

# World Journal of *Gastrointestinal Oncology*

*World J Gastrointest Oncol* 2020 November 15; 12(11): 1216-1380



### ORIGINAL ARTICLE

#### Basic Study

- 1216** Pathological significance of abnormal receptor d'origine nantaïs and programmed death ligand 1 expression in colorectal cancer  
*Liu YZ, Han DT, Shi DR, Hong B, Qian Y, Wu ZG, Yao SH, Tang TM, Wang MH, Xu XM, Yao HP*
- 1237** Decreased expression of the long non-coding RNA HOXD-AS2 promotes gastric cancer progression by targeting HOXD8 and activating PI3K/Akt signaling pathway  
*Yao L, Ye PC, Tan W, Luo YJ, Xiang WP, Liu ZL, Fu ZM, Lu F, Tang LH, Xiao JW*
- 1255** Programmed death 1, ligand 1 and 2 correlated genes and their association with mutation, immune infiltration and clinical outcomes of hepatocellular carcinoma  
*Sheng QJ, Tian WY, Dou XG, Zhang C, Li YW, Han C, Fan YX, Lai PP, Ding Y*

#### Case Control Study

- 1272** LncRNA C9orf139 can regulate the growth of pancreatic cancer by mediating the miR-663a/Sox12 axis  
*Ge JN, Yan D, Ge CL, Wei MJ*

#### Retrospective Cohort Study

- 1288** Cancer-related microangiopathic hemolytic anemia in patients with advanced gastric cancer: A retrospective single-center analysis  
*Berger AK, Allgäuer M, Apostolidis L, Schulze-Schleithoff AE, Merle U, Jaeger D, Haag GM*
- 1296** Influence of primary tumor location and resection on survival in metastatic colorectal cancer  
*Tharin Z, Blanc J, Charifi Alaoui I, Bertaut A, Ghiringhelli F*

#### Retrospective Study

- 1311** Highly accurate colorectal cancer prediction model based on Raman spectroscopy using patient serum  
*Ito H, Urugami N, Miyazaki T, Yang W, Issha K, Matsuo K, Kimura S, Arai Y, Tokunaga H, Okada S, Kawamura M, Yokoyama N, Kushima M, Inoue H, Fukagai T, Kamijo Y*
- 1325** Subtotal gastrectomy combined with chemotherapy: An effective therapy for patients with circumscribed Borrmann type IV gastric cancer  
*Huang HB, Gao ZM, Sun AQ, Liang WT, Li K*

#### Randomized Controlled Trial

- 1336** Diagnostic value of novel retroflexion colonoscopy in the right colon: A randomized controlled trial  
*Li WK, Wang Y, Wang YD, Liu KL, Guo CM, Su H, Liu H, Wu J*



**META-ANALYSIS**

- 1346** Efficacy and safety of anti-PD-1/anti-PD-L1 antibody therapy in treatment of advanced gastric cancer or gastroesophageal junction cancer: A meta-analysis

*Yang L, Dong XZ, Xing XX, Cui XH, Li L, Zhang L*

**CASE REPORT**

- 1364** Inferior mesenteric arteriovenous fistula during treatment with bevacizumab in colorectal cancer patient: A case report

*Doi A, Takeda H, Umemoto K, Oumi R, Wada S, Hamaguchi S, Mimura H, Arai H, Horie Y, Mizukami T, Izawa N, Ogura T, Nakajima TE, Sunakawa Y*

- 1372** Cutaneous metastases of pancreatic carcinoma to the labia majora: A case report and review of literature

*Shi Y, Li SS, Liu DY, Yu Y*

**ABOUT COVER**

Editorial Board Member of *World Journal of Gastrointestinal Oncology*, Tomohide Hori, PhD, MD, FACS, is an Attending Surgeon at the Affiliated Hospital with Kyoto University (Kyoto, Japan). Dr. Hori obtained his medical doctor license from Tokyo Medical University (Japan) in 1997 and his Doctor of Philosophy degree from Mie University Graduate School of Medicine (Japan) in 2007. Dr. Hori is certified and qualified by many international and domestic societies, including the American College of Surgeons and Japan Society of Endoscopic Surgery. From 2009 to 2011, he worked at Mayo Clinic (Jacksonville, FL, United States). Dr. Hori's research career has spanned the fields of gastroenterology, hepatology, transplant immunology, and gastrointestinal, colorectal, hepatobiliary, pancreatic, transplant and pediatric surgeries, yielding more than 200 medical publications in international journals. (L-Editor: Filipodia)

**AIMS AND SCOPE**

The primary aim of *World Journal of Gastrointestinal Oncology* (WJGO, *World J Gastrointest Oncol*) is to provide scholars and readers from various fields of gastrointestinal oncology with a platform to publish high-quality basic and clinical research articles and communicate their research findings online.

WJGO mainly publishes articles reporting research results and findings obtained in the field of gastrointestinal oncology and covering a wide range of topics including liver cell adenoma, gastric neoplasms, appendiceal neoplasms, biliary tract neoplasms, hepatocellular carcinoma, pancreatic carcinoma, cecal neoplasms, colonic neoplasms, colorectal neoplasms, duodenal neoplasms, esophageal neoplasms, gallbladder neoplasms, etc.

**INDEXING/ABSTRACTING**

The WJGO is now indexed in Science Citation Index Expanded (also known as SciSearch®), PubMed, and PubMed Central. The 2020 edition of Journal Citation Reports® cites the 2019 impact factor (IF) for WJGO as 2.898; IF without journal self cites: 2.880; 5-year IF: 3.316; Ranking: 143 among 244 journals in oncology; Quartile category: Q3; Ranking: 55 among 88 journals in gastroenterology and hepatology; and Quartile category: Q3.

**RESPONSIBLE EDITORS FOR THIS ISSUE**

Production Editor: Jia-Hui Li; Production Department Director: Xiang Li; Editorial Office Director: Jin-Lei Wang.

**NAME OF JOURNAL**

*World Journal of Gastrointestinal Oncology*

**ISSN**

ISSN 1948-5204 (online)

**LAUNCH DATE**

February 15, 2009

**FREQUENCY**

Monthly

**EDITORS-IN-CHIEF**

Rosa M Jimenez Rodriguez, Pashtoon Kasi, Monjur Ahmed

**EDITORIAL BOARD MEMBERS**

<https://www.wjgnet.com/1948-5204/editorialboard.htm>

**PUBLICATION DATE**

November 15, 2020

**COPYRIGHT**

© 2020 Baishideng Publishing Group Inc

**INSTRUCTIONS TO AUTHORS**

<https://www.wjgnet.com/bpg/gerinfo/204>

**GUIDELINES FOR ETHICS DOCUMENTS**

<https://www.wjgnet.com/bpg/GerInfo/287>

**GUIDELINES FOR NON-NATIVE SPEAKERS OF ENGLISH**

<https://www.wjgnet.com/bpg/gerinfo/240>

**PUBLICATION ETHICS**

<https://www.wjgnet.com/bpg/GerInfo/288>

**PUBLICATION MISCONDUCT**

<https://www.wjgnet.com/bpg/gerinfo/208>

**ARTICLE PROCESSING CHARGE**

<https://www.wjgnet.com/bpg/gerinfo/242>

**STEPS FOR SUBMITTING MANUSCRIPTS**

<https://www.wjgnet.com/bpg/GerInfo/239>

**ONLINE SUBMISSION**

<https://www.f6publishing.com>



Basic Study

## Pathological significance of abnormal recepteur d'origine nantais and programmed death ligand 1 expression in colorectal cancer

Yi-Zhi Liu, Da-Ting Han, Dan-Rong Shi, Bo Hong, Yun Qian, Zhi-Gang Wu, Shu-Hao Yao, Tao-Ming Tang, Ming-Hai Wang, Xiang-Ming Xu, Hang-Ping Yao

**ORCID number:** Yi-Zhi Liu 0000-0003-0350-4477; Da-Ting Han 0000-0002-4305-7045; Dan-Rong Shi 0000-0002-6364-2321; Bo Hong 0000-0003-2100-8880; Yun Qian 0000-0003-3158-9412; Zhi-Gang Wu 0000-0003-2405-1702; Shu-Hao Yao 0000-0003-3408-5615; Tao-Ming Tang 0000-0002-7852-2728; Ming-Hai Wang 0000 0002 5173 2987; Xiang-Ming Xu 0000-0003-4402-5018; Hang-Ping Yao 0000-0001-6742-7074.

**Author contributions:** Yao HP, Xu XM, and Wang MH carried out the experimental design and supervision; Yao HP, Liu YZ, Hong B, Qian Y, Tang TM, Wu ZG, Yao SH, and Xu XM conducted the sample collection, immunohistochemistry, and multiplex immunofluorescence analysis; Liu YZ, Shi DR, and Han DT performed the *in vitro* cellular experiments and data analysis; Yao HP, Wang MH, and Liu YZ drafted the manuscript; all authors read and approved the final manuscript.

**Supported by** the National Natural Science Foundation of China, No. 81872883 (to Yao HP); Zhejiang Major Medical Health & Sciences Technology Foundation Projects, No. WKJ-ZJ-13 (to Yao HP); and Zhejiang Provincial Natural Science Foundation of China, No.

**Yi-Zhi Liu, Da-Ting Han, Dan-Rong Shi, Zhi-Gang Wu, Tao-Ming Tang, Hang-Ping Yao**, Department of Cancer Biology Research, State Key Laboratory for Diagnosis and Treatment of Infectious Diseases, National Clinical Research Center for Infectious Diseases, The First Affiliated Hospital, Zhejiang University School of Medicine, Hangzhou 310003, Zhejiang Province, China

**Bo Hong**, Department of Pathology, The Second Affiliated Hospital, Zhejiang University School of Medicine, Hangzhou 310003, Zhejiang Province, China

**Yun Qian**, Department of Clinical Laboratory, The Second Affiliated Hospital, Zhejiang University School of Medicine, Hangzhou 310003, Zhejiang Province, China

**Shu-Hao Yao**, Department of Stomatology, Wenzhou Medical University Renji College, Wenzhou 325035, Zhejiang Province, China

**Ming-Hai Wang**, Cancer Biology Research Center and Department of Pharmaceutical Sciences, School of Pharmacy, Texas Tech University Health Sciences Center, Amarillo, TX 79106, United States

**Xiang-Ming Xu**, Department of Cancer Biology Research, The First Affiliated Hospital, Zhejiang University School of Medicine, Hangzhou 310003, Zhejiang Province, China

**Corresponding author:** Hang-Ping Yao, PhD, Professor, Department of Cancer Biology Research, State Key Laboratory for Diagnosis and Treatment of Infectious Diseases, National Clinical Research Center for Infectious Diseases, The First Affiliated Hospital, Zhejiang University School of Medicine, No. 79 Qingchun Road, Hangzhou 310003, Zhejiang Province, China. [yaohangping@zju.edu.cn](mailto:yaohangping@zju.edu.cn)

### Abstract

#### BACKGROUND

Programmed death ligand 1 (PD-L1) immunotherapy remains poorly efficacious in colorectal cancer (CRC). The recepteur d'origine nantais (RON) receptor tyrosine kinase plays an important role in regulating tumor immunity.

#### AIM

To identify the patterns of RON and PD-L1 expression and explore their clinical significance in CRC.

LY18H160014 (to Xu XM).

#### Institutional review board

**statement:** The study was reviewed and approved by the First Affiliated Hospital, Zhejiang University School of Medicine (reference number: 2017427-1).

**Conflict-of-interest statement:** The authors confirm that there are no known conflicts of interest associated with this publication. The manuscript has been read and approved by all authors and there are no other persons who satisfied the criteria for authorship but are not listed. We further confirm that the order of authors listed in the manuscript has been approved by all of authors.

**Data sharing statement:** All data generated or analyzed during this study are included in the published paper. More details can be provided on request.

**ARRIVE guidelines statement:** The authors have read the ARRIVE guidelines, and the manuscript was prepared and revised according to the ARRIVE guidelines.

**Open-Access:** This article is an open-access article that was selected by an in-house editor and fully peer-reviewed by external reviewers. It is distributed in accordance with the Creative Commons Attribution NonCommercial (CC BY-NC 4.0) license, which permits others to distribute, remix, adapt, build upon this work non-commercially, and license their derivative works on different terms, provided the original work is properly cited and the use is non-commercial. See: <http://creativecommons.org/licenses/by-nc/4.0/>

**Manuscript source:** Invited manuscript

**Specialty type:** Pathology

**Country/Territory of origin:** China

**Peer-review report's scientific quality classification**

Grade A (Excellent): 0

## METHODS

Gene expression data from the Gene Expression Omnibus database (GEO;  $n = 290$ ) and patients at the First Affiliated Hospital, Zhejiang University School of Medicine (FAHZUSM;  $n = 381$ ) were analyzed to determine the prognostic value of RON and PD-L1 expression within the tumor microenvironment of CRC. HT29 cell line was treated with BMS-777607 to explore the relationship between RON activity and PD-L1 expression. Signaling pathways and protein expression perturbed by RON inhibition were evaluated by cellular immunofluorescence and Western blot.

## RESULTS

In the GEO patient cohort, cut-off values for RON and PD-L1 expression were determined to be 7.70 and 4.3, respectively. Stratification of patients based on these cutoffs demonstrated that high expression of RON and PD-L1 was associated with a poor prognosis. In the FAHZUSM cohort, rates of high expression of RON in tumor cells, high PD-L1 expression in tumor cells and tumor infiltrating monocytes, and both high RON and high PD-L1 expression in the tumor microenvironment were 121 (32%), 43 (11%), 91 (24%), and 51 (13.4%), respectively. High expression of RON was significantly correlated with high expression of PD-L1 in the tumor cell compartment ( $P < 0.001$ ). High expression of RON and that of PD-L1 were independent prognostic factors for poorer overall survival. Concurrent high expression of both RON and PD-L1 in the tumor microenvironment was significantly associated with a poor prognosis. *In vitro*, BMS-777607 inhibited the phosphorylation of RON, inhibited PD-L1 expression, and attenuated activation of the ERK1/2 and AKT signaling pathways in CRC cells.

## CONCLUSION

RON, PD-L1, and their crosstalk are significant in predicting the prognostic value of CRC. Moreover, phosphorylation of RON upregulates PD-L1 expression, which provides a novel approach to immunotherapy in CRC.

**Key Words:** Colorectal cancer; Programmed death ligand 1; Prognosis; Recepteur d'origine nantais; Tumor infiltrating mononuclear cells; Tumor microenvironment

©The Author(s) 2020. Published by Baishideng Publishing Group Inc. All rights reserved.

**Core Tip:** Recepteur d'origine nantais (RON) expression plays an important role in regulating tumor immunity, and the efficacy of programmed death ligand 1 (PD-L1) immunotherapy in colorectal cancer (CRC) is still not satisfactory. This inspired us to study the clinical significance and correlation of RON and PD-L1 in CRC. The major discoveries and findings in this study are: (1) The abnormal expression of RON and PD-L1 was not only correlated, but was also significant biomarkers for poor prognosis of CRC. This finding was identified in 389 primary CRC clinical samples *via* multiplex immunofluorescence staining and immunohistochemistry staining; and (2) In *in vitro* experiments, activation of RON phosphorylation up-regulated the expression of PD-L1 in CRC cells.

**Citation:** Liu YZ, Han DT, Shi DR, Hong B, Qian Y, Wu ZG, Yao SH, Tang TM, Wang MH, Xu XM, Yao HP. Pathological significance of abnormal recepteur d'origine nantais and programmed death ligand 1 expression in colorectal cancer. *World J Gastrointest Oncol* 2020; 12(11): 1216-1236

**URL:** <https://www.wjgnet.com/1948-5204/full/v12/i11/1216.htm>

**DOI:** <https://dx.doi.org/10.4251/wjgo.v12.i11.1216>

## INTRODUCTION

Colorectal cancer (CRC) is the fourth most common malignancy worldwide in 2018<sup>[1]</sup>.



Grade B (Very good): B  
 Grade C (Good): C  
 Grade D (Fair): 0  
 Grade E (Poor): 0

**Received:** August 9, 2020

**Peer-review started:** August 9, 2020

**First decision:** August 22, 2020

**Revised:** September 6, 2020

**Accepted:** September 18, 2020

**Article in press:** September 18, 2020

**Published online:** November 15, 2020

**P-Reviewer:** Koustas E, Zhu Y

**S-Editor:** Gong ZM

**L-Editor:** Wang TQ

**P-Editor:** Li JH



Despite advances in CRC treatment methods, it still has a poor prognosis, and many patients will have local recurrence and/or distant metastasis within 5 years after treatment<sup>[2]</sup>.

Immunotherapy has become a promising strategy for treating a wide variety of malignancies<sup>[3]</sup>. Therapeutic antibodies that block the activity of programmed death ligand 1 (PD-L1, also known as CD274) protein are effective against many cancer types<sup>[4]</sup>. PD-L1 is a transmembrane immune checkpoint protein that can be expressed on both immune cells and cancer cells, including CRC cells<sup>[5-7]</sup>. When expressed on immune cells, PD-L1 can be regulated by a variety of inflammatory mediators and cytokines. When expressed on the surface of tumor cells (TCs), PD-L1 enables TCs to evade the immune system<sup>[8,9]</sup>. Cancer cells can induce the expression of PD-L1 through activation of oncogenic pathways, such as the RAS-ERK or PI3K-AKT pathways, to facilitate immune escape<sup>[10-12]</sup>.

However, the efficacy of PD-L1 immunosuppressive agents in CRC is poor<sup>[13,14]</sup>. The overall poor response of CRC to PD-L1 blockade may be due to the activity of multiple oncogenes<sup>[15,16]</sup>. For example, KRAS mutations can up-regulate the expression of PD-L1 in CRC cells, thereby reducing the efficacy of PD-L1 immunosuppressive agents<sup>[17]</sup>. RON (macrophage-stimulating 1 receptor, MST1R), a member of the MET proto-oncogene family and a receptor for MSP, is an effector of KRAS signaling, and exhibits "KRAS addiction", a phenomenon that plays an important role in the initiation and development of tumors<sup>[18-20]</sup>. RON is overexpressed pathologically in various types of cancer, including CRC, and many small-molecule inhibitors are being developed to target RON and its associated compounds<sup>[20-22]</sup>. BMS-777607 is a highly selective small molecule inhibitor of RON (IC<sub>50</sub> 1.8nM for RON)<sup>[23]</sup>. Activation of RON leads to RON phosphorylation, which then activates different signaling pathways in cancer cells, including the RAS-ERK and PI3K-AKT pathways<sup>[24-26]</sup>. Interactions between RON and other membrane receptors further promote pathway activation, enhancing the migration and invasion of CRC cells<sup>[20,22]</sup>. In addition, overexpression of RON can damage immune cells and inhibit anti-tumor immunity<sup>[27,28]</sup>. Thus, abnormal expression of RON may affect the efficacy of PD-L1 immunotherapy in CRC.

In this study, we investigated the clinical significance of expression patterns of RON and PD-L1 in primary CRC samples, and evaluated the potential for RON and PD-L1 as prognostic biomarkers in CRC. We treated CRC cells with BMS777607 *in vitro* to explore if RON inhibition affects the expression of PD-L1 and results in changes in related signaling pathways in CRC cells. Our data suggested that RON inhibition may be a novel approach to augment immunotherapy in CRC.

## MATERIALS AND METHODS

### Patient demographics

This study involved a GEO (Gene Expression Omnibus) cohort and a FAHZUSM (The First Affiliated Hospital, Zhejiang University School of Medicine) cohort. In the GEO cohort, the median age of all 287 CRC patients was 70 years (range: 24-97 years). There were 158 (55.1%) male patients and 129 (44.9%) female patients. The median survival time was 58 months, and 94 patients died during follow-up. In the FAHZUSM cohort, the median age of the CRC patients undergoing tumor resection was 61 years (range: 29-94 years). In this cohort, 215 (56.4%) patients were male and 166 (43.6%) were female. The median survival time was 100 months, and 91 patients died during follow-up. The primary site of a tumor, pathological grade, TNM stage, disease stage, histological type, and treatment status of CRC patients are shown in [Table 1](#).

### Cell lines and reagents

The CRC cell line HT29 was obtained from the American Type Cell Culture (ATCC, Manassas, VA, United States). Flow cytometric analysis revealed that RON and PD-L1 were strongly expressed in HT29 cells ([Supplementary Figure 1](#)). Cells were cultured in growth medium supplemented with 10% fetal bovine serum and incubated under standard cell culture conditions at 37 °C and 5% CO<sub>2</sub>. Rabbit anti-RON antibody (5029) and mouse anti-RON monoclonal antibodies (Zt/f2 and Zt/g4) were used as previously described<sup>[28]</sup>. Macrophage-stimulating protein (MSP) is an activation factor for RON receptor tyrosine kinase phosphorylation and catalytic activity of a number of signal transduction proteins<sup>[29]</sup>. Human mature MSP was obtained from R&D Systems (Minneapolis, MN, United States). Antibodies against phospho-tyrosine (P-Tyr-100, Cat # 9411), AKT (Cat # 4685), phospho-AKT (Cat # 4060), extracellular signaling regulated kinase (ERK) 1/2 (Cat # 4695), and phospho-ERK1/2 (p44/42) (Cat # 4376)

**Table 1 Comparison of RON and PD-L1 expression and clinicopathological characteristics of patients with colorectal cancer in the FAHZUSM and Gene Expression Omnibus cohorts, *n* (%)**

Characteristic	FAHZUSM cohort (n = 381)							GEO cohort (n = 287)									
	Cases	RON expression			PD-L1 expression				Cases No (%)	RON expression			PD-L1 expression				
		Low	High	<sup>1</sup> P value	Low	High (TIMC)	<sup>2</sup> P value	Low		High (TC)	<sup>3</sup> P value	Low	High	<sup>1</sup> P value	Low	High (TC)	<sup>3</sup> P value
No. of cases number	381	260	121		247	91		247	43		287	193	94		48	239	
Age (mean ± SD)	61.16 ± 12.419	60.40 ± 12.560	62.81 ± 11.997	0.859	60.94 ± 12.37	62.04 ± 13.080	0.771	60.94 ± 12.37	61.16 ± 12.419	0.938	68.44 ± 14.00	66.87 ± 13.18	71.65 ± 15.12	0.006	66.94 ± 14.33	68.74 ± 13.95	0.417
Sex																	
Man	215 (56.4)	157 (60.4)	58 (47.9)	0.023	143 (57.9)	54 (59.3)	0.811	143 (57.9)	18 (41.9)	0.051	158 (55.1)	111 (57.5)	47 (50)	0.230	30 (62.5)	128 (53.6)	0.256
Women	166 (43.6)	103 (39.6)	63 (52.1)		104 (42.1)	37 (40.7)		104 (42.1)	25 (58.1)		129 (44.9)	82 (42.5)	47 (50)		18 (37.5)	111 (46.4)	
Principal diagnosis																	
Rectum	229 (60.1)	158 (61.1)	71 (58.7)	0.698	153 (61.9)	47 (51.6)	0.088	153 (61.9)	29 (67.4)	0.491	165 (57.5)	111 (57.5)	54 (57.4)	0.920	34 (70.8)	131 (54.8)	0.040
Colon	152 (39.9)	102 (38.9)	50 (41.3)		94 (38.1)	44 (48.4)		94 (38.1)	14 (32.6)		122 (42.5)	82 (42.5)	40 (42.6)		14 (29.2)	108 (45.2)	
Pathological grade																	
Well/moderate	9 (2.4)	6 (2.3)	3 (2.5)	0.177	5 (2)	3 (3.3)	0.778	5 (2)	1 (2.3)	0.898	NA						
Poor	346 (90.8)	232 (89.2)	114 (94.2)		224 (90.7)	82 (90.1)		224 (90.7)	40 (93)								
Unknown	26 (6.8)	22 (8.5)	4 (3.3)		18 (7.1)	6 (6.3)		18 (7.3)	2 (4.7)								
T stage																	
Tis-T2	107 (28.1)	85 (32.7)	22 (18.2)	0.001	73 (29.6)	23 (25.3)	0.105	73 (29.6)	11 (25.6)	0.864	28 (9.7)	18 (9.3)	10 (10.6)	0.459	3 (6.3)	25 (10.5)	0.437
T3	177 (46.5)	121 (46.5)	56 (46.3)		118 (47.8) (46.8%)	37 (40.7)		118 (47.8)	22 (51.2)		208 (72.5)	144 (74.6)	64 (68.1)20		39 (81.3)	169 (70.7)	
T4	97 (25.5)	54 (20.8)	43 (35.5)		56 (22.7)	31 (34.1)		56 (22.7)	10 (23.3)		51 (17.8)	31 (16.1)	20 (21.3)		6 (12.5)	45 (18.8)	
N stage																	
N0	251 (65.9)	184 (70.8)	67 (55.4)	0.003	164 (66.4)	62 (68.1)	0.764	164 (66.4)	25 (58.1)	0.294	141 (49.1)	97 (50.3)	44 (46.8)	0.583	27 (56.3)	114 (44.7)	0.279
N (1-2)	91 (23.9)	76 (29.2)	54 (44.6)		83 (33.6)	29 (31.9)		83 (33.6)	12 (27.9)		146 (50.9)	96 (49.7)	50 (53.2)		21 (43.7)	125 (52.3)	
M stage																	
M0	368 (96.6)	252 (96.9)	116 (95.9) (96.3%)	0.822	241 (97.6)	85 (93.4)	0.133	241 (97.6)	42 (97.7)	1.000	268 (93.4)	183 (94.8)	85 (90.4)	0.160	47 (97.9)	221 (92.5)	0.216

M1	13 (3.4)	8 (3.1)	5 (4.1)		6 (2.4)	6 (6.6)		6 (2.4)	1 (2.3)		19 (6.6)	10 (5.2)	9 (9.6)		1 (2.1)	18 (7.5)	
Disease stage																	
0-II	246 (64.6)	180 (69.2)	66 (54.5)	<b>0.016</b>	162 (65.6)	59 (64.8)	0.897	162 (65.6)	25 (58.1)	0.346	139 (48.4)	95 (49.2)	44 (46.8)	0.701	27 (56.3)	112 (46.9)	0.235
III-IV	135 (35.4)	80 (30.8)	55 (45.5)		85 (34.4)	32 (35.2)		85 (34.4)	18 (41.9)		148 (51.6)	98 (50.8)	50 (53.2)		21 (43.8)	127 (53.1)	
Histological type																	
Adenocarcinoma	335 (87.9)	227 (87.3)	108 (89.3)	0.706	214 (86.6)	84 (92.3)	0.130	214 (86.6)	37 (86)	0.488	287 (100)	193 (100)	94 (100)		48 (100)	239 (100)	
Mucinous/SRCC	36 (9.4)	25 (9.6)	11 (9.1)		28 (11.3)	4 (4.4)		28 (11.3)	4 (9.3)		0 (0)	0 (0)	0 (0)		0 (0)	0 (0)	
Other	10 (2.6)	8 (3.1)	2 (1.7)		5 (2.0)	3 (3.3)		5 (2.0)	2 (4.7)		0 (0)	0 (0)	0 (0)		0 (0)	0 (0)	
Treatment																	
Yes	173 (45.4)	110 (42.3)	63 (52.1)	<b>0.043</b>	112 (45.3)	38 (41.8)	0.694	112 (45.3)	23 (32.6)	0.472	115 (40.1)	89 (46.1)	26 (27.7)	<b>0.003</b>	22 (45.8)	93 (38.9)	0.372
No	158 (41.5)	119 (45.8)	39 (32.2)		105 (42.5)	39 (42.9)		105 (42.5)	14 (53.5)		172 (59.9)	104 (53.9)	68 (72.3)		26 (54.2)	146 (61.1)	
Unknown	50 (13.1)	31 (11.9)	19 (15.7)		30 (12.1)	14 (15.4)		30 (12.1)	6 (14)			0 (0)	0 (0)				
PD-L1 (protein)																	
Low	247 (64.8)	177 (73.1)	70 (26.9)	0.976 <sup>4</sup>							NA						
High (TIMCs)	91 (23.9)	65 (26.9)	26 (27.1)														
High (TCs)	43 (11.3)	18 (9.2)	25 (26.3)	<b>&lt; 0.001<sup>5</sup></b>													
PD-L1 (mRNA)																	
Low	NA										48 (16.7)	31 (16.1)	17 (18.1)	0.666			
High											239 (83.3)	162 (83.9)	77 (81.9)				

<sup>1</sup>Comparing RON high expression and RON low expression.

<sup>2</sup>Comparing PD-L1 low expression and PD-L1 expression in TIMCs.

<sup>3</sup>Comparing PD-L1 low expression and PD-L1 expression in TCs.

<sup>4</sup>PD-L1 low (both TCs and TIMCs) *vs* PD-L1 high (TIMCs).

<sup>5</sup>PD-L1 low (both TCs and TIMCs) *vs* PD-L1 high TCs. Bold entries indicate statistical significance ( $P < 0.05$ ). GEO: The Gene Expression Omnibus; RON: Recepteur d'origine nantais; PD-L1: Programmed death ligand 1; TCs: Tumor cells; TIMCs: Tumor-infiltrating mononuclear cells; FAHZUSM: The First Affiliated Hospital, Zhejiang University School of Medicine.

were obtained from Cell Signaling Technology (Beverly, MA, United States). CK antibody was from ZSGB-BIO (Cat # ZM-0069, Beijing, China). The BMS-777607 RON inhibitor was from Medchem Express (Monmouth Junction, NJ, United States). BMS-777607 was dissolved in dimethyl sulfoxide (DMSO) to a final concentration of 10 mmol/L and stored at -20 °C. The PD-L1 antibody (Cat # 13864) for immunohistochemistry and multiplex immunofluorescence was obtained from Cell

Signaling Technology (Beverly, MA, United States). The PD-L1 antibody (Cat # 205921) used for cell experiments was from Abcam (Burlingame, CA, United States). Opal tyramine signal amplification (TSA) staining kit was from PerkinElmer (Hopkinton, MA, United States).

### **The Gene Expression Omnibus database**

Gene expression data for RON and PD-L1 and clinical data for CRC patients are available from the GEO database and accessed through the browser web site (<https://geonames.org/>)<sup>[30]</sup>. A total of 290 primary CRC tumors from patients with detailed RON and PD-L1 expression data were selected from the GEO database, based on the completeness of patient clinical data. Only patients with complete tumor characteristics, overall survival (OS), and RNA-seq information, and patients whose tumor samples were obtained prior to treatment were included. The clinicopathologic features of the patients included age, sex, tumor location, histological type, tumor-lymph node-metastasis (TNM) stage, treatment regimen, and OS.

### **Patients and tissue samples**

The CRC specimens used for this study were obtained from 381 CRC patients who were pathologically diagnosed and treated between January 2006 and November 2009 at the FAHZUSM. Clinical data for patients included age, sex, tumor location, histological type, TNM stage, tumor differentiation, treatment pattern, and OS rate (Table 1). CRC tissues were fixed in 10% buffered formalin, embedded in paraffin, and were available for immunohistochemical (IHC) evaluation. Detailed demographic data and clinical features of the FAHZUSM cohort are provided in Table 1. This study was approved by the Ethics Committee of the First Affiliated Hospital, Zhejiang University School of Medicine (reference number: 2017427-1).

### **Multiplex immunofluorescence**

Multiplex immunofluorescence staining of paraffin-embedded sections was performed using Zt/f2 (5 µg/mL) as the primary antibody for RON, rabbit anti-PD-L1 antibody (1:150, 13684, CST) for PD-L1, and mouse anti-CK mAb (1:200, ZM-0069, ZSGB-BIO) for CK, and visualized using the Opal tyramine signal amplification (TSA) staining kit. First, the concentration and sequence of the RON, PD-L1, and CK antibodies were optimized. The primary antibodies/fluorescent dyes for PD-L1/Opal 530, RON/Opal 690, and CK /Opal 520 were applied to the CRC tissues in sequence. Finally, sections were stained with DAPI and mounted with an anti-fading mounting agent. PerkinElmer software version 2.1 was used to analyze multispectral images.

### **Immunohistochemistry**

IHC staining was performed according to standard protocols. Primary antibodies were incubated overnight using a dilution of 1:150 for PD-L1 (13684, CST, United States) and 1:800 for RON. Mouse anti-RON mAb (Zt/f2) was used as previously described<sup>[31]</sup>. The primary antibody was visualized with diaminobenzidine until a brown precipitate appeared at the antigenic site using EnVision + System-HRP (Dako, Carpinteria, CA, United States). Then, sections were counterstained with hematoxylin.

### **Evaluation of RON and PD-L1 expression in CRC samples**

The IHC-stained sections were independently scored by two pathologists who were blinded to the clinicopathological data. RON expression was determined using a semi-quantitative system. According to the percentage of positive staining area in the whole cancer area, the scoring was as follows: 0 (< 5%), 1 (5%-25%), 2 (26%-50%), 3 (51%-75%), and 4 (> 75%). The staining intensity was scored as 0 (negative), 1 (weak), 2 (medium), or 3 (strong). The total score was obtained by adding the positive proportion score and the staining level score. Samples were categorized as follows: Samples with a final staining score ≤ 4 were considered to be low and those with a score of > 4 were considered to be high for RON expression.

PD-L1 expression was evaluated using an anti-PD-L1 rabbit antibody (13684, CST, United States). A cutoff of 5% for the total proportion of cells that were positive for PD-L1 was used, such that samples with < 5% PD-L1 positive cells were considered to be low and samples with ≥ 5% PD-L1 positive cells were considered to be high for PD-L1 expression. This standard has been established in various types of cancer<sup>[32-34]</sup>.

### **Phosphorylation and Western blot analysis**

The result of Cell Counting Kit 8 illustrated that the half-maximal inhibitory concentration (IC50) of BMS-777607 in HT29 cells at 72 h was 2 µmol/L (



**Supplementary Figure 2).** HT29 cells were treated with 2 nmol/L MSP, 2  $\mu$ mol/L BMS-777607, or 2 nmol/L MSP + 2  $\mu$ mol/L BMS-777607 for 24 h. The culture medium was removed and the cells were washed with ice-cold phosphate buffered saline (PBS). Cells were digested with trypsin, collected, and washed with PBS to remove residual trypsin. Cells were lysed in radioimmunoprecipitation (RIPA) buffer, and 25  $\mu$ g of total protein per sample was separated by 8% SDS-PAGE. Western blot was performed using antibodies against RON, phospho-RON, PD-L1, ERK1/2, phospho-ERK1/2, AKT, and phospho-AKT; GAPDH protein was evaluated as an internal control to ensure equal sample loading. Immunoreactive protein bands were visually detected using enhanced chemiluminescence reagents.

### **Immunofluorescence analysis**

HT29 cells were cultured overnight in a 6-well plate on a cover slide. After treatment with 2 nmol/L MSP, 2  $\mu$ mol/L BMS-777607, or 2 nmol/L MSP + 2  $\mu$ mol/L BMS-777607 for 24 h, cells were fixed with 4% paraformaldehyde at 37 °C for 20 min, then washed with PBS five times for 3 min. Cover slides were then blocked with 5% BSA in PBS at room temperature for 30 min. After that, the cells were incubated with primary antibody against PD-L1 (205921, Abcam, United States) and mouse anti-RON mAb (Zt/f2) overnight at 4 °C. Primary antibodies were then removed by washing with PBS five times for 3 min. The cells were then incubated with a fluorescently labeled secondary antibody in the dark at room temperature for 1 h. Excess secondary antibody was removed and the cells were counterstained with DAPI. Slides were mounted with an anti-quenching agent and sealed. The fluorescently labeled cells were observed using a LEICA DMi8 microscope (Leica). Representative images were selected and photographed.

### **Statistical analysis**

Clinical quantitative data are expressed as the mean  $\pm$  standard deviation (SD) and count data are expressed as constituent ratio (%) or ratio (%). Statistical evaluation was conducted with SPSS 25.0 (IBM Corp., Armonk, NY, United States) and GraphPad Prism v.8 (La Jolla, CA, United States). X-tile 3.6.1 software (Yale University, New Haven, CT, United States) was used to determine the optimal cut-off values for RON and PD-L1 expression in the GEO cohort<sup>[35]</sup>.  $\chi^2$  tests were used to analyze relationships between clinicopathological parameters and RON and PD-L1 expression. Differences between quantitative data with a normal distribution were compared using two independent samples *t*-tests between two groups and one-way analysis of variance among three groups and SNK-q test between groups. Kaplan-Meier method and log-rank test were used for OS analysis. Univariate and multivariate Cox regression analyses were used for identifying the risk factors for OS. A *P* value < 0.05 was considered statistically significant. All confidence intervals (CIs) are stated at the 95% confidence level.

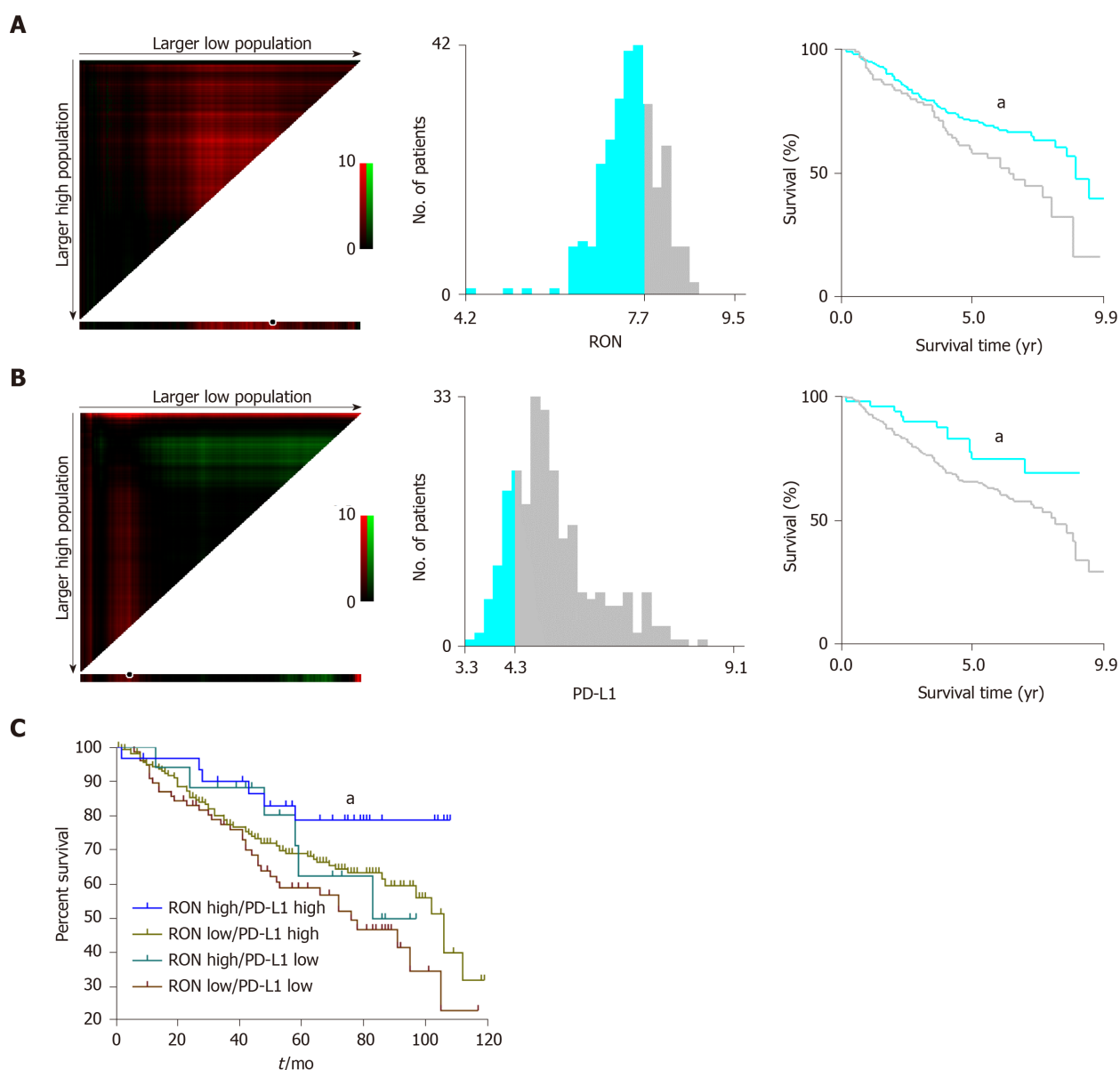
## **RESULTS**

### **Expression patterns of RON and PD-L1 in the GEO cohort**

In the GEO cohort, X-tile was used to find the optimal cutoff values to divide the data of RON (the upper panel) and PD-L1 (the lower panel) mRNA expression into either low or high expression by selecting the highest  $\chi^2$  value and the smallest *P* value of a standard log-rank test. The cut-off values for RON and PD-L1 mRNA in TCs were determined as 7.70 and 4.30, respectively (Figure 1A and B), and the log-rank  $\chi^2$  values for RON and PD-L1 were 4.544 and 4.078, respectively. Patients in the GEO cohort were stratified according to RON and PD-L1 status: RON  $\leq$  7.70 and RON > 7.70, and PD-L1  $\leq$  4.30 and PD-L1 > 4.30 (Figure 1A and B). We found that the high expression of RON and PD-L1 was associated with a poor prognosis.

### **Expression of RON and PD-L1 in CRC tumor tissue**

In CRC tissue samples, multiple immunofluorescence staining was used to show the expression patterns of RON in TCs and PD-L1 in the tumor microenvironment. We found that both RON and PD-L1 exhibited membrane-enhanced expression in TCs (Figure 2A); elevated RON expression on the tumor cell membrane was accompanied by enhanced PD-L1 expression in tumor-infiltrating mononuclear cells (TIMCs) (Figure 2B). We also observed cases where PD-L1 expression was enhanced on the tumor cell membrane (Figure 2C) or in TIMCs (Figure 2D), but RON expression was

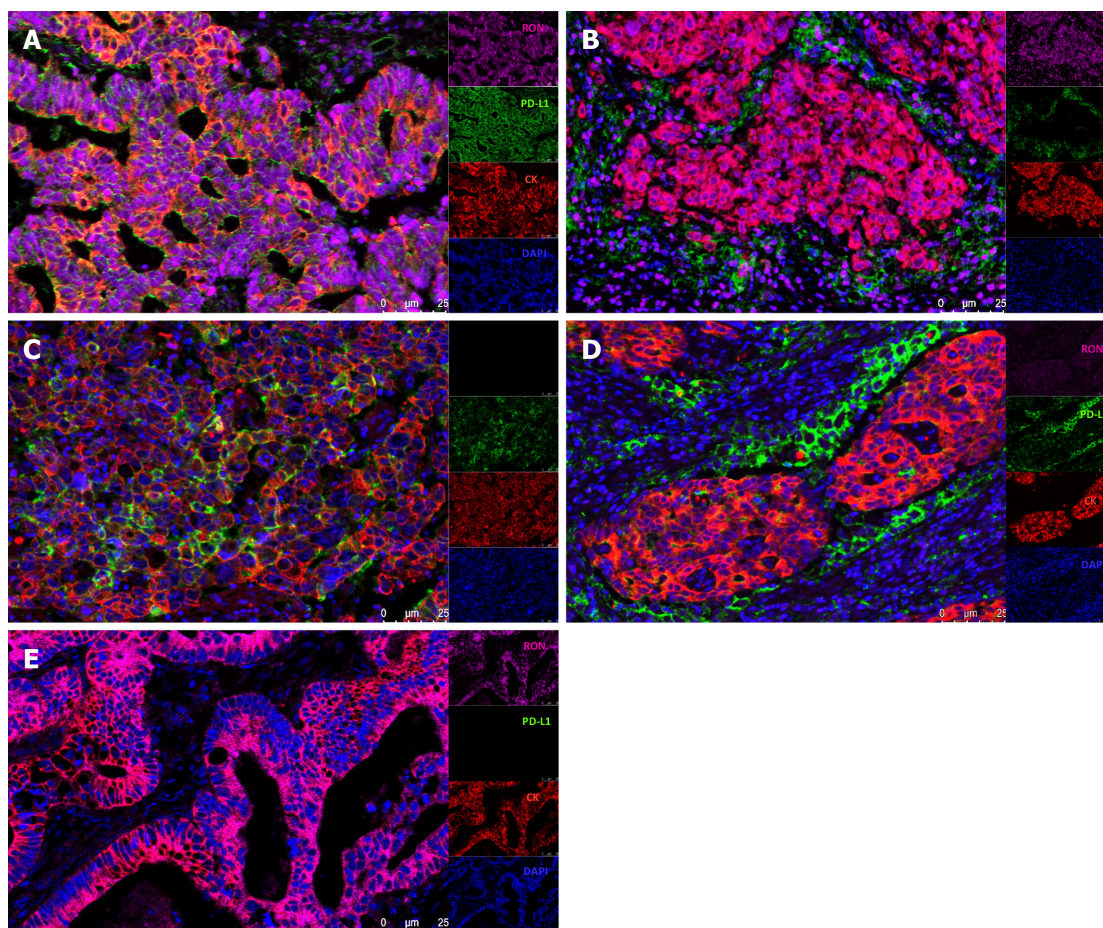


**Figure 1** X-tile analysis to determine the optimal cut-off values for RON and PD-L1 expression and survival analysis in the GEO dataset. The optimal cut-off values are highlighted by black circles (left panels) and shown in histograms for the entire cohort (middle panels). Kaplan-Meier survival plots are shown in right panels. A: The optimal cut-off value for RON was 7.50 ( $\chi^2 = 4.544$ ,  $P = 0.033$ ); B: The optimal cut-off value for PD-L1 was 4.30 ( $\chi^2 = 4.078$ ,  $P = 0.043$ ); C: Effect of different RON and PD-L1 expression states on patient survival. <sup>a</sup> $P < 0.05$ .

low. Additionally, there were cases where RON expression was enhanced on the TC membrane, but PD-L1 was not expressed in the tumor microenvironment (Figure 2E). In addition, RON and PD-L1 were often accompanied by a cytoplasmic expression of cancer cells. In general, when RON and PD-L1 were enhanced in the tumor cell membrane and cytoplasm, PD-L1 was also expressed in TIMCs. The results of multiplex immunofluorescence are consistent with the evaluation of RON and PD-L1 by immunohistochemical staining (Figure 3A-C).

#### Association of RON and PD-L1 expression with clinicopathological features in the FAHZUSM cohort

In the FAHZUSM cohort, CRC patients were divided into two groups based on high or low expression of RON and PD-L1 detected by IHC staining. In 381 CRC patients, high and low RON expression in TCs was observed in 121 (31.8%) and 260 (68.2%), respectively. High and low expression of PD-L1 in TCs and TIMCs was noted in 43 (11.3%) and 91 (23.9%) patients, respectively, and PD-L1 was lowly expressed in TIMCs in 247 (64.8%) cases. None of the patients had high PD-L1 expression in both TCs and TIMCs. Among all samples expressing RON and PD-L1 in TCs, the proportion with both high RON and high PD-L1 expression was 8.6% (25/290), while



**Figure 2 Four-color multiplex immunofluorescence staining of paraffin-embedded colorectal cancer tissues.** A: High expression of RON and PD-L1 in tumor cells (TCs); B: High expression of RON in TCs and high expression of PD-L1 in tumor-infiltrating mononuclear cells (TIMCs); C: Lack of RON expression and high PD-L1 expression in TCs; D: Low expression of RON in TC and high PD-L1 expression in TIMCs; E: High RON expression in TCs and no PD-L1 expression in either TCs or TIMCs. Blue (DAPI) shows nuclei, green shows PD-L1, pink indicates RON, and red displays CK.

the proportion of samples expressing high PD-L1 in TIMCs and high RON in TCs was 7.7% (26/338). Chi-square tests were used to determine the correlation between the expression of RON and PD-L1 in tumor tissues. Compared to samples with low expression of RON, samples with high RON expression levels were more likely to have high levels of PD-L1 in TCs, demonstrating a significant correlation between high RON expression and high PD-L1 expression in TCs ( $P < 0.001$ , Table 1). The expression of PD-L1 in TIMCs was not significantly correlated with RON expression in TCs (Table 1).

We compared the clinical characteristics of patient groups categorized based on the expression of RON and PD-L1. High expression of RON was associated with gender, T stage, N stage, disease stage, and treatment. High RON and high PD-L1 expression in TCs was related to T stage (Table 2). High expression of RON and PD-L1 (TIMCs) was associated with T stage, principal diagnosis, histological type, and treatment ( $P < 0.05$ ; Table 3).

### Prognostic significance of RON and PD-L1 expression in CRC

In the GEO cohort, univariate Cox regression analysis showed that age, T stage, M stage, disease stage, RON, and PD-L1 (TCs) expression were significantly correlated with a poor prognosis in CRC patients ( $P < 0.05$ ). Multivariate analysis after adjustment showed that only age, T stage, and M stage were independent prognostic factors for OS in CRC patients ( $P < 0.05$ ); disease stage, RON expression, and PD-L1 expression were not significant factors in the multivariate analysis ( $P > 0.05$ ; Table 4). Kaplan-Meier analysis showed that high expression of RON or PD-L1 (TCs), and both high RON and PD-L1 expression were all associated with a poor OS ( $P < 0.05$ ; Figure 1A-C). High expression of RON was associated with patient age and treatment type, and high expression of PD-L1 (TCs) was associated with the primary site of the tumor ( $P < 0.05$ ; Table 1).

**Table 2 Comparison of RON (tumor cells) and PD-L1 (tumor cells) expression and clinicopathological characteristics of patients with colorectal cancer in the FAHZUSM cohort, *n* (%)**

Characteristic	Cases	RON and PD-L1 (TCs) expression in the tumor microenvironment				<i>P</i> value
		RON low/PD-L1 low	RON high/PD-L1 low	RON low/PD-L1 high	RON high/PD-L1 high	
Number of cases	290	177	70	18	25	
Age (mean $\pm$ SD)	60.89 $\pm$ 12.215	60.37 $\pm$ 12.299	62.40 $\pm$ 12.518	58.39 $\pm$ 12.930	62.12 $\pm$ 10.179	0.495
Sex						
Man	161 (55.5)	108 (61)	35 (50.0)	9 (50.0)	9 (36.0)	0.061
Women	129 (44.5)	68 (39)	35 (50.0)	9 (50.0)	16 (64.0)	
Principal diagnosis				s		
Rectum	182 (62.8)	116 (65.5)	37 (52.9)	14 (77.8)	15 (60.0)	0.149
Colon	108 (37.2)	61 (34.5)	33 (47.1)	4 (22.2)	10 (40.0)	
Pathological grade						
Well/moderate	6 (2.1)	3 (1.7)	2 (2.9)	0 (0.0)	1 (4.0)	0.264
Poor	264 (9.1)	158 (89.3)	66 (94.3)	16 (88.9)	24 (96.0)	
Unknown	20 (6.9)	16 (9.0)	2 (2.9)	2 (11.1)	0 (0.0)	
T stage						
Tis-T2	84 (29)	64 (36.2)	9 (12.9)	5 (27.8)	6 (24.0)	<b>0.003</b>
T3	140 (48.3)	82 (46.3)	36 (51.4)	11 (61.1)	11 (44.0)	
T4	66 (22.8)	31 (17.5)	25 (35.7)	2 (11.1)	8 (32.0)	
N stage						
N0	238 (66.9)	125 (70.6)	39 (55.7)	12 (66.7)	13 (66.4)	0.072
N (1-2)	118 (33.1)	52 (29.4)	31 (44.3)	6 (33.3)	12 (33.6)	
M stage						
M0	283 (97.6)	173 (97.7)	68 (97.1)	18 (100)	24 (96.0)	0.735
M1	7 (2.4)	4 (2.3)	2 (2.9)	0 (0.0)	1 (4.0)	
Stage						
0-II	187 (64.5)	123 (69.5)	39 (55.7)	12 (66.7)	13 (52.0)	0.110
III-IV	103 (35.5)	54 (30.5)	31 (33.3)	6 (33.3)	12 (48.0)	
Histological type						
Adenocarcinoma	251 (86.6)	152 (85.9)	62 (88.6)	15 (83.3)	22 (88.0)	0.493
Mucinous/SRCC	32 (11)	21 (11.9)	7 (10.0)	1 (5.6)	3 (12.0)	
Other	7 (2.4)	4 (2.3)	1 (1.4)	2 (11.1)	0 (0.0)	
Treatment						
Yes	135 (46.6)	83 (46.9)	22 (31.4)	6 (33.3)	12 (48.0)	0.158
No	119 (41.0)	74 (41.8)	38 (54.3)	11 (61.1)	8 (32.0)	
Unknown	36 (12.4)	20 (11.3)	10 (14.3)	1 (5.6)	5 (20.0)	

Bold entries indicate statistical significance ( $P < 0.05$ ). RON: Recepteur d'origine nantais; PD-L1: Programmed death ligand 1; TCs: Tumor cells; FAHZUSM: The First Affiliated Hospital, Zhejiang University School of Medicine.



In the FAHZUSM cohort, Kaplan-Meier analysis showed that high expression of RON in TCs, high PD-L1 expression in TCs, or high PD-L1 expression in TIMCs in CRC tissue samples was correlated with a lower OS ( $P < 0.05$ ) (Figure 4A-C). Univariate Cox regression analysis showed that age, gender, TNM stage, disease stage, pathological grade, RON expression, and PD-L1 expression were associated with a poor OS in patients with CRC ( $P < 0.05$ ). Multivariate analysis after adjustment showed that age, gender, T stage, M stage, pathological grade, RON expression, and PD-L1 expression remained independent prognostic factors for OS in CRC patients ( $P < 0.05$ ), while N and disease stage were not significant ( $P > 0.05$ ; Table 4). We further analyzed the relationship between OS and RON and PD-L1 expression in the tumor microenvironment. High expression of both RON and PD-L1 in TCs predicted a significantly worse OS, and high RON expression in TCs and high PD-L1 expression in TIMCs were associated with a significantly worse prognosis ( $P < 0.001$ ; Figure 4D and E).

### Effects of regulating RON phosphorylation on PD-L1 expression

In order to study the relationship between RON and PD-L1 in CRC cells, HT29 cells (following serum starvation) were treated with MSP, BMS-777607, or MSP + BMS-777607 for 24 h. The effects of treatment on RON and PD-L1 expression were analyzed by cellular immunofluorescence. Activating RON phosphorylation promoted PD-L1 expression, while inhibiting RON phosphorylation down-regulated PD-L1 expression (Figure 5A). This result was confirmed by analysis of protein expression by Western blot ( $P < 0.05$ ; Figure 5B and C). In addition, we found that RON inhibition significantly reduced the phosphorylation of AKT and ERK1/2, which signal downstream of RON (Figure 6A-D).

## DISCUSSION

The application of PD-L1 immunotherapy in cancer treatment is becoming more and more important, but its therapeutic effect has been limited in CRC. This may be due in part to the prevalence of the mismatch repair (MMR) proficient or microsatellite stabilization (MSS) subtypes of CRC<sup>[36]</sup>. In addition, c-MET plays an important role in regulating PD-L1 expression<sup>[37,38]</sup>. Therefore, RON may promote the expression of PD-L1 in tumor tissue to affect the efficacy of PD-L1 immunosuppressants.

RON and PD-L1 play important roles in cancer initiation and development and are important targets for tumor therapy. However, few studies have explored the relationship between RON and PD-L1 expression in CRC and the impact that RON and PD-L1 expression patterns may have on pathological characteristics and disease outcomes. It was our hypothesis that activation of the RON receptor tyrosine kinase may promote the expression of PD-L1 in CRC tissue and impair the efficacy of PD-L1 immunotherapy. The purpose of our study was to analyze the expression and clinical significance of RON and PD-L1 in the tumor microenvironment in CRC samples, and to determine whether RON can regulate the expression of PD-L1 in CRC. We discovered that high expression of both RON and PD-L1 in the tumor microenvironment was associated with the poorest OS rate compared to CRC tumors with other RON and PD-L1 expression states. RON and PD-L1 were independent prognostic factors for OS in CRC patients. In addition, we showed that RON phosphorylation led to increased expression of PD-L1 in CRC cells, and that inhibiting RON phosphorylation can reduce PD-L1 expression.

We used publicly available data from the GEO database to investigate the relationship between RON and PD-L1 expression and clinical outcomes in CRC. We used X-tile to determine the optimal cut-off values for RON and PD-L1 levels in the GEO cohort. Kaplan-Meier survival analysis revealed a positive correlation of high RON or PD-L1 expression with worse OS, and high expression of RON and PD-L1 together was associated with the worst OS for CRC patients. However, RON and PD-L1 levels in the GEO dataset were determined by RNA sequencing using RNA extracted from tumor tissue to quantify the expression level in TCs, and it is difficult to determine the interactions between RON and PD-L1 that may arise within the tumor microenvironment from the GEO dataset. Therefore, we used the FAHZUSM cohort, a larger patient cohort with pathological tumor samples, to further study the expression of RON and PD-L1 in CRC tissues and to determine the pathological significance of elevated RON and PD-L1 expression in the tumor microenvironment.

Dysregulation of RON and PD-L1 signal transduction is a key feature of many tumors. Our results and previous studies demonstrated that high expression of RON

**Table 3 Comparison of RON (tumor cells) and PD-L1 (tumor-infiltrating mononuclear cells) expression and clinicopathological characteristics of patients with colorectal cancer in the FAHZUSM cohort, *n* (%)**

Characteristic	Cases	RON and PD-L1 (TIMCs) expression in the tumor microenvironment				<i>P</i> value
		RON low/PD-L1 low	RON high/PD-L1 low	RON low/PD-L1 high	RON high/PD-L1 high	
Number of cases	338	177	70	65	26	
Age (mean ± SD)	61.24 ± 12.555	60.37 ± 12.299	62.40 ± 12.518	61.03 ± 13.286	64.58 ± 12.436	0.348
Sex						
Man	197 (58.3)	108 (61)	35 (50.0)	40 (61.5)	14 (52.8)	0.368
Women	141 (41.7)	68 (39)	35 (50.0)	25 (38.5)	12 (46.2)	
Principal diagnosis						
Rectum	200 (59.2)	116 (65.5)	37 (52.9)	28 (43.1)	19 (73.1)	<b>0.004</b>
Colon	138 (40.8)	61 (34.5)	33 (47.1)	37 (56.9)	7 (26.9)	
Pathological grade						
Well/moderate	8 (2.4)	3 (1.7)	2 (2.9)	3 (4.6)	0 (0)	0.492
Poor	306 (90.5)	158 (89.3)	66 (94.3)	58 (89.2)	24 (92.3)	
Unknown	24 (7.1)	16 (9.0)	2 (2.9)	4 (6.2)	2 (7.7)	
T stage						
Tis-T2	96 (28.4)	64 (36.2)	9 (12.9)	16 (2.6)	7 (26.9)	<b>0.002</b>
T3	155 (45.9)	82 (46.3)	36 (51.4)	28 (43.1)	9 (34.6)	
T4	87 (25.7)	31 (17.5)	25 (35.7)	21 (32.3)	10 (38.5)	
N stage						
N0	226 (66.9)	125 (70.6)	39 (55.7)	47 (72.3)	15 (57.7)	0.075
N (1-2)	112 (33.1)	52 (29.4)	31 (44.3)	18 (27.7)	11 (42.3)	
M stage						
M0	326 (96.4)	173 (97.7)	68 (97.1)	61 (93.8)	24 (92.3)	0.235
M1	12 (3.6)	4 (2.3)	2 (2.9)	4 (2.3)	2 (7.7)	
Stage						
0-II	221 (65.4)	123 (69.5)	39 (55.7)	45 (69.2)	14 (53.8)	0.104
III-IV	117 (34.6)	54 (30.5)	31 (33.3)	20 (30.8)	12 (46.2)	
Histological type						
Adenocarcinoma	287 (84.9)	152 (85.9)	62 (88.6)	60 (92.3)	13 (50)	<b>&lt; 0.001</b>
Mucinous/SRCC	40 (11.8)	21 (11.9)	7 (10.0)	3 (4.6)	9 (34.6)	
Other	11 (3.3)	4 (2.3)	1 (1.4)	2 (3.1)	4 (15.4)	
Treatment						
Yes	298 (88.2)	83 (46.9)	22 (31.4)	30 (46.2)	24 (92.3)	<b>&lt; 0.001</b>
No	32 (9.5)	74 (41.8)	38 (54.3)	25 (38.5)	1 (3.8)	
Unknown	8 (2.4)	20 (11.3)	10 (14.3)	10 (15.4)	1 (3.8)	

Bold entries indicate statistical significance ( $P < 0.05$ ). RON: Recepteur d'origine nantais; PD-L1: Programmed death ligand 1; TCs: Tumor cells; TIMCs: Tumor-infiltrating mononuclear cells; FAHZUSM: The First Affiliated Hospital, Zhejiang University School of Medicine.

or PD-L1 in CRC tumor tissues correlated with the extent of primary tumor, lymph node metastasis, and distant metastasis<sup>[39,40]</sup>. Furthermore, high expression of RON or PD-L1 in the tumor microenvironment was associated with a poor survival in CRC patients<sup>[22,39-42]</sup>.

We demonstrated that high expression of both RON and PD-L1 in TCs was associated with a poor OS in CRC patients. Interestingly, the expression levels of RON were positively correlated with those of PD-L1 in TCs, which has not been previously reported. This may be related to the fact that RON can regulate both the production of and response to IFN- $\gamma$ <sup>[43]</sup>. In TCs, long-term continuous activation of IFN- $\gamma$  can mediate adaptive resistance to PD-L1 tumor immunosuppression; high expression of RON may attenuate resistance, restore the efficacy of PD-L1 targeted therapy, and may even have a promoting effect on the expression of PD-L1 by inhibiting the production of IFN- $\gamma$ <sup>[10,43-45]</sup>.

MEK/ERK and PI3K/AKT signaling pathways play a central role towards understanding the mechanisms underlying tumorigenesis and tumor development, prevention, and treatment. For example, autophagy caused by the activation of PI3K/AKT pathway plays a significant role in tumors<sup>[46,47]</sup>. In our study, we demonstrated that RON phosphorylation increased the expression of PD-L1 in CRC cells, proving that RON activation promotes the expression of PD-L1, likely acting through the downstream AKT and ERK1/2 signaling pathways. Previous studies have shown that there is crosstalk between RON phosphorylation and other receptors, which can affect the surface expression of other receptors<sup>[22]</sup>. Phosphorylation of RON activates downstream oncogenic signaling pathways, such as the RAS-ERK and PI3K-AKT pathways, thereby promoting tumor initiation, growth, invasion, and metastasis<sup>[20]</sup>. Treatment with BRAF inhibitors or MEK inhibitors, or down-regulation of ERK1/2 can lead to down-regulation of PD-L1 expression in TCs<sup>[48]</sup>. Thus, RON phosphorylation may promote the expression of PD-L1 in TCs through the RAS-ERK signaling pathway. In addition, PTEN interacts with RTK-dependent signals at multiple levels<sup>[48]</sup>, and has an antagonistic effect on PI3K, which plays an important role in mediating RTK-dependent cell signaling and tumor immune escape<sup>[10,48,49]</sup>. Therefore, RON phosphorylation may interact with PTEN to activate the PI3K-AKT signaling pathway, thereby promoting PD-L1 expression in TCs.

TIMCs are regarded as an indicator of host immune response to a tumor, and have long been considered an unfavorable prognostic marker in CRC<sup>[41,42]</sup>. Moreover, RON expression plays an important role in anti-tumor immune responses<sup>[27,50]</sup>. Previous studies also have shown that RON activation reduced the polarization of inflammatory M1 macrophages and induced the differentiation of immunosuppressive M2 macrophages. M2 macrophages promote PD-L1 expression through autocrine VEGF signaling<sup>[51]</sup>. In our study, we demonstrated that high expression of both RON and PD-L1 (TIMCs) was associated with a poor OS in patients with CRC. Thus, high expression of RON may impair the anti-tumor immune response by promoting the expression of PD-L1 in TIMCs, leading to tumor growth, invasion, and metastasis.

There were some limitations in this study. First, although we have analyzed a large patient cohort, this was a retrospective analysis and there is the potential for selection bias. Second, we did not evaluate which specific immune cell components in TIMCs expressed PD-L1. Third, although we have preliminarily studied that RON phosphorylation promotes the expression of PD-L1 in CRC cells, the mechanism by which RON promotes PD-L1 expression still needs to be further studied.

## CONCLUSION

In summary, high expression of RON and/or PD-L1 in CRC samples is associated with a poor prognosis in CRC patients. The expression status of RON and PD-L1 may be helpful as biomarkers to evaluate the prognosis of patients with CRC. In addition, RON phosphorylation can promote the expression of PD-L1 in CRC cells, possibly through activation of the AKT and ERK1/2 signaling pathways, which provides a new idea for the immunotherapy of CRC.

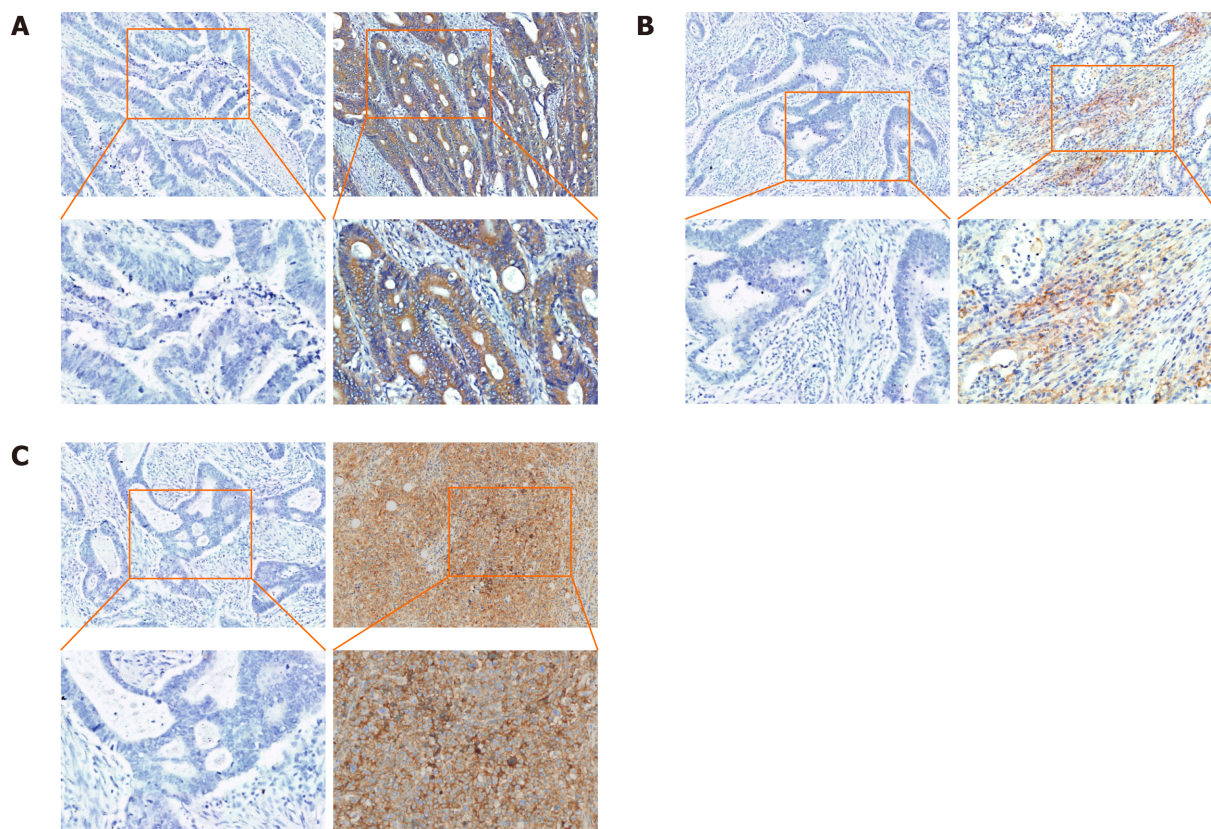
**Table 4 Univariate and multivariate Cox proportional hazard analyses of overall survival in patients with colorectal cancer in the FAHZUSM and Gene Expression Omnibus cohorts**

Variable	FAHZUSM cohort				GEO cohort			
	Univariate analysis, HR (95%CI)	P value	Multivariate analysis, HR (95%CI)	P value	Univariate analysis, HR (95%CI)	P value	Multivariate analysis, HR (95%CI)	P value
Age (mean $\pm$ SD)	1.029 (1.011-1.048)	<b>0.002</b>	1.031 (1.011-1.050)	<b>0.002</b>	1.025 (1.009-1.041)	<b>0.002</b>	1.028 (1.012-1.045)	<b>0.001</b>
Gender								
Male	1.000	<b>0.011</b>	1.000	<b>0.008</b>	1.000	0.293	1.000	0.076
Female	0.562 (0.362-0.874)		0.527 (0.328-0.847)		0.814 (0.555-1.194)		0.698 (0.469-1.039)	
Principal diagnosis								
Rectum	1.000	0.298	1.000	0.318	1.000	0.688	1.000	0.544
Colon	0.796 (0.518-1.224)		0.790 (0.497-1.255)		1.081 (0.738-1.585)		0.882 (0.589-1.322)	
Histological type								
Adenocarcinoma	1.000	0.408	1.000	0.387	NA			
Mucinous/SRCC	2.464 (0.343-17.710)		2.720 (0.263-28.122)					
Unknown	3.355 (0.433-25.986)		1.232 (0.129-11.795)					
T stage								
Tis-T2	1.000	<b>&lt; 0.001</b>	1.000	<b>0.003</b>	1.000	<b>0.001</b>	1.000	<b>0.007</b>
T3	0.211 (0.108-0.413)		0.298 (0.141-0.632)		0.333 (0.145-0.766)		0.381 (0.159-0.914)	
T4	0.503 (0.325-0.781)		0.596 (0.361-0.897)		0.455 (0.292-0.709)		0.476 (0.295-0.769)	
N stage								
N0	1.000	<b>&lt; 0.001</b>	1.000	0.111	1.000	0.062	1.000	0.141
N (1-2)	3.156 (2.083-4.783)		5.376 (0.678-42.660)		1.435 (0.982-2.097)		0.306 (0.063-1.479)	
M stage								
M0	1.000	<b>&lt; 0.001</b>	1.000	0.039	1.000	<b>&lt; 0.001</b>	1.000	<b>0.008</b>
M1	4.338 (2.094-8.985)		2.445 (1.048-5.701)		3.546 (2.013-6.247)		2.481 (1.269-4.852)	
Stage								
0-II	1.000	<b>&lt; 0.001</b>	1.000	0.406	1.000	<b>0.029</b>	1.000	0.099
III-IV	3.102 (2.044-4.708)		0.409 (0.050-3.366)		1.530 (1.045-2.242)		3.924 (0.774-19.888)	
Pathological grade								
Well/moderate	1.000	<b>&lt; 0.001</b>	1.000	<b>0.003</b>	NA			
Poor	7.689 (2.434-24.290)		4.044 (1.103-14.830)					
Unknown	1.266 (0.513-3.126)		0.375 (0.104-1.357)					
RON (protein)								
Low	1.000	<b>0.001</b>	1.000	<b>0.012</b>	1.000	<b>0.035</b>	1.000	0.466
High	2.060 (1.364-3.112)		1.788 (1.138-2.808)		1.515 (1.030-2.228)		1.170 (0.767-1.785)	
RON (mRNA)								
Low	NA				1.000	<b>0.035</b>	1.000	0.466
High					1.515 (1.030-2.228)		1.170 (0.767-1.785)	
PD-L1 (protein)								
Low	1.000	<b>&lt; 0.001</b>	1.000	<b>0.001</b>	NA			

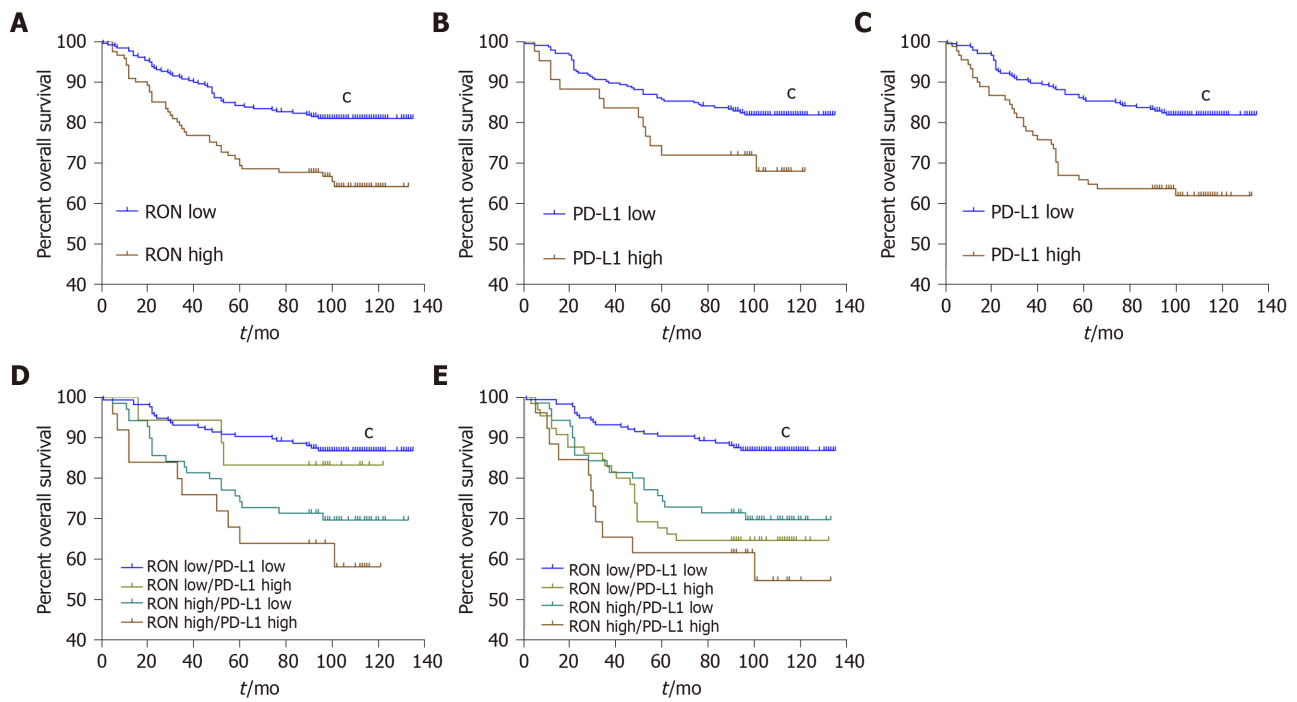


High (TIMCs)	0.544 (0.293-1.011)	0.676 (0.350-1.304)				
High (TCs)	1.325 (0.669-2.511)	1.654 (0.819-3.338)				
PD-L1 (mRNA)						
Low	NA		1.000	<b>0.047</b>	1.000	0.083
High			1.835 (1.007-3.345)		1.719 (0.931-3.173)	

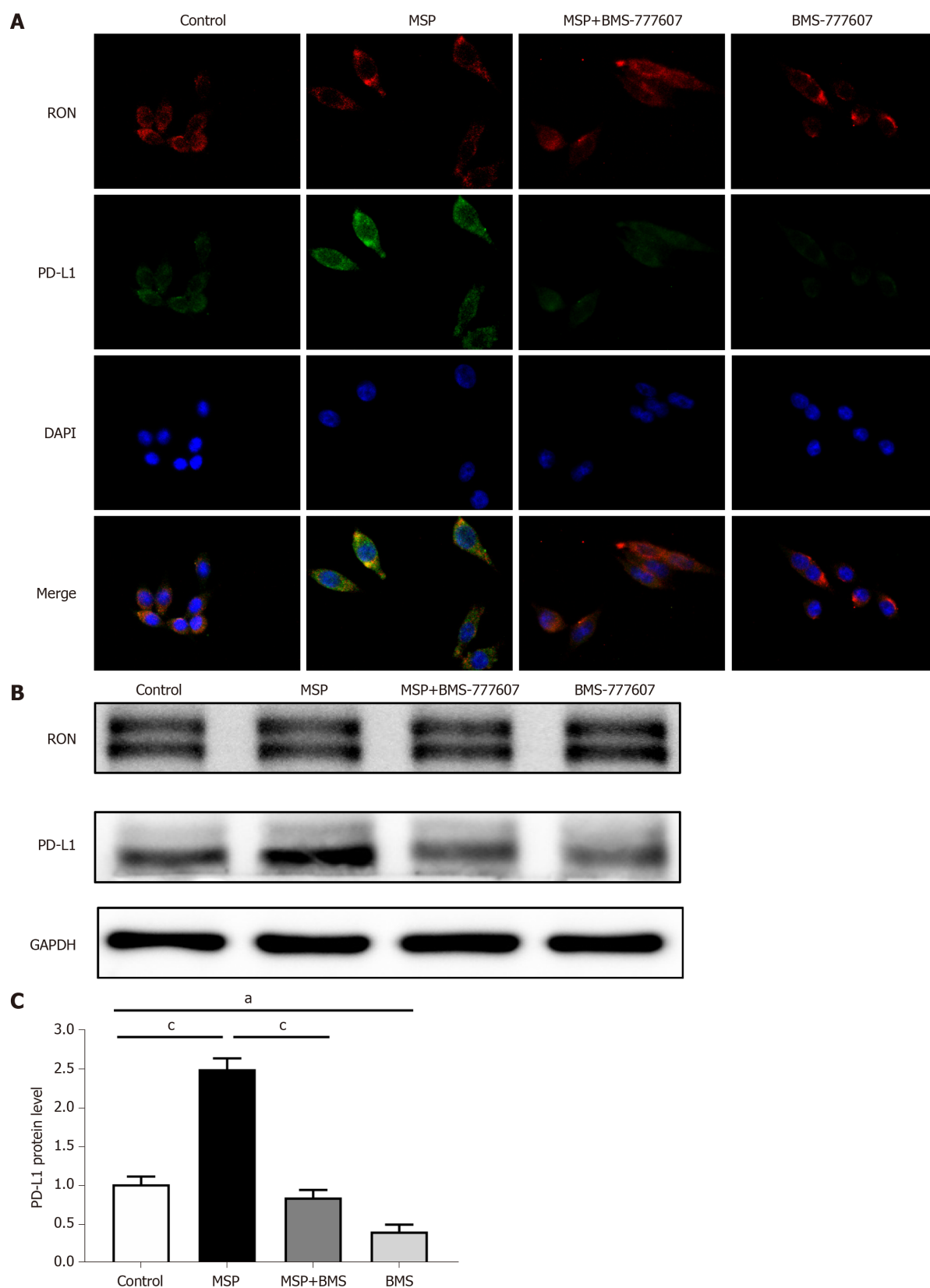
All variables are adjusted by the Cox proportional hazard model. Bold entries indicate statistical significance ( $P < 0.05$ ). GEO: The Gene Expression Omnibus; RON: Recepteur d'origine nantais; PD-L1: Programmed death ligand 1; TCs: Tumor cells; TIMCs: Tumor-infiltrating mononuclear cells; FAHZUSM: The First Affiliated Hospital, Zhejiang University School of Medicine.



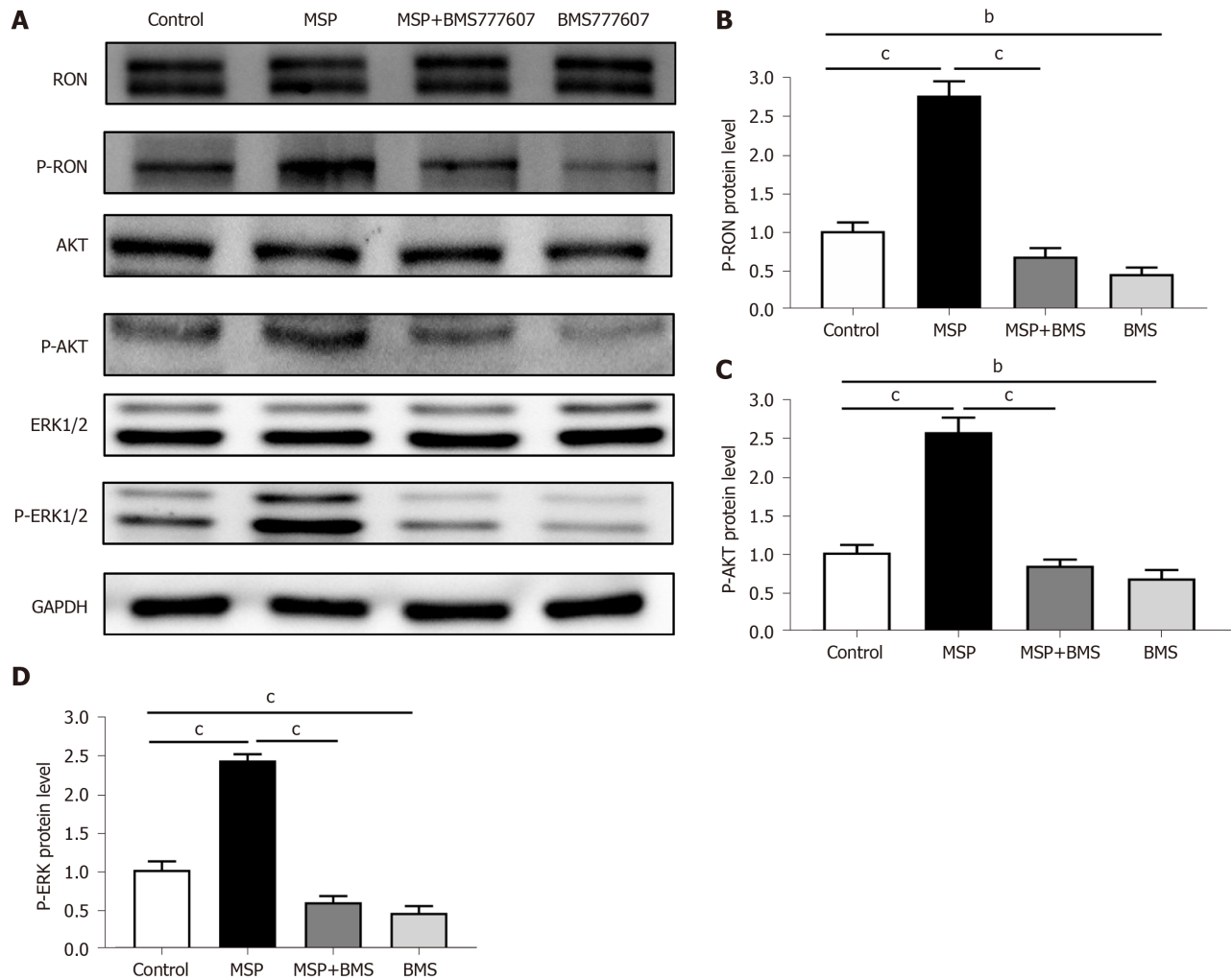
**Figure 3 Immunohistochemical expression of RON and PD-L1 in colorectal cancer tissues.** A: High (right) and negative (left) expression of RON in tumor cells (TCs); B: High (right) and negative (left) expression of PD-L1 in tumor-infiltrating mononuclear cells; C: High and negative expression of PD-L1 in TCs (original magnification,  $\times 100$  and  $\times 200$ ).



**Figure 4** Kaplan-Meier analysis of overall survival of patients with colorectal cancer stratified by RON and/or PD-L1 expression. A: Overall survival (OS) according to RON expression in tumor cells (TCs); B: OS according to PD-L1 expression in TCs; C: OS according to PD-L1 expression in tumor-infiltrating mononuclear cells (TIMCs); D: OS according to RON and PD-L1 expression in TCs; E: OS according to RON expression in TCs and PD-L1 expression in TIMCs. <sup>a</sup>*P* < 0.05, <sup>b</sup>*P* < 0.01, <sup>c</sup>*P* < 0.001.



**Figure 5** Expression of RON and PD-L1 in HT29 cells after treatment with 2 nmol/L MSP, 2 nmol/L MSP + 2  $\mu$ mol/L BMS-777607, or 2  $\mu$ mol/L BMS-777607. A: Cellular immunofluorescence indicating the expression of RON and PD-L1 after treatment of HT29 cells with 2 nmol/L MSP, 2 nmol/L MSP + 2  $\mu$ mol/L BMS-777607, or 2  $\mu$ mol/L BMS-777607 for 24 h, respectively. DAPI indicates nuclei (blue color), FITC indicates PD-L1 (green color), and PE indicates RON (red color). Original magnification  $\times 400$  (all photomicrographs). B-C: HT29 cells were treated with 2 nmol/L MSP, 2 nmol/L MSP + 2  $\mu$ mol/L BMS-777607, or 2  $\mu$ mol/L BMS-777607 for 24 h, and the expression of RON and PD-L1 was detected by Western blot and quantified according to the immunoblots. <sup>a</sup> $P < 0.05$ , <sup>b</sup> $P < 0.01$ , <sup>c</sup> $P < 0.001$ .



**Figure 6** Expression of RON and PD-L1, and activation of signaling pathways in HT29 cells. A: HT29 cells were treated with 2 nmol/L MSP, 2 nmol/L MSP + 2  $\mu$ mol/L BMS-777607, or 2  $\mu$ mol/L BMS-777607 for 1 h. The proteins analyzed include RON, phosphorylated RON, AKT, ERK1/2, phosphorylated AKT, and phosphorylated-ERK1/2. GAPDH was used as a loading control; B-D: The expression of p-RON, p-AKT, and p-ERK1/2 was detected by Western blot and quantified. <sup>a</sup>  $P < 0.05$ , <sup>b</sup>  $P < 0.01$ , <sup>c</sup>  $P < 0.001$ .

## ARTICLE HIGHLIGHTS

### Research background

Programmed death ligand 1 (PD-L1) protein expression on immune cells enables tumor cells to evade the immune system in a wide variety of malignancies. However, the efficacy of PD-L1 immunosuppressive agents in colorectal cancer (CRC) is poor. The receptor d'origine nantais (RON) receptor tyrosine kinase plays an important role in regulating tumor immunity.

### Research motivation

The poor anti-tumor effect of PD-1 inhibitors in CRC promoted the research on the mechanism of PD-1 expression, so as to improve the therapeutic effect of PD-1 inhibitors on CRC.

### Research objectives

The present study aimed to identify patterns of RON and PD-L1 expression and explore the clinical significance of these patterns in CRC.

### Research methods

The gene expression data from the Gene Expression Omnibus database (GEO;  $n = 290$ ) and patients at the First Affiliated Hospital, Zhejiang University School of Medicine (FAHZUSM;  $n = 381$ ) were analyzed to determine the prognostic value of RON and PD-L1 expression in the tumor microenvironment of CRC. HT29 cells were treated

with BMS-777607 to explore the relationship between RON activity and PD-L1 expression. Signaling pathways and protein expression perturbed by RON inhibition were evaluated by cellular immunofluorescence and Western blot.

### Research results

In the GEO patient cohort, the cut-off values for RON and PD-L1 expression were determined to be 7.70 and 4.30, respectively. Stratification of patients based on these cutoffs demonstrated that high expression of RON and PD-L1 was associated with a poor prognosis. In the FAHZUSM cohort, rates of high expression of RON in tumor cells, high PD-L1 expression in tumor cells and tumor infiltrating monocytes, and both high RON and high PD-L1 expression in the tumor microenvironment were 121 (32%), 43 (11%), 91 (24%), and 51 (13.4%), respectively. High expression of RON was significantly correlated with high expression of PD-L1 in the tumor cell compartment ( $P < 0.001$ ). High expression of RON and PD-L1 were independent prognostic factors for poorer overall survival. Concurrent high expression of both RON and PD-L1 in the tumor microenvironment was significantly associated with a poor prognosis. *In vitro*, BMS-777607 inhibited the phosphorylation of RON and PD-L1 expression, and attenuated the activation of the ERK1/2 and AKT signaling pathways in CRC cells.

### Research conclusions

RON, PD-L1, and their crosstalk are significant in predicting the prognostic value of CRC. Moreover, phosphorylation of RON upregulates PD-L1 expression, which provides a novel approach to immunotherapy in CRC.

### Research perspectives

The study of RON and PD-L1 expression will help improve the efficacy of PD-L1 immunosuppressive agents for CRC.

## REFERENCES

- 1 **Bray F**, Ferlay J, Soerjomataram I, Siegel RL, Torre LA, Jemal A. Global cancer statistics 2018: GLOBOCAN estimates of incidence and mortality worldwide for 36 cancers in 185 countries. *CA Cancer J Clin* 2018; **68**: 394-424 [PMID: 30207593 DOI: 10.3322/caac.21492]
- 2 **Arshad U**, Sutton PA, Ashford MB, Treacher KE, Liptrott NJ, Rannard SP, Goldring CE, Owen A. Critical considerations for targeting colorectal liver metastases with nanotechnology. *Wiley Interdiscip Rev Nanomed Nanobiotechnol* 2020; **12**: e1588 [PMID: 31566913 DOI: 10.1002/wnan.1588]
- 3 **Topalian SL**, Drake CG, Pardoll DM. Immune checkpoint blockade: a common denominator approach to cancer therapy. *Cancer Cell* 2015; **27**: 450-461 [PMID: 25858804 DOI: 10.1016/j.ccell.2015.03.001]
- 4 **Masugi Y**, Nishihara R, Yang J, Mima K, da Silva A, Shi Y, Inamura K, Cao Y, Song M, Nowak JA, Liao X, Nosho K, Chan AT, Giannakis M, Bass AJ, Hodi FS, Freeman GJ, Rodig S, Fuchs CS, Qian ZR, Ogino S. Tumour CD274 (PD-L1) expression and T cells in colorectal cancer. *Gut* 2017; **66**: 1463-1473 [PMID: 27196573 DOI: 10.1136/gutjnl-2016-311421]
- 5 **Hamanishi J**, Mandai M, Matsumura N, Abiko K, Baba T, Konishi I. PD-1/PD-L1 blockade in cancer treatment: perspectives and issues. *Int J Clin Oncol* 2016; **21**: 462-473 [PMID: 26899259 DOI: 10.1007/s10147-016-0959-z]
- 6 **Dong H**, Zhu G, Tamada K, Chen L. B7-H1, a third member of the B7 family, co-stimulates T-cell proliferation and interleukin-10 secretion. *Nat Med* 1999; **5**: 1365-1369 [PMID: 10581077 DOI: 10.1038/70932]
- 7 **Baeten JM**, Palanee-Phillips T, Brown ER, Schwartz K, Soto-Torres LE, Govender V, Mgodini NM, Matovu Kiweewa F, Nair G, Mhlana F, Siva S, Bekker LG, Jeenarain N, Gaffoor Z, Martinson F, Mkanani B, Pather A, Naidoo L, Husnik M, Richardson BA, Parikh UM, Mellors JW, Marzinke MA, Hendrix CW, van der Straten A, Ramjee G, Chirenje ZM, Nakabiito C, Taha TE, Jones J, Mayo A, Scheckter R, Berthiaume J, Livant E, Jacobson C, Ndase P, White R, Patterson K, Germuga D, Galaska B, Bunge K, Singh D, Szyldo DW, Montgomery ET, Mensch BS, Torjesen K, Grossman CI, Chakhtoura N, Nel A, Rosenberg Z, McGowan I, Hillier S; MTN-020-ASPIRE Study Team. Use of a Vaginal Ring Containing Dapivirine for HIV-1 Prevention in Women. *N Engl J Med* 2016; **375**: 2121-2132 [PMID: 26900902 DOI: 10.1056/NEJMoa1506110]
- 8 **Prall F**, Hühns M. The PD-1 expressing immune phenotype of T cell exhaustion is prominent in the 'immunoreactive' microenvironment of colorectal carcinoma. *Histopathology* 2017; **71**: 366-374 [PMID: 28383777 DOI: 10.1111/his.13231]
- 9 **Ji S**, Xu Y, Han D, Peng X, Lu X, Brockmeyer NH, Wu N. Changes in Lipid Indices in HIV+ Cases on HAART. *Biomed Res Int* 2019; **2019**: 2870647 [PMID: 30868068 DOI: 10.1155/2019/2870647]
- 10 **Kalbasi A**, Ribas A. Tumour-intrinsic resistance to immune checkpoint blockade. *Nat Rev Immunol* 2020; **20**: 25-39 [PMID: 31570880 DOI: 10.1038/s41577-019-0218-4]
- 11 **Feng D**, Qin B, Pal K, Sun L, Dutta S, Dong H, Liu X, Mukhopadhyay D, Huang S, Sinicrope FA. BRAF<sup>V600E</sup>-induced, tumor intrinsic PD-L1 can regulate chemotherapy-induced apoptosis in human colon cancer cells and in tumor xenografts. *Oncogene* 2019; **38**: 6752-6766 [PMID: 31406255 DOI: 10.1038/s41388-019-0919-y]



- 12 **Peng S**, Wang R, Zhang X, Ma Y, Zhong L, Li K, Nishiyama A, Arai S, Yano S, Wang W. EGFR-TKI resistance promotes immune escape in lung cancer *via* increased PD-L1 expression. *Mol Cancer* 2019; **18**: 165 [PMID: [31747941](#) DOI: [10.1186/s12943-019-1073-4](#)]
- 13 **Topalian SL**, Hodi FS, Brahmer JR, Gettinger SN, Smith DC, McDermott DF, Powderly JD, Carvajal RD, Sosman JA, Atkins MB, Leming PD, Spigel DR, Antonia SJ, Horn L, Drake CG, Pardoll DM, Chen L, Sharfman WH, Anders RA, Taube JM, McMiller TL, Xu H, Korman AJ, Jure-Kunkel M, Agrawal S, McDonald D, Kollia GD, Gupta A, Wigginton JM, Sznol M. Safety, activity, and immune correlates of anti-PD-1 antibody in cancer. *N Engl J Med* 2012; **366**: 2443-2454 [PMID: [22658127](#) DOI: [10.1056/NEJMoa1200690](#)]
- 14 **Brahmer JR**, Tykodi SS, Chow LQ, Hwu WJ, Topalian SL, Hwu P, Drake CG, Camacho LH, Kauh J, Odunsi K, Pitot HC, Hamid O, Bhatia S, Martins R, Eaton K, Chen S, Salay TM, Alaparthi S, Grosso JF, Korman AJ, Parker SM, Agrawal S, Goldberg SM, Pardoll DM, Gupta A, Wigginton JM. Safety and activity of anti-PD-L1 antibody in patients with advanced cancer. *N Engl J Med* 2012; **366**: 2455-2465 [PMID: [22658128](#) DOI: [10.1056/NEJMoa1200694](#)]
- 15 **Ng C**, Li H, Wu WKK, Wong SH, Yu J. Genomics and metagenomics of colorectal cancer. *J Gastrointest Oncol* 2019; **10**: 1164-1170 [PMID: [31949936](#) DOI: [10.21037/jgo.2019.06.04](#)]
- 16 **Arai H**, Battaglin F, Wang J, Lo JH, Soni S, Zhang W, Lenz HJ. Molecular insight of regorafenib treatment for colorectal cancer. *Cancer Treat Rev* 2019; **81**: 101912 [PMID: [31715423](#) DOI: [10.1016/j.ctrv.2019.101912](#)]
- 17 **Ledys F**, Klopfenstein Q, Truntzer C, Arnould L, Vincent J, Bengrine L, Remark R, Boidot R, Ladoire S, Ghiringhelli F, Derangere V. RAS status and neoadjuvant chemotherapy impact CD8+ cells and tumor HLA class I expression in liver metastatic colorectal cancer. *J Immunother Cancer* 2018; **6**: 123 [PMID: [30454021](#) DOI: [10.1186/s40425-018-0438-3](#)]
- 18 **Singh A**, Greninger P, Rhodes D, Koopman L, Violette S, Bardeesy N, Settleman J. A gene expression signature associated with "K-Ras addiction" reveals regulators of EMT and tumor cell survival. *Cancer Cell* 2009; **15**: 489-500 [PMID: [19477428](#) DOI: [10.1016/j.ccr.2009.03.022](#)]
- 19 **Ronsin C**, Muscatelli F, Mattei MG, Brethnach R. A novel putative receptor protein tyrosine kinase of the met family. *Oncogene* 1993; **8**: 1195-1202 [PMID: [8386824](#)]
- 20 **Yao HP**, Zhou YQ, Zhang R, Wang MH. MSP-RON signalling in cancer: pathogenesis and therapeutic potential. *Nat Rev Cancer* 2013; **13**: 466-481 [PMID: [23792360](#) DOI: [10.1038/nrc3545](#)]
- 21 **Graves-Deal R**, Bogatcheva G, Rehman S, Lu Y, Higginbotham JN, Singh B. Broad-spectrum receptor tyrosine kinase inhibitors overcome *de novo* and acquired modes of resistance to EGFR-targeted therapies in colorectal cancer. *Oncotarget* 2019; **10**: 1320-1333 [PMID: [30863492](#) DOI: [10.18632/oncotarget.26663](#)]
- 22 **Lee CT**, Chow NH, Su PF, Lin SC, Lin PC, Lee JC. The prognostic significance of RON and MET receptor coexpression in patients with colorectal cancer. *Dis Colon Rectum* 2008; **51**: 1268-1274 [PMID: [18536971](#) DOI: [10.1007/s10350-008-9297-1](#)]
- 23 **Schroeder GM**, An Y, Cai ZW, Chen XT, Clark C, Cornelius LA, Dai J, Gullo-Brown J, Gupta A, Henley B, Hunt JT, Jeyaseelan R, Kamath A, Kim K, Lippy J, Lombardo LJ, Manne V, Oppenheimer S, Sack JS, Schmidt RJ, Shen G, Stefanski K, Tokarski JS, Trainor GL, Wautlet BS, Wei D, Williams DK, Zhang Y, Zhang Y, Fargnoli J, Borzilleri RM. Discovery of N-(4-(2-amino-3-chloropyridin-4-yloxy)-3-fluorophenyl)-4-ethoxy-1-(4-fluorophenyl)-2-oxo-1,2-dihydropyridine-3-carboxamide (BMS-777607), a selective and orally efficacious inhibitor of the Met kinase superfamily. *J Med Chem* 2009; **52**: 1251-1254 [PMID: [19260711](#) DOI: [10.1021/jm801586s](#)]
- 24 **Wang J**, Rajput A, Kan JL, Rose R, Liu XQ, Kuropatwinski K, Hauser J, Beko A, Dominguez I, Sharratt EA, Brattain L, Levea C, Sun FL, Keane DM, Gibson NW, Brattain MG. Knockdown of Ron kinase inhibits mutant phosphatidylinositol 3-kinase and reduces metastasis in human colon carcinoma. *J Biol Chem* 2009; **284**: 10912-10922 [PMID: [19224914](#) DOI: [10.1074/jbc.M809551200](#)]
- 25 **Xu XM**, Wang D, Shen Q, Chen YQ, Wang MH. RNA-mediated gene silencing of the RON receptor tyrosine kinase alters oncogenic phenotypes of human colorectal carcinoma cells. *Oncogene* 2004; **23**: 8464-8474 [PMID: [15378025](#) DOI: [10.1038/sj.onc.1207907](#)]
- 26 **Yao HP**, Zhou YQ, Ma Q, Guin S, Padhye SS, Zhang RW, Wang MH. The monoclonal antibody Zt/f2 targeting RON receptor tyrosine kinase as potential therapeutics against tumor growth-mediated by colon cancer cells. *Mol Cancer* 2011; **10**: 82 [PMID: [21749705](#) DOI: [10.1186/1476-4598-10-82](#)]
- 27 **Eyob H**, Ekiz HA, Welm AL. RON promotes the metastatic spread of breast carcinomas by subverting antitumor immune responses. *Oncoimmunology* 2013; **2**: e25670 [PMID: [24327933](#) DOI: [10.4161/onci.25670](#)]
- 28 **Eyob H**, Ekiz HA, Derosé YS, Waltz SE, Williams MA, Welm AL. Inhibition of ron kinase blocks conversion of micrometastases to overt metastases by boosting antitumor immunity. *Cancer Discov* 2013; **3**: 751-760 [PMID: [23612011](#) DOI: [10.1158/2159-8290.CD-12-0480](#)]
- 29 **Danilkovitch A**, Donley S, Skeel A, Leonard EJ. Two independent signaling pathways mediate the antiapoptotic action of macrophage-stimulating protein on epithelial cells. *Mol Cell Biol* 2000; **20**: 2218-2227 [PMID: [10688668](#) DOI: [10.1128/mcb.20.6.2218-2227.2000](#)]
- 30 **Clough E**, Barrett T. The Gene Expression Omnibus Database. *Methods Mol Biol* 2016; **1418**: 93-110 [PMID: [27008011](#) DOI: [10.1007/978-1-4939-3578-9\\_5](#)]
- 31 **Feng L**, Yao HP, Wang W, Zhou YQ, Zhou J, Zhang R, Wang MH. Efficacy of anti-RON antibody Zt/g4-drug maytansinoid conjugation (Anti-RON ADC) as a novel therapeutics for targeted colorectal cancer therapy. *Clin Cancer Res* 2014; **20**: 6045-6058 [PMID: [25294907](#) DOI: [10.1158/1078-0432.CCR-14-0898](#)]
- 32 **Herbst RS**, Soria JC, Kowanetz M, Fine GD, Hamid O, Gordon MS, Sosman JA, McDermott DF, Powderly JD, Gettinger SN, Kohrt HE, Horn L, Lawrence DP, Rost S, Leabman M, Xiao Y, Mokatrik A, Koeppen H, Hegde PS, Mellman I, Chen DS, Hodi FS. Predictive correlates of response to the anti-PD-L1 antibody MPDL3280A in cancer patients. *Nature* 2014; **515**: 563-567 [PMID: [25428504](#) DOI: [10.1038/nature14011](#)]
- 33 **Fehrenbacher L**, Spira A, Ballinger M, Kowanetz M, Vansteenkiste J, Mazieres J, Park K, Smith D, Artal-Cortes A, Lewanski C, Braithe F, Waterkamp D, He P, Zou W, Chen DS, Yi J, Sandler A, Rittmeyer A;



- POPLAR Study Group. Atezolizumab versus docetaxel for patients with previously treated non-small-cell lung cancer (POPLAR): a multicentre, open-label, phase 2 randomised controlled trial. *Lancet* 2016; **387**: 1837-1846 [PMID: [26970723](#) DOI: [10.1016/S0140-6736\(16\)00587-0](#)]
- 34 **Rosenberg JE**, Hoffman-Censits J, Powles T, van der Heijden MS, Balar AV, Necchi A, Dawson N, O'Donnell PH, Balmanoukian A, Loriot Y, Srinivas S, Retz MM, Grivas P, Joseph RW, Galsky MD, Fleming MT, Petrylak DP, Perez-Gracia JL, Burris HA, Castellano D, Canil C, Bellmunt J, Bajorin D, Nickles D, Bourgon R, Frampton GM, Cui N, Mariathasan S, Abidoye O, Fine GD, Dreicer R. Atezolizumab in patients with locally advanced and metastatic urothelial carcinoma who have progressed following treatment with platinum-based chemotherapy: a single-arm, multicentre, phase 2 trial. *Lancet* 2016; **387**: 1909-1920 [PMID: [26952546](#) DOI: [10.1016/S0140-6736\(16\)00561-4](#)]
  - 35 **Camp RL**, Dolled-Filhart M, Rimm DL. X-tile: a new bio-informatics tool for biomarker assessment and outcome-based cut-point optimization. *Clin Cancer Res* 2004; **10**: 7252-7259 [PMID: [15534099](#) DOI: [10.1158/1078-0432.Ccr-04-0713](#)]
  - 36 **Gelsomino F**, Barbolini M, Spallanzani A, Pugliese G, Cascinu S. The evolving role of microsatellite instability in colorectal cancer: A review. *Cancer Treat Rev* 2016; **51**: 19-26 [PMID: [27838401](#) DOI: [10.1016/j.ctrv.2016.10.005](#)]
  - 37 **Chun HW**, Hong R. Significance of PD-L1 clones and C-MET expression in hepatocellular carcinoma. *Oncol Lett* 2019; **17**: 5487-5498 [PMID: [31186768](#) DOI: [10.3892/ol.2019.10222](#)]
  - 38 **Kammerer-Jacquet SF**, Medane S, Bensalah K, Bernhard JC, Yacoub M, Dupuis F, Ravaud A, Verhoest G, Mathieu R, Peyronnet B, Brunot A, Laguerre B, Lespagnol A, Mosser J, Dugay F, Belaud-Rotureau MA, Rioux-Leclercq N. Correlation of c-MET Expression with PD-L1 Expression in Metastatic Clear Cell Renal Cell Carcinoma Treated by Sunitinib First-Line Therapy. *Target Oncol* 2017; **12**: 487-494 [PMID: [28550387](#) DOI: [10.1007/s11523-017-0498-1](#)]
  - 39 **Park YL**, Lee GH, Kim KY, Myung E, Kim JS, Myung DS, Park KJ, Cho SB, Lee WS, Jung YD, Kim HS, Joo YE. Expression of RON in colorectal cancer and its relationships with tumor cell behavior and prognosis. *Tumori* 2012; **98**: 652-662 [PMID: [23235762](#) DOI: [10.1700/1190.13208](#)]
  - 40 **Koganemaru S**, Inoshita N, Miura Y, Miyama Y, Fukui Y, Ozaki Y, Tomizawa K, Hanaoka Y, Toda S, Suyama K, Tanabe Y, Moriyama J, Fujii T, Matoba S, Kuroyanagi H, Takano T. Prognostic value of programmed death-ligand 1 expression in patients with stage III colorectal cancer. *Cancer Sci* 2017; **108**: 853-858 [PMID: [28267224](#) DOI: [10.1111/cas.13229](#)]
  - 41 **Wang L**, Ren F, Wang Q, Baldrige LA, Monn MF, Fisher KW, Sheng W, Zhou X, Du X, Cheng L. Significance of Programmed Death Ligand 1 (PD-L1) Immunohistochemical Expression in Colorectal Cancer. *Mol Diagn Ther* 2016; **20**: 175-181 [PMID: [26891728](#) DOI: [10.1007/s40291-016-0188-1](#)]
  - 42 **Lee LH**, Cavalcanti MS, Segal NH, Hechtman JF, Weiser MR, Smith JJ, Garcia-Aguilar J, Sadot E, Ntiamoah P, Markowitz AJ, Shike M, Stadler ZK, Vakiani E, Klimstra DS, Shia J. Patterns and prognostic relevance of PD-1 and PD-L1 expression in colorectal carcinoma. *Mod Pathol* 2016; **29**: 1433-1442 [PMID: [27443512](#) DOI: [10.1038/modpathol.2016.139](#)]
  - 43 **Wilson CB**, Ray M, Lutz M, Sharda D, Xu J, Hankey PA. The RON receptor tyrosine kinase regulates IFN-gamma production and responses in innate immunity. *J Immunol* 2008; **181**: 2303-2310 [PMID: [18684919](#) DOI: [10.4049/jimmunol.181.4.2303](#)]
  - 44 **Wilson EB**, Yamada DH, Elsaesser H, Herskovitz J, Deng J, Cheng G, Aronow BJ, Karp CL, Brooks DG. Blockade of chronic type I interferon signaling to control persistent LCMV infection. *Science* 2013; **340**: 202-207 [PMID: [23580528](#) DOI: [10.1126/science.1235208](#)]
  - 45 **Teijaro JR**, Ng C, Lee AM, Sullivan BM, Sheehan KC, Welch M, Schreiber RD, de la Torre JC, Oldstone MB. Persistent LCMV infection is controlled by blockade of type I interferon signaling. *Science* 2013; **340**: 207-211 [PMID: [23580529](#) DOI: [10.1126/science.1235214](#)]
  - 46 **Kousta E**, Papavassiliou AG, Karamouzis MV. The role of autophagy in the treatment of BRAF mutant colorectal carcinomas differs based on microsatellite instability status. *PLoS One* 2018; **13**: e0207227 [PMID: [30427914](#) DOI: [10.1371/journal.pone.0207227](#)]
  - 47 **Kousta E**, Sarantis P, Kyriakopoulou G, Papavassiliou AG, Karamouzis MV. The Interplay of Autophagy and Tumor Microenvironment in Colorectal Cancer-Ways of Enhancing Immunotherapy Action. *Cancers (Basel)* 2019; **11**: 533 [PMID: [31013961](#) DOI: [10.3390/cancers11040533](#)]
  - 48 **Jiang X**, Zhou J, Giobbie-Hurder A, Wargo J, Hodi FS. The activation of MAPK in melanoma cells resistant to BRAF inhibition promotes PD-L1 expression that is reversible by MEK and PI3K inhibition. *Clin Cancer Res* 2013; **19**: 598-609 [PMID: [23095323](#) DOI: [10.1158/1078-0432.CCR-12-2731](#)]
  - 49 **Atefi M**, Avramis E, Lassen A, Wong DJ, Robert L, Foulad D, Cerniglia M, Titz B, Chodon T, Graeber TG, Comin-Anduix B, Ribas A. Effects of MAPK and PI3K pathways on PD-L1 expression in melanoma. *Clin Cancer Res* 2014; **20**: 3446-3457 [PMID: [24812408](#) DOI: [10.1158/1078-0432.CCR-13-2797](#)]
  - 50 **Babicky ML**, Harper MM, Chakedis J, Cazes A, Mose ES, Jaquish DV, French RP, Childers B, Alakus H, Schmid MC, Foubert P, Miyamoto J, Holman PJ, Walterscheid ZJ, Tang CM, Varki N, Sicklick JK, Messer K, Varner JA, Waltz SE, Lowy AM. MST1R kinase accelerates pancreatic cancer progression via effects on both epithelial cells and macrophages. *Oncogene* 2019; **38**: 5599-5611 [PMID: [30967626](#) DOI: [10.1038/s41388-019-0811-9](#)]
  - 51 **Lai YS**, Wahyuningtyas R, Aui SP, Chang KT. Autocrine VEGF signalling on M2 macrophages regulates PD-L1 expression for immunomodulation of T cells. *J Cell Mol Med* 2019; **23**: 1257-1267 [PMID: [30456891](#) DOI: [10.1111/jcmm.14027](#)]



Basic Study

## Decreased expression of the long non-coding RNA *HOXD-AS2* promotes gastric cancer progression by targeting *HOXD8* and activating *PI3K/Akt* signaling pathway

Lin Yao, Peng-Cheng Ye, Wang Tan, Ya-Jun Luo, Wan-Ping Xiang, Zi-Lin Liu, Zhi-Ming Fu, Fei Lu, Ling-Han Tang, Jiang-Wei Xiao

**ORCID number:** Lin Yao 0000-0002-1123-7789; Peng-Cheng Ye 0000-0003-3574-5128; Wang Tan 0000-0002-7780-8855; Ya-Jun Luo 0000-0002-8924-580X; Wan-Ping Xiang 0000-0003-1883-5180; Zi-Lin Liu 0000-0003-0113-9912; Zhi-Ming Fu 0000-0003-2468-899X; Fei Lu 0000-0002-1566-8746; Ling-Han Tang 0000-0001-8531-0304; Jiang-Wei Xiao 0000-0002-4288-7581.

**Author contributions:** Yao L and Xiao JW conceived and designed the experiments; Yao L and Ye PC did most of the experiments and data analysis; Yao L wrote the manuscript; Ye PC, Fu ZM, Lu F, and Tang LH collected the clinical samples; Tan W, Yao L, and Xiang WP performed data analysis; Xiao JW revised the manuscript; and all authors read and approved the final manuscript.

**Supported by** National Natural Science Foundation of China, No. 30700773, No. 81070378, and No. 81270561; and Sichuan Outstanding Youth Fund Project, No. 2015JQ0060.

**Institutional review board**

**statement:** All the gastric cancer tissue samples were collected with written informed consent in

**Lin Yao,** Department of Gastrointestinal Surgery, Clinical Medical College and The First Affiliated Hospital of Chengdu Medical College, Chengdu 610000, Sichuan Province, China, The Hepatobiliary Research Institute, North Sichuan Medical College, Nanchong 637000, Sichuan Province, China

**Lin Yao, Peng-Cheng Ye, Zhi-Ming Fu, Fei Lu, Ling-Han Tang,** Department of Gastrointestinal Surgery, The Affiliated Hospital of North Sichuan Medical College, The Hepatobiliary Research Institute, North Sichuan Medical College, Nanchong 637000, Sichuan Province, China

**Wang Tan,** Department of Gastrointestinal Surgery, Yaan People's Hospital, Yaan 625000, Sichuan Province, China

**Ya-Jun Luo,** Department of Gastrointestinal Surgery, The First Affiliated Hospital of Chongqing Medical University, Chongqing 400010, China

**Wan-Ping Xiang,** Department of Thoracic Surgery, Nanchong Central Hospital, Nanchong 637000, Sichuan Province, China

**Zi-Lin Liu, Jiang-Wei Xiao,** Department of Gastrointestinal Surgery, Clinical Medical College and The First Affiliated Hospital of Chengdu Medical College, Chengdu 610000, Sichuan Province, China

**Corresponding author:** Jiang-Wei Xiao, MD, PhD, Postdoc, Professor, Surgeon, Surgical Oncologist, Teacher, Department of Gastrointestinal Surgery, Clinical Medical College and The First Affiliated Hospital of Chengdu Medical College, No. 278 Baoguang Road, Xindu District, Chengdu 610000, Sichuan Province, China. [xiaojiangwei2018@163.com](mailto:xiaojiangwei2018@163.com)

### Abstract

#### BACKGROUND

Long non-coding RNAs (lncRNAs) have been shown to be associated with many tumors. However, the specific mechanism of lncRNAs in the occurrence and development of gastric cancer (GC) has not been fully elucidated.

#### AIM

accordance with the Declaration of Helsinki and with the approval of The Ethical Committee of The Affiliated Hospital of North Sichuan Medical College.

**Conflict-of-interest statement:** The authors declare that they have no competing interests to disclose.

**Data sharing statement:** No additional data are available.

**Open-Access:** This article is an open-access article that was selected by an in-house editor and fully peer-reviewed by external reviewers. It is distributed in accordance with the Creative Commons Attribution NonCommercial (CC BY-NC 4.0) license, which permits others to distribute, remix, adapt, build upon this work non-commercially, and license their derivative works on different terms, provided the original work is properly cited and the use is non-commercial. See: <http://creativecommons.org/License/by-nc/4.0/>

**Manuscript source:** Unsolicited manuscript

**Specialty type:** Oncology

**Country/Territory of origin:** China

**Peer-review report's scientific quality classification**

Grade A (Excellent): 0  
Grade B (Very good): 0  
Grade C (Good): C, C, C  
Grade D (Fair): 0  
Grade E (Poor): 0

**Received:** July 24, 2020

**Peer-review started:** July 24, 2020

**First decision:** September 17, 2020

**Revised:** September 27, 2020

**Accepted:** October 21, 2020

**Article in press:** October 21, 2020

**Published online:** November 15, 2020

**P-Reviewer:** Matsuo Y, Nakajima N

**S-Editor:** Huang P

**L-Editor:** Wang TQ

**P-Editor:** Li JH



To explore the expression level and molecular mechanism of *HOXD-AS2* in GC tissues and cells, and analyze its significance in the prognosis of GC.

## METHODS

Real-time quantitative PCR was used to detect the expression of *HOXD-AS2* in 79 pairs of GC tissues and five cell lines. The pc*HOXD-AS2* plasmid vector was constructed and transfected into SGC-7901 and SNU-1 GC cells. Matrigel Transwell and wound healing assays were used to confirm the effect of *HOXD-AS2* on invasion and migration of GC cells. Cell counting kit-8 assay and flow cytometry were used to verify the effect of *HOXD-AS2* on the proliferation, cell cycle, and apoptosis of GC cells. The relevant regulatory mechanism between *HOXD-AS2* and *HOXD8* and PI3K/Akt signaling pathway was verified by Western blot analysis.

## RESULTS

The low expression of lncRNA *HOXD-AS2* was associated with lymph node metastasis and tumor-node-metastasis stage in GC. *In vitro* functional experiments demonstrated that overexpression of *HOXD-AS2* inhibited GC cell progression. Mechanistic studies revealed that *HOXD-AS2* regulated the expression of its nearby gene *HOXD8* and inhibited the activity of the PI3K/Akt signaling pathway.

## CONCLUSION

These results indicate that downregulation of *HOXD-AS2* significantly promotes the progression of GC cells by regulating *HOXD8* expression and activating the PI3K/Akt signaling pathway. *HOXD-AS2* may be a novel diagnostic biomarker and effective therapeutic target for GC.

**Key Words:** Long non-coding RNA; Gastric cancer; *HOXD-AS2*; *HOXD8*; PI3K/Akt; Progression

©The Author(s) 2020. Published by Baishideng Publishing Group Inc. All rights reserved.

**Core Tip:** In this study we found that the expression of long non-coding RNA *HOXD-AS2* was down-regulated in gastric cancer (GC) tissues and cells. The low expression of *HOXD-AS2* was associated with lymph node metastasis and tumor-node-metastasis stage in GC. Overexpression of *HOXD-AS2* inhibited the progression of GC cells. Decreased expression of *HOXD-AS2* promotes GC cell progression by targeting *HOXD8* and activating the PI3K/Akt signaling pathway. *HOXD-AS2* may be a novel diagnostic biomarker and effective therapeutic target for GC.

**Citation:** Yao L, Ye PC, Tan W, Luo YJ, Xiang WP, Liu ZL, Fu ZM, Lu F, Tang LH, Xiao JW. Decreased expression of the long non-coding RNA *HOXD-AS2* promotes gastric cancer progression by targeting *HOXD8* and activating PI3K/Akt signaling pathway. *World J Gastrointest Oncol* 2020; 12(11): 1237-1254

**URL:** <https://www.wjgnet.com/1948-5204/full/v12/i11/1237.htm>

**DOI:** <https://dx.doi.org/10.4251/wjgo.v12.i11.1237>

## INTRODUCTION

According to the latest statistics, in 2018 there were more than 1000000 new cases of gastric cancer (GC) and an estimated 783000 deaths from GC worldwide. The incidence rate of GC is fifth among all malignant tumors, and the mortality rate ranks third. GC seriously affects human health<sup>[1]</sup>. China is one of the countries with a high incidence of GC, and with new cases of GC in China accounting for more than 40% of the world's GC cases, GC has become the second leading cause of cancer death in China<sup>[2]</sup>. Because most patients with GC are asymptomatic at the early stage<sup>[3]</sup>, many are in advanced stage at the time of initial diagnosis, and the prognosis is often poor<sup>[4]</sup>. At present, the therapeutic effects on GC are still not satisfactory. Therefore, further

understanding of the molecular mechanisms of gastric carcinogenesis, development, invasion, and migration and searching for new targeted drugs and methods are of great significance for the treatment of GC and improvement of the patient survival rate.

Long non-coding RNAs (lncRNAs) are a class of non-coding RNAs that are more than 200 nucleotides in length and lack an open reading frame<sup>[5]</sup>. lncRNAs have been shown to regulate RNA transcription and mRNA splicing, and play an important role in regulating the stability of RNA in the cytoplasm and the activity of microRNAs<sup>[6,7]</sup>. An increasing number of studies have shown that abnormally expressed lncRNAs are involved in the process of tumor genesis and development and have a close relationship with tumor cell proliferation, apoptosis, invasion, and metastasis and poor prognosis<sup>[8-12]</sup>. In recent years, many studies have also found that abnormally expressed lncRNAs are involved in the occurrence and development of GC. For instance, lncRNA *SLC7A11-AS1* is expressed at low levels in GC and significantly associated with tumor macroscopic type, distant migration, and tumor-node-metastasis (TNM) stage. *SLC7A11-AS1* can be used as a biomarker for the diagnosis and prognosis of GC, and provides a potential target for GC treatment<sup>[13]</sup>. lncRNA *LINC01606* is highly expressed in GC. *LINC01606* can act as an endogenous competitive RNA (ceRNA) to adsorb miR-423-5p, attenuating the inhibitory effect of miR-423-5p on the *Wnt3a* gene, thereby activating the Wnt/ $\beta$ -catenin signaling pathway and promoting the invasion and migration of GC cells<sup>[14]</sup>. lncRNA *LINC01133* is downregulated in GC tissues and cells. Low expression of *LINC01133* is significantly associated with tumor size, depth of invasion, lymph node metastasis, and TNM stage and predicts poor prognosis. *LINC01133* can act as a ceRNA to adsorb miR-106a-3p and thereby regulate the expression of the *APC* gene and affect the Wnt/ $\beta$ -catenin signaling pathway. The results suggest that *LINC01133* can be used as a potential biomarker for poor prognosis of GC<sup>[15]</sup>. Although a major breakthrough has been achieved in the study of lncRNAs in the pathogenesis of GC, the specific mechanism of lncRNAs in the occurrence and development of GC has not been fully elucidated.

We screened for abnormally expressed lncRNA *HOXD-AS2* in GC by gene chip analysis. *HOXD-AS2*, which is located at 2q31.1 and is encoded by three exons, was mapped to chromosome 2 region 176134841-176137098. In the present study, we used quantitative polymerase chain reaction (qPCR) to detect the expression of *HOXD-AS2* in 79 pairs of GC tissues and 5 GC cell lines. Based on the clinical and pathological features of GC patients, we found that *HOXD-AS2* may be involved in the progression of GC. Then, a *HOXD-AS2* plasmid was constructed and transfected into SGC-7901 and SNU-1 cells. After transfection, the effect of *HOXD-AS2* on the progression of GC cells was analyzed. Furthermore, we illustrated a potential mechanism by which *HOXD-AS2* may modulate the expression of *HOXD8* and activate the PI3K/Akt signaling pathway in SGC-7901 and SNU-1 GC cells. The objective of our study was to explore the role of *HOXD-AS2* in the development and progression of GC and to elucidate its possible regulatory mechanisms.

## MATERIALS AND METHODS

### *Patients and tumor tissues*

A total of 79 human GC tissues and matched adjacent non-cancerous tissues (ANTs) (at a distance of 5 cm from the tumor margin) were obtained at the time of surgery from April 2015 to May 2017 at The Affiliated Hospital of North Sichuan Medical College (Sichuan, China). None of the patients received radiotherapy, chemotherapy, or other anti-tumor treatments before surgery. Following excision, the GC and non-cancerous tissues were immediately frozen in liquid nitrogen and preserved at -80 °C until use. The clinicopathological parameters of patients with GC were collected. All patients provided written informed consent, and the entire study protocol was approved by The Ethics Committee of the Affiliated Hospital of North Sichuan Medical College, Nanchong, China.

### *Cell culture and cell transfection*

Five human GC cell lines, AGS, MGC-803, BGC-823, SNU-1, and SGC-7901, and the normal gastric mucosal cell line GES-1 were purchased from Shanghai Cell Bank (Shanghai, China). The results of short tandem repeat (STR) analysis showed that there was no tri-allelic phenomenon in any locus, and no cross-contamination of other human cells was found. STR analysis found a 100% match to the reference data in the



ATCC cell bank. Cells were cultured in DMEM or RPMI-1640 (Gibco BRL, Gaithersburg, MD, United States) supplemented with 10% fetal bovine serum (FBS; Gibco BRL, Gaithersburg, MD, United States) and antibiotics (100 IU/mL penicillin and 100 µg/mL streptomycin) at 37 °C in a humidified atmosphere with 5% CO<sub>2</sub>.

The pc-*HOXD-AS2* plasmid vector was purchased from Beijing Syngentech (Beijing, China). The plasmid was transfected into SGC-7901 and SNU-1 cells using Lipofectamine 3000 (Invitrogen, United States). After 48 h, the efficiency of each transfection group was compared with regard to the expression of *HOXD-AS2*.

The PI3K inhibitor LY294002 was purchased from MedChemExpress (United States). LY294002 was dissolved in DMSO (100 mmol/L) and stored at -20 °C for 1 wk. Before use, LY294002 was quickly diluted into culture medium at a final concentration of 10 µmol/L.

### Reverse transcription quantitative PCR

Total RNA was extracted from GC tissues, ANTs, and GC cell lines using TRIzol reagent (Invitrogen, Carlsbad, CA, United States), and reverse transcription reactions were performed using the GoScript Reverse Transcription System (Promega, Madison, United States) according to the manufacturer's instructions. Real-time PCR was performed according to the instructions using standard Roche fluorescence quantitative PCR reagents (Roche, United States) and Roche fluorescent PCR instruments. *β-actin* or *GAPDH* was used as an internal reference. Each sample was detected three times. After the end of PCR, the dissolution profile of each specimen was stringently checked to ensure that there was only a single amplification product. *HOXD-AS2*, *HOXD8*, *GAPDH*, *β-actin*, *PI3K*, *Akt*, *MAM2*, and *p53* primers were purchased from Shanghai Biotech (Shanghai, China). The primer sequences are shown in [Supplementary Table 1](#). Analysis of the relative quantification of gene expression was performed using the classical 2<sup>-ΔΔC<sub>t</sub></sup> method.

### Transwell migration and invasion assays

The invasive ability of GC cells (SGC-7901 and SNU-1) was detected by Matrigel Transwell assay. A 24-well Transwell plate was used with membranes separated by 8 µm pores (Costar, Cambridge, MA, United States), and 50 mg/L Matrigel (BD Pharmingen, San Jose, CA, United States) was added to the upper chamber. Then, the 24-well plate was incubated at 37 °C in a humidified incubator containing 5% CO<sub>2</sub> for 2 h. SGC-7901 and SNU-1 cells transfected for 48 h were inoculated into the upper chamber at 5 × 10<sup>5</sup> cells per well, and complete medium containing 10% FBS was added to the lower chamber. After 48 h of incubation, the cells that did not invade the Matrigel were wiped off with a cotton swab, and the invaded cells attached to the lower surface of the membrane were fixed with 4% paraformaldehyde (Sigma Aldrich, St. Louis, MO, United States), and stained with 1% crystal violet (Beyotime, Shanghai, China). The migration assay was similar to the invasion assay except that Matrigel was not added. Finally, three fields of view were randomly selected under a microscope for invasive and migratory cell counting. Three replicate wells were set in all experiments.

### Wound healing assay

Cell migration ability was measured using a scratch wound healing assay. A straight line was marked with a marker in the middle on the back of a 3.5 cm dish. The SGC-7901 and SNU-1 GC cells transfected 24 h after each group were inoculated into a culture dish. After 24 h, a scratch was made on the bottom of the culture dish with a 200 µL tip, and the cell fragments were washed with sterile phosphate buffered saline (PBS). After incubation at 37 °C and 5% CO<sub>2</sub> for 48 h, the distance between the two edges of the scratch was observed under a microscope.

### Cell proliferation assays

Cell counting kit-8 assay (CCK-8, Beyotime Institute of Biotechnology, Shanghai, China) was used to detect the cell viability. Cells were seeded at 5000 cells per well in a 96-well plate. After the cells were transfected with plasmids for 24 h, 10 µL of CCK-8 was added to each well at 0 h, 24 h, 48 h, and 72 h. The absorbance at 450 nm of each well was measured with a spectrophotometer. All experiments were performed in triplicate.

### Flow cytometry assay

Cell apoptosis was analyzed with Annexin V-APC/7-AAD Apoptosis Detection kit (KeyGEN BioTECH, China) and a NovoCyte flow cytometer (ACEA, China). Forty-eight hours after cell transfection, the cells were digested with trypsin without EDTA

and washed twice with cold PBS. Then the digested cells were put into the flow sampling tube, and 500  $\mu$ L of Binding Buffer was added to the tube according to the ratio of 100:1, followed by the addition of 5  $\mu$ L Annexin V-APC and 5  $\mu$ L 7-AAD staining solution. After 15 min of reaction at room temperature and protection from light, samples were taken on the machine for apoptosis analysis. Each experiment was repeated three times.

For cell cycle detection, the cells were collected into a brown EP tube. Add pre-cooled 70% alcohol was added, the tube was shaken gently, and put in a refrigerator at 4 °C for 4 h. After the cell membrane was broken, 0.5 mL of propidium iodide staining solution was added to the tube for staining at room temperature in the dark for 30 min, and then the sample was subject to cell cycle analysis. This experiment was performed in triplicate.

### Western blot analysis

Total protein was extracted, and the concentration was determined using a BCA protein assay kit (Thermo Fisher Scientific, Waltham, MA, United States). Sample lysates (10  $\mu$ g of protein) were separated by SDS-PAGE and transferred to a PVDF membrane. The membrane was incubated with specific antibodies against *HOXD8* (1:1000), *PI3K* (1:1000), *Akt* (1:2000), *MDM2* (1:500), or *p53* (1:1000) (Abcam, Cambridge, MA, United States) at 4 °C overnight, followed by incubation with secondary antibody. Protein levels were normalized to those of total GAPDH, which were detected using a monoclonal anti-GAPDH antibody (1:10000; Sigma-Aldrich Corporation, St. Louis, MO, United States). Autoradiograms were quantified by densitometry (Quantity One software; Bio-Rad).

### Statistical analysis

All experimental data were analyzed using SPSS20.0 (SPSS, Chicago, IL, United States) and GraphPad Prism 7.0 (GraphPad Software, La Jolla, CA, United States), and the measurement data are expressed as the mean  $\pm$  SD. Two-tailed Student's *t*-test was used to compare two groups of measurement data. The relationship between lncRNA expression levels and clinical indicators of patients was calculated by Chi-square test or Fisher's exact probability test (two-sided). Survival analysis for patients with GC was performed by the Kaplan-Meier method, and the differences between survival curves were estimated by the log-rank test. Spearman correlation analyses were performed to investigate correlations between gene expression levels. All tests were two-tailed, and *P* < 0.05 was considered statistically significant.

## RESULTS

### Decreased expression of lncRNA *HOXD-AS2* is associated with a poor prognosis in patients with GC

As shown in Figure 1A, the relative expression level of lncRNA *HOXD-AS2* in 79 GC tissues was significantly decreased in comparison with that in the corresponding adjacent tissues (*P* = 0.030). As shown in Figure 1B, decreased expression of *HOXD-AS2* was observed in 49 (62.03%) out of 79 cases, while high expression was observed in the 30 remaining cases (37.97%). The relationship between the expression level of *HOXD-AS2* and the clinicopathological features of GC patients was analyzed. As shown in Table 1, low expression of *HOXD-AS2* was associated with lymph node metastasis (*P* = 0.009) and TNM stage (*P* = 0.040). Data from the Kaplan-Meier Plotter database (<http://kmplot.com/>) was used to analyze the relationship between *HOXD-AS2* expression and the overall survival rate of 348 patients with GC (109 patients with low *HOXD-AS2* expression and 239 with high *HOXD-AS2* expression). The prognosis of the *HOXD-AS2* low expression group was worse than that of the *HOXD-AS2* high expression group, and the difference was statistically significant (*P* = 0.012, Figure 1C).

### lncRNA *HOXD-AS2* is downregulated in GC cells

As shown in Figure 2A, the relative expression level of lncRNA *HOXD-AS2* in the five GC cell lines SGC-7901, MGC-803, BGC-823, SNU-1, and AGS was lower than that in the normal gastric mucosal cell line GES-1 (*P* = 0.005, = 0.006, < 0.001, = 0.004, and < 0.001, respectively). The expression of *HOXD-AS2* was the lowest in SGC-7901 and SNU-1 cells, so we selected these two cell lines for subsequent experimental studies. As shown in Figure 2B, after transfection of SGC-7901 and SNU-1 cells, the expression of *HOXD-AS2* in the pc*HOXD-AS2* group was significantly increased compared with

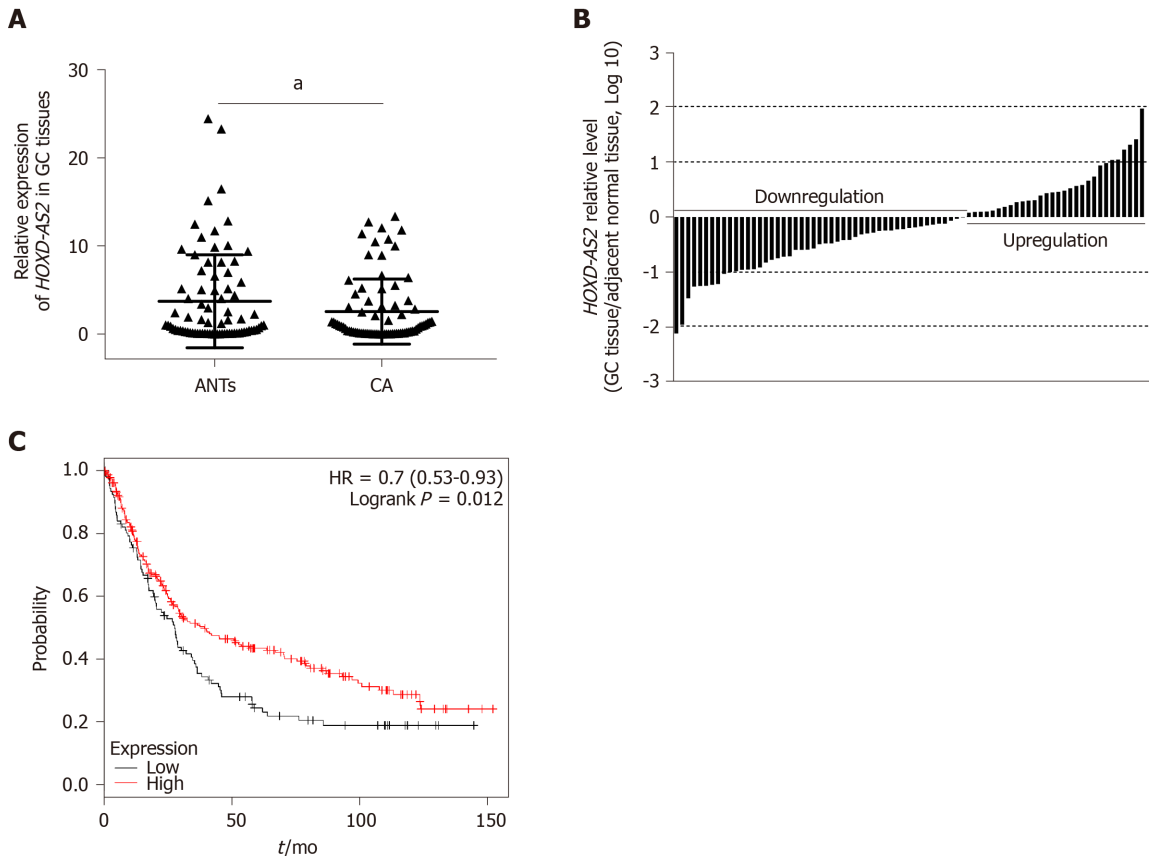


**Table 1 Association between *HOXD-AS2* expression and clinicopathological factors of human gastric cancer patients**

Characteristic	Each group (n)	<i>HOXD-AS2</i> expression		P value
		High	Low	
All cases	79	30	49	
Age (yr, mean $\pm$ SD)	79	64.10 $\pm$ 9.323	62.04 $\pm$ 9.648	0.354
BMI	79	21.04 $\pm$ 2.797	21.90 $\pm$ 3.196	0.224
Gender	79			0.594
Male	63	23	40	
Female	16	7	9	
Smoking	79			0.179
Yes	32	15	17	
No	47	15	32	
Drinking alcohol	79			0.096
Yes	23	12	11	
No	56	18	38	
Maximum tumor diameter (cm, mean $\pm$ SD)	79	4.36 $\pm$ 1.856	4.87 $\pm$ 2.613	0.355
Histology	79			1.000
Undifferentiated	7	3	4	
Differentiated	72	27	45	
Depth of invasion	79			0.430
pT 1-2	9	5	4	
pT 3-4	70	25	45	
Lymph node metastasis	79			0.009
pN0	19	12	7	
pN1-3	60	18	42	
Distant metastasis	79			1.000
pM0	75	28	47	
pM1	4	2	2	
Tumor TNM stage	79			0.040
I-II	19	11	8	
III-IV	60	19	41	
Venous/lymphatic invasion	79			0.376
Positive	11	6	5	
Negative	68	24	44	
Nervous invasion	79			1.000
Positive	10	4	6	
Negative	69	26	43	
Liver metastasis	79			0.300
Absent	75	27	48	
Present	4	3	1	
Ascitic fluid	79			0.965
Negative	63	24	39	
Positive	16	6	10	

Fatty nodules	79		1.000
Positive	9	3	6
Negative	70	27	43

BMI: Body mass index; TNM: Tumor-node-metastasis.

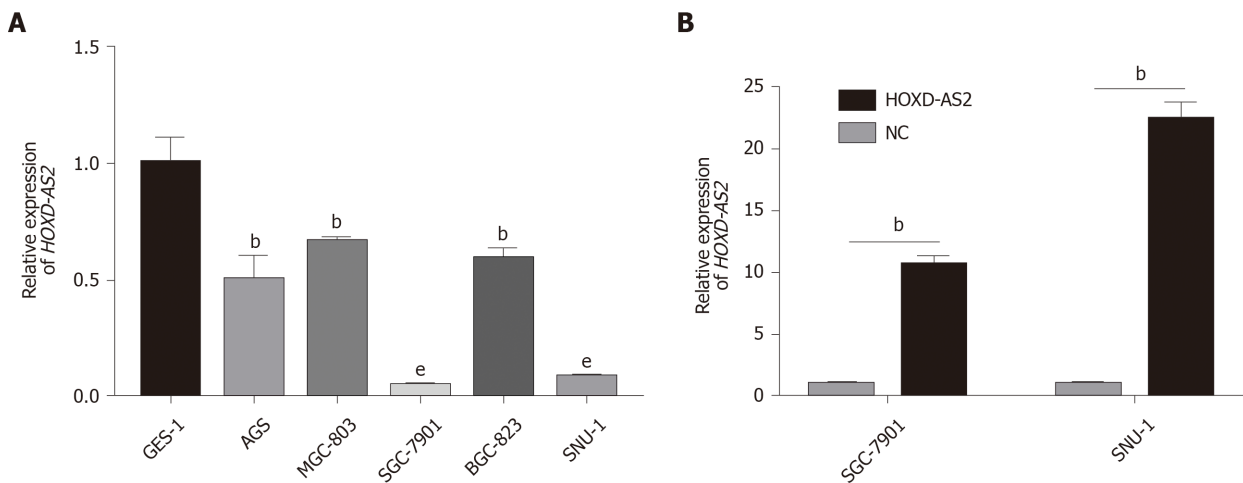


**Figure 1** *HOXD-AS2* is downregulated in gastric cancer tissues and is associated with a poor prognosis in gastric cancer patients. A: The relative expression level of *HOXD-AS2* in gastric cancer (GC) tissues was significantly lower than that in adjacent non-cancerous tissues (ANTs;  $P = 0.030$ ,  $n = 79$ ); B: *HOXD-AS2* expression levels were decreased in human GC tissues and ANTs. Bars represent the ratio between the expression levels in GC tissues and ANTs (C/N, log scale) from the 79 patients. GC tissues expressed significantly lower levels of *HOXD-AS2* than ANTs in the majority of patients (62.03%); C: Kaplan-Meier survival analysis showed that patients with low *HOXD-AS2* expression had a poorer prognosis than those with high expression. Low: The expression level of *HOXD-AS2* is lower than that of ANTs. High: The expression level of *HOXD-AS2* is higher than that of ANTs. Expression levels were normalized to  $\beta$ -actin levels. The results are shown as the mean  $\pm$  SD. <sup>a</sup> $P < 0.05$ , two-tailed Student's *t*-test. GC: Gastric cancer; ANTs: Adjacent non-cancerous tissues.

that in the control group ( $P = 0.002$  and  $0.002$ , respectively).

### Overexpression of *HOXD-AS2* inhibits the invasion and migration of GC cells SGC-7901 and SNU-1

The effects of *HOXD-AS2* on the invasion and migration of SGC-7901 and SNU-1 cells were detected by wound healing assay and Transwell assay. It was found that overexpression of *HOXD-AS2* inhibited the invasion and migration of SGC-7901 and SNU-1 cells (Figure 3A). We calculated the number of invasive and migratory cells in the pc-*HOXD-AS2* group and control group, and cell migration and invasion in the pc-*HOXD-AS2* group were significantly decreased compared with those in the control group (Figure 3A). The wound healing assay also confirmed the ability to inhibit the migration of SGC-7901 and SNU-1 cells after overexpression of *HOXD-AS2* (Figure 3B). These results show that *HOXD-AS2* is involved in the regulation of invasion and migration of GC cells.



**Figure 2** *HOXD-AS2* is downregulated in gastric cancer cells. A: The expression of *HOXD-AS2* was downregulated in gastric cancer AGS, MGC-803, SGC-7901, BGC-823, and SNU-1 cells compared with gastric epithelial GES-1 cells; B: The expression of *HOXD-AS2* in SGC-7901 and SNU-1 cells after transfections. The results are shown as the mean  $\pm$  SD. <sup>b</sup> $P < 0.01$ , <sup>e</sup> $P < 0.001$ .

### ***HOXD-AS2* regulates the proliferation, cell cycle progression, and apoptosis of SGC-7901 and SNU-1 cells**

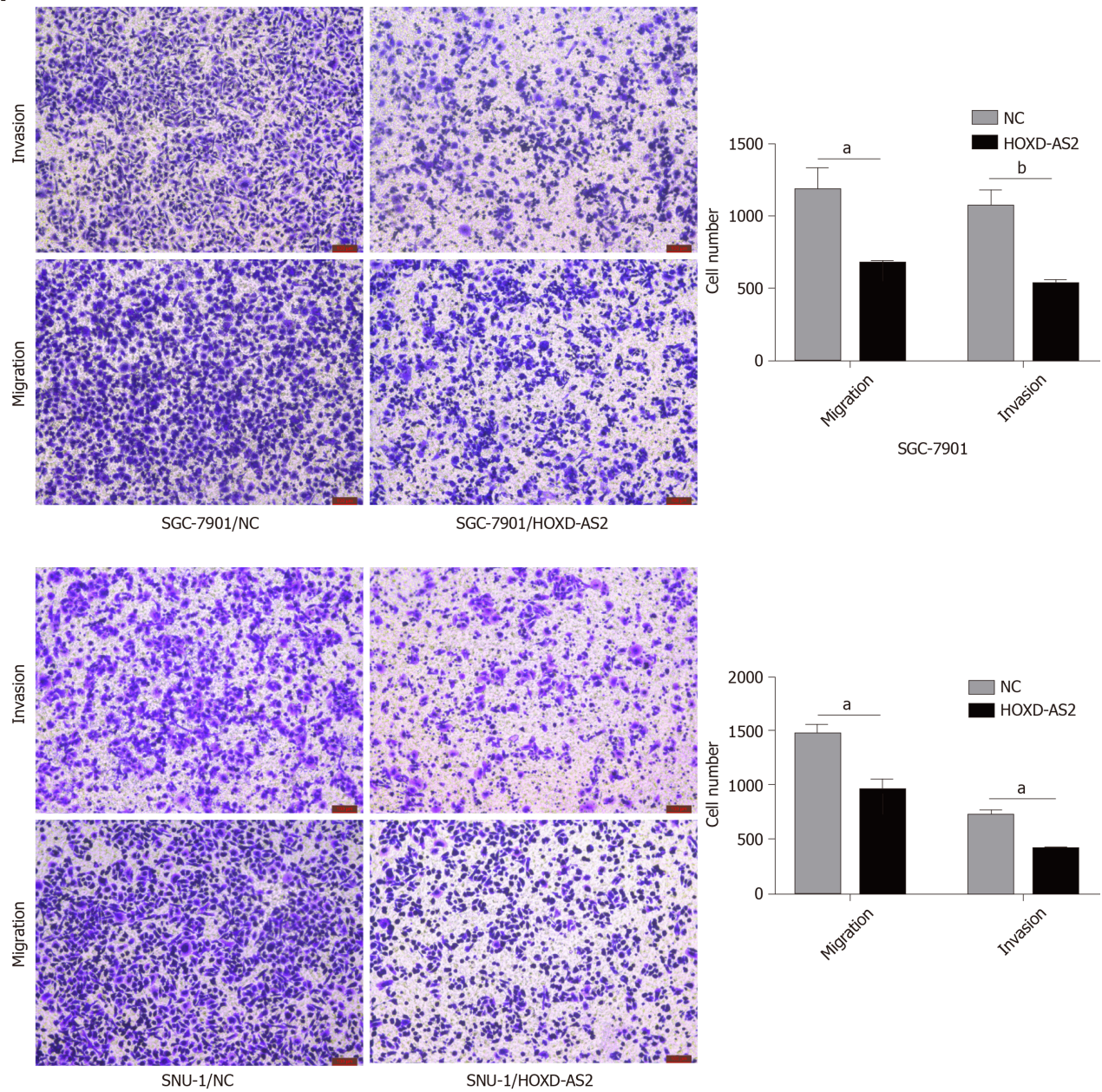
The cell proliferation activity was detected by the CCK8 experiment, and it was found that overexpression of *HOXD-AS2* can inhibit the proliferation ability of SGC-7901 and SNU-1 cells (Figure 4A and B). We examined the effect of *HOXD-AS2* on the apoptosis of SGC-7901 and SNU-1 cells by flow cytometry. The results showed that the apoptosis rate of the *HOXD-AS2* overexpression group was higher than that of the control group (Figure 4C). Cell cycle detection results showed that in SGC-7901 and SNU-1 cells, overexpression of *HOXD-AS2* can increase the number of G0/G1 phase cells, reduce the number of S phase cells, and block the cell cycle in G0/G1 phase (Figure 4D).

### ***HOXD8* is downregulated in human GC tissues and positively correlated with *HOXD-AS2* expression**

To explore the regulatory mechanism of *HOXD-AS2* in GC, we predicted the co-expressed genes associated with lncRNA *HOXD-AS2* via circIncrNAet (<http://app.cgu.edu.tw/circIncrNAet/>) and found that *HOXD-AS2* was positively correlated with its nearby gene *HOXD8* ( $r = 0.785$ ,  $P < 0.05$ ) (Figure 5A). Then, we included our qPCR data in the analysis and confirmed that *HOXD-AS2* had a positive correlation with *HOXD8* ( $r = 0.9157$ ,  $P < 0.05$ ) (Figure 5B). As shown in Figure 5C, G, and H, the relative mRNA expression level of *HOXD8* in 79 GC tissues was significantly decreased in comparison with that in the corresponding adjacent tissues ( $P = 0.048$ ), and the protein expression levels of *HOXD8* in six GC tissues was significantly decreased in comparison with that in the corresponding adjacent tissues ( $P < 0.001$ ). As shown in Figure 5D, E, and F, the relative mRNA and protein expression levels of *HOXD8* in the five GC cell lines SGC-7901, MGC-803, BGC-823, SNU-1, and AGS were lower than those in the normal gastric mucosal cell line GES-1 ( $P < 0.001$ ). In SGC-7901 and SNU-1 cells, we overexpressed *HOXD-AS2* and found that *HOXD8* protein levels also increased (Figure 6A, D, and E). According to these results, we speculate that *HOXD-AS2* is likely to participate in the progression of GC cells via interaction with *HOXD8*.

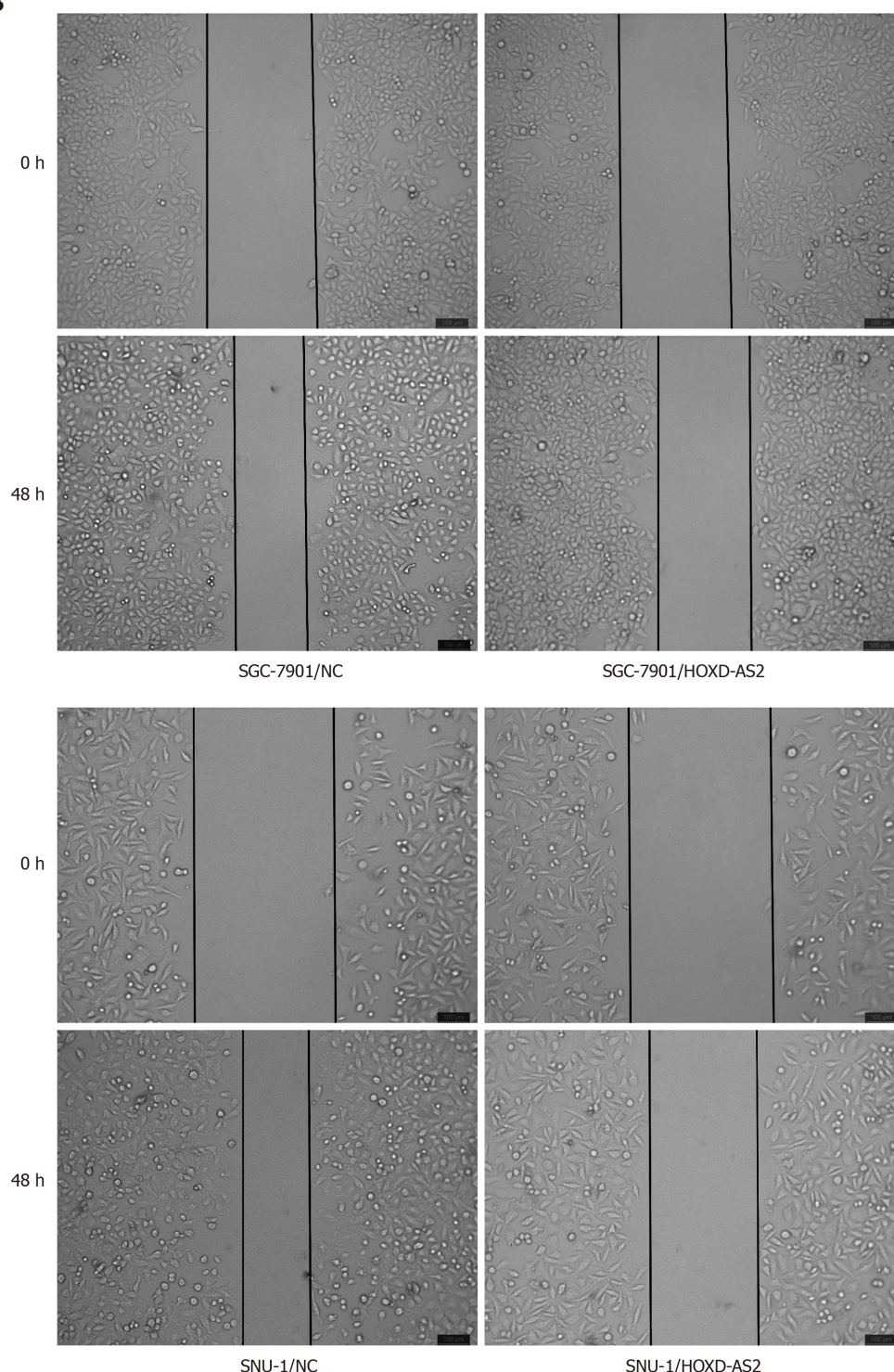
### **Overexpression of *HOXD-AS2* inhibits the PI3K/Akt signaling pathway in SGC-7901 and SNU-1 cells**

In our previous research, through Gene Ontology (GO) analysis and KEGG signaling pathway enrichment analysis of GC-related signaling pathways, we identified the top 10 most enriched signal pathways in GC<sup>[14]</sup>. In this study, we found that lncRNA *HOXD-AS2* may play an important role in regulating the progression of GC cells through the PI3K/Akt signaling pathway. The results showed that in SGC-7901 and SNU-1 cells, the protein levels of p-PI3K, p-Akt, and p-MDM2 in the pc-*HOXD-AS2* group were lower than those in the control group, while the level of p53 was higher than that in the control group (Figure 6A, D, and E). To further demonstrate whether

**A**


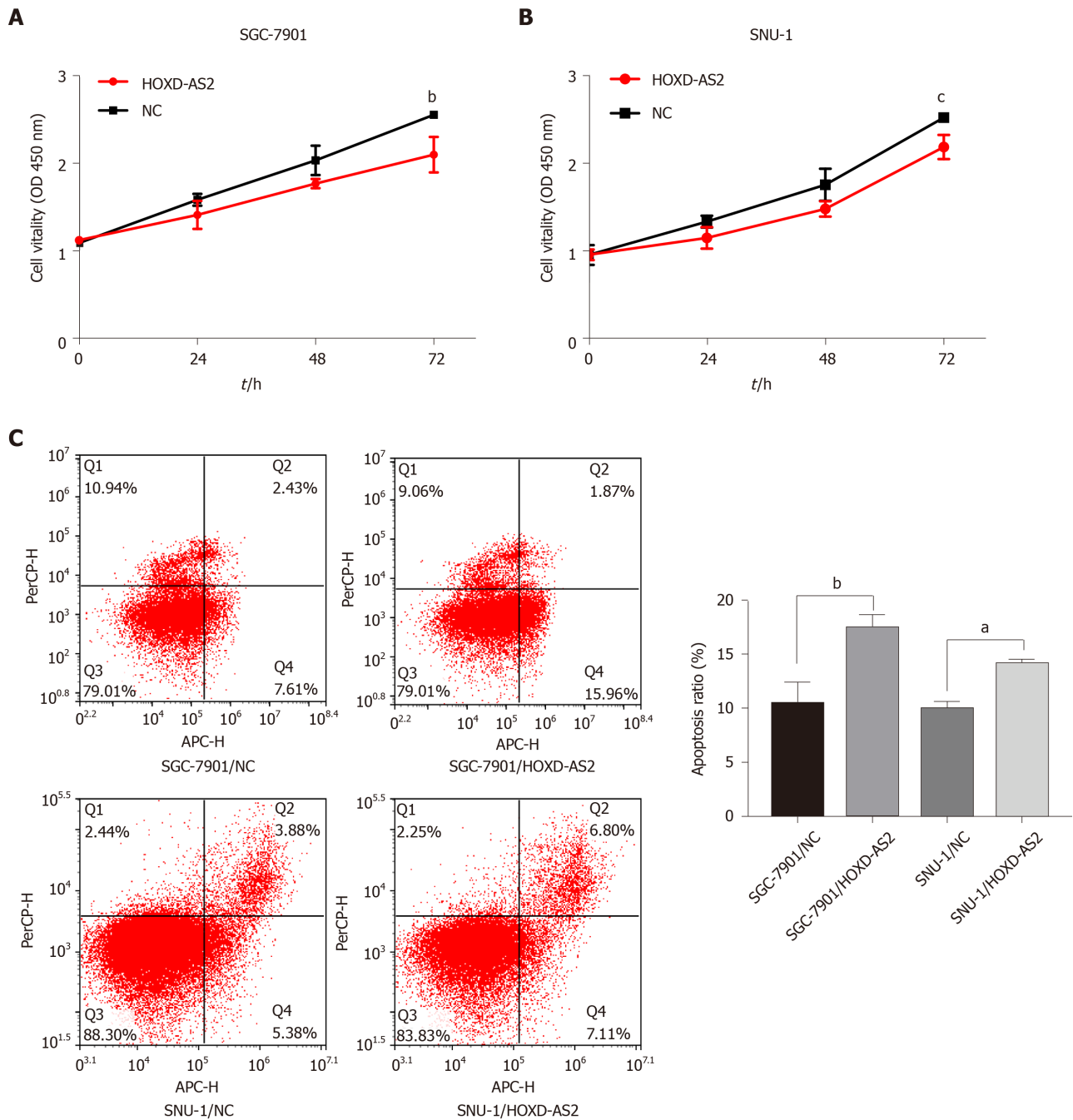


**B**

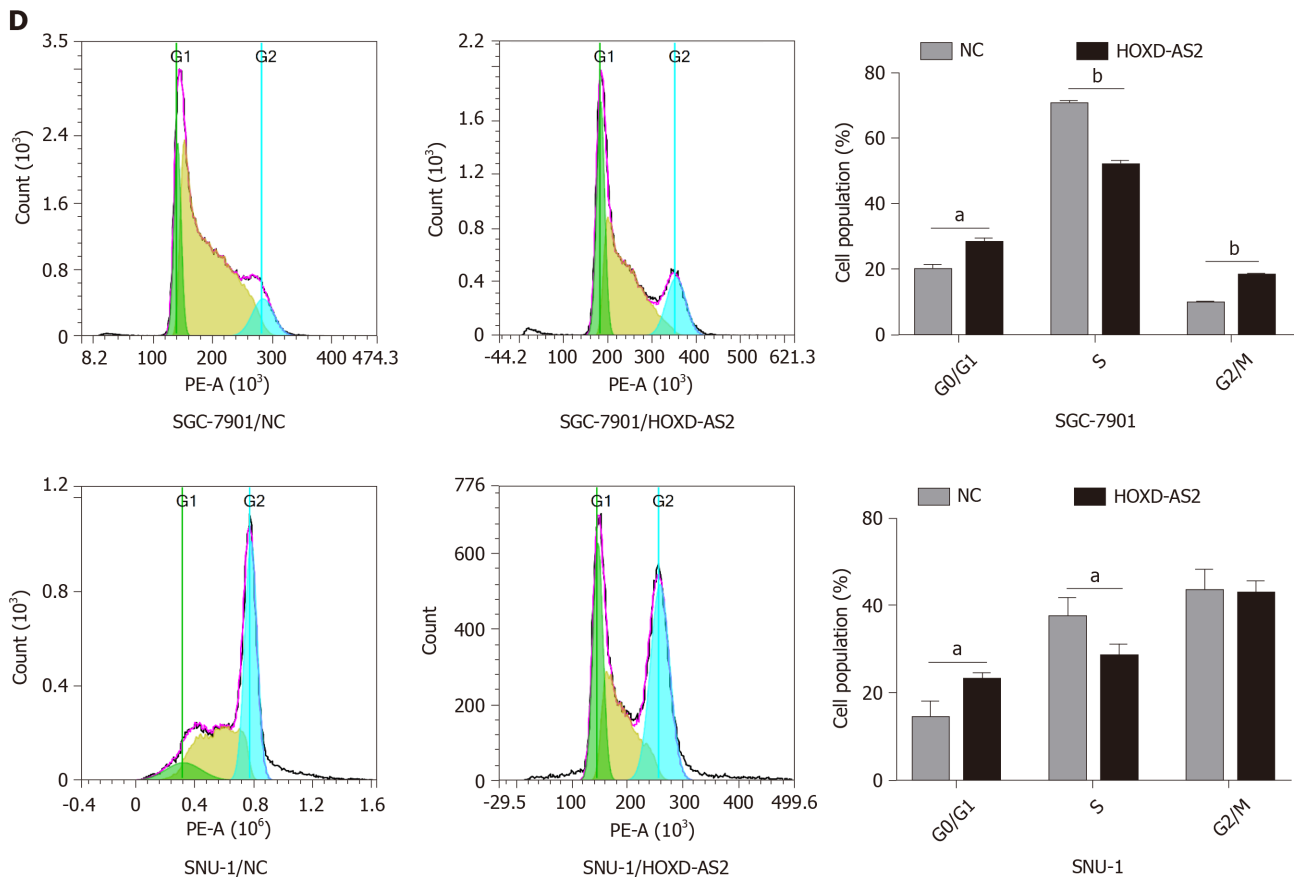


**Figure 3 Overexpression of *HOXD-AS2* inhibits gastric cancer cell migration and invasion *in vitro*.** A: Transwell assays were performed to detect the effect of *HOXD-AS2* on the migration and invasion of SGC-7901 and SNU-1 cells. The results revealed that overexpression of *HOXD-AS2* inhibited the migration and invasion of SGC-7901 and SNU-1 cells; B: Wound healing assay further showed that overexpression of *HOXD-AS2* inhibited gastric cancer cell migration and invasion. <sup>a</sup> $P < 0.05$ , <sup>b</sup> $P < 0.01$ . Data are shown as the mean  $\pm$  SD. All the experiments were performed in triplicate.

*HOXD-AS2* regulates the progression of GC cells *via* the PI3K/Akt signaling pathway, we added 10  $\mu\text{mol/L}$  PI3K inhibitor to SGC-7901 and SNU-1 cells. After the use of the PI3K-specific inhibitor LY294002, a similar effect was obtained as with transfection of the *HOXD-AS2* plasmid. The results also showed that the expression of *HOXD-AS2* increased and the expression of HOXD8 protein increased, which further demonstrated that *HOXD-AS2* regulates the progression of GC cells by inhibiting the activation of the PI3K/Akt signaling pathway (Figure 6B, C, F, and G).





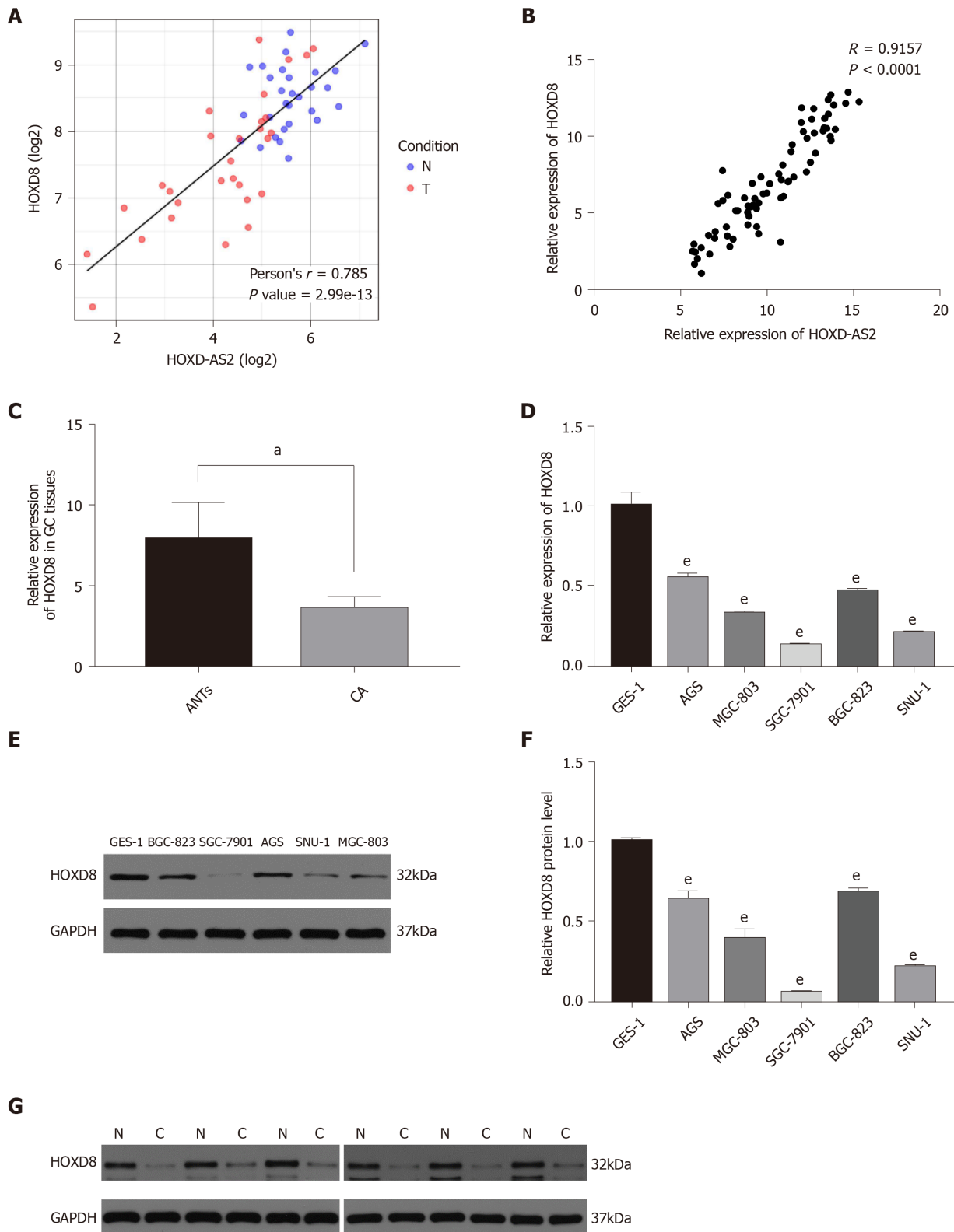


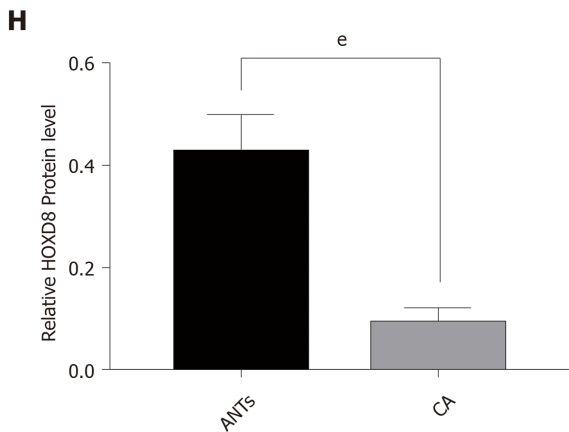
**Figure 4** Overexpression of *HOXD-AS2* inhibits gastric cancer cell proliferation and cell cycle progression and promotes apoptosis *in vitro*. A and B: The effect of *HOXD-AS2* on cell proliferation was determined by cell counting kit-8 assay. Cell proliferation was decreased after overexpression of *HOXD-AS2* in SGC-7901 ( $P = 0.0019$ ) and SNU-1 ( $P < 0.001$ ) cells; C: Flow cytometry was used to detect the percentage of apoptotic cells in the pc-*HOXD-AS2* and the control groups. The percentage of apoptotic cells was increased after overexpression of *HOXD-AS2* in SGC-7901 ( $P = 0.007$ ) and SNU-1 ( $P = 0.021$ ) cells; D: The effect of *HOXD-AS2* on cell cycle was measured by flow cytometry after 7-AAD staining in SGC-7901 and SNU-1 cells. <sup>a</sup> $P < 0.05$ , <sup>b</sup> $P < 0.01$ , <sup>c</sup> $P < 0.001$ .

## DISCUSSION

LncRNAs have diverse biological functions and mainly regulate gene expression at three levels: Epigenetic, transcriptional, and post-transcriptional. Regulation at the epigenetic level is mainly through DNA methylation and demethylation. Transcriptional regulation mainly affects the expression of genes through promoters and enhancers. Regulation at the post-transcriptional level is mainly through the regulation of post-transcriptional processing and modification processes such as mRNA splicing, editing, and degradation<sup>[16-18]</sup>. Many studies have found that lncRNAs are closely related to GC, and lncRNAs can act as tumor suppressor genes or oncogenes to play an important role in the regulation of malignant biological behaviors in GC such as proliferation, apoptosis, invasion, and metastasis<sup>[19]</sup>. However, the specific molecular mechanism of lncRNAs in GC has not been fully elucidated. In our previous study, we constructed an lncRNA expression chip to compare differentially expressed lncRNAs in GC tissues and matched paracancerous tissues<sup>[13,14,20]</sup>. *HOXD-AS2* has great expression differences between GC tissues and matched paracancerous tissues, but its specific role in GC remains unclear. The purpose of this study was to detect the expression of *HOXD-AS2* in GC tissues and cells, analyze its relationship with the clinicopathological features of GC patients, and explore its role and specific molecular regulatory mechanism in the occurrence and development of GC.

In the present study, we verified the expression of *HOXD-AS2* in 79 GC tissues and 5 GC cell lines by qRT-PCR. The relationship between the expression of *HOXD-AS2* and the clinicopathological features of GC patients was analyzed. It was found that low expression of *HOXD-AS2* was significantly associated with lymph node metastasis and TNM stage. We analyzed data from the Kaplan-Meier plotter database and found that the *HOXD-AS2* low expression group had a lower overall survival rate and worse prognosis than the *HOXD-AS2* high expression group. Lymph node metastasis and



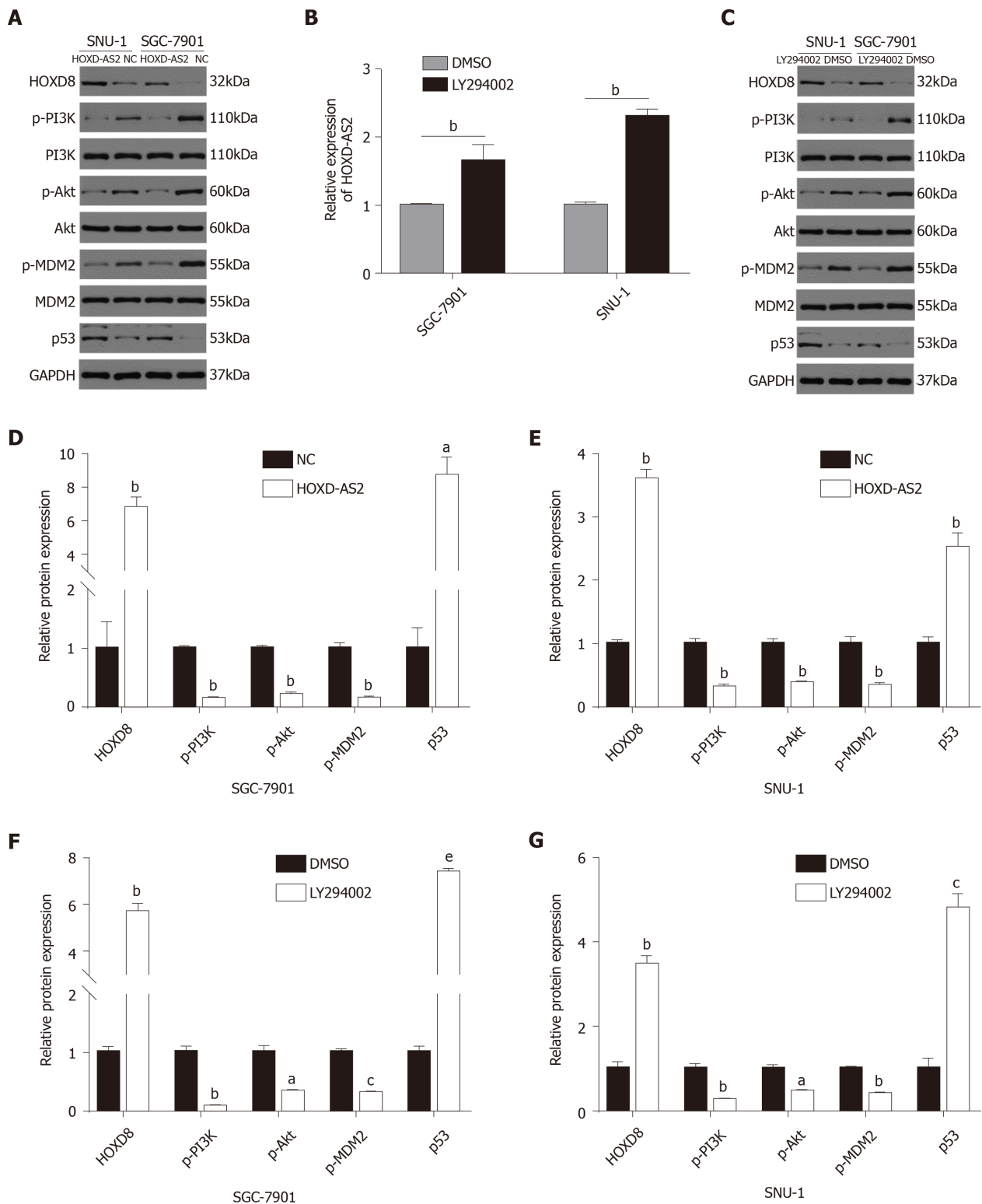


**Figure 5** *HOXD8* is downregulated in human gastric cancer tissues and positively correlated with *HOXD-AS2* expression. A: CircIncrNA database analysis results show that *HOXD-AS2* is positively correlated with *HOXD8* ( $r = 0.785$ ,  $P < 0.05$ ); B: Bivariate correlation analysis of the relationship between *HOXD-AS2* and *HOXD8* expression levels, and the resulting Spearman correlation coefficient was calculated as 0.9157 with  $P < 0.0001$  ( $n = 79$ ); C and D: The relative mRNA expression level of *HOXD8* was decreased in human gastric cancer (GC) tissues ( $P = 0.048$ ); E and F: The relative protein expression levels of *HOXD8* were decreased in human GC cells ( $P < 0.001$ ); G and H: The relative protein expression level of *HOXD8* was decreased in human GC tissues ( $P < 0.001$ ). The results are shown as the mean  $\pm$  SD. <sup>a</sup> $P < 0.05$ , <sup>e</sup> $P < 0.001$ . GC: Gastric cancer; ANTs: Adjacent non-cancerous tissues.

TNM stage are closely related to the progression of tumors. We speculated that *HOXD-AS2* may be involved in the biological behavior of GC cells. To confirm our hypothesis, we specifically upregulated the expression of *HOXD-AS2* in GC cells *in vitro* and found that the invasion, migration, and proliferation ability of GC cells was significantly inhibited. All the results indicated that *HOXD-AS2* may play an important regulatory role in the progression of GC.

Many studies have found that the natural antisense transcript types of lncRNAs can regulate the expression of their nearby genes. For example, lncRNA *FOXP4-AS1* can act as a ceRNA to adsorb miR-3184-5p, attenuating the inhibitory effect of miR-3184-5p on its target gene *FOXP4*, thereby promoting prostate cancer cell proliferation<sup>[21]</sup>. LncRNA *SLC7A11-AS1* is negatively regulated by its adjacent gene *SLC7A11*. Decreasing *SLC7A11-AS1* can increase the expression of *SLC7A11*. *SLC7A11-AS1* can also regulate the proliferation of GC cells by activating the ASK1-p38MAPK/JNK signaling pathway<sup>[13]</sup>. LncRNA *MACC1-AS1* is highly expressed in GC tissues, and it can upregulate the expression of *MACC1* by enhancing the stability of *MACC1* mRNA, thereby enhancing the glycolysis process and antioxidant capacity of GC cells to promote their proliferation, invasion, and migration. *MACC1-AS1* can be used as a biomarker for the diagnosis and prognosis of GC<sup>[22]</sup>. Similarly, when we predicted the co-expressed genes related to *HOXD-AS2* through an online database, we found that the expression of the nearby gene *HOXD8* was positively correlated with the expression of *HOXD-AS2*. Therefore, we speculated that *HOXD-AS2* may be involved in the regulation of *HOXD8* through a ceRNA mechanism and may play a role in regulating the process of GC cells. We used qRT-PCR assay to further verify that there was a significant positive correlation between the expression of the two genes in clinical GC tissues and GC cells. After overexpression of *HOXD-AS2*, we found that the protein level of *HOXD8* was higher than that of the control group, further confirming that *HOXD-AS2* can regulate the expression of *HOXD8*. However, little is known about the role of *HOXD8* in tumorigenesis and development and the specific regulatory mechanisms. *HOXD8*, which is located at 2q31.1 and contains two exons, has been mapped to chromosome 2 region 176129705-176132695. The expression of *HOXD8* is decreased in colorectal cancer. Overexpression of *HOXD8* can inhibit the proliferation, invasion, and migration of colorectal cancer cells and promote their apoptosis<sup>[23]</sup>. *HOXD8* is highly expressed in non-small cell lung cancer. Overexpression of *HOXD8* can upregulate the expression of proliferation-related genes *p53*, *PTEN*, and *p21* and promote the proliferation of non-small cell lung cancer cells. In addition, miR-520a-3p can inhibit the proliferation of non-small cell lung cancer cells by downregulating the expression of *HOXD8*<sup>[24]</sup>. The specific regulatory mechanism of *HOXD8* in tumors still needs further exploration and confirmation.

The PI3K/Akt signaling pathway has been well documented in a number of studies as a key mechanism regulating tumor cell processes, including proliferation, apoptosis, invasion, and migration<sup>[25-27]</sup>. Many lncRNAs have also been found to be closely related to the PI3K/Akt signaling pathway in GC. Huang *et al*<sup>[28]</sup> found that



**Figure 6** Overexpression of *HOXD-AS2* inhibits the PI3K/Akt signaling pathway. A, D, and E: Overexpression of *HOXD-AS2* reduced p-PI3K, p-Akt, and p-MDM2 protein levels, and increased p53 and HOXD8 protein levels; B: *HOXD-AS2* mRNA levels were significantly increased following treatment with LY294002 in SGC-7901 ( $P = 0.009$ ) and SNU-1 ( $P = 0.001$ ) cells for 48 h. Expression levels were normalized to GAPDH levels. The results are shown as the mean  $\pm$  SD; C, F, and G: HOXD8 and p53 protein levels were significantly increased but p-PI3K, p-Akt, and p-MDM2 protein levels were significantly reduced following treatment with LY294002 in SGC-790 and SNU-1 cells for 48 h.  $^aP < 0.05$ ,  $^bP < 0.01$ ,  $^cP < 0.001$ .

lncRNA *AK023391* promotes the development and progression of GC by activating the PI3K/Akt signaling pathway. Cheng *et al*<sup>[29]</sup> found that downregulation of lncRNA *HOTAIR* can upregulate the expression of miR-34a, inhibit the PI3K/Akt and Wnt/ $\beta$ -catenin signaling pathways, and attenuate the resistance of GC cells to cisplatin. In this study, we found a possible link between the PI3K/Akt signaling pathway and GC by GO and KEGG analysis. After overexpression of *HOXD-AS2* in GC cells SGC-7901 and

SNU-1, we found that the PI3K/Akt signaling pathway is inhibited. *In vitro*, after we specifically overexpressed *HOXD-AS2* in GC cells SGC-7901 and SNU-1, we found that the expression levels of several key genes in the PI3K/Akt signaling pathway were downregulated and that the signaling pathway was inhibited. In the positive control group, we obtained similar results after adding the PI3K inhibitor LY294002. We found that the expression level of *HOXD-AS2* increased, the protein level of *HOXD8* also increased, and the PI3K/Akt signaling pathway was inhibited. The invasion, migration, and proliferation ability of GC cells also decreased. Based on the above findings, we speculate that the low expression of *HOXD-AS2* may regulate the activation of the PI3K/Akt signaling pathway *via HOXD8* through a ceRNA mechanism, which may promote the progression of GC.

## CONCLUSION

In summary, our current results demonstrate that *HOXD-AS2* might play an important role in suppressing the progression of GC cells by regulating *HOXD8* gene expression and inhibiting the PI3K/Akt signaling pathway. These results suggest that *HOXD-AS2* may be a key molecule in tumor development and a potential target for the treatment of GC.

## ARTICLE HIGHLIGHTS

### Research background

Long non-coding RNAs (lncRNAs) are a class of non-coding RNAs with a length of more than 200 nucleotides and lack an open reading frame. They mainly regulate RNA transcription and mRNA splicing and play an important role in regulating the stability of RNA in the cytoplasm and the activity of microRNAs. More and more studies have shown that abnormally expressed lncRNAs are involved in all aspects of tumor occurrence and development, and are closely related to tumor proliferation, apoptosis, invasion, metastasis, drug resistance, and poor prognosis. In recent years, more and more studies have found that abnormally expressed lncRNAs are involved in the occurrence and development of gastric cancer (GC), and they are expected to become new biomarkers for the diagnosis and treatment of GC.

### Research motivation

GC is one of the most common malignant tumors in the world. The incidence and mortality of GC are in the forefront of all malignant tumors. Although a major breakthrough has been achieved in the study of lncRNAs in the pathogenesis of GC, the specific mechanism of lncRNAs in the occurrence and development of GC has not yet been fully elucidated. Exploring new lncRNAs can help to understand the molecular mechanism of GC more deeply.

### Research objectives

The main purpose of this study was to explore the effect of downregulation of *HOXD-AS2* on the biological behavior of GC cells SGC-7901 and SNU-1 and the underlying mechanism. Studies have found that the downregulation of *HOXD-AS2* can regulate the expression of its neighboring gene *HOXD8*, and can also activate the PI3K/Akt signaling pathway, thereby promoting the progression of GC cells. The results of this study may provide a new idea for the treatment of GC.

### Research methods

The pc*HOXD-AS2* plasmid vector was constructed and transfected into SGC-7901 and SNU-1 GC cells. Matrigel Transwell and wound healing assays were used to confirm the effect of *HOXD-AS2* on invasion and migration of GC cells. Cell counting kit-8 assay and flow cytometry were used to verify the effect of *HOXD-AS2* on proliferation, cell cycle, and apoptosis of GC cells. The relevant regulatory mechanism between *HOXD-AS2* and *HOXD8* and PI3K/Akt signaling pathway was verified by Western blot analysis.

### Research results

In this study, we found that the low expression of lncRNA *HOXD-AS2* was associated



with lymph node metastasis and tumor-node-metastasis stage in GC. *In vitro* functional experiments demonstrated that overexpression of *HOXD-AS2* inhibited GC cell progression. Mechanistic studies revealed that *HOXD-AS2* regulated the expression of its nearby gene *HOXD8* and inhibited the activity of the PI3K/Akt signaling pathway.

### Research conclusions

These results indicate that downregulation of *HOXD-AS2* significantly promotes the progression of GC cells by regulating *HOXD8* expression and activating the PI3K/Akt signaling pathway. *HOXD-AS2* may be a novel diagnostic biomarker and effective therapeutic target for GC.

### Research perspectives

This study combines basic experimental research and bioinformatics results to reach a relatively novel conclusion. To further confirm the results of this study, siRNA and animal experiments may be better.

## REFERENCES

- 1 **Bray F**, Ferlay J, Soerjomataram I, Siegel RL, Torre LA, Jemal A. Global cancer statistics 2018: GLOBOCAN estimates of incidence and mortality worldwide for 36 cancers in 185 countries. *CA Cancer J Clin* 2018; **68**: 394-424 [PMID: 30207593 DOI: 10.3322/caac.21492]
- 2 **Chen W**, Zheng R, Baade PD, Zhang S, Zeng H, Bray F, Jemal A, Yu XQ, He J. Cancer statistics in China, 2015. *CA Cancer J Clin* 2016; **66**: 115-132 [PMID: 26808342 DOI: 10.3322/caac.21338]
- 3 **Van Cutsem E**, Sagaert X, Topal B, Haustermans K, Prenen H. Gastric cancer. *Lancet* 2016; **388**: 2654-2664 [PMID: 27156933 DOI: 10.1016/S0140-6736(16)30354-3]
- 4 **Yamaguchi K**, Yoshida K, Tanahashi T, Takahashi T, Matsuhashi N, Tanaka Y, Tanabe K, Ohdan H. The long-term survival of stage IV gastric cancer patients with conversion therapy. *Gastric Cancer* 2018; **21**: 315-323 [PMID: 28616743 DOI: 10.1007/s10120-017-0738-1]
- 5 **Ulitsky I**, Bartel DP. lincRNAs: genomics, evolution, and mechanisms. *Cell* 2013; **154**: 26-46 [PMID: 23827673 DOI: 10.1016/j.cell.2013.06.020]
- 6 **Qi P**, Du X. The long non-coding RNAs, a new cancer diagnostic and therapeutic gold mine. *Mod Pathol* 2013; **26**: 155-165 [PMID: 22996375 DOI: 10.1038/modpathol.2012.160]
- 7 **Lee JT**. Epigenetic regulation by long noncoding RNAs. *Science* 2012; **338**: 1435-1439 [PMID: 23239728 DOI: 10.1126/science.1231776]
- 8 **Zhang J**, Li Z, Liu L, Wang Q, Li S, Chen D, Hu Z, Yu T, Ding J, Li J, Yao M, Huang S, Zhao Y, He X. Long noncoding RNA TSLNC8 is a tumor suppressor that inactivates the interleukin-6/STAT3 signaling pathway. *Hepatology* 2018; **67**: 171-187 [PMID: 28746790 DOI: 10.1002/hep.29405]
- 9 **Xiao ZD**, Han L, Lee H, Zhuang L, Zhang Y, Baddour J, Nagrath D, Wood CG, Gu J, Wu X, Liang H, Gan B. Energy stress-induced lncRNA FILNC1 represses c-Myc-mediated energy metabolism and inhibits renal tumor development. *Nat Commun* 2017; **8**: 783 [PMID: 28978906 DOI: 10.1038/s41467-017-00902-z]
- 10 **Tan DSW**, Chong FT, Leong HS, Toh SY, Lau DP, Kwang XL, Zhang X, Sundaram GM, Tan GS, Chang MM, Chua BT, Lim WT, Tan EH, Ang MK, Lim TKH, Sampath P, Chowbay B, Skanderup AJ, DasGupta R, Iyer NG. Long noncoding RNA EGFR-AS1 mediates epidermal growth factor receptor addiction and modulates treatment response in squamous cell carcinoma. *Nat Med* 2017; **23**: 1167-1175 [PMID: 28920960 DOI: 10.1038/nm.4401]
- 11 **Kim J**, Piao HL, Kim BJ, Yao F, Han Z, Wang Y, Xiao Z, Siverly AN, Lawhon SE, Ton BN, Lee H, Zhou Z, Gan B, Nakagawa S, Ellis MJ, Liang H, Hung MC, You MJ, Sun Y, Ma L. Long noncoding RNA MALAT1 suppresses breast cancer metastasis. *Nat Genet* 2018; **50**: 1705-1715 [PMID: 30349115 DOI: 10.1038/s41588-018-0252-3]
- 12 **Shang Z**, Yu J, Sun L, Tian J, Zhu S, Zhang B, Dong Q, Jiang N, Flores-Morales A, Chang C, Niu Y. LncRNA PCAT1 activates AKT and NF- $\kappa$ B signaling in castration-resistant prostate cancer by regulating the PHLPP/FKBP51/IKK $\alpha$  complex. *Nucleic Acids Res* 2019; **47**: 4211-4225 [PMID: 30773595 DOI: 10.1093/nar/gkz108]
- 13 **Luo Y**, Wang C, Yong P, Ye P, Liu Z, Fu Z, Lu F, Xiang W, Tan W, Xiao J. Decreased expression of the long non-coding RNA SLC7A11-AS1 predicts poor prognosis and promotes tumor growth in gastric cancer. *Oncotarget* 2017; **8**: 112530-112549 [PMID: 29348845 DOI: 10.18632/oncotarget.22486]
- 14 **Luo Y**, Tan W, Jia W, Liu Z, Ye P, Fu Z, Lu F, Xiang W, Tang L, Yao L, Huang Q, Xiao J. The long non-coding RNA LINC01606 contributes to the metastasis and invasion of human gastric cancer and is associated with Wnt/ $\beta$ -catenin signaling. *Int J Biochem Cell Biol* 2018; **103**: 125-134 [PMID: 30142387 DOI: 10.1016/j.biocel.2018.08.012]
- 15 **Yang XZ**, Cheng TT, He QJ, Lei ZY, Chi J, Tang Z, Liao QX, Zhang H, Zeng LS, Cui SZ. LINC01133 as ceRNA inhibits gastric cancer progression by sponging miR-106a-3p to regulate APC expression and the Wnt/ $\beta$ -catenin pathway. *Mol Cancer* 2018; **17**: 126 [PMID: 30134915 DOI: 10.1186/s12943-018-0874-1]
- 16 **Huarte M**. The emerging role of lncRNAs in cancer. *Nat Med* 2015; **21**: 1253-1261 [PMID: 26540387 DOI: 10.1038/nm.3981]
- 17 **Li M**, Izpisua Belmonte JC. Roles for noncoding RNAs in cell-fate determination and regeneration. *Nat Struct Mol Biol* 2015; **22**: 2-4 [PMID: 25565025 DOI: 10.1038/nsmb.2946]
- 18 **Ponting CP**, Oliver PL, Reik W. Evolution and functions of long noncoding RNAs. *Cell* 2009; **136**: 629-641

- [PMID: 19239885 DOI: 10.1016/j.cell.2009.02.006]
- 19 **Fang XY**, Pan HF, Leng RX, Ye DQ. Long noncoding RNAs: novel insights into gastric cancer. *Cancer Lett* 2015; **356**: 357-366 [PMID: 25444905 DOI: 10.1016/j.canlet.2014.11.005]
  - 20 **Feng Y**, Fu Z, Luo Y, Tan W, Liu Z, Ye P, Lu F, Xiang W, Tang L, Yao L, Song M, Huang Q, Liu Y, Xiao J. Long non-coding RNA RP11-6O2.4 indicates poor prognosis and suppresses cell cycle progression through the p38-MAPK signaling pathway in gastric cancer. *Mol Cell Toxicol* 2019; **15**: 335-344 [DOI: 10.1007/s13273-019-0037-5]
  - 21 **Wu X**, Xiao Y, Zhou Y, Zhou Z, Yan W. LncRNA FOXP4-AS1 is activated by PAX5 and promotes the growth of prostate cancer by sequestering miR-3184-5p to upregulate FOXP4. *Cell Death Dis* 2019; **10**: 472 [PMID: 31209207 DOI: 10.1038/s41419-019-1699-6]
  - 22 **Zhao Y**, Liu Y, Lin L, Huang Q, He W, Zhang S, Dong S, Wen Z, Rao J, Liao W, Shi M. The lncRNA MACC1-AS1 promotes gastric cancer cell metabolic plasticity via AMPK/Lin28 mediated mRNA stability of MACC1. *Mol Cancer* 2018; **17**: 69 [PMID: 29510730 DOI: 10.1186/s12943-018-0820-2]
  - 23 **Mansour MA**, Senga T. HOXD8 exerts a tumor-suppressing role in colorectal cancer as an apoptotic inducer. *Int J Biochem Cell Biol* 2017; **88**: 1-13 [PMID: 28457970 DOI: 10.1016/j.biocel.2017.04.011]
  - 24 **Liu Y**, Miao L, Ni R, Zhang H, Li L, Wang X, Li X, Wang J. microRNA-520a-3p inhibits proliferation and cancer stem cell phenotype by targeting HOXD8 in non-small cell lung cancer. *Oncol Rep* 2016; **36**: 3529-3535 [PMID: 27748920 DOI: 10.3892/or.2016.5149]
  - 25 **Xue G**, Restuccia DF, Lan Q, Hynx D, Dirnhofer S, Hess D, Rüegg C, Hemmings BA. Akt/PKB-mediated phosphorylation of Twist1 promotes tumor metastasis via mediating cross-talk between PI3K/Akt and TGF- $\beta$  signaling axes. *Cancer Discov* 2012; **2**: 248-259 [PMID: 22585995 DOI: 10.1158/2159-8290.CD-11-0270]
  - 26 **Wang H**, Yang X, Guo Y, Shui L, Li S, Bai Y, Liu Y, Zeng M, Xia J. HERG1 promotes esophageal squamous cell carcinoma growth and metastasis through TXNDC5 by activating the PI3K/AKT pathway. *J Exp Clin Cancer Res* 2019; **38**: 324 [PMID: 31331361 DOI: 10.1186/s13046-019-1284-y]
  - 27 **Xu W**, Yang Z, Xie C, Zhu Y, Shu X, Zhang Z, Li N, Chai N, Zhang S, Wu K, Nie Y, Lu N. PTEN lipid phosphatase inactivation links the hippo and PI3K/Akt pathways to induce gastric tumorigenesis. *J Exp Clin Cancer Res* 2018; **37**: 198 [PMID: 30134988 DOI: 10.1186/s13046-018-0795-2]
  - 28 **Huang Y**, Zhang J, Hou L, Wang G, Liu H, Zhang R, Chen X, Zhu J. LncRNA AK023391 promotes tumorigenesis and invasion of gastric cancer through activation of the PI3K/Akt signaling pathway. *J Exp Clin Cancer Res* 2017; **36**: 194 [PMID: 29282102 DOI: 10.1186/s13046-017-0666-2]
  - 29 **Cheng C**, Qin Y, Zhi Q, Wang J, Qin C. Knockdown of long non-coding RNA HOTAIR inhibits cisplatin resistance of gastric cancer cells through inhibiting the PI3K/Akt and Wnt/ $\beta$ -catenin signaling pathways by up-regulating miR-34a. *Int J Biol Macromol* 2018; **107**: 2620-2629 [PMID: 29080815 DOI: 10.1016/j.ijbiomac.2017.10.154]



Basic Study

# Programmed death 1, ligand 1 and 2 correlated genes and their association with mutation, immune infiltration and clinical outcomes of hepatocellular carcinoma

Qiu-Ju Sheng, Wen-Yue Tian, Xiao-Guang Dou, Chong Zhang, Yan-Wei Li, Chao Han, Yao-Xin Fan, Ping-Ping Lai, Yang Ding

**ORCID number:** Qiu-Ju Sheng 0000-0001-7561-7396; Wen-Yue Tian 0000-0002-5572-6904; Xiao-Guang Dou 0000-0003-1856-7331; Chong Zhang 0000-0001-5322-1091; Yan-Wei Li 0000-0001-6679-7460; Chao Han 0000-0002-4627-6200; Yao-Xin Fan 0000-0001-8874-3789; Ping-Ping Lai 0000-0003-0391-7693; Yang Ding 0000-0002-7066-2865.

**Author contributions:** Sheng QJ, Tian WY, and Dou XG designed the research study; Sheng QJ, Zhang C, and Ding Y performed the research; Li YW, Han C, and Fan YX contributed new reagents and analytic tools; Shen QJ, Ding Y, and Lai PP analyzed the data and wrote the manuscript; all authors have read and approved the final manuscript.

**Supported by** National Science and Technology Major Project, No. 2017ZX10201201 and No. 2017ZX10202202; and Liaoning Province Natural Science Foundation, No. 20180550096.

**Institutional review board statement:** This research did not involve any human or animal experiments.

**Conflict-of-interest statement:** All

Qiu-Ju Sheng, Wen-Yue Tian, Xiao-Guang Dou, Chong Zhang, Yan-Wei Li, Chao Han, Yao-Xin Fan, Ping-Ping Lai, Yang Ding, Department of Infectious Diseases, Shengjing Hospital of China Medical University, Shenyang 110022, Liaoning Province, China

**Corresponding author:** Yang Ding, PhD, Professor, Department of Infectious Diseases, Shengjing Hospital of China Medical University, No. 39 Huaxiang Road, Tiexi District, Shenyang 110022, Liaoning Province, China. [yding0903@sina.com](mailto:yding0903@sina.com)

## Abstract

### BACKGROUND

The exact regulation network of programmed death 1 (PD-1), programmed death ligand 1 (PD-L1), and programmed death ligand 2 (PD-L2) signaling in immune escape is largely unknown. We aimed to describe the gene expression profiles related to PD-1 as well as its ligands PD-L1 and PD-L2, thus deciphering their possible biological processes in hepatocellular carcinoma (HCC).

### AIM

To find the possible mechanism of function of PD-1, PD-L1, and PD-L2 in HCC.

### METHODS

Based on the expression data of HCC from The Cancer Genome Atlas, the PD-1/PD-L1/PD-L2 related genes were screened by weighted correlation network analysis method and the biological processes of certain genes were enriched. Relation of PD1/PD-L1/PD-L2 with immune infiltration and checkpoints was investigated by co-expression analysis. The roles of PD-1/PD-L1/PD-L2 in determination of clinical outcome were also analyzed.

### RESULTS

Mutations of calcium voltage-gated channel subunit alpha1 E, catenin beta 1, ryanodine receptor 2, tumor suppressor protein p53, and Titin altered PD-1/PD-L1/PD-L2 expression profiles in HCC. PD-1, PD-L1, and PD-L2 related genes were mainly enriched in biological procedures of T cell activation, cell adhesion, and other important lymphocyte effects. In addition, PD-1/PD-L1/PD-L2 was related with immune infiltration of CD8 T cells, cytotoxic lymphocytes,

of the authors declare that there is no conflict of interest to disclose.

**Data sharing statement:** No additional data are available.

**Open-Access:** This article is an open-access article that was selected by an in-house editor and fully peer-reviewed by external reviewers. It is distributed in accordance with the Creative Commons Attribution NonCommercial (CC BY-NC 4.0) license, which permits others to distribute, remix, adapt, build upon this work non-commercially, and license their derivative works on different terms, provided the original work is properly cited and the use is non-commercial. See: <http://creativecommons.org/licenses/by-nc/4.0/>

**Manuscript source:** Unsolicited manuscript

**Specialty type:** Oncology

**Country/Territory of origin:** China

**Peer-review report's scientific quality classification**

Grade A (Excellent): A  
Grade B (Very good): B  
Grade C (Good): 0  
Grade D (Fair): 0  
Grade E (Poor): 0

**Received:** June 12, 2020

**Peer-review started:** June 12, 2020

**First decision:** July 21, 2020

**Revised:** August 6, 2020

**Accepted:** September 25, 2020

**Article in press:** September 25, 2020

**Published online:** November 15, 2020

**P-Reviewer:** Emi M, Lucchesi A

**S-Editor:** Gao CC

**L-Editor:** Wang TQ

**P-Editor:** Li JH



fibroblasts, and myeloid dendritic cells. Immune checkpoints of CTLA4, CD27, CD80, CD86, and CD28 were significantly related to the PD-1/PD-L1/PD-L2 axis. Clinically, PD-1 and PD-L2 expression was correlated with recurrence ( $P = 0.005$  for both), but there was no significant correlation between their expression and HCC patient survival.

## CONCLUSION

Mutations of key genes influence PD-1, PD-L1, and PD-L2 expression. PD-1, PD-L1, and PD-L2 related genes participate in T cell activation, cell adhesion, and other important lymphocyte effects. The finding that PD-1/PD-L1/PD-L2 is related to immune infiltration and other immune checkpoints would expand our understanding of promising anti-PD-1 immunotherapy.

**Key Words:** Programmed death 1; Programmed death ligand 1; Programmed death ligand 2; Immune; Hepatocellular carcinoma; Cancer

©The Author(s) 2020. Published by Baishideng Publishing Group Inc. All rights reserved.

**Core Tip:** This study mainly investigated the relationship between programmed death 1 (PD-1)/programmed death ligand 1 (PD-L1)/programmed death ligand 2 (PD-L2) and hepatocellular carcinoma, and explored the possible mechanism of PD-1/PD-L1/PD-L2 in this malignancy.

**Citation:** Sheng QJ, Tian WY, Dou XG, Zhang C, Li YW, Han C, Fan YX, Lai PP, Ding Y. Programmed death 1, ligand 1 and 2 correlated genes and their association with mutation, immune infiltration and clinical outcomes of hepatocellular carcinoma. *World J Gastrointest Oncol* 2020; 12(11): 1255-1271

**URL:** <https://www.wjgnet.com/1948-5204/full/v12/i11/1255.htm>

**DOI:** <https://dx.doi.org/10.4251/wjgo.v12.i11.1255>

## INTRODUCTION

In the past decade, the tumor immunotherapy targeting critical immune checkpoints has tremendously changed the anti-cancer therapy<sup>[1]</sup>. One of the most effective immune checkpoints is programmed death 1 (PD-1) and its ligand programmed death ligand 1 (PD-L1)<sup>[2]</sup>. The interaction of PD-1 expressed on T cells with PD-L1 on the membrane of cancer cells leads to T cell exhaustion and inhibits subsequent immune reaction, thus bypassing immune surveillance<sup>[3,4]</sup>. Besides, it has been found that programmed death ligand 2 (PD-L2) is another ligand that interacts with PD1, which suppresses T cell proliferation and cytokine release<sup>[5]</sup>. Until now, the specific mechanism of PD-L1 and PD-L2 regulation in tumor immune escape remains largely elusive<sup>[6]</sup>.

Hepatocellular carcinoma (HCC), one of the most frequent malignant tumor of the digestive tract, remains a leading cause of cancer-related death worldwide with limited therapeutic regimens<sup>[7,8]</sup>. It has been proved that HCC is caused mainly by hepatitis virus infection, alcohol drinking, drug abuse, and unhealthy habits<sup>[9]</sup>. In addition to surgery, chemical therapy, and liver transplantation, a number of molecular therapy regimens have been approved for treating advanced HCC, such as sorafenib and lenvatinib<sup>[10]</sup>. Recently, immune checkpoint blockade therapy targeting essential immune markers including PD-1, PD-L1 and CTLA-4 has been approved for HCC in which chemotherapeutics are ineffective<sup>[11-13]</sup>.

Previously, the effect and mechanisms of antibodies to PD-1 and its ligands have been investigated in HCC therapy by a number of studies. It has been reported that CD8 positive T cells promoted PD-L1 expression on HCC cells in a IFN- $\gamma$ -dependent manner, which in turn leads to apoptosis of CD8(+) T cells<sup>[14,15]</sup>. PD-1 expression was significantly elevated in CD8+ and CD4+ T cells obtained from HCC tissue compared with control tissue as well as blood. Antibodies to PD-L1, TIM3, or LAG3 elicit reactions of HCC-derived T cells against tumor antigens, which might become essential treatment strategies for HCC<sup>[16]</sup>. In addition, PD-1 expression in HCC has also

been suggested to increase tumor proliferation independently of adaptive immunity *via* interacting with downstream target of rapamycin effectors eukaryotic initiation factor 4E and ribosomal protein S6. Moreover, PD-1 checkpoint blockade in combination with rapamycin inhibitor resulted in more durable and synergistic tumor regression<sup>[17,18]</sup>. For HCC prognosis, it was suggested that increased expression of PD-L1 instead of PD-L2 predicted an unfavorable survival in HCC patients<sup>[19]</sup>.

Although satisfactory effect of anti-PD-1/PD-L1 therapy has been observed in several types of cancers, the potential complicated interaction network of PD-1/PD-L1/PD-L2 related genes in immune escape and immune surveillance remains unclear. In the present study, we analyzed the gene expression profiles associated with PD-1 and its ligands PD-L1 and PD-L2, deciphered the possible biological processes of the identified genes based on transcriptional data of HCC from The Cancer Genome Atlas (TCGA), explored the influence of PD-1 and its ligands on immune cell infiltration and other immune checkpoints, and investigated the prognostic potential of PD-1, PD-L1, and PD-L2 in HCC to explore their prognostic potential as predictors of survival.

## MATERIALS AND METHODS

### Analyzed datasets

The RNA expression, copy-number variants, and clinical information of HCC individuals of TCGA datasets were obtained *via* UCSC XENA (<https://xena.ucsc.edu/>). We marked gene expression data as transcripts per million reads (TPM). Clinical information included age, gender, tumor stage, recurrence, and survival time. We explored the association of PD-1, PD-L1, and PD-L2 expression with these clinical parameters.

### Co-expression gene and enrichment analyses

Weighted correlation network analysis (WGCNA)<sup>[20]</sup> represents a method to identify gene-gene interactions considering the weighted aspect. Co-expression genes identified by the WGCNA method can generate more specific and robust results. Through WGCNA exploration, we analyzed the genes co-expressed with PD-1, PD-L1, and PD-L2. Gene expression variation was evaluated *via* median absolute deviation (MAD). After identification of the interaction genes, protein-protein interaction investigation was performed to identify the interaction of genes with STRING (<https://string-db.org>)<sup>[21]</sup>. Enrichment analysis is a method for analyzing gene expression information. It classifies genes based on the data of gene annotations to help understand the way that genes function. Using clusterprofiler, we adopted the Gene Ontology to perform enrichment analysis<sup>[22]</sup>.

### Association of immune regulators with PD-1/PD-L1/PD-L2

Multiple studies have reported that immune cell infiltration was related to tumor in many aspects. MCP-counter is a R package to evaluate immune infiltration of individuals<sup>[23]</sup>. Considering the matrix of gene expression, it generates CD3 + T cells, B lymphocytes, cytotoxic lymphocytes, NK cells, CD8 + T cells, cells derived from monocytes, myeloid dendritic cells, neutrophils, endothelial cells, and fibroblasts for each sample. Thus, the relation of PD-1, PD-L1, and PD-L2 with immune infiltration was investigated. Since immune checkpoints were the key indicators of immune status, we then explored the relation of PD-1/PD-L1/PD-L2 with immune checkpoints.

### Statistical analysis

In the present study, we performed statistical analyses *via* R language (<https://www.r-project.org/>) by using important packages. Rank sum test was adopted to assess the differential expression of PD-1, PD-L1, and PD-L2 in different groups. Spearman correlation analysis was adopted to investigate the associations of PD-1, PD-L1, and PD-L2 expression with immune infiltration and immune checkpoints. Survival analysis was then performed by Kaplan-Meier method and log-rank test. Other figures were plotted with several R packages, including ComplexHeatmap<sup>[24]</sup>, circlize<sup>[25]</sup>, and corrrplot. The multiple tests were all corrected using BH method.  $P < 0.05$  was considered significant.



## RESULTS

### PD-1/PD-L1/PD-L2 expression in different clinical subgroups

After the preliminary screening, we finally included 374 HCC patients from the TCGA database for the following analysis. Using TCGA datasets, we analyzed the PD-1/PD-L1/PD-L2 expression in different groups according to the clinical data. As shown in [Figure 1A](#), PD-1 and PD-L2 expression was correlated with the recurrence events of HCC patients ( $P = 0.005$ ), while the expression of PD-L1 showed no significant association with recurrence events ( $P = 0.155$ ). Moreover, all of the three genes showed no correlation with clinical stage ( $P = 0.95$ ,  $0.97$ , and  $0.475$ , respectively) ([Figure 1B](#)).

Survival of the HCC patients showed no significant difference in the overall survival (OS) analysis of patients with high PD-1/PD-L1/PD-L2 expression (defined as over median expression) or low PD-1/PD-L1/PD-L2 expression (defined as below median expression) with a hazard ratio (HR) of 1.01, 0.88, and 0.91, respectively ( $P > 0.05$ ) ([Figure 1C](#)).

### Copy number variation and mutation analysis

Copy number variants of 270 patients derived from the TCGA database were analyzed. A total of 20 mutations with high occurrence were selected ([Figure 2](#)). Expression of PD-1/PD-L1/PD-L2 was not directly correlated to the total mutation load of each patient ( $r = 0.02/0.07/0.04$ , respectively). However, after differential expression analysis, mutations of genes including calcium voltage-gated channel subunit alpha1 E (*CACNA1E*,  $P = 0.046$ ), catenin beta 1 (*CTNNB1*,  $P = 0.020$ ), ryanodine receptor 2 (*RYR2*,  $P = 0.030$ ), tumor suppressor protein p53 (*TP53*,  $P = 0.016$ ), and Titin (*TTN*,  $P = 0.014$ ) could alter PD-1 expression; *TP53* mutations ( $P = 0.003$ ) correlated with high PD-L1 expression; *TP53* ( $P = 0.041$ ) and *TTN* mutations ( $P = 0.028$ ) were associated with PD-L2 expression ([Table 1](#)).

### Co-expression analysis of genes associated with PD-1, PD-L1, and PD-L2

Using WGCNA, we analyzed the co-expressed genes with PD-1, PD-L1, and PD-L2. The connectivity among genes had a scale-free network distribution when the value of soft thresholding power  $\beta$  equals to 14 ([Figure 3A](#)). Altogether 22 modules were obtained according to WGCNA analysis ([Figure 3B](#)). Among these modules, PD-1 belonged to the brown module while PD-L1 and PD-L2 belonged to the blue module. We finally obtained 371 genes that interacted with PD-1 and 747 PD-L1/PD-L2 related genes. Then, we verified the two module interaction in STRING datasets ([Figure 3C](#)). After verification, PD-L1/PD-L2 interacted with 7 genes while PD-1 showed co-expression with 39 genes ([Supplementary Table 1](#)). Finally, we selected the interacted genes for further enrichment analysis. PD-1 related genes were mainly enriched in biological processes of T cell activation, regulation of T cell activation, regulation of lymphocyte activation, leukocyte cell-cell adhesion, cytosolic calcium ion concentration, T cell receptor signaling pathway, calcium ion homeostasis, release of sequestered calcium ion into cytosol, and cellular defense response; PD-L1/PD-L2 related genes were enriched in cellular defense response, positive regulation of cell activation, regulation of cell-cell adhesion, interferon-gamma-mediated signaling pathway, negative regulation of activated T cell proliferation, interleukin-10 production, and response to hypoxia ([Figure 3D](#) and [Table 2](#)).

### PD-1/PD-L1/ PD-L2 expression and immune infiltration

Using MCP-counter, we evaluated the profiles of immune infiltration among various subtypes and stages of HCC ([Figure 4](#)). The heatmap in [Figure 4](#) (middle) shows the associations of PD-1, PD-L1, and PD-L2 with immune cell populations according to analysis of the transcriptomic data. The results indicated that PD-1 was mainly related with CD8 T cells ( $r = 0.608$ ) and cytotoxic lymphocytes ( $r = 0.60$ ); PD-L1 was mainly related with fibroblasts ( $r = 0.671$ ); PD-L2 showed a significant correlation with myeloid dendritic cells ( $r = 0.805$ ). Moreover, we also presented the correlation among different infiltrated immune cell types. As shown in the right correlation heatmap in [Figure 4](#), CD8 T cells were associated with cytotoxic lymphocytes ( $r = 0.93$ ).

### PD-1/PD-L1/PD-L2 expression and immune checkpoints

As previous reported, the immune checkpoints of the PD1/PD-L1/PDL2 regulatory axis mainly included CD28, CD80, CD86, CTLA4, RGMB, CD58, CD27, CD70, HLA-A, and CD74. We then analyzed the correlation between PD-1/PD-L1/PD-L2 expression and these important immune checkpoints. As shown in [Figure 5](#) and [Table 3](#), PD-1 was mainly associated with CTLA4 ( $r = 0.828$ ) and CD27 ( $r = 0.855$ ), PD-L1 correlated with

Table 1 Co-mutation analysis for programmed death 1/programmed death ligand 1/programmed death ligand 2

Gene	Mutation	PD-1 (mean $\pm$ SD)	PD-1 <i>P</i> value	PD-L1 (mean $\pm$ SD)	PD-L1 <i>P</i> value	PD-L2 (mean $\pm$ SD)	PD-L2 <i>P</i> value
ABCA13	NO	0.38 $\pm$ 1.47		0.14 $\pm$ 0.54		0.34 $\pm$ 3.31	
	Yes	0.3 $\pm$ 0.69	0.675	0.1 $\pm$ 0.21	0.431	0.08 $\pm$ 0.1	0.705
ALB	NO	0.38 $\pm$ 1.46		0.14 $\pm$ 0.53		0.33 $\pm$ 3.26	
	Yes	0.11 $\pm$ 0.23	0.242	0.12 $\pm$ 0.27	0.545	0.11 $\pm$ 0.27	0.121
APOB	NO	0.39 $\pm$ 1.46		0.14 $\pm$ 0.53		0.34 $\pm$ 3.27	
	Yes	0.04 $\pm$ 0.05	0.102	0.05 $\pm$ 0.03	0.858	0.05 $\pm$ 0.04	0.835
ARID1A	NO	0.37 $\pm$ 1.43		0.14 $\pm$ 0.52		0.33 $\pm$ 3.22	
	Yes	0.59 $\pm$ 1.03	0.316	0.1 $\pm$ 0.14	0.699	0.13 $\pm$ 0.17	0.495
AXIN1	NO	0.37 $\pm$ 1.43		0.14 $\pm$ 0.52		0.32 $\pm$ 3.2	
	Yes	0.16 $\pm$ 0.08	0.206	0.06 $\pm$ 0.02	0.418	0.03 $\pm$ 0	0.741
CACNA1E	NO	0.39 $\pm$ 1.48		0.14 $\pm$ 0.53		0.34 $\pm$ 3.32	
	Yes	0.13 $\pm$ 0.44	0.046	0.09 $\pm$ 0.26	0.083	0.07 $\pm$ 0.17	0.076
CSMD3	NO	0.35 $\pm$ 1.42		0.14 $\pm$ 0.53		0.34 $\pm$ 3.29	
	Yes	0.67 $\pm$ 1.49	0.286	0.07 $\pm$ 0.09	0.981	0.12 $\pm$ 0.14	0.633
CTNNB1	NO	0.43 $\pm$ 1.61		0.17 $\pm$ 0.6		0.42 $\pm$ 3.75	
	Yes	0.22 $\pm$ 0.75	0.02	0.06 $\pm$ 0.1	0.428	0.07 $\pm$ 0.09	0.554
FLG	NO	0.39 $\pm$ 1.48		0.1 $\pm$ 0.27		0.13 $\pm$ 0.55	
	Yes	0.22 $\pm$ 0.52	0.78	0.49 $\pm$ 1.53	0.893	2.34 $\pm$ 10.8	0.204
LRP1B	NO	0.39 $\pm$ 1.48		0.14 $\pm$ 0.54		0.34 $\pm$ 3.32	
	Yes	0.2 $\pm$ 0.41	0.519	0.1 $\pm$ 0.17	0.554	0.12 $\pm$ 0.3	0.886
MUC16	NO	0.32 $\pm$ 1.31		0.14 $\pm$ 0.55		0.35 $\pm$ 3.47	
	Yes	0.64 $\pm$ 1.93	0.697	0.13 $\pm$ 0.3	0.521	0.18 $\pm$ 0.53	0.997
MUC4	NO	0.38 $\pm$ 1.44		0.14 $\pm$ 0.52		0.33 $\pm$ 3.23	
	Yes	0.13 $\pm$ 0.3	0.196	0.1 $\pm$ 0.11	0.641	0.08 $\pm$ 0.1	0.753
OBSCN	NO	0.4 $\pm$ 1.49		0.1 $\pm$ 0.27		0.14 $\pm$ 0.55	
	Yes	0.15 $\pm$ 0.42	0.267	0.46 $\pm$ 1.46	0.087	2.13 $\pm$ 10.37	0.518
PCLO	NO	0.33 $\pm$ 1.3		0.14 $\pm$ 0.54		0.35 $\pm$ 3.36	
	Yes	0.75 $\pm$ 2.29	0.712	0.1 $\pm$ 0.22	0.422	0.1 $\pm$ 0.17	0.974
RYY1	NO	0.34 $\pm$ 1.29		0.14 $\pm$ 0.54		0.34 $\pm$ 3.31	
	Yes	0.74 $\pm$ 2.59	0.101	0.05 $\pm$ 0.04	0.872	0.06 $\pm$ 0.05	0.705
RYY2	NO	0.36 $\pm$ 1.41		0.13 $\pm$ 0.5		0.34 $\pm$ 3.34	
	Yes	0.47 $\pm$ 1.58	0.03	0.24 $\pm$ 0.67	0.113	0.12 $\pm$ 0.2	0.321
SPTA1	NO	0.39 $\pm$ 1.48		0.14 $\pm$ 0.54		0.33 $\pm$ 3.31	
	Yes	0.18 $\pm$ 0.4	0.737	0.1 $\pm$ 0.21	0.201	0.15 $\pm$ 0.36	0.384
TP53	NO	0.3 $\pm$ 1.22		0.08 $\pm$ 0.18		0.1 $\pm$ 0.28	
	Yes	0.65 $\pm$ 2.04	0.016	0.35 $\pm$ 1.08	0.003	1.19 $\pm$ 7.04	0.041
TTN	NO	0.45 $\pm$ 1.62		0.15 $\pm$ 0.59		0.4 $\pm$ 3.66	
	Yes	0.14 $\pm$ 0.38	0.014	0.08 $\pm$ 0.18	0.291	0.08 $\pm$ 0.2	0.028
XIRP2	NO	0.31 $\pm$ 1.12		0.13 $\pm$ 0.51		0.31 $\pm$ 3.31	
	Yes	1.02 $\pm$ 3.15	0.26	0.19 $\pm$ 0.63	0.235	0.39 $\pm$ 1.54	0.329

PD-1: Programmed death 1; PD-L1: Programmed death ligand 1; PD-L2: Programmed death ligand 2; SD: Standard deviation.

CD80 ( $r = 0.675$ ) and CD86 ( $r = 0.695$ ), and PD-L2 correlated with CD86 ( $r = 0.797$ ) and CD28 ( $r = 0.714$ ).

## DISCUSSION

Previous clinical trials indicated that immune checkpoint blockade therapies demonstrated satisfactory curative effect for multiple types of cancer, with persistent responses and acceptable toxicity<sup>[3]</sup>. However, only part of individuals who received antibody immunotherapy greatly benefit from the treatment<sup>[26]</sup>. It is therefore urgent to unravel the underlying signaling pathway of important immune checkpoints such as PD-1 and its ligands PD-L1 and PD-L2 to improve the therapeutic sensitivity. Here, we presented an integrative analysis of PD-1, PD-L1, and PD-L2 based on the HCC data from TCGA. We identified potential molecular and genetic alterations correlating with the PD-1/PD-L1/PD-L2 and revealed their biological functions. The relation of PD-1/PD-L1/PD-L2 with immune infiltration and HCC survival were also explored to elucidate their role as prognostic biomarkers.

We first described the PD-1/PD-L1/PD-L2 expression profiles in different clinical subtypes. The results indicated that PD-1 and PD-L2 expression was associated with the recurrence events of HCC patients. However, none of the three genes showed a significant correlation with clinical stage. In a previous research of 217 HCC patients, PD-L1 expression demonstrated a significant relation with multiple markers of cancer aggressiveness including satellite nodules, macrovascular invasion, microvascular invasion, and poor differentiation<sup>[27]</sup>. Besides, PD-1 and PD-L1 expression was upregulated in HCC tissues compared with adjacent normal tissues, which was positively related with the clinical stage and lymph node metastasis, but negatively related with the survival of HCC patients<sup>[28]</sup>. These results suggested that the PD-1/PD-L1/PD-L2 axis might correlate with multiple clinical parameters of HCC.

Prognostic analysis of the HCC patients showed no significant association between PD-1/PD-L1/PD-L2 expression and the OS of HCC patients. In a study of 85 HCC patients, PD-L1 or PD-L2 expression was associated with a poor survival according to immunohistochemical investigation<sup>[29-31]</sup>. Elevated PD-L1 expression has been reported to be an independent adverse prognosis predictor of disease-free survival in addition to previously reported factors<sup>[32]</sup>. One study performing immunohistochemical staining of 136 HCC tissues demonstrated that PD-L1 high expression exhibited a significant correlation with clinical and pathological parameters indicating worse HCC progression and prognosis<sup>[33]</sup>. In another study of PD-L1 in HCC, however, PD-L1 expression was inversely correlated with P53 and associated with a longer survival of patients with HCC<sup>[34]</sup>. There was also a study reporting that PD-L1 expression failed to have a markedly significant prognostic association with survival in 143 patients with HCC<sup>[35]</sup>. According to the analysis of TCGA data and previous studies on PD-1/PD-L1/PD-L2, the relation of PD-1/PD-L1/PD-L2 expression with HCC prognosis still requires to be confirmed in future studies with large samples.

Based on the copy number variations and mutation analysis, a total of 20 mutations with high occurrence were selected. Expression of PD-1/PD-L1/PD-L2 was not directly correlated to the total mutation load of each patient. After differential expression analysis, however, mutations of genes including *CACNA1E*, *CTNNB1*, *RYR2*, *TP53*, and *TTN* could alter PD-1 expression; *TP53* mutations correlated with high PD-L1 expression, and *TP53* and *TTN* mutations were associated with PD-L2 expression. Interestingly, *TP53* mutation significantly increased the expression of PD-1, PD-L1, and PD-L2, suggesting a probable molecular link between *TP53* and PD-1 axis regulation. Admittedly, change of PD-1-PD-L1 immune regulator and p53 alternation promote cancer development in activated B-cell diffuse large B-cell lymphomas<sup>[36]</sup>. In addition, the prognosis of Kras-p53-associated lung cancer is regulated by MEK and PD-1/PD-L1 immune checkpoint<sup>[37-40]</sup>. The underlying mechanisms of critical mutations such as *TP53*, *TTN*, and *CTNNB1* mutations in modulating PD-1 signaling might provide novel strategies for immunotherapies. In the future, we may be able to perform different immunotherapies by stratifying patients based on the mutation types of these genes.

Using WGCNA, we next analyzed the co-expressed genes with PD-1, PD-L1, and PD-L2. After verification, PD-L1/PD-L2 interacted with 7 genes while PD-1 showed

Table 2 GO analysis for programmed death 1/programmed death ligand 1/programmed death ligand 2 co-expression gene

ID	Description	Gene ratio	P value	P adjust	Gene ID	Count
GO: 0042110	T cell activation	16/27	$1.23 \times 10^{-19}$	$1.10 \times 10^{-16}$	PTPN6/CD3E/LCK/PDCD1/CD3G/IDO1/TNFRSF4/TIGIT/PTPRC/CD40LG/PRDM1/EOMES/CD2/CD5/CD8A/IRF4	16
GO: 0050863	Regulation of T cell activation	12/27	$4.55 \times 10^{-15}$	$2.05 \times 10^{-12}$	PTPN6/CD3E/LCK/PDCD1/IDO1/TIGIT/PTPRC/CD40LG/PRDM1/CD2/CD5/IRF4	12
GO: 0051249	Regulation of lymphocyte activation	13/27	$2.40 \times 10^{-14}$	$5.40 \times 10^{-12}$	PTPN6/CD3E/LCK/PDCD1/IDO1/TNFRSF4/TIGIT/PTPRC/CD40LG/PRDM1/CD2/CD5/IRF4	13
GO: 1903037	Regulation of leukocyte cell-cell adhesion	10/27	$5.69 \times 10^{-12}$	$1.02 \times 10^{-9}$	PTPN6/CD3E/LCK/PDCD1/IDO1/TIGIT/PTPRC/CD40LG/CD5/ITGA4	10
GO: 0007159	Leukocyte cell-cell adhesion	10/27	$1.68 \times 10^{-11}$	$2.53 \times 10^{-9}$	PTPN6/CD3E/LCK/PDCD1/IDO1/TIGIT/PTPRC/CD40LG/CD5/ITGA4	10
GO: 0007204	Positive regulation of cytosolic calcium ion concentration	9/27	$3.25 \times 10^{-10}$	$2.66 \times 10^{-8}$	PTPN6/LCK/CD19/PTPRC/CXCR3/FASLG/CXCR4/CD52/CXCL9	9
GO: 0050852	T cell receptor signaling pathway	9/27	$1.56 \times 10^{-9}$	$1.00 \times 10^{-7}$	PTPN6/CD3E/LCK/HLA-DQB1/CD3G/PTPRC/CD247	7
GO: 0055074	Calcium ion homeostasis	9/27	$1.08 \times 10^{-8}$	$4.87 \times 10^{-7}$	PTPN6/LCK/CD19/PTPRC/CXCR3/FASLG/CXCR4/CD52/CXCL9	9
GO: 0051209	Release of sequestered calcium ion into cytosol	6/27	$1.42 \times 10^{-8}$	$5.81 \times 10^{-7}$	PTPN6/LCK/CD19/PTPRC/FASLG/CXCL9	6
GO: 0006968	Cellular defense response	5/27	$2.52 \times 10^{-8}$	$8.11 \times 10^{-7}$	TNFRSF4/CD19/PRF1/CXCL9/SH2D1A	5
GO: 0050867	Positive regulation of cell activation	5/8	$2.00 \times 10^{-7}$	$5.23 \times 10^{-5}$	PDCD1LG2/JAK2/CD274/ITPKB/PDGFRB	5
GO: 0022407	Regulation of cell-cell adhesion	5/8	$2.11 \times 10^{-7}$	$5.23 \times 10^{-5}$	PDCD1LG2/JAK2/CD44/CD274/ITPKB	5
GO: 0045785	Positive regulation of cell adhesion	5/8	$2.36 \times 10^{-7}$	$5.23 \times 10^{-5}$	PDCD1LG2/JAK2/CD44/CD274/ITPKB	5
GO: 0060333	Interferon-gamma-mediated signaling pathway	3/8	$6.13 \times 10^{-6}$	0.000528087	JAK2/CD44/NCAM1	3
GO: 0007159	Leukocyte cell-cell adhesion	4/8	$6.35 \times 10^{-6}$	0.000528087	PDCD1LG2/CD44/CD274/ITPKB	4
GO: 2001269	Positive regulation of cysteine-type endopeptidase activity involved in apoptotic signaling pathway	2/8	$7.36 \times 10^{-6}$	0.000543547	JAK2/FAS	2
GO:	Negative regulation of activated T cell proliferation	2/8	$8.99 \times 10^{-6}$	0.000597772	PDCD1LG2/CD274	2

0046007						
GO: 0032693	Negative regulation of interleukin-10 production	2/8	$2.22 \times 10^{-5}$	0.001230174	PDCD1LG2/CD274	2
GO: 0032516	Positive regulation of phosphoprotein phosphatase activity	2/8	$3.42 \times 10^{-5}$	0.001626763	JAK2/PDGFRB	2
GO: 0055093	Response to hyperoxia	2/8	$3.42 \times 10^{-5}$	0.001626763	FAS/PDGFRB	2

$P < 0.05$  was considered significant.

co-expression with 39 genes. PD-1 related genes were mainly enriched in T cell activation, lymphocyte activation, leukocyte cell-cell adhesion, cytosolic calcium ion concentration, T cell receptor signaling pathway, calcium ion homeostasis, release of sequestered calcium ion into cytosol, and cellular defense response; PD-L1/PD-L2 related genes were enriched in cellular defense response, cell activation, cell-cell adhesion, interferon-gamma-mediated signaling pathway, negative regulation of activated T cell proliferation, interleukin-10 production, and response to hyperoxia. As indicated by the enrichment analysis, PD-1/PD-L1/PD-L2 signaling is a key regulator of T cell activation and other important lymphocyte functions, which was consistent with the results of multiple previous investigations<sup>[41-44]</sup>. It is worthy elucidating the immune modulating mechanisms of PD-1 axis in the future to unravel its specific role in cancer immunity.

Immune cell infiltration reflects the immune microenvironment around the tumor tissues and is reportedly correlated with outcome of cancer progression. We subsequently evaluated PD-1/PD-L1/PD-L2 expression and immune infiltration in HCC, the results of which suggested that PD-1 was correlated with CD8 T cells and cytotoxic lymphocytes, PD-L1 was related with fibroblasts, and PD-L2 was significantly correlated with myeloid dendritic cells. It has been reported that CD8+ cytotoxic T lymphocytes greatly increase PD-L1 expression on cancer cell lines, and PD-L1 expression and CD8+ T-cell density showed a significant positive correlation in HCC patients<sup>[45]</sup>. Besides, PD-1 and PD-L1 expression was suggested to be significantly related to high levels of CD8+ tumor-infiltrating lymphocytes (TILs)<sup>[32,44]</sup>. In addition to T lymphocytes, PD-1 expression on dendritic cells has been found to restrict CD8+ T cell function and anti-cancer immunity<sup>[46]</sup>. Understanding the correlation of PD-1/PD-L1/PD-L2 immune checkpoints with immune cell infiltration might greatly benefit the tumor immunotherapy targeting PD-1 signaling. After analyzing the immune checkpoints of PD1/PD-L1/PDL2 regulatory axis including CD28, CD74, CD86, CD58, CTLA4, RGMB, CD70, CD27, CD80, and HLA-A, we suggested that PD-1 was mainly associated with CD27 and CTLA4, PD-L1 related with CD86 as well as CD80, and PD-L2 related with CD28 and CD86. The combined inhibition of different immune checkpoints might generate more satisfactory clinical outcome. Thus, future studies



**Table 3 Correlation analysis for immune checkpoints and programmed death 1/programmed death ligand 1/programmed death ligand 2**

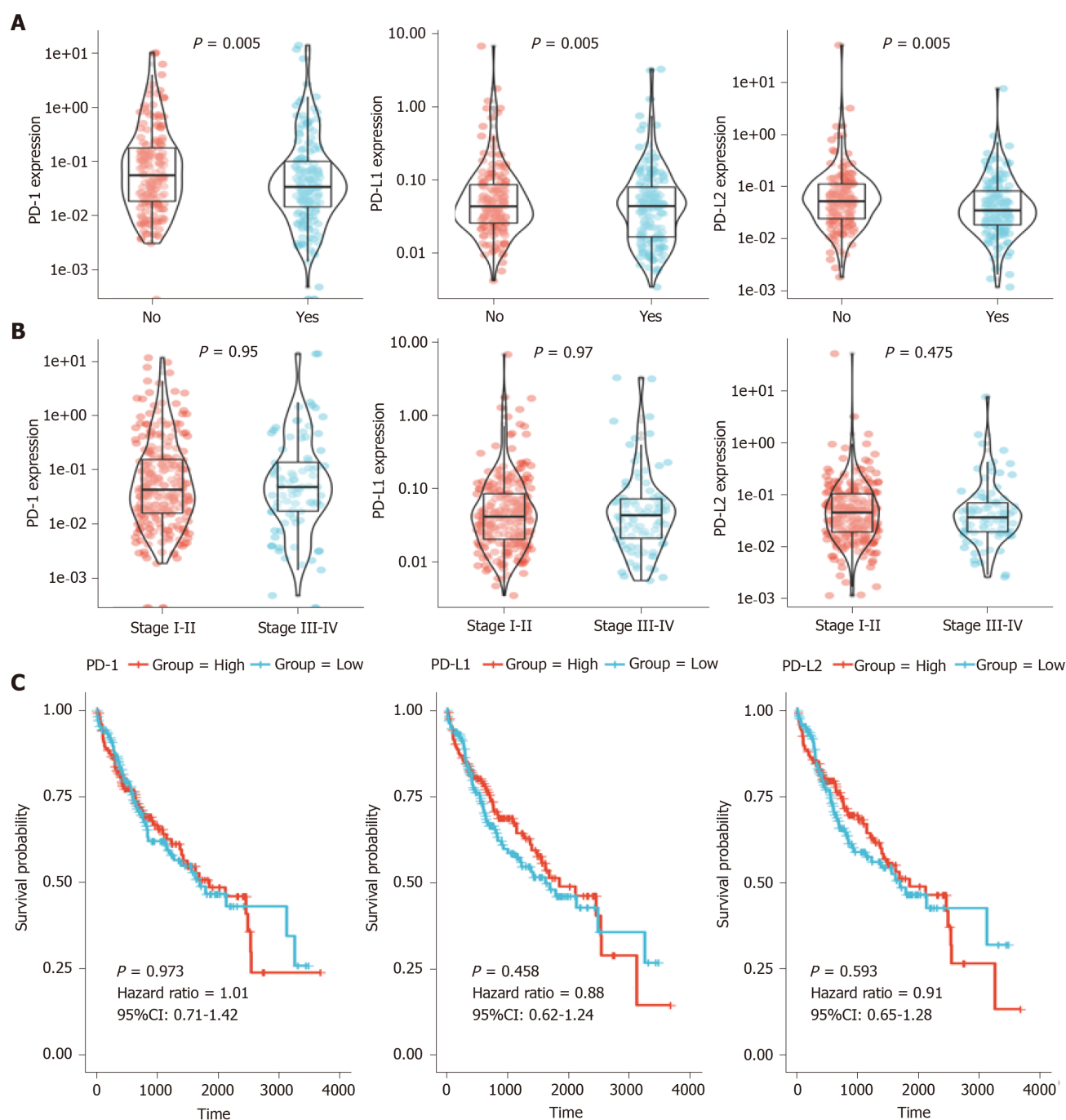
	PD-1 <i>r</i>	PD-1 <i>padj</i>	PD-L1 <i>r</i>	PD-L1 <i>padj</i>	PD-L2 <i>r</i>	PD-L2 <i>padj</i>
CD28	0.57465488	$4.28 \times 10^{-34}$	0.6660232	$9.08 \times 10^{-49}$	0.71414661	$6.86 \times 10^{-59}$
CD80	0.63623359	$1.59 \times 10^{-43}$	0.67510422	$2.19 \times 10^{-50}$	0.70070417	$4.16 \times 10^{-56}$
CD86	0.72311298	$2.38 \times 10^{-61}$	0.69521618	$2.70 \times 10^{-54}$	0.79715204	$1.59 \times 10^{-82}$
CTLA4	0.82827652	$6.53 \times 10^{-95}$	0.53400839	$9.77 \times 10^{-29}$	0.62325084	$2.09 \times 10^{-41}$
RGMB	0.08079832	0.11878686	0.31356282	$5.62 \times 10^{-10}$	0.15655839	0.00239497
CD58	0.4020193	$6.49 \times 10^{-16}$	0.44699953	$1.00 \times 10^{-19}$	0.34510312	$7.46 \times 10^{-12}$
CD27	0.8554091	$2.51 \times 10^{-107}$	0.564041	$1.70 \times 10^{-32}$	0.70361681	$1.23 \times 10^{-56}$
CD70	0.73757481	$6.84 \times 10^{-65}$	0.49791513	$1.14 \times 10^{-24}$	0.5810653	$5.35 \times 10^{-35}$
HLA-A	0.49005962	$6.82 \times 10^{-24}$	0.45628329	$1.56 \times 10^{-20}$	0.47535158	$2.20 \times 10^{-22}$
CD74	0.62377393	$1.71 \times 10^{-41}$	0.57693716	$3.59 \times 10^{-34}$	0.68544635	$6.61 \times 10^{-53}$

PD-1: Programmed death 1; PD-L1: Programmed death ligand 1; PD-L2: Programmed death ligand 2.

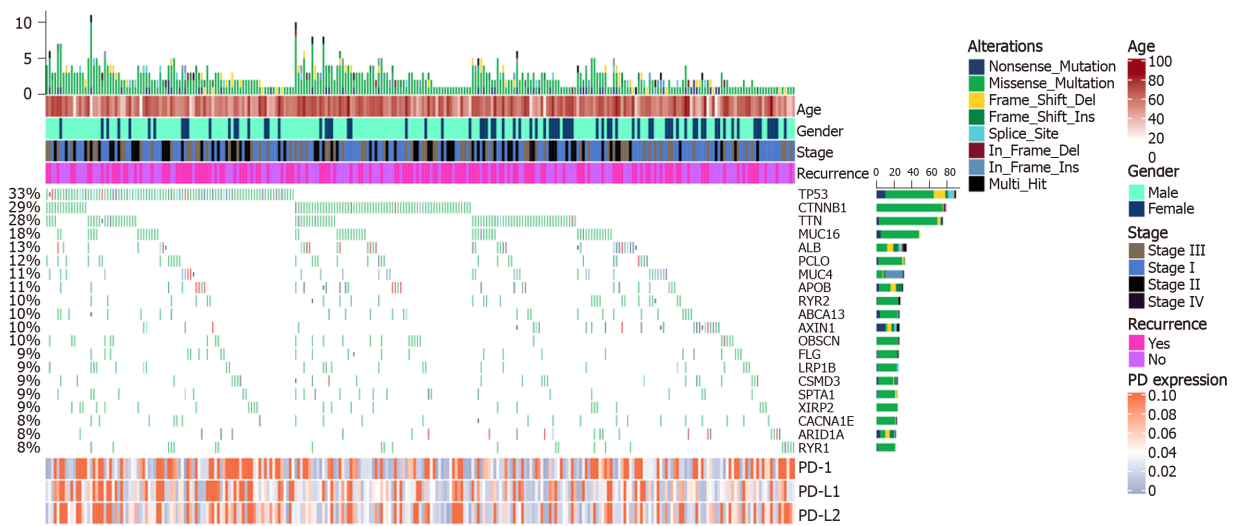
focusing on PD-1/PD-L1/PD-L2 related immune checkpoints including CTLA4, CD27, CD80, CD86, and CD28 are required to obtain an optimal immunotherapy effect.

## CONCLUSION

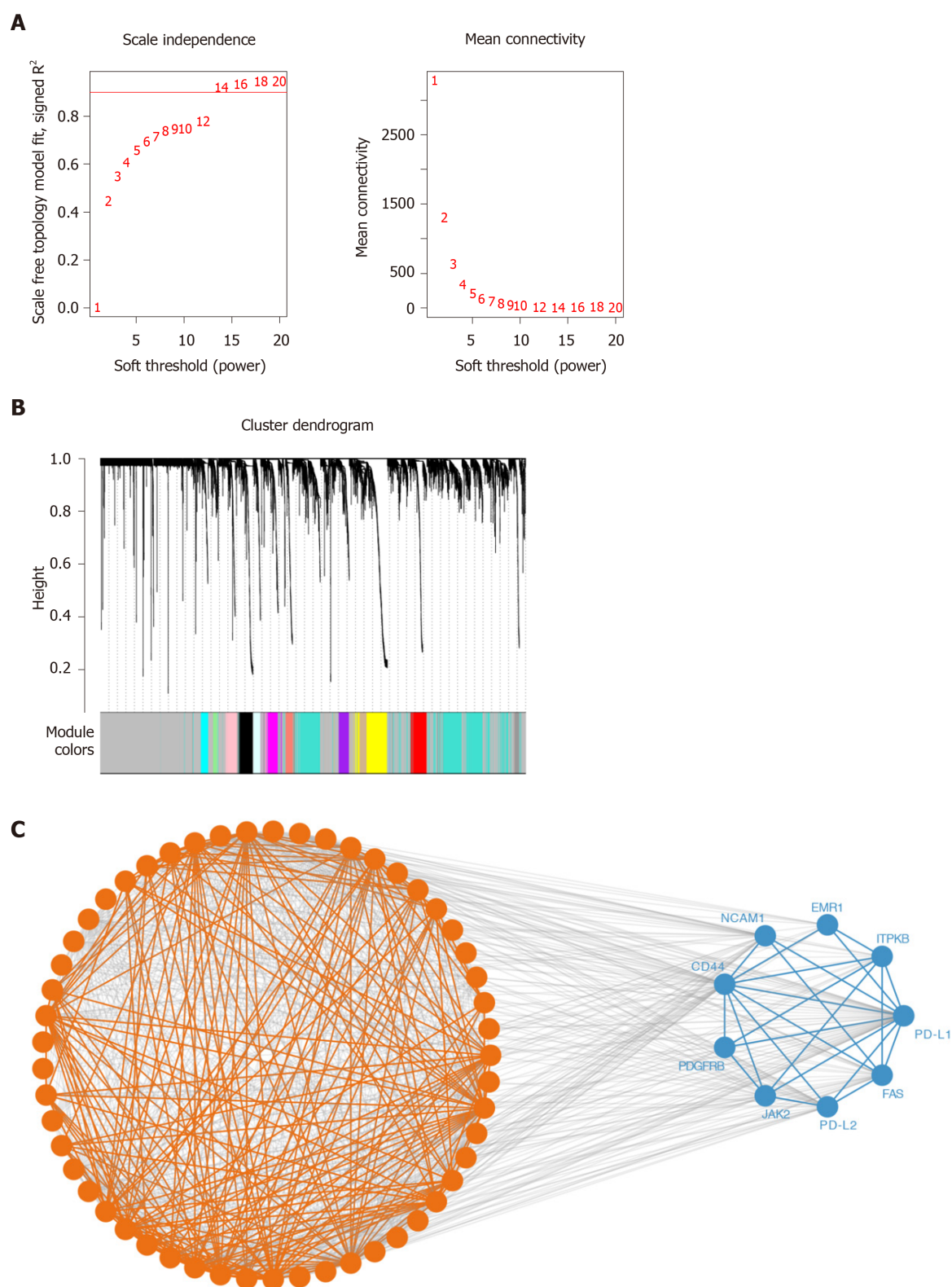
Mutations of *CACNA1E*, *CTNNB1*, *RYR2*, *TP53*, and *TTN* alter PD-1/PD-L1/PD-L2 expression profiles in HCC. The limitation on the effect of mutations on gene expression is that only statistical differences have been observed so far. We will conduct follow-up research on its detailed mechanism. PD-1/PD-L1/PD-L2 related genes are enriched in the biological processes of T cell activation, cell-cell adhesion, and other important lymphocyte effects. In addition, PD-1/PD-L1/PD-L2 is related to immune infiltration of CD8 T cells, cytotoxic lymphocytes, fibroblasts, and myeloid dendritic cells. Immune checkpoints CTLA4, CD27, CD80, CD86, and CD28 are significantly associated with PD-1/PD-L1/PD-L2 axis. Clinically, PD-1 and PD-L2 expression is correlated with recurrence, but there is no significant correlation between PD-1/PD-L1/PD-L2 expression and survival of HCC patients.

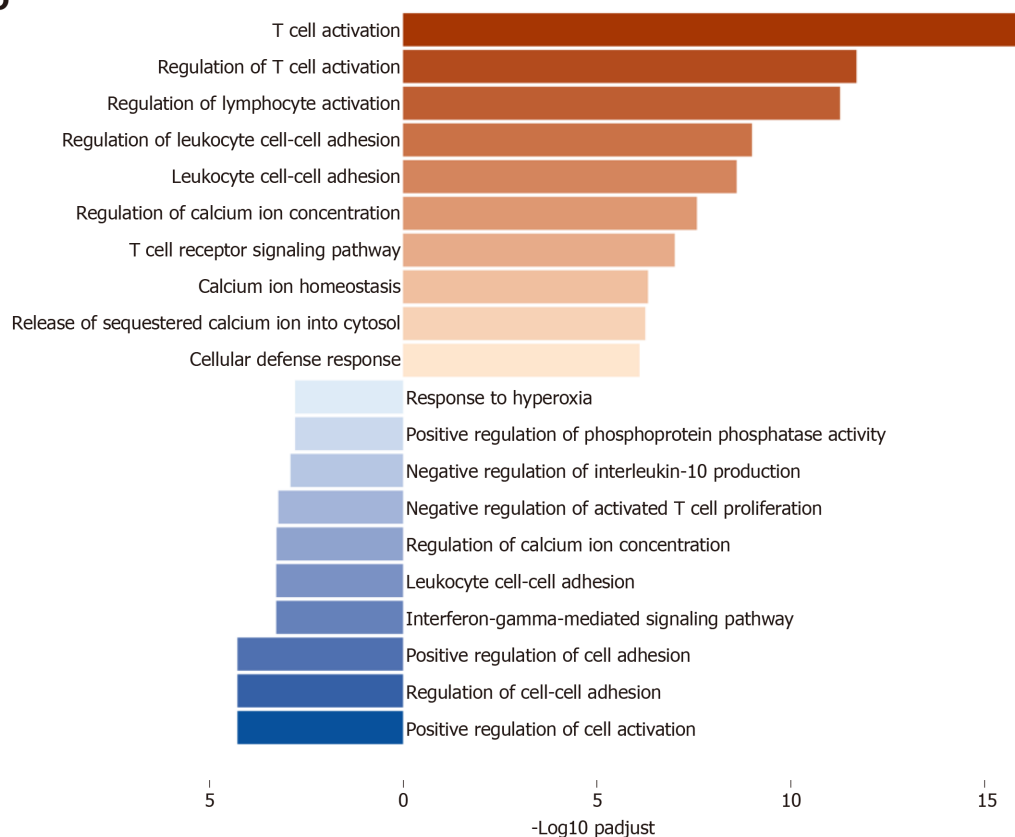


**Figure 1 Relationship between gene expression and clinical data.** A: Programmed death 1 (PD-1)/programmed death ligand 1 (PD-L1)/programmed death ligand 2 (PD-L2) expression in recurrence and non-recurrence groups; B: PD-1/PD-L1/PD-L2 expression in stage I-II and stage III-IV groups; C: Prognostic analysis of PD-1/PD-L1/PD-L2 in hepatocellular carcinoma. The median of the expression value was selected as the cut-off point. KM plotter was used for prognosis analysis. PD-1: Programmed death 1; PD-L1: Programmed death ligand 1; PD-L2: Programmed death ligand 2; CI: Confidence interval.



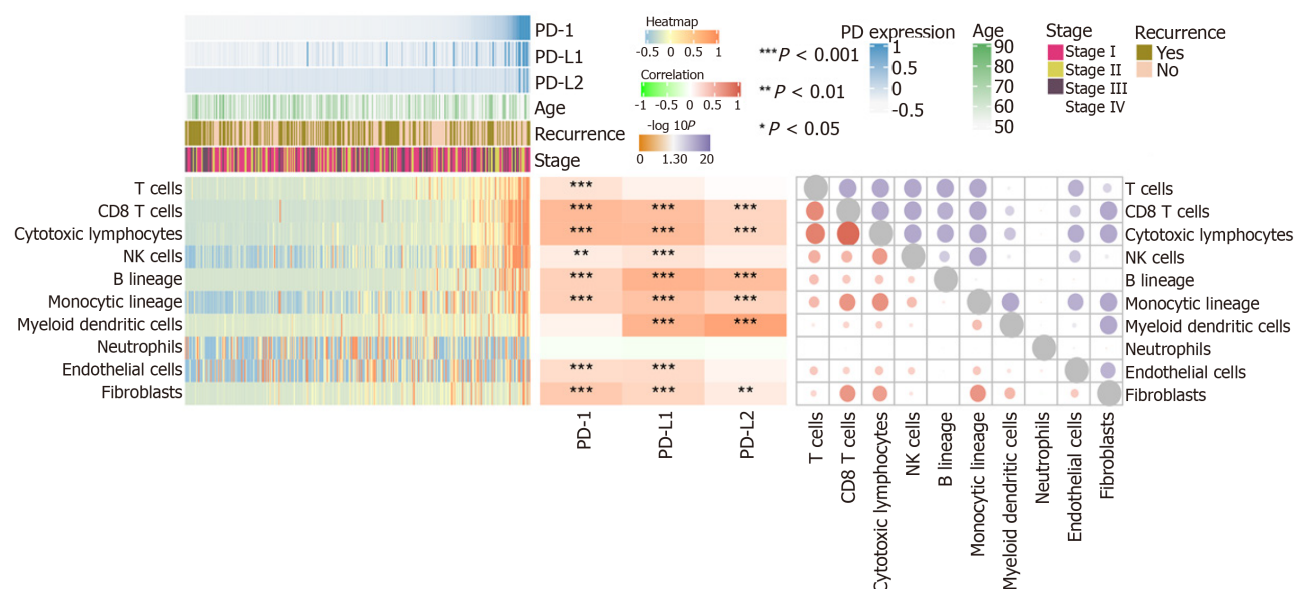
**Figure 2 Co-mutation plot of highly frequent mutations in liver cancer.** Mutational frequencies are given in a bar plot beside the co-mutation plot. Overall mutation load as the total number of mutations in each patient is presented in the top barplot. Programmed death 1/programmed death ligand 1/programmed death ligand 2 expression is illustrated in a heatmap in the panel below. Clinical data including age, stage, and recurrence event are shown in the top panel. TP53: Tumor suppressor protein p53; CTNNB1: Catenin beta 1; TTN: TITIN; CACNA1E: Calcium voltage-gated channel subunit alpha 1 E; RYR: Ryanodine receptor; PD-1: Programmed death 1; PD-L1: Programmed death ligand 1; PD-L2: Programmed death ligand 2.



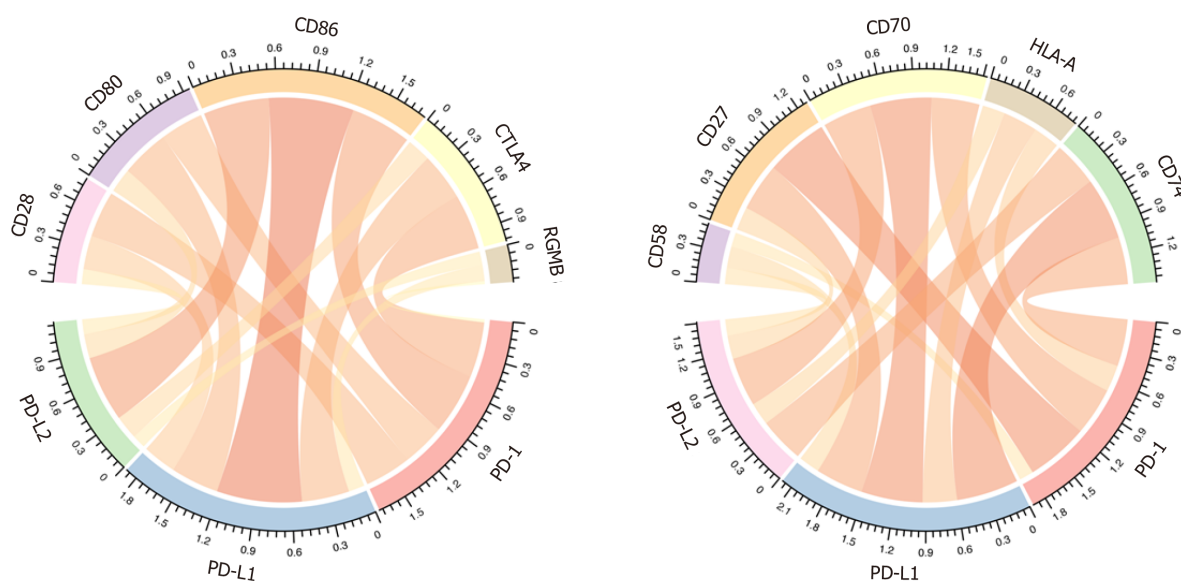
**D**

**Figure 3 Co-expression analysis of genes associated with programmed death 1, programmed death ligand 1, and programmed death ligand 2.** The weighted correlation network analysis (WGCNA) and string datasets were used to select the co-expressed genes. We used WGCNA to identify gene-related modules, and then used STRING database to determine the true interaction of genes. A: Soft threshold selected in the WGCNA analysis. We selected the threshold for R2 to exceed 0.9 for the first time as the soft threshold, and for subsequent analysis 14 was selected as the threshold; B: Distribution of genes in WGCNA; C: Protein-protein interaction of the co-expression genes in the STRING datasets. We put the module genes obtained by WGCNA analysis into the STRING database for protein interaction analysis; D: Biological processes of Gene Ontology (GO) analysis in the co-expression gene. The top ten enrichment results are used for visualization. PD-L1: Programmed death ligand 1; PD-L2: Programmed death ligand 2.





**Figure 4 Programmed death 1/programmed death ligand 1/programmed death ligand 2 expression and immune infiltration.** The score of immune infiltration is calculated based on the MCP-counter algorithm. The left heatmap shows the immune infiltration score in hepatocellular carcinoma. The lower part is the immune infiltration score in each sample. The upper part is the gene expression of each sample and some common clinical features. The middle heatmap shows the relationship between gene expression and immune infiltration, and the right heatmap shows the relation among immune infiltration. The lower part is the interaction coefficient, and the upper part is the  $-\log_{10}(P \text{ value})$  of the correlation analysis. PD-1: Programmed death 1; PD-L1: Programmed death ligand 1; PD-L2: Programmed death ligand 2; NK: Natural killer.



**Figure 5 Correlation between programmed death 1/programmed death ligand 1/programmed death ligand 2 expression and immune checkpoint genes.** In the correlation diagram, each bar represents the interaction between two genes. The width of the strip represents the size of the correlation coefficient. PD-1: Programmed death 1; PD-L1: Programmed death ligand 1; PD-L2: Programmed death ligand 2.

## ARTICLE HIGHLIGHTS

### Research background

The potential regulating network of programmed death 1 (PD-1)/programmed death ligand 1 (PD-L1)/programmed death ligand 2 (PD-L2) signaling in the immune escape is unclear. We aimed to describe the gene expression profiles related with PD-1 and its ligands PD-L1 and PD-L2 to decipher their possible biological processes in hepatocellular carcinoma (HCC).

### Research motivation

Although satisfactory effect of anti-PD-1/PD-L1 therapy has been observed in several types of cancers, the potential complicated interaction network of PD-1/PD-L1/PD-L2 related genes in immune escape and immune surveillance still remains unclear.

### Research objectives

The aim of the study was to explore the possible mechanism of function of PD-1, PD-L1, and PD-L2 in HCC.

### Research methods

Based on transcriptional data of HCC from TCGA, PD-1/PD-L1/PD-L2 related genes were screened by weighted correlation network analysis and the biological processes of certain genes were enriched. The relation of PD1/PD-L1/PD-L2 expression with immune infiltration and checkpoints was investigated by co-expression analysis. The role of PD-1/PD-L1/PD-L2 in the determination of clinical outcome was also analyzed.

### Research results

Mutations of calcium voltage-gated channel subunit alpha1 E (*CACNA1E*), catenin beta 1 (*CTNNB1*), ryanodine receptor 2 (*RYR2*), tumor suppressor protein p53 (*TP53*), and Titin (*TTN*) altered PD-1/PD-L1/PD-L2 expression profiles in HCC. PD-1/PD-L1/PD-L2 related genes were mainly enriched in biological processes of T cell activation, cell-cell adhesion, and other important lymphocyte effects. In addition, PD-1/PD-L1/PD-L2 was related with immune infiltration of CD8 T cells, cytotoxic lymphocytes, fibroblasts, and myeloid dendritic cells. Immune checkpoints CTLA4, CD27, CD80, CD86, and CD28 were significantly correlated with PD-1/PD-L1/PD-L2 axis. Clinically, PD-1 and PD-L2 expression was correlated with recurrence ( $P = 0.005$  for both), but there was no significant correlation between PD-1/PD-L1/PD-L2 expression and HCC patient survival.

### Research conclusions

Mutations of key genes influence PD-1/PD-L1/PD-L2 expression. PD-1/PD-L1/PD-L2 related genes participate in T cell activation, cell-cell adhesion, and other important lymphocyte effects. Correlation of PD-1/PD-L1/PD-L2 with immune infiltration and other immune checkpoints would expand our understanding of promising anti-PD-1 immunotherapy.

### Research perspectives

Mutations of *CACNA1E*, *CTNNB1*, *RYR2*, *TP53*, and *TTN* altered PD-1/PD-L1/PD-L2 expression profiles in HCC. The limitation on the effect of mutations on gene expression is that only statistical differences have been observed so far. We will conduct follow-up research on its detailed mechanism. PD-1/PD-L1/PD-L2 related genes were enriched in biological processes of T cell activation, cell-cell adhesion, and other important lymphocyte effects. In addition, PD-1/PD-L1/PD-L2 was related with immune infiltration of CD8 T cells, cytotoxic lymphocytes, fibroblasts, and myeloid dendritic cells. Immune checkpoints CTLA4, CD27, CD80, CD86, and CD28 were significantly correlated with PD-1/PD-L1/PD-L2 axis. Clinically, PD-1 and PD-L2 expression was correlated with recurrence, but there was no significant correlation between PD-1/PD-L1/PD-L2 and survival of HCC patients.

## REFERENCES

- 1 Yang Y. Cancer immunotherapy: harnessing the immune system to battle cancer. *J Clin Invest* 2015; **125**: 3335-3337 [PMID: 26325031 DOI: 10.1172/JCI83871]
- 2 Zak KM, Grudnik P, Magiera K, Dömling A, Dubin G, Holak TA. Structural Biology of the Immune Checkpoint Receptor PD-1 and Its Ligands PD-L1/PD-L2. *Structure* 2017; **25**: 1163-1174 [PMID: 28768162 DOI: 10.1016/j.str.2017.06.011]
- 3 Alsaab HO, Sau S, Alzhrani R, Tatiparti K, Bhise K, Kashaw SK, Iyer AK. PD-1 and PD-L1 Checkpoint Signaling Inhibition for Cancer Immunotherapy: Mechanism, Combinations, and Clinical Outcome. *Front Pharmacol* 2017; **8**: 561 [PMID: 28878676 DOI: 10.3389/fphar.2017.00561]
- 4 Iwai Y, Hamanishi J, Chamoto K, Honjo T. Cancer immunotherapies targeting the PD-1 signaling pathway. *J Biomed Sci* 2017; **24**: 26 [PMID: 28376884 DOI: 10.1186/s12929-017-0329-9]
- 5 Keir ME, Butte MJ, Freeman GJ, Sharpe AH. PD-1 and its ligands in tolerance and immunity. *Annu Rev Immunol* 2008; **26**: 677-704 [PMID: 18173375 DOI: 10.1146/annurev.immunol.26.021607.090331]

- 6 **Dyck L**, Mills KHG. Immune checkpoints and their inhibition in cancer and infectious diseases. *Eur J Immunol* 2017; **47**: 765-779 [PMID: 28393361 DOI: 10.1002/eji.201646875]
- 7 **Sia D**, Villanueva A, Friedman SL, Llovet JM. Liver Cancer Cell of Origin, Molecular Class, and Effects on Patient Prognosis. *Gastroenterology* 2017; **152**: 745-761 [PMID: 28043904 DOI: 10.1053/j.gastro.2016.11.048]
- 8 **Yu LX**, Schwabe RF. The gut microbiome and liver cancer: mechanisms and clinical translation. *Nat Rev Gastroenterol Hepatol* 2017; **14**: 527-539 [PMID: 28676707 DOI: 10.1038/nrgastro.2017.72]
- 9 **Allaire M**, Nault JC. Advances in management of hepatocellular carcinoma. *Curr Opin Oncol* 2017; **29**: 288-295 [PMID: 28509806 DOI: 10.1097/CCO.0000000000000378]
- 10 **Hartke J**, Johnson M, Ghabril M. The diagnosis and treatment of hepatocellular carcinoma. *Semin Diagn Pathol* 2017; **34**: 153-159 [PMID: 28108047 DOI: 10.1053/j.semdp.2016.12.011]
- 11 **Iñarrairaegui M**, Melero I, Sangro B. Immunotherapy of Hepatocellular Carcinoma: Facts and Hopes. *Clin Cancer Res* 2018; **24**: 1518-1524 [PMID: 29138342 DOI: 10.1158/1078-0432.CCR-17-0289]
- 12 **Kudo M**. Immune Checkpoint Inhibition in Hepatocellular Carcinoma: Basics and Ongoing Clinical Trials. *Oncology* 2017; **92** Suppl 1: 50-62 [PMID: 28147363 DOI: 10.1159/000451016]
- 13 **Abad-Belando R**, Varas-Lorenzo MJ, Pons-Villardell C, Puig-Torres X, Pla-Alcaraz M, Monleón-Getino A, Sánchez-Vizcaíno-Mengual E. Canalization technique to obtain deep tissue biopsy of gastrointestinal subepithelial tumors as an alternative to conventional known techniques. *Endosc Ultrasound* 2018; **7**: 184-190 [PMID: 28707653 DOI: 10.4103/eus.eus\_13\_17]
- 14 **Shi F**, Shi M, Zeng Z, Qi RZ, Liu ZW, Zhang JY, Yang YP, Tien P, Wang FS. PD-1 and PD-L1 upregulation promotes CD8(+) T-cell apoptosis and postoperative recurrence in hepatocellular carcinoma patients. *Int J Cancer* 2011; **128**: 887-896 [PMID: 20473887 DOI: 10.1002/ijc.25397]
- 15 **Adler DG**. Single-operator experience with a 20-mm diameter lumen apposing metal stent to treat patients with large pancreatic fluid collections from pancreatic necrosis. *Endosc Ultrasound* 2018; **7**: 422-423 [PMID: 30531025 DOI: 10.4103/eus.eus\_39\_18]
- 16 **Zhou G**, Sprengers D, Boor PPC, Doukas M, Schutz H, Mancham S, Pedroza-Gonzalez A, Polak WG, de Jonge J, Gaspersz M, Dong H, Thielemans K, Pan Q, IJzermans JNM, Bruno MJ, Kwekkeboom J. Antibodies Against Immune Checkpoint Molecules Restore Functions of Tumor-Infiltrating T Cells in Hepatocellular Carcinomas. *Gastroenterology* 2017; **153**: 1107-1119. e10 [PMID: 28648905 DOI: 10.1053/j.gastro.2017.06.017]
- 17 **Li H**, Li X, Liu S, Guo L, Zhang B, Zhang J, Ye Q. Programmed cell death-1 (PD-1) checkpoint blockade in combination with a mammalian target of rapamycin inhibitor restrains hepatocellular carcinoma growth induced by hepatoma cell-intrinsic PD-1. *Hepatology* 2017; **66**: 1920-1933 [PMID: 28732118 DOI: 10.1002/hep.29360]
- 18 **Adler DG**. EUS-guided gallbladder drainage: Current status and future prospects. *Endosc Ultrasound* 2018; **7**: 1-3 [PMID: 29451163 DOI: 10.4103/eus.eus\_3\_18]
- 19 **Ma LJ**, Feng FL, Dong LQ, Zhang Z, Duan M, Liu LZ, Shi JY, Yang LX, Wang ZC, Zhang S, Ding ZB, Ke AW, Cao Y, Zhang XM, Zhou J, Fan J, Wang XY, Gao Q. Clinical significance of PD-1/PD-Ls gene amplification and overexpression in patients with hepatocellular carcinoma. *Theranostics* 2018; **8**: 5690-5702 [PMID: 30555574 DOI: 10.7150/thno.28742]
- 20 **Langfelder P**, Horvath S. WGCNA: an R package for weighted correlation network analysis. *BMC Bioinformatics* 2008; **9**: 559 [PMID: 19114008 DOI: 10.1186/1471-2105-9-559]
- 21 **Szklarczyk D**, Morris JH, Cook H, Kuhn M, Wyder S, Simonovic M, Santos A, Doncheva NT, Roth A, Bork P, Jensen LJ, von Mering C. The STRING database in 2017: quality-controlled protein-protein association networks, made broadly accessible. *Nucleic Acids Res* 2017; **45**: D362-D368 [PMID: 27924014 DOI: 10.1093/nar/gkw937]
- 22 **The Gene Ontology Consortium**. Expansion of the Gene Ontology knowledgebase and resources. *Nucleic Acids Res* 2017; **45**: D331-D338 [PMID: 27899567 DOI: 10.1093/nar/gkw1108]
- 23 **Becht E**, Giraldo NA, Lacroix L, Buttard B, Elarouci N, Petitprez F, Selves J, Laurent-Puig P, Sautès-Fridman C, Fridman WH, de Reyniès A. Estimating the population abundance of tissue-infiltrating immune and stromal cell populations using gene expression. *Genome Biol* 2016; **17**: 218 [PMID: 27765066 DOI: 10.1186/s13059-016-1070-5]
- 24 **Gu Z**, Eils R, Schlesner M. Complex heatmaps reveal patterns and correlations in multidimensional genomic data. *Bioinformatics* 2016; **32**: 2847-2849 [PMID: 27207943 DOI: 10.1093/bioinformatics/btw313]
- 25 **Gu Z**, Gu L, Eils R, Schlesner M, Brors B. circlize Implements and enhances circular visualization in R. *Bioinformatics* 2014; **30**: 2811-2812 [PMID: 24930139 DOI: 10.1093/bioinformatics/btu393]
- 26 **Curry WT**, Lim M. Immunomodulation: checkpoint blockade *etc.* *Neuro Oncol* 2015; **17** Suppl 7: vii26-vii31 [PMID: 26516223 DOI: 10.1093/neuonc/nov174]
- 27 **Calderaro J**, Rousseau B, Amaddeo G, Mercey M, Charpy C, Costentin C, Luciani A, Zafrani ES, Laurent A, Azoulay D, Lafdil F, Pawlotsky JM. Programmed death ligand 1 expression in hepatocellular carcinoma: Relationship With clinical and pathological features. *Hepatology* 2016; **64**: 2038-2046 [PMID: 27359084 DOI: 10.1002/hep.28710]
- 28 **Long J**, Qu T, Pan XF, Tang X, Wan HH, Qiu P, Xu YH. Expression of programmed death ligand-1 and programmed death 1 in hepatocellular carcinoma and its clinical significance. *J Cancer Res Ther* 2018; **14**: S1188-S1192 [PMID: 30539869 DOI: 10.4103/0973-1482.204850]
- 29 **Jung HI**, Jeong D, Ji S, Ahn TS, Bae SH, Chin S, Chung JC, Kim HC, Lee MS, Baek MJ. Overexpression of PD-L1 and PD-L2 Is Associated with Poor Prognosis in Patients with Hepatocellular Carcinoma. *Cancer Res Treat* 2017; **49**: 246-254 [PMID: 27456947 DOI: 10.4143/crt.2016.066]
- 30 **Adler DG**, Mallery S, Amateau S, Nieto J, Taylor LJ, Siddiqui A. A pilot study of a 20-mm lumen-apposing metal stent to treat pancreatic fluid collections: First reported multicenter use of a new device. *Endosc Ultrasound* 2019; **8**: 136-138 [PMID: 31006708 DOI: 10.4103/eus.eus\_58\_18]
- 31 **Adler DG**, Muthusamy VR, Ehrlich DS, Parasher G, Thosani NC, Chen A, Buscaglia JM, Appannagari A, Quintero E, Aslanian H, Taylor LJ, Siddiqui A. A multicenter evaluation of a new EUS core biopsy needle:

- Experience in 200 patients. *Endosc Ultrasound* 2019; **8**: 99-104 [PMID: 29623911 DOI: 10.4103/eus.eus\_53\_17]
- 32 **Chang H**, Jung W, Kim A, Kim HK, Kim WB, Kim JH, Kim BH. Expression and prognostic significance of programmed death protein 1 and programmed death ligand-1, and cytotoxic T lymphocyte-associated molecule-4 in hepatocellular carcinoma. *APMIS* 2017; **125**: 690-698 [PMID: 28493410 DOI: 10.1111/apm.12703]
  - 33 **Hu K**, Wang ZM, Li JN, Zhang S, Xiao ZF, Tao YM. CLEC1B Expression and PD-L1 Expression Predict Clinical Outcome in Hepatocellular Carcinoma with Tumor Hemorrhage. *Transl Oncol* 2018; **11**: 552-558 [PMID: 29525632 DOI: 10.1016/j.tranon.2018.02.010]
  - 34 **Kan G**, Dong W. The expression of PD-L1 APE1 and P53 in hepatocellular carcinoma and its relationship to clinical pathology. *Eur Rev Med Pharmacol Sci* 2015; **19**: 3063-3071 [PMID: 26367730]
  - 35 **Pei R**, Zhang W, Wang S, Huang X, Zou Y. Prognostic Value of PD-L1 in Patients with Hepatocellular Carcinoma. *Clin Lab* 2019; **65** [PMID: 31115210 DOI: 10.7754/Clin.Lab.2018.180839]
  - 36 **Pascual M**, Mena-Varas M, Robles EF, Garcia-Barchino MJ, Panizo C, Hervás-Stubbbs S, Alignani D, Sagardoy A, Martínez-Ferrandis JI, Bunting KL, Meier S, Sagaert X, Bagnara D, Guruceaga E, Blanco O, Celay J, Martínez-Baztan A, Casares N, Lasarte JJ, MacCarthy T, Melnick A, Martínez-Climent JA, Roa S. PD-1/PD-L1 immune checkpoint and p53 Loss facilitate tumor progression in activated B-cell diffuse large B-cell lymphomas. *Blood* 2019; **133**: 2401-2412 [PMID: 30975638 DOI: 10.1182/blood.2018889931]
  - 37 **Lee JW**, Zhang Y, Eoh KJ, Sharma R, Sanmamed MF, Wu J, Choi J, Park HS, Iwasaki A, Kaftan E, Chen L, Papadimitrakopoulou V, Herbst RS, Koo JS. The Combination of MEK Inhibitor With Immunomodulatory Antibodies Targeting Programmed Death 1 and Programmed Death Ligand 1 Results in Prolonged Survival in Kras/p53-Driven Lung Cancer. *J Thorac Oncol* 2019; **14**: 1046-1060 [PMID: 30771521 DOI: 10.1016/j.jtho.2019.02.004]
  - 38 **Ang TL**, Li JW, Kwek ABE, Thuraiarah PH, Wang LM. The difference in histological yield between 19G EUS-FNA and EUS-fine-needle biopsy needles. *Endosc Ultrasound* 2019; **8**: 255-260 [PMID: 31115385 DOI: 10.4103/eus.eus\_12\_19]
  - 39 **Antonini F**, Delconte G, Fuccio L, De Nucci G, Fabbri C, Armellini E, Frazzoni L, Fornelli A, Magarotto A, Mandelli E, Occhipinti P, Masci E, Manes G, Macarri G. EUS-guided tissue sampling with a 20-gauge core biopsy needle for the characterization of gastrointestinal subepithelial lesions: A multicenter study. *Endosc Ultrasound* 2019; **8**: 105-110 [PMID: 29770781 DOI: 10.4103/eus.eus\_1\_18]
  - 40 **Bhatia V**, Dhir V. Radial EUS imaging of the liver: A pictorial guide. *Endosc Ultrasound* 2019; **8**: 76-81 [PMID: 31006705 DOI: 10.4103/eus.eus\_17\_19]
  - 41 **Cubillos-Zapata C**, Avendaño-Ortiz J, Hernández-Jimenez E, Toledano V, Casas-Martin J, Varela-Serrano A, Torres M, Almendros I, Casitas R, Fernández-Navarro I, García-Sánchez A, Aguirre LA, Farre R, López-Collazo E, García-Río F. Hypoxia-induced PD-L1/PD-1 crosstalk impairs T-cell function in sleep apnoea. *Eur Respir J* 2017; **50** [PMID: 29051270 DOI: 10.1183/13993003.00833-2017]
  - 42 **Hui E**, Cheung J, Zhu J, Su X, Taylor MJ, Wallweber HA, Sasmal DK, Huang J, Kim JM, Mellman I, Vale RD. T cell costimulatory receptor CD28 is a primary target for PD-1-mediated inhibition. *Science* 2017; **355**: 1428-1433 [PMID: 28280247 DOI: 10.1126/science.aaf1292]
  - 43 **Seifert AM**, Zeng S, Zhang JQ, Kim TS, Cohen NA, Beckman MJ, Medina BD, Maltback JH, Loo JK, Crawley MH, Rossi F, Besmer P, Antonescu CR, DeMatteo RP. PD-1/PD-L1 Blockade Enhances T-cell Activity and Antitumor Efficacy of Imatinib in Gastrointestinal Stromal Tumors. *Clin Cancer Res* 2017; **23**: 454-465 [PMID: 27470968 DOI: 10.1158/1078-0432.CCR-16-1163]
  - 44 **Adler DG**, Gabr M, Taylor LJ, Witt B, Pleskow D. Initial report of transesophageal EUS-guided intraparenchymal lung mass core biopsy: Findings and outcomes in two cases. *Endosc Ultrasound* 2018; **7**: 413-417 [PMID: 29786035 DOI: 10.4103/eus.eus\_13\_18]
  - 45 **Huang CY**, Wang Y, Luo GY, Han F, Li YQ, Zhou ZG, Xu GL. Relationship Between PD-L1 Expression and CD8<sup>+</sup> T-cell Immune Responses in Hepatocellular Carcinoma. *J Immunother* 2017; **40**: 323-333 [PMID: 29028787 DOI: 10.1097/CJI.0000000000000187]
  - 46 **Lim TS**, Chew V, Sieow JL, Goh S, Yeong JP, Soon AL, Ricciardi-Castagnoli P. PD-1 expression on dendritic cells suppresses CD8<sup>+</sup> T cell function and antitumor immunity. *Oncoimmunology* 2016; **5**: e1085146 [PMID: 27141339 DOI: 10.1080/2162402x.2015.1085146]



Case Control Study

# LncRNA C9orf139 can regulate the growth of pancreatic cancer by mediating the miR-663a/Sox12 axis

Jin-Nian Ge, Di Yan, Chun-Lin Ge, Min-Jie Wei

**ORCID number:** Jin-Nian Ge 0000-0001-5596-151X; Di Yan 0000-0001-6456-1059; Chun-Lin Ge 0000-0003-3728-8610; Min-Jie Wei 0000-0002-5014-2088.

**Author contributions:** Ge JN and Yan D contributed to the study design and reviewed the manuscript; Ge CL and Wei MJ analyzed the data and wrote the manuscript; Yan D contributed to the data collection, data interpretation, and manuscript writing; and all authors read and approved the final manuscript.

**Institutional review board statement:** The study was reviewed and approved for publication by the First Affiliated Hospital of China Medical University.

**Informed consent statement:** All study participants or their legal guardian provided informed written consent about personal and medical data collection prior to study enrollment.

**Conflict-of-interest statement:** All the authors have no conflict of interest related to the manuscript.

**Data sharing statement:** No additional data are available.

**STROBE statement:** The authors

**Jin-Nian Ge, Chun-Lin Ge,** Department of General Surgery, The First Affiliated Hospital of China Medical University, Shenyang 110001, Liaoning Province, China

**Di Yan,** Intensive Care Unit, The Central Affiliated Hospital of Shenyang Medical College, Shenyang 110024, Liaoning Province, China

**Min-Jie Wei,** Department of Pharmacology, School of Pharmacy, China Medical University, Shenyang 110122, Liaoning Province, China

**Corresponding author:** Min-Jie Wei, PhD, Doctor, Department of Pharmacology, School of Pharmacy, China Medical University, No. 155 Nanjing North Street, Heping District, Shenyang 110122, Liaoning Province, China. [weiminjie112233@163.com](mailto:weiminjie112233@163.com)

## Abstract

### BACKGROUND

Recent studies have proved the important role of many oncogenic long non-coding RNAs (lncRNAs) in the progression of pancreatic cancer, but little is known about the mechanisms of tumor suppression in pancreatic cancer.

### AIM

To evaluate the function of tumor suppressor lncRNA C9orf139 in pancreatic cancer progression and to study the underlying mechanism.

### METHODS

We assigned 54 patients with pancreatic ductal adenocarcinoma treated at our hospital to the patient group and 30 normal subjects undergoing physical examination to the control group. RT-qPCR was used to measure the relative expression of C9orf139 in the tissue and serum of patients, in an attempt to investigate the prognostic value of C9orf139 in pancreatic cancer patients. The luciferase reporter gene assay was performed to determine the interaction between C9orf139 and miR-663a. The biological function of C9orf139 was assessed by *in vitro* assays and *in vivo* subcutaneous tumor formation tests in animal models. To figure out the molecular mechanism of C9orf139 to act on miR-663a/Sox12, RNA pull-down, Western blot assay, RNA immunoprecipitation assay, and co-immunoprecipitation assay were performed.

### RESULTS

C9orf139 level significantly increased in the tissue and serum of patients, which



have read the STROBE Statement—checklist of items, and the manuscript was prepared and revised according to the STROBE Statement—checklist of items.

**Open-Access:** This article is an open-access article that was selected by an in-house editor and fully peer-reviewed by external reviewers. It is distributed in accordance with the Creative Commons Attribution NonCommercial (CC BY-NC 4.0) license, which permits others to distribute, remix, adapt, build upon this work non-commercially, and license their derivative works on different terms, provided the original work is properly cited and the use is non-commercial. See: <http://creativecommons.org/licenses/by-nc/4.0/>

**Manuscript source:** Unsolicited manuscript

**Specialty type:** Oncology

**Country/Territory of origin:** China

**Peer-review report's scientific quality classification**

Grade A (Excellent): 0  
Grade B (Very good): B, B, B, B, B  
Grade C (Good): C  
Grade D (Fair): 0  
Grade E (Poor): 0

**Received:** June 1, 2020

**Peer-review started:** June 1, 2020

**First decision:** September 11, 2020

**Revised:** September 24, 2020

**Accepted:** October 12, 2020

**Article in press:** October 12, 2020

**Published online:** November 15, 2020

**P-Reviewer:** Aykan NF, Casella C, Dinc T, Moschovi MA, Ooi L

**S-Editor:** Huang P

**L-Editor:** Wang TQ

**P-Editor:** Li JH



had clinical diagnostic value for pancreatic cancer. Patients with high C9orf139 expression had a higher risk of progressing to stage III + IV, lymph node metastasis, and poor differentiation. Cox regression analysis suggested that C9orf139, tumor-node-metastasis stage, and lymph node metastasis were independent prognostic factors in patients. The underlying mechanism of C9orf139 was that it promoted the growth of pancreatic cancer cells by modulating the miR-663a/Sox12 axis.

## CONCLUSION

C9orf139 is highly expressed in pancreatic cancer, qualified to be used as a potential diagnostic and prognostic marker for pancreatic cancer. Its promotion of pancreatic cancer cell growth is achieved by mediating the miR-663a/Sox12 axis.

**Key Words:** C9orf139; miR-663a; Sox12; Pancreatic cancer; Prognosis; Tumor formation in nude mice

©The Author(s) 2020. Published by Baishideng Publishing Group Inc. All rights reserved.

**Core Tip:** C9orf139 is highly expressed in pancreatic cancer, qualified to be used as a potential diagnostic and prognostic marker for pancreatic cancer. Its promotion of pancreatic cancer cell growth is achieved by mediating the miR-663a/Sox12 axis.

**Citation:** Ge JN, Yan D, Ge CL, Wei MJ. LncRNA C9orf139 can regulate the growth of pancreatic cancer by mediating the miR-663a/Sox12 axis. *World J Gastrointest Oncol* 2020; 12(11): 1272-1287

**URL:** <https://www.wjgnet.com/1948-5204/full/v12/i11/1272.htm>

**DOI:** <https://dx.doi.org/10.4251/wjgo.v12.i11.1272>

## INTRODUCTION

Pancreatic cancer is the most lethal malignant gastrointestinal tumor in the clinic and is reported to be the fourth leading cause of death from cancer worldwide<sup>[1]</sup>. According to the latest global tumor statistics<sup>[2]</sup>, new cases and death cases of pancreatic cancer surpassed 400000 last year, and its increasing incidence among younger people has a serious impact on people's life. The best existing treatment for pancreatic cancer is surgical resection. But most patients are already at the middle and advanced tumor stage and are with metastasis at the time of diagnosis, no longer suitable for surgery<sup>[3,4]</sup>. Radiotherapy is a choice for those unsuitable for surgery, but its treatment outcome is unsatisfactory, which is one of the main reasons for the poor 5-year survival of pancreatic cancer no more than 10%<sup>[5,6]</sup>. Therefore, it is urgent to figure out the molecular mechanism of pancreatic cancer progression and explore more therapeutic regimens for pancreatic cancer.

The study on non-coding RNAs has been popular in various fields in recent years. The well-known mainstream non-coding RNAs are long non-coding RNAs (lncRNAs), microRNAs, and circular RNAs (circRNAs)<sup>[7-9]</sup>. MicroRNAs have been frequently studied recently, and they are involved in the development and progression of pancreatic cancer, as well as in tumor resistance and autophagy<sup>[10-12]</sup>. LncRNAs are a group of non-coding RNAs with more than 200 nt, which were first discovered as "metabolism waste" produced during transcription<sup>[13]</sup>. Scientific advancement revealed differential expression of lncRNAs and their function of gene regulation in various tumors such as lung cancer<sup>[14]</sup>, liver cancer<sup>[15]</sup>, breast cancer<sup>[16]</sup>, gastric cancer<sup>[17]</sup>, and pancreatic cancer<sup>[18]</sup>. More and more studies in recent years have found that lncRNAs can compete with sponge microRNAs as competing endogenous RNAs (ceRNAs) to regulate mRNA<sup>[19]</sup>. C9orf139 is an important member of the lncRNA family. Song *et al*<sup>[20]</sup> found that C9orf139 was differentially expressed in various tumors and was highly expressed in pancreatic cancer, which is expected to be a potential target for pancreatic cancer. But whether it can interact with sponge microRNA to regulate tumor growth is unclear. The result of bioinformatics analysis implied a targeting site between C9orf139 and miR-663a. Previous studies have found that miR-663a is lowly

expressed in pancreatic cancer, and the up-regulation of miR-663a can inhibit tumor growth<sup>[21]</sup>.

This study analyzed the possibility of C9orf139 as a target to inhibit tumor growth and provide a potential target for clinical treatment of pancreatic cancer by acting as a ceRNA to sponge miR-663a.

## MATERIALS AND METHODS

### Subjects

We recruited 54 patients with pancreatic ductal adenocarcinoma admitted to our hospital from May 2013 to May 2014 into this study and assigned them to the patient group. This study has obtained ethical approval from the Ethics Committee of the First Affiliated Hospital of China Medical University. Cancer tissue samples and tumor-adjacent tissue samples were collected from the 54 patients during the operation, transported by liquid nitrogen to the laboratory for testing, and then stored at -80 °C. The peripheral blood of patients from the patient group was also collected before treatment. We also recruited 30 normal people undergoing physical examination during the same period to the control group and collected their peripheral blood. All peripheral blood samples were separated to obtain the serum and then sent to the laboratory for testing immediately. The inclusion criteria were: Patients diagnosed with pancreatic ductal adenocarcinoma by pathological examination; patients in line with the tumor-node-metastasis (TNM) staging criteria issued in 2009; patients with no previous anti-tumor treatment before the study. All patients provided informed consent. Normal people from the control group were not affected by diseases involving the pancreatic system according to imaging test results. The exclusion criteria were: Patients with other tumors; patients not capable of participating in the follow-up; patients with an expected survival of less than 1 mo. The tumor tissue was collected during the surgery. This study followed the Declaration of Helsinki<sup>[22]</sup>. Patients from the patient group were comparable to people from the control group in age and sex.

### Cell culture and transfection

The human pancreatic cancer cell lines AsPC-1, BxPC-3, PANC-1, PaCa-2, and SW1990, and the human pancreatic ductal epithelial cell line HPDE6-C7 were from ATCC (Rockville, MD, United States). The cells were cultured in RPMI-1640 or DMEM (Gibco, Waltham, MA, United States) containing 10% fetal bovine serum (FBS). Overexpression plasmid containing C9orf139 (sh-C9orf139), plasmids for knockdown (si-C9orf139-#1, si-C9orf139-#2, and si-C9orf139-#3), and Sox12 expression plasmid (pcDNA3.1-Sox12) were constructed by Shanghai GenePharma Co., Ltd. Sox12 shRNA, Sox12 siRNA, control siRNA, miR-663a mimic, miR-NC, miR-663a inhibitor, and control inhibitor were obtained from RiboBio (Guangzhou, China). Cell transfection was performed using Lipofectamine 2000 (Invitrogen, Carlsbad, CA, United States) according to the manufacturer's instructions.

### Proliferation test (CCK-8)

Cells transfected with plasmids were used to prepare a cell suspension at a density of  $4 \times 10^4$  cells/mL, which was then seeded in 96-well plates, at 0.1 mL ( $4 \times 10^3$ ) per well, and incubated at 37 °C under 5% CO<sub>2</sub>. Then, 10 µL of CCK-8 reagent (Beyotime Biotechnology, Shanghai, CHN) was added to the plates at the 24th, 48th, 72th, and 96th hours of the incubation and cultured for 4 h. The optical density was measured with a microplate reader (Multiskan™ FC Microplate Photometer, CA, Thermo Scientific) at 450 nm.

### Cell invasion and migration assays

Cells transfected with plasmids were used to prepare a cell suspension at a density of  $4 \times 10^4$  cells/mL and suspended in a serum-free medium containing 1 µg/mL mitomycin C to inhibit cell proliferation. Then, the cell suspension was inoculated into the upper chamber of transwell, while 10% FBS was added to the lower chamber and cultured at 37 °C for 24 h. The matrix and cells remaining in the upper chamber that did not migrate through the membrane were wiped off. Then the system was washed three times with PBS and fixed with paraformaldehyde for 10 min, followed by three times of washing with double distilled water. After drying, cells were stained with 0.5% crystal violet and placed under a microscope to observe the cell migration. For

wound healing assay, cells were seeded in 6-well plates and scratched artificially with a 200  $\mu$ L pipette. Wound closure was observed after 24 h and imaged under a microscope.

### **Apoptosis assay**

Cells transfected with plasmids were digested with 0.25% trypsin (Gibco) and washed twice with PBS. Next, cells were added to 100  $\mu$ L of binding buffer to prepare a suspension at a density of  $1 \times 10^6$  cells/mL, and the suspension was inoculated with Annexin V-FITC (Yeasen Biotech Co., Ltd.) and PI at room temperature in the dark for 5 min. Finally, cell apoptosis was measured using the FC500MCL flow cytometry system. The assay was repeated three times to obtain the mean value.

### **RT-qPCR**

Total RNA was extracted from tissues and sera using a TRIzol kit (Invitrogen, United States). The purity, concentration, and integrity of total RNA were measured by ultraviolet spectrophotometry and agarose gel electrophoresis. Reverse transcription was subsequently performed using the TaqMan™ Reverse Reverse Transcription Kit (Invitrogen) according to the kit manual, and cDNA was then synthesized for subsequent studies. PCR amplification was performed using the PrimeScript RT Master Mix kit (Takara Bio, Japan). The amplification system was 20  $\mu$ L in total, containing 10  $\mu$ L of SYBR qPCR Mix, 0.8  $\mu$ L of upstream primer, 0.8  $\mu$ L of downstream primer, 2  $\mu$ L of cDNA product, 0.4  $\mu$ L of  $50 \times$  ROX reference dye, and RNase-free water to adjust the volume. PCR conditions were pre-denaturation at 95 °C for 60 s and 40 cycles of denaturation at 95 °C for 30 s, and annealing and extension at 60 °C for 40 s. We designed three parallel replicate wells and all specimens were tested three times. U6 was used as the internal reference of microRNAs, and GAPDH was used as the internal reference of other genes. The data were analyzed using  $2^{-\Delta\Delta Ct}$  method<sup>[23]</sup>. The PCR reaction was performed using the 7500 PCR instrument from ABI.

### **Western blot analysis**

The cultured cells were lysed using RIPA buffer (Thermo Scientific, Inc., United States) and the protein concentration was measured using a BCA kit (Thermo Scientific, Inc.). The protein was adjusted to a density of 4  $\mu$ g/ $\mu$ L and separated by 12% SDS-PAGE electrophoresis. The protein was transferred to a 0.22  $\mu$ m PVDF membrane and blocked with 5% skim milk for 2 h, followed by overnight incubation at 4 °C with Sox12 antibody (dilution 1:1000; Abcam, United States). The primary antibody was washed and the horseradish peroxidase-labeled goat anti-rabbit secondary antibody (dilution 1:5000; Abcam) was added and incubated at 37 °C for 1 h. The membrane was rinsed three times with PBS, 5 min each time. The excess liquid on the membrane was dried with a filter paper, and the ECL reagent was used for color development. The protein bands were scanned and the gray values were analyzed using Quantity One software. GAPDH was used as the internal reference.

### **RNA immunoprecipitation**

RNA immunoprecipitation (RIP) assay was conducted in line with the manual of the EZMagna RIP kit (Millipore, Billerica, MA, United States) to investigate the possibility that C9orf139 and miR-663a interact or bind to the potential binding protein Ago2 in LoVo and HCT116 cells. PaCa-2 cells were lysed and incubated with protein A magbeads that were conjugated with the antibody at 4 °C. Six hours later, the magbeads were washed with washing buffer and then incubated with 0.1% SDS/0.5 mg/mL proteinase K for 30 min at 55 °C to detach proteins. Finally, qRT-PCR analysis of the immunoprecipitated RNA was performed to demonstrate the presence of C9orf139 and miR-663a using specific primers.

### **RNA pull-down assay**

PaCa-2 cells were transfected with biotinylated miR-663a-wt, miR-663a-mut, and a negative control (GenePharma, Shanghai, China), respectively. After 48 h, the cell lysate was incubated with M-280 Streptomyces magbeads (Invitrogen) according to the manufacturer's instructions. The level of LINC00152 in the RNA complex bound to the beads was determined using the qRT-PCR method.

### **Dual-luciferase reporter assay**

A cDNA fragment containing the wild type (C9orf139-WT) or mutant type (C9orf139-mut) fragment was subcloned to the downstream of the luciferase gene of psi-CHECK2 luciferase reporter vector. The 3' untranslated region (UTR) of Sox12-wt and

the corresponding mutant (Sox12-mut) were subcloned to downstream of the luciferase gene of the psi-check2 luciferase reporter vector. The miR-663a mimic or inhibitor was co-transfected with the C9orf139-WT or C9orf139-mut reporter vector (Invitrogen, United States). After 48 h of transfection, the luciferase activity of firefly and renin in the cell lysates was continuously determined using a dual-luciferase reporter kit (Promega, United States). Similarly, Sox12-WT or Sox12-mut was co-transfected with miR-663a mimic.

### ***Tumor formation in nude mice***

This animal experiment was approved by the ethics committee of our hospital. Nude mice (4-5 wk old, male,  $n = 5$  per group) were from Charles River Laboratories (China). Subcutaneous injection of 200  $\mu$ L of transfected PaCa-2 cells ( $2 \times 10^6$ ) was performed on the left side of the back of each nude mouse. Tumor size was measured periodically using the formula:  $0.52 \times L \times W^2$  (L refers to the tumor length, W refers to tumor width). Mice were euthanized on the 30<sup>th</sup> day after the injection, and the tumor was collected.

### ***Follow-up***

The survival of patients was followed for 5 years *via* the telephone or the records of reexamination on the 1<sup>st</sup>, 3<sup>rd</sup>, 6<sup>th</sup>, 9<sup>th</sup>, and 12<sup>th</sup> months of each year.

### ***Statistical analysis***

Data visualization and data analyses were performed using GraphPad 7 software package. The analysis of independent prognostic factors was conducted using SPSS20.0 software. The distribution of the measurement data was analyzed by the K-S test. Data with a normal distribution are expressed as the mean  $\pm$  standard deviation (means  $\pm$  SD) and were compared between the two groups by the independent sample *t*-test. Count data are expressed as percentages (%) and were compared between the two groups by the chi-square test. The comparison between multiple groups was performed by one-way ANOVA. The LSD-*t* test was used for post-hoc pairwise comparison. The comparison between multiple time points was performed by repeated measure ANOVA. The Bonferroni test was used for post-hoc test. Receiver operating characteristic (ROC) curve analysis was employed to assess the diagnostic value of C9orf139 in pancreatic cancer. Pearson correlation coefficient was used to analyze the correlation between genes. Kaplan-Meier survival curve was plotted to display the overall survival that was analyzed by the Log-rank test. Multivariate Cox regression was conducted to predict the prognosis of patients.  $P < 0.05$  indicated a statistical difference.

## **RESULTS**

### ***Clinical value of C9orf139 in patients***

Clinical detection revealed a marked increase in C9orf139 expression in patients' tissues or sera. The area under the ROC curve was 0.923. To investigate the relationship between C9orf139 and pathological data of patients with pancreatic cancer, we divided patients into the high expression group and low expression group according to the median value of C9orf139 level. Patients with high expression had markedly higher risks of progressing to stage III + IV, lymph node metastasis, and poor differentiation. The 5-year survival of patients in the high expression group was significantly reduced. Cox regression analysis demonstrated that C9orf139, TNM stage, and lymph node metastasis were independent prognostic factors for pancreatic cancer patients. More details are shown in Figures 1 and 2 and Tables 1 and 2.

### ***Knockdown of lncRNA C9orf139 inhibits the growth of pancreatic cancer cells***

Clinical detection revealed high expression of C9orf139 in pancreatic cancer cells. For further verification, we tested C9orf139 expression in each group of cells and confirmed that C9orf139 was highly expressed in all pancreatic cancer cells. We selected PaCa-2 and SW1990 cells in which C9orf139 expression was especially high for the following experiments. To investigate the effect of C9orf139 on pancreatic cancer cells, we established three C9orf139 knockout expression vectors (si-C9orf139#1-#3) and transfected them into PaCa-2 and SW199 cells. We detected that si-C9orf139 #2 had the lowest relative expression of C9orf139, so we selected si-C9orf139#2 for subsequent experiments. We conducted relevant experiments to test

**Table 1 Relationship between long non-coding RNA C9orf139 and pathological data of patients**

Variable	LncRNA C9orf139		$\chi^2$	P value
	High expression (n = 27)	Low expression (n = 27)		
Age			0.260	1.271
	≥ 60 yr (n = 20)	12 (44.44)	8 (29.63)	
	< 60 yr (n = 34)	15 (55.56)	19 (70.37)	
Sex			0.307	0.580
	Male (n = 32)	15 (55.56)	17 (62.96)	
	Female (n = 22)	12 (44.44)	10 (37.04)	
Tumor size			0.333	0.564
	≥ 3 cm (n = 18)	10 (37.04)	8 (29.63)	
	< 3 cm (n = 36)	17 (62.96)	19 (70.37)	
TNM stage			9.826	0.002
	I-II (n = 35)	12 (44.44)	23 (85.19)	
	III-IV (n = 19)	15 (55.56)	4 (14.81)	
Degree of differentiation			4.207	0.040
	Poor (n = 17)	12 (44.44)	5 (18.52)	
	Moderate and high (n = 37)	15 (55.56)	22 (81.48)	
Lymph node metastasis			5.206	0.004
	Yes (n = 13)	11 (40.74)	2 (7.41)	
	No (n = 41)	16 (59.26)	25 (92.59)	

LncRNA: Long non-coding RNA; TNM: Tumor-node-metastasis.

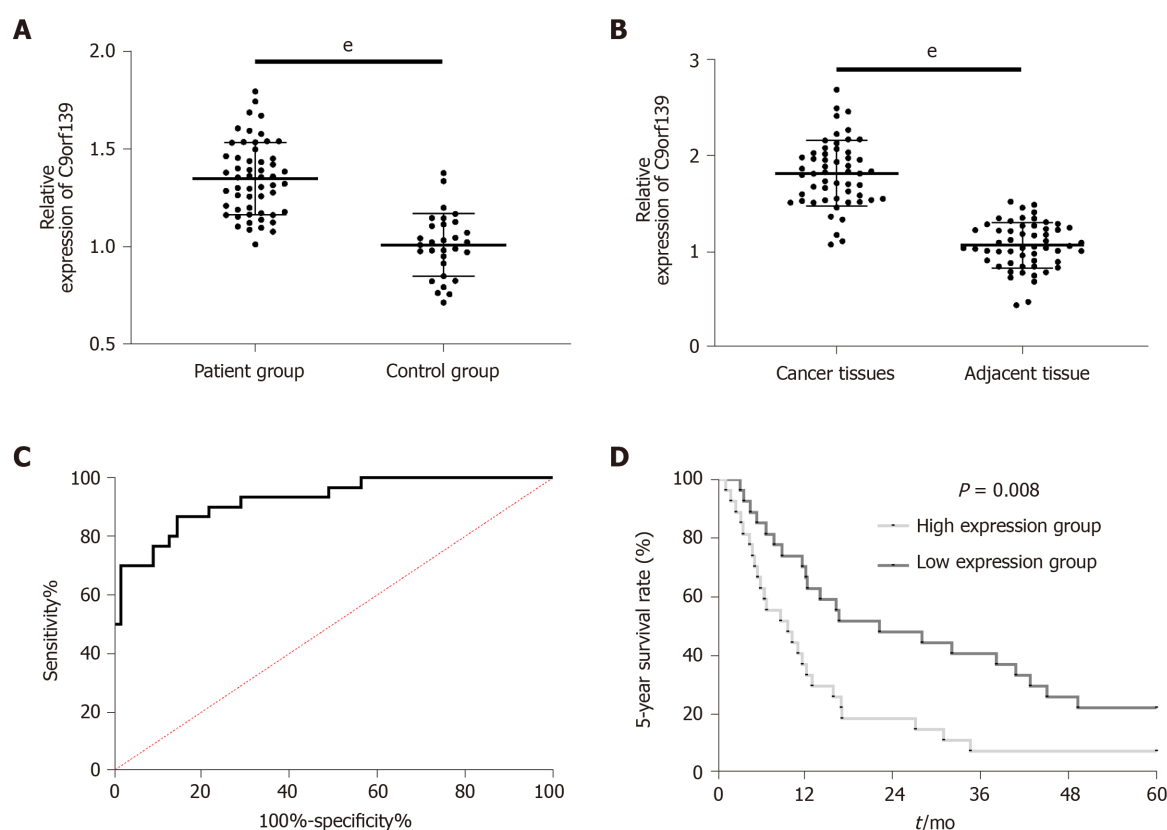
**Table 2 Prognostic analysis of long non-coding RNA C9orf139 in patients**

Variable	Univariate Cox regression analysis			Multivariate Cox regression analysis		
	P value	HR	95CI%	P value	HR	95CI%
Age (≥ 60 yr vs < 60 yr)	0.637	1.158	0.631-2.125			
Sex (male vs female)	0.885	0.957	0.528-1.734			
Tumor size (≥ 3 cm vs < 3 cm)	0.160	0.648	0.354-1.187			
TNM stage (I + II vs III + IV)	0.035	1.932	1.047-3.564	0.109	1.724	0.886-3.353
Degree of differentiation (poor vs moderate and high)	0.019	0.477	0.257-0.886	0.045	0.526	0.281-0.987
Lymph node metastasis (yes vs no)	0.019	0.456	0.237-0.877	0.167	0.622	0.317-1.219
C9orf139 (low expression vs high expression)	0.010	0.455	0.251-0.825	0.020	0.488	0.267-0.893

TNM: Tumor-node-metastasis.

the biological condition of the transfected cells. The results of CCK-8 assay revealed great inhibition of cell growth in pancreatic cancer cells transfected with si-C9orf139#2, and Transwell assay and wound-healing assay demonstrated a marked decrease in the number of cells migrating through the membrane and the migration rate in cells transfected with si-C9orf139#2. Flow cytometry showed a marked increase in the apoptosis of cells transfected with si-C9orf139#2. Such results suggested that knockdown of lncRNA C9orf139 inhibits the growth of pancreatic cancer cells. More details are shown in Figure 2.





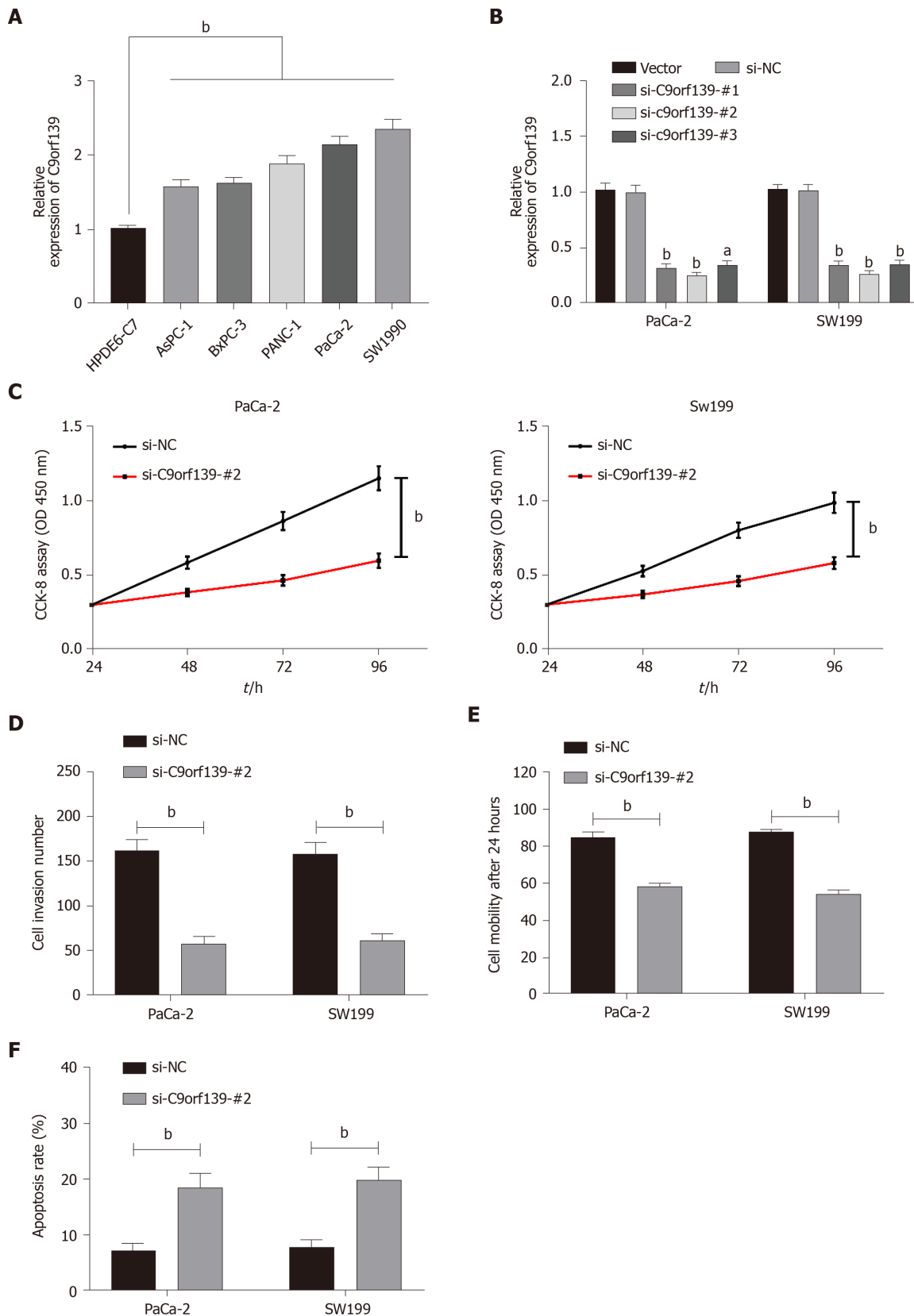
**Figure 1** Clinical value of long non-coding RNA C9orf139 in patients with pancreatic cancer. A: Relative serum expression of long non-coding RNA (lncRNA) C9orf139 in the patient group and control group; B: Expression of lncRNA C9orf139 in cancer tissues and adjacent tissues; C: Receiver operating characteristic curve of lncRNA C9orf139 for the diagnosis of pancreatic cancer; D: The 5-year survival of patients was higher in the low expression group than in the high expression group. \* $P < 0.001$  for the comparison between two groups.

### ***Up-regulation of lncRNA C9orf139 promotes pancreatic cancer cell growth by inhibiting miR-663a***

Online miR target prediction of C9orf139 (<http://starbase.sysu.edu.cn/>) found a potential binding target between C9orf139 and miR-663a. We conducted dual-luciferase reporter assay, RIP assay, and RNA pull-down assay to confirm this. The dual-luciferase report assay showed that the fluorescence activity of C9orf139-WT was significantly inhibited by miR-663a-mimic. RIP assay showed that the levels of C9orf139 and miR-663a precipitated by Ago2 antibody were significantly higher than those precipitated by IgG. RNA pull-down assay revealed that C9orf139 could be pulled down by biotin-labeled miR-663a-WT, not by miR-663a-mut. The detection of miR-663a expression in the patient tissue showed that miR-663a expression was significantly decreased in the patient tissue, and correlation analysis revealed a negative correlation between miR-663a and C9orf139 in the patient tissue. To further confirm the effects of C9orf139 and miR-663a on pancreatic cancer cells, we transfected pancreatic cancer cells with miR-663a-mimic, sh-C9orf139 + miR-663a-mimic, and miR-NC, respectively. We found that cell proliferation, invasion, and migration were significantly inhibited, and the apoptosis was significantly increased in cells transfected with miR-663a-mimic, while the biological behaviors of cells transfected with sh-C9orf139 + miR-663a-mimic were reversed and contrary to cells transfected with miR-663a-mimic alone. Such results indicated that up-regulated C9orf139 can inhibit the expression of miR-663a and promote tumor cell growth. More details are shown in Figure 3.

### ***lncRNA C9orf139 targets miR-663a to promote pancreatic cancer cell growth via regulating Sox12 expression***

The main regulatory mode of microRNAs is performed through the regulation of transcription of downstream target genes. Bioinformatics analysis revealed a targeted binding site for miR-663a and Sox12. We conducted the dual-luciferase reporter assay and detected Sox12 expression in cells after the transfection and confirmed that there was targeting binding between Sox12 and miR-663a. We transfected cells with miR-



**Figure 2 Effect of long non-coding RNA C9orf139 on pancreatic cancer cell behaviors.** A: Relative expression of long non-coding RNA (lncRNA) C9orf139 in pancreatic cancer cell lines; B: Relative expression of lncRNA C9orf139 in cells after transfection; C: Inhibited cell proliferation after knockdown of lncRNA C9orf139; D: Decreased cell invasion after knockdown of lncRNA C9orf139; E: Inhibited cell migration after knockdown of lncRNA C9orf139; F: Increased cell apoptosis after knockdown of lncRNA C9orf139. <sup>b</sup>*P* < 0.01 for the comparison between two groups. si-NC was the irrelevant sequence and vector was the control group.

NC, miR-663a-mimic, miR-663a-mimic + vector, and sh-C9orf139 + miR-663a-mimic and then detected the expression of Sox12. The results demonstrated that the expression of Sox12 protein and mRNA was suppressed in cells with up-regulated miR-663a, but the expression results were reversed after the co-transfection of sh-C9orf139 and miR-663a-mimic. We detected significantly higher Sox12 expression in the cancer tissues than in the adjacent tissues. Further correlation analysis showed that Sox12 was positively correlated with C9orf139 expression, but negatively correlated with miR-663a. To verify the effect of Sox12 on pancreatic cancer cells, we transfected pancreatic cancer cells with si-Sox12 and si-NC. The results showed that knockdown of Sox12 led to inhibited proliferation, invasion, migration, and increased apoptosis. More details are shown in [Figure 4](#).

#### ***lncRNA C9orf139 promotes tumor formation in nude mice via miR-663a/Sox12***

Tumor formation in nude mice was conducted to observe whether lncRNA C9orf139 affects solid tumors through the miR-663a/Sox12 axis. We subcutaneously injected miR-NC, miR-663a-mimic, or sh-C9orf139 + miR-663a-mimic into nude mice, and found that the tumor size and weight were markedly decreased in nude mice injected with miR-663a-mimic, while the tumor size and weight in nude mice injected with sh-C9orf139 + miR-663a-mimic were not significantly different from those in nude mice injected with miR-NC. The expression of Sox12 protein and mRNA in the tumor in nude mice injected with miR-663a-mimic and mice injected with miR-663a-mimic + vector was significantly inhibited, while the inhibition on Sox12 protein and mRNA was reversed in mice injected with C9orf139 + miR-663a-mimic. More details are shown in [Figure 5](#).

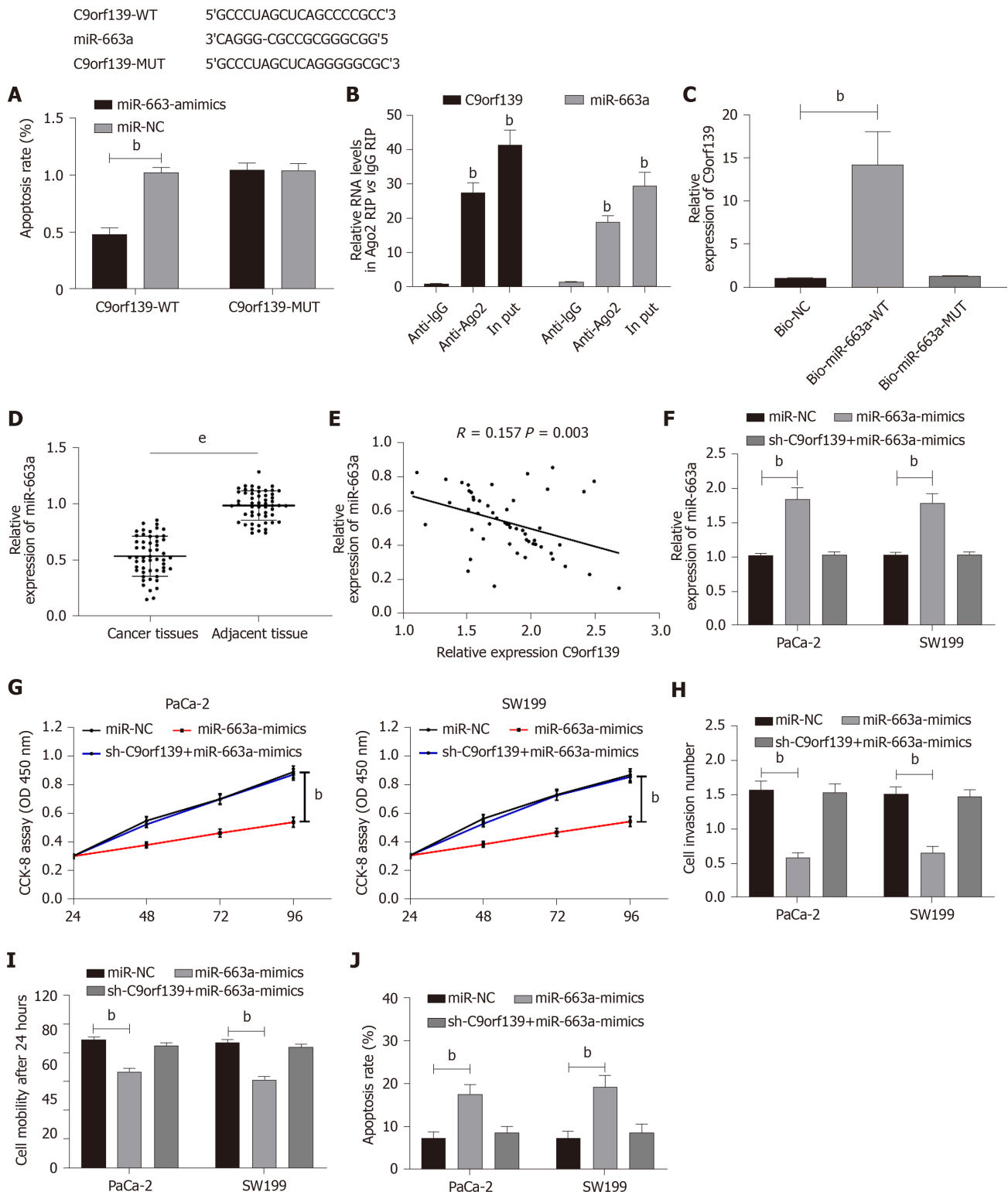
## **DISCUSSION**

In this study, we detected high C9orf139 expression in pancreatic cancer and found that patients with higher C9orf139 expression had markedly decreased 5-year survival and increased risks of progressing to stage III + IV, poor differentiation, and lymph node metastasis. We also found that C9orf139 could promote the growth of pancreatic cancer cells *via* the miR-663a/Sox12 axis, which indicates the capacity of C9orf139 to be a potential indicator for the treatment of pancreatic cancer.

The 5-year survival of pancreatic cancer patients was at the bottom among digestive tract tumors and even among all malignant tumors<sup>[24]</sup>. The low 5-year survival of pancreatic cancer is mostly attributed to the fact that most patients are already at middle or advanced stages with high risks of lesion metastasis at the time of diagnosis, which disqualifies patients for surgery. Chemoradiotherapy can improve the prognosis of patients, but its treatment efficacy is poor, so the relevant mechanisms of pancreatic cancer should be figured out<sup>[25,26]</sup>.

lncRNAs are non-coding RNAs longer than 200 nt. They have been found to play an important role in epigenetic, transcriptional, and post-transcriptional regulation of gene expression<sup>[27]</sup>. It is also reported to be closely related to the prognosis of a variety of tumors. Huang *et al*<sup>[28]</sup> found that the overexpression of lncRNA PVT1 led to a poor prognosis in patients with pancreatic cancer. A previous study<sup>[29]</sup> reported that lncRNA-ATB low expression was an independent predictor of poor prognosis in patients with pancreatic cancer. C9orf139, a newly discovered lncRNA located on human 9q34.3 chromosome, was found to be highly expressed in pancreatic cancer and a promising prognostic indicator for pancreatic cancer in the studies by Shi *et al*<sup>[30]</sup> and Wei *et al*<sup>[31]</sup>. The mechanism of C9orf139 in pancreatic cancer remains unclear. In this study, we found that C9orf139 was highly expressed in tissues and sera of pancreatic cancer patients and in pancreatic cancer cell lines, which was consistent with the results of the above-mentioned studies. Then we further analyzed the relationship between C9orf139 and pathological data and survival prognosis of patients with pancreatic cancer. The results demonstrated that patients with higher expression of C9orf139 were subjected to higher risks of progressing to stage III + IV, poor differentiation, and lymph node metastasis. ROC curve analysis revealed high diagnostic value of C9orf139 for pancreatic cancer and a markedly reduced 5-year survival in patients with high C9orf139 expression. Cox regression analysis found that high C9orf139 expression was an independent predictor of poor prognosis in patients with pancreatic cancer. Such results proved that C9orf139 is close related to the development of pancreatic cancer.

The underlying mechanism of action of C9orf139 in pancreatic cancer has not been figured out. The main mechanism of lncRNAs lies in their regulation of gene



**Figure 3 Effect of long non-coding RNA C9orf139 and miR-663a on pancreatic cancer cell behaviors.** A: Dual-luciferase reporter assay revealed a target binding between C9orf139 and miR-663a; B: RNA immunoprecipitation assay showed the enrichment of C9orf139 and miR-663a in PaCa-2 cells containing Ago2 antibody, with IgG antibody as a negative control; C: RNA pull-down assay was performed in PaCa-2 cells with biotin-labeled miR-663a, and then qRT-PCR was conducted to measure C9orf139 expression; D: Expression of miR-663a in patients with pancreatic cancer; E: Correlation analysis between miR-663a and C9orf139 in patients with pancreatic cancer; F: Relative expression of miR-663a in cells after the transfection; G: Cell proliferation after the transfection; H: Cell invasion after the transfection; I: The 24 h migration after the transfection; J: Cell apoptosis after the transfection. <sup>b</sup> $P < 0.01$  compared with the control group; <sup>e</sup> $P < 0.001$  compared with the control group.

expression by competing with microRNA elements as ceRNAs<sup>[32]</sup>. Our bioinformatics prediction suggested binding sites between miR-663a and C9orf139. miR-663a is an important member of the microRNA family. A former study concluded that<sup>[33]</sup> miR-663a was lowly expressed in the serum of patients with pancreatic cancer and could be used as a potential diagnostic marker for pancreatic cancer, suggesting that miR-663a may also be involved in the progression of pancreatic cancer. We conducted a dual-luciferase reporter assay, RIP assay, and RNA pull-down assay to verify the relationship between the miR-663a and C9orf139. Dual-luciferase reporter assay revealed targeting binding between miR-663a and C9orf139. RIP assay showed that the levels of C9orf139 and miR-663a precipitated with Ago2 antibody were significantly higher than those precipitated with IgG. RNA pull-down assay found that C9orf139 could be pulled down by biotin-labeled miR-663a-wt, not by miR-663a-mut. The above assays suggested that C9orf139 can regulate miR-663a as a ceRNA. To investigate the effects of C9orf139 and miR-663a on the growth of pancreatic cancer cells, we transfected pancreatic cancer cells with si-C9orf139 and miR-663a-mimic and discovered that the up-regulation of miR-663a and knockout of C9orf139 resulted in inhibited cell proliferation, invasion, and migration, as well as increased apoptosis. Such results indicated that the growth of pancreatic cancer cells can be affected by the expression of C9orf139 and miR-663a. To verify this, we co-transfected pancreatic cancer cells with miR-663a-mimic and sh-C9orf139 and found that the inhibited cell proliferation, invasion, and migration, and increased apoptosis caused by the up-regulated miR-663a were completely reversed by the transfection with sh-C9orf139. This demonstrates that the up-regulation of C9orf139 can regulate miR-663a to promote the growth of pancreatic cancer cells.

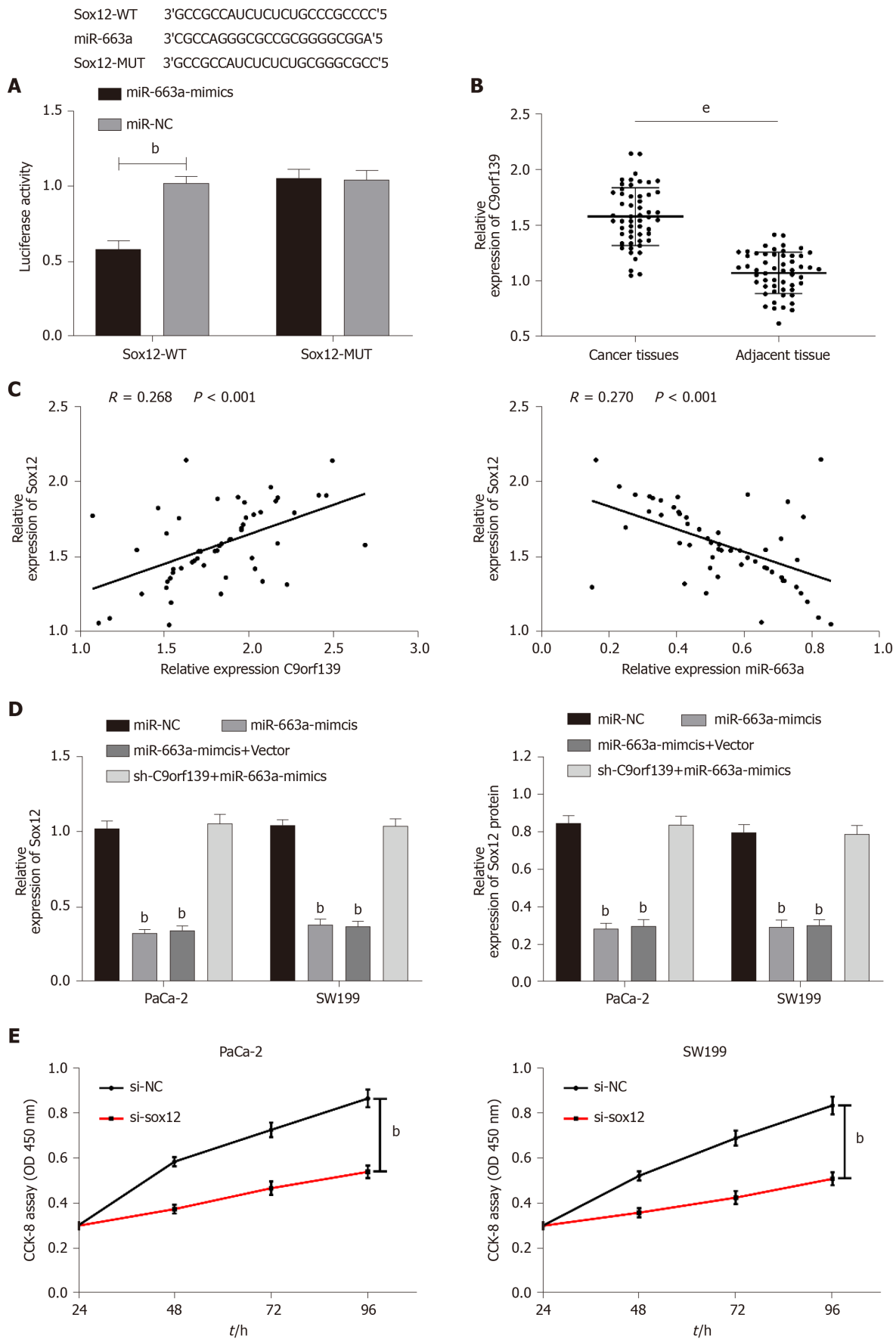
One of the important mechanisms of microRNAs lies in their regulation of mRNA to affect the biological functions<sup>[34]</sup>. Our bioinformatics analysis discovered a targeted binding site between miR-663a and Sox12. Sox12 is a member of the SOX transcription factor family. In the study by Wang *et al*<sup>[35]</sup>, Sox12 was found to be highly expressed in pancreatic cancer and miR-26a could inhibit the proliferation, migration, and invasion of pancreatic cancer cells by regulating Sox12. Dual-luciferase report assay revealed a targeting binding site between miR-663a and Sox12. In this study, knockdown of Sox12 led to inhibited proliferation, invasion, migration, and increased apoptosis. In order to confirm whether C9orf139 can affect pancreatic cancer *via* the miR-663a/Sox12 axis, we tested the expression of C9orf139, miR-663a, and Sox12 in patient tissues and conducted correlation analysis. It was found that Sox12 was positively correlated with C9orf139 expression and negatively correlated with miR-663a, and miR-663a was negatively correlated with C9orf139. We also found that up-regulated miR-663a led to inhibited Sox12 expression, but the expression of Sox12 mRNA and protein was reversed by the co-transfection with up-regulated C9orf139 plasmid. At the end of this study, we conducted tumor formation in nude mice and confirmed that the C9orf139-mediated miR-663a/Sox12 axis was involved in the growth of pancreatic cancer.

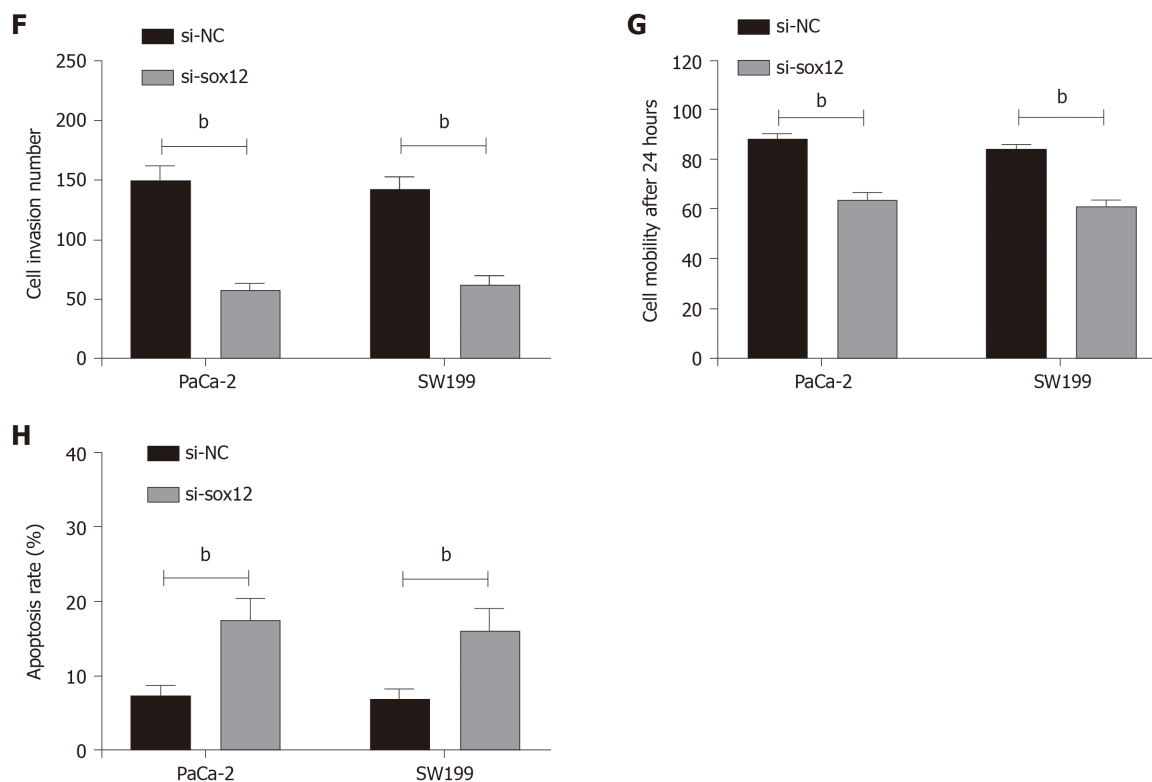
This study was subject to some limitations. First, we did not collect patients with benign pancreatic lesions to measure their C9orf139 expression, so whether C9orf139 can be used as the diagnostic indicator for benign pancreatic lesions and pancreatic cancer has not confirmed. Second, the presence or absence of the connection between C9orf139 and drug resistance, which is the most common condition in patients with pancreatic cancer, is not clear. To perfect our findings, we will collect more samples and research cases with different types and conduct bioinformatics analysis to explore the potential links between C9orf139 and drug resistance in pancreatic cancer.

## CONCLUSION

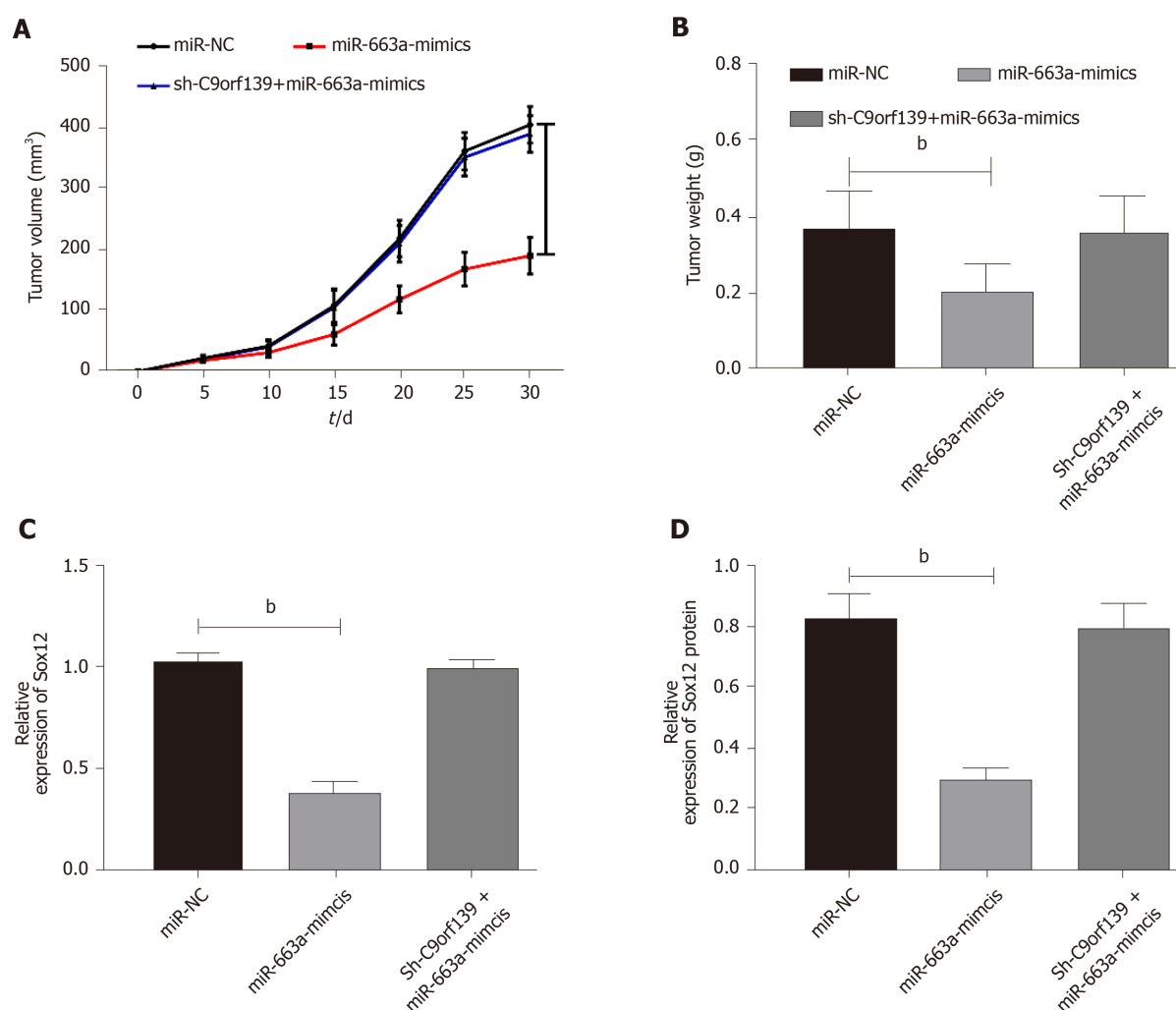
In conclusion, C9orf139 is highly expressed in pancreatic cancer, qualified to be used as a potential diagnostic and prognostic marker for pancreatic cancer. Its promotion of pancreatic cancer cell growth is achieved *via* the miR-663a/Sox12 axis.







**Figure 4 miR-663a inhibits pancreatic cancer cell growth by targeting Sox12.** A: Dual-luciferase reporter assay confirmed the relationship between miR-663a and Sox12; B: Expression of Sox12 in patients with pancreatic cancer; C: Sox12 was negatively correlated with miR-663a and positively correlated with C9orf139; D: Relative expression of Sox12 mRNA and protein in cells after transfection; E: Inhibited cell proliferation in pancreatic cancer cells transfected with si-Sox12; F: Inhibited cell invasion in pancreatic cancer cells transfected with si-Sox12; G: Inhibited cell migration in pancreatic cancer cells transfected with si-Sox12; H: Increased cell apoptosis in pancreatic cancer cells transfected with si-Sox12. <sup>b</sup> $P < 0.01$  compared with the control group; <sup>a</sup> $P < 0.001$  compared with the control group.



**Figure 5** Effect of long non-coding RNA C9orf139 and miR-663a on tumor formation in nude mice. A: The change of subcutaneous tumor size in nude mice during 30 d; B: Tumor size in nude mice on the 30th day; C: Expression of Sox12 mRNA in nude mouse tumors; D: Expression of Sox12 protein in nude mouse tumors. <sup>b</sup> $P < 0.01$  compared with the control group; <sup>a</sup> $P < 0.001$  compared with the control group.

## ARTICLE HIGHLIGHTS

### Research background

Pancreatic cancer is one of the tumors with the lowest 5-year survival rate, and its incidence has been surging in recent years. Many studies have confirmed the critical role of long non-coding RNAs (lncRNAs) in the development and progression of pancreatic cancer, but little has been known about C9orf139 in pancreatic cancer.

### Research motivation

To identify biomarkers for the diagnosis and treatment of pancreatic cancer.

### Research objectives

To explore the mechanism of action of lncRNA-C9orf139 in pancreatic cancer.

### Research methods

The relative expression of C9orf139 in tissues and sera of patients with pancreatic cancer was tested by RT-qPCR. The predictive value of C9orf139 for pancreatic cancer prognosis and the interaction between C9orf139 and miR-663a were assessed. The biological functions of C9orf139 were evaluated by *in vitro* assays and *in vivo* subcutaneous tumor formation experiments in animal models. The molecular mechanism of C9orf139 on miR-663a/Sox12 was investigated through assays including RNA pull-down, Western blot, RNA immunoprecipitation, and co-immunoprecipitation.

### Research results

RT-qPCR results revealed markedly high C9orf139 levels in the serum and tissue of pancreatic cancer patients, which showed clinical diagnostic and prognostic value. Biological and functional analyses suggested that C9orf139 may promote the growth of pancreatic cancer cells by regulating the miR-663a/Sox12 axis.

### Research conclusions

C9orf139 is highly expressed in pancreatic cancer and may work as a diagnostic and prognostic marker for pancreatic cancer. It promotes pancreatic cancer cell growth *via* the miR-663a/Sox12 axis.

### Research perspectives

The role of C9orf139 in other tumors may be uncovered in the future, and its application in anti-cancer therapy will be promoted.

## REFERENCES

- 1 **Kamisawa T**, Wood LD, Itoi T, Takaori K. Pancreatic cancer. *Lancet* 2016; **388**: 73-85 [PMID: [26830752](#) DOI: [10.1016/S0140-6736\(16\)00141-0](#)]
- 2 **Bray F**, Ferlay J, Soerjomataram I, Siegel RL, Torre LA, Jemal A. Global cancer statistics 2018: GLOBOCAN estimates of incidence and mortality worldwide for 36 cancers in 185 countries. *CA Cancer J Clin* 2018; **68**: 394-424 [PMID: [30207593](#) DOI: [10.3322/caac.21492](#)]
- 3 **Suker M**, Beumer BR, Sadot E, Marthey L, Faris JE, Mellon EA, El-Rayes BF, Wang-Gillam A, Lacy J, Hosein PJ, Moorcraft SY, Conroy T, Hohla F, Allen P, Taieb J, Hong TS, Shridhar R, Chau I, van Eijck CH, Koerkamp BG. FOLFIRINOX for locally advanced pancreatic cancer: a systematic review and patient-level meta-analysis. *Lancet Oncol* 2016; **17**: 801-810 [PMID: [27160474](#) DOI: [10.1016/S1470-2045\(16\)00172-8](#)]
- 4 **Ferrone CR**, Marchegiani G, Hong TS, Ryan DP, Deshpande V, McDonnell EI, Sabbatino F, Santos DD, Allen JN, Blaszkowsky LS, Clark JW, Faris JE, Goyal L, Kwak EL, Murphy JE, Ting DT, Wo JY, Zhu AX, Warshaw AL, Lillmoen KD, Fernández-del Castillo C. Radiological and surgical implications of neoadjuvant treatment with FOLFIRINOX for locally advanced and borderline resectable pancreatic cancer. *Ann Surg* 2015; **261**: 12-17 [PMID: [25599322](#) DOI: [10.1097/SLA.0000000000000867](#)]
- 5 **Zhang L**, Sanagapalli S, Stoita A. Challenges in diagnosis of pancreatic cancer. *World J Gastroenterol* 2018; **24**: 2047-2060 [PMID: [29785074](#) DOI: [10.3748/wjg.v24.i19.2047](#)]
- 6 **Khadka R**, Tian W, Hao X, Koirala R. Risk factor, early diagnosis and overall survival on outcome of association between pancreatic cancer and diabetes mellitus: Changes and advances, a review. *Int J Surg* 2018; **52**: 342-346 [PMID: [29535016](#) DOI: [10.1016/j.ijssu.2018.02.058](#)]
- 7 **Zhang HD**, Jiang LH, Sun DW, Hou JC, Ji ZL. CircRNA: a novel type of biomarker for cancer. *Breast Cancer* 2018; **25**: 1-7 [PMID: [28721656](#) DOI: [10.1007/s12282-017-0793-9](#)]
- 8 **Peng WX**, Koirala P, Mo YY. LncRNA-mediated regulation of cell signaling in cancer. *Oncogene* 2017; **36**: 5661-5667 [PMID: [28604750](#) DOI: [10.1038/onc.2017.184](#)]
- 9 **Qu S**, Yang X, Li X, Wang J, Gao Y, Shang R, Sun W, Dou K, Li H. Circular RNA: A new star of noncoding RNAs. *Cancer Lett* 2015; **365**: 141-148 [PMID: [26052092](#) DOI: [10.1016/j.canlet.2015.06.003](#)]
- 10 **Lin YH**. MicroRNA Networks Modulate Oxidative Stress in Cancer. *Int J Mol Sci* 2019; **20** [PMID: [31514389](#) DOI: [10.3390/ijms20184497](#)]
- 11 **Rupaimoole R**, Slack FJ. MicroRNA therapeutics: towards a new era for the management of cancer and other diseases. *Nat Rev Drug Discov* 2017; **16**: 203-222 [PMID: [28209991](#) DOI: [10.1038/nrd.2016.246](#)]
- 12 **Acunzo M**, Romano G, Wernicke D, Croce CM. MicroRNA and cancer—a brief overview. *Adv Biol Regul* 2015; **57**: 1-9 [PMID: [25294678](#) DOI: [10.1016/j.jbior.2014.09.013](#)]
- 13 **Jathar S**, Kumar V, Srivastava J, Tripathi V. Technological Developments in LncRNA Biology. *Adv Exp Med Biol* 2017; **1008**: 283-323 [PMID: [28815544](#) DOI: [10.1007/978-981-10-5203-3\\_10](#)]
- 14 **Chen R**, Li WX, Sun Y, Duan Y, Li Q, Zhang AX, Hu JL, Wang YM, Gao YD. Comprehensive Analysis of LncRNA and mRNA Expression Profiles in Lung Cancer. *Clin Lab* 2017; **63**: 313-320 [PMID: [28182363](#) DOI: [10.7754/Clin.Lab.2016.160812](#)]
- 15 **Jiang B**, Yang B, Wang Q, Zheng X, Guo Y, Lu W. LncRNA PVT1 promotes hepatitis B virus-positive liver cancer progression by disturbing histone methylation on the c-Myc promoter. *Oncol Rep* 2020; **43**: 718-726 [PMID: [31894346](#) DOI: [10.3892/or.2019.7444](#)]
- 16 **Lin A**, Li C, Xing Z, Hu Q, Liang K, Han L, Wang C, Hawke DH, Wang S, Zhang Y, Wei Y, Ma G, Park PK, Zhou J, Zhou Y, Hu Z, Zhou Y, Marks JR, Liang H, Hung MC, Lin C, Yang L. The LINK-A lncRNA activates normoxic HIF1 $\alpha$  signalling in triple-negative breast cancer. *Nat Cell Biol* 2016; **18**: 213-224 [PMID: [26751287](#) DOI: [10.1038/ncb3295](#)]
- 17 **Sun M**, Nie F, Wang Y, Zhang Z, Hou J, He D, Xie M, Xu L, De W, Wang Z, Wang J. LncRNA HOXA11-AS Promotes Proliferation and Invasion of Gastric Cancer by Scaffolding the Chromatin Modification Factors PRC2, LSD1, and DNMT1. *Cancer Res* 2016; **76**: 6299-6310 [PMID: [27651312](#) DOI: [10.1158/0008-5472.CAN-16-0356](#)]
- 18 **Wei W**, Liu Y, Lu Y, Yang B, Tang L. LncRNA XIST Promotes Pancreatic Cancer Proliferation Through miR-133a/EGFR. *J Cell Biochem* 2017; **118**: 3349-3358 [PMID: [28295543](#) DOI: [10.1002/jcb.25988](#)]
- 19 **Paraskevopoulou MD**, Hatzigeorgiou AG. Analyzing MiRNA-LncRNA Interactions. *Methods Mol Biol* 2016; **1402**: 271-286 [PMID: [26721498](#) DOI: [10.1007/978-1-4939-3378-5\\_21](#)]
- 20 **Song J**, Xu Q, Zhang H, Yin X, Zhu C, Zhao K, Zhu J. Five key lncRNAs considered as prognostic targets

- for predicting pancreatic ductal adenocarcinoma. *J Cell Biochem* 2018; **119**: 4559-4569 [PMID: 29239017 DOI: 10.1002/jcb.26598]
- 21 **Huang B**, Wang J, Chen Q, Qu C, Zhang J, Chen E, Zhang Y, Wang Y, Ni L, Liang T. Gemcitabine enhances OSI-027 cytotoxicity by upregulation of miR-663a in pancreatic ductal adenocarcinoma cells. *Am J Transl Res* 2019; **11**: 473-485 [PMID: 30788003]
  - 22 Issue Information-Declaration of Helsinki. *J Bone Miner Res* 2018; **33**: BM i-BM ii [PMID: 30521121 DOI: 10.1002/jbmr.3277]
  - 23 **Livak KJ**, Schmittgen TD. Analysis of relative gene expression data using real-time quantitative PCR and the 2(-Delta Delta C(T)) Method. *Methods* 2001; **25**: 402-408 [PMID: 11846609 DOI: 10.1006/meth.2001.1262]
  - 24 **Chen W**, Zheng R, Baade PD, Zhang S, Zeng H, Bray F, Jemal A, Yu XQ, He J. Cancer statistics in China, 2015. *CA Cancer J Clin* 2016; **66**: 115-132 [PMID: 26808342 DOI: 10.3322/caac.21338]
  - 25 **Qi Q**, Geng Y, Sun M, Chen H, Wang P, Chen Z. Hyperfibrinogen Is Associated With the Systemic Inflammatory Response and Predicts Poor Prognosis in Advanced Pancreatic Cancer. *Pancreas* 2015; **44**: 977-982 [PMID: 25931258 DOI: 10.1097/MPA.0000000000000353]
  - 26 **Luo G**, Guo M, Liu Z, Xiao Z, Jin K, Long J, Liu L, Liu C, Xu J, Ni Q, Yu X. Blood neutrophil-lymphocyte ratio predicts survival in patients with advanced pancreatic cancer treated with chemotherapy. *Ann Surg Oncol* 2015; **22**: 670-676 [PMID: 25155401 DOI: 10.1245/s10434-014-4021-y]
  - 27 **Li J**, Meng H, Bai Y, Wang K. Regulation of lncRNA and Its Role in Cancer Metastasis. *Oncol Res* 2016; **23**: 205-217 [PMID: 27098144 DOI: 10.3727/096504016X14549667334007]
  - 28 **Huang C**, Yu W, Wang Q, Cui H, Wang Y, Zhang L, Han F, Huang T. Increased expression of the lncRNA PVT1 is associated with poor prognosis in pancreatic cancer patients. *Minerva Med* 2015; **106**: 143-149 [PMID: 25668599]
  - 29 **Qu S**, Yang X, Song W, Sun W, Li X, Wang J, Zhong Y, Shang R, Ruan B, Zhang Z, Zhang X, Li H. Downregulation of lncRNA-ATB correlates with clinical progression and unfavorable prognosis in pancreatic cancer. *Tumour Biol* 2016; **37**: 3933-3938 [PMID: 26482611 DOI: 10.1007/s13277-015-4252-y]
  - 30 **Shi X**, Zhao Y, He R, Zhou M, Pan S, Yu S, Xie Y, Li X, Wang M, Guo X, Qin R. Three-lncRNA signature is a potential prognostic biomarker for pancreatic adenocarcinoma. *Oncotarget* 2018; **9**: 24248-24259 [PMID: 29849937 DOI: 10.18632/oncotarget.24443]
  - 31 **Wei C**, Liang Q, Li X, Li H, Liu Y, Huang X, Chen X, Guo Y, Li J. Bioinformatics profiling utilized a nine immune-related long noncoding RNA signature as a prognostic target for pancreatic cancer. *J Cell Biochem* 2019; **120**: 14916-14927 [PMID: 31016791 DOI: 10.1002/jcb.28754]
  - 32 **Zhou M**, Diao Z, Yue X, Chen Y, Zhao H, Cheng L, Sun J. Construction and analysis of dysregulated lncRNA-associated ceRNA network identified novel lncRNA biomarkers for early diagnosis of human pancreatic cancer. *Oncotarget* 2016; **7**: 56383-56394 [PMID: 27487139 DOI: 10.18632/oncotarget.10891]
  - 33 **Mody HR**, Hung SW, AlSaggar M, Griffin J, Govindarajan R. Inhibition of S-Adenosylmethionine-Dependent Methyltransferase Attenuates TGFβ1-Induced EMT and Metastasis in Pancreatic Cancer: Putative Roles of miR-663a and miR-4787-5p. *Mol Cancer Res* 2016; **14**: 1124-1135 [PMID: 27624777 DOI: 10.1158/1541-7786.MCR-16-0083]
  - 34 **Amirkhah R**, Schmitz U, Linnebacher M, Wolkenhauer O, Farazmand A. MicroRNA-mRNA interactions in colorectal cancer and their role in tumor progression. *Genes Chromosomes Cancer* 2015; **54**: 129-141 [PMID: 25620079 DOI: 10.1002/gcc.22231]
  - 35 **Wang L**, Wang Z, Huang L, Wu C, Zhang B. MiR-29b suppresses proliferation and mobility by targeting SOX12 and DNMT3b in pancreatic cancer. *Anticancer Drugs* 2019; **30**: 281-288 [PMID: 30601190 DOI: 10.1097/CAD.0000000000000719]





Retrospective Cohort Study

## Cancer-related microangiopathic hemolytic anemia in patients with advanced gastric cancer: A retrospective single-center analysis

Anne Katrin Berger, Michael Allgäuer, Leonidas Apostolidis, Anna Elisa Schulze-Schleithoff, Uta Merle, Dirk Jaeger, Georg Martin Haag

**ORCID number:** Anne Katrin Berger 0000-0002-0906-4401; Michael Allgäuer 0000-0003-4518-7887; Leonidas Apostolidis 0000-0002-6358-8206; Anna Elisa Schulze-Schleithoff 0000-0003-1914-0866; Uta Merle 0000-0003-1386-3350; Dirk Jaeger 0000-0002-1276-7802; Georg Martin Haag 0000-0002-9410-9968.

**Author contributions:** Berger AK completed conception and design, acquisition of data, analysis and interpretation of data, writing and revision of the manuscript; Allgäuer M and Apostolidis L finished analysis and interpretation of data, rewriting and review of the manuscript, technical support; Schulze-Schleithoff AE, Merle U and Jaeger D completed acquisition of data, writing and review of the manuscript; Haag GM finished conception and design, acquisition of data, analysis and interpretation of data, writing and review of the manuscript; All authors approved the final manuscript version.

**Institutional review board**

**statement:** The study was approved by the local Ethics Committee University of Heidelberg, No. S-335/2014.

**Informed consent statement:**

According to local ethics policy for retrospective analysis of own

Anne Katrin Berger, Leonidas Apostolidis, Dirk Jaeger, Georg Martin Haag, Department of Medical Oncology, National Center for Tumor Diseases, University Hospital of Heidelberg, Heidelberg 69120, Germany

Michael Allgäuer, Department of Pathology, Institute of Pathology, University Hospital of Heidelberg, Heidelberg 69120, Germany

Anna Elisa Schulze-Schleithoff, Department of Gastroenterology, University Hospital of Heidelberg, Heidelberg 69120, Germany

Uta Merle, Department of Gastroenterology and Hepatology, University Hospital of Heidelberg, Heidelberg 69120, Germany

**Corresponding author:** Anne Katrin Berger, MD, Attending Doctor, Department of Medical Oncology, National Center for Tumor Diseases, University Hospital of Heidelberg, Im Neuenheimer Feld 460, Heidelberg 69120, Germany. [anne.berger@med.uni-heidelberg.de](mailto:anne.berger@med.uni-heidelberg.de)

### Abstract

#### BACKGROUND

Microangiopathic hemolytic anemia (MAHA) with thrombocytopenia and organ failure caused by tumor-associated thrombotic microangiopathy (TMA) is a life-threatening oncological emergency. Rapid diagnosis and precise distinction from other forms of TMA is crucial for appropriate therapy, which aims at treating the underlying malignancy. However, the prognosis of patients with cancer-related (CR)-MAHA is limited. To date, less than 50 patients with gastric cancer and CR-MAHA have been reported, mainly as single case reports, and detailed information on treatment strategies and outcome are scarce. We analyzed the characteristics and outcomes data of CR-MAHA patients with gastric cancer treated at our center between 2012 and 2019.

#### AIM

To gain knowledge about CR-MAHA and the course of disease.

#### METHODS

We retrospectively analyzed patients using an institutional prospectively maintained database. Patients who had CR-MAHA but other cancer types or cancer of unknown primary were excluded. The basic requirements for inclusion

anonymized clinical data, informed consent was not obtained.

#### Conflict-of-interest statement:

Haag MG has received fees for consulting or advisory role: Bristol-Myers Squibb, MSD Sharp & Dohme (Inst), EsoCap. Honoraria: Servier, MSD Sharp & Dohme. Research Funding: Nordic Pharma (Inst); Taiho Pharmaceutical (Inst), MSD (Inst). Travel, Accommodations: Bristol-Myers Squibb; Lilly, all outside the submitted work. Leonidas Apostolidis: reports grants, personal fees and non-financial support from Ipsen, personal and non-financial support from Novartis, all outside the submitted work. All other authors have no conflicts to declare.

**Data sharing statement:** The dataset is available from the corresponding author.

**STROBE statement:** The authors have read the STROBE Statement-checklist of items, and the manuscript was prepared and revised according to the STROBE Statement-checklist of item.

**Open-Access:** This article is an open-access article that was selected by an in-house editor and fully peer-reviewed by external reviewers. It is distributed in accordance with the Creative Commons Attribution NonCommercial (CC BY-NC 4.0) license, which permits others to distribute, remix, adapt, build upon this work non-commercially, and license their derivative works on different terms, provided the original work is properly cited and the use is non-commercial. See: <http://creativecommons.org/licenses/by-nc/4.0/>

**Manuscript source:** Unsolicited manuscript

**Specialty type:** Oncology

**Country/Territory of origin:** Germany

**Peer-review report's scientific quality classification**  
Grade A (Excellent): 0

were: Histologically proven gastric adenocarcinoma; and clinical diagnosis of hemolytic anemia with schistocytes with or without thrombocytopenia. The observation period for each patient started with the first day of documented symptoms. The follow-up period for this analysis ended on February 1, 2020.

#### RESULTS

We identified eight patients with a median age of 54 years. Histologically, all patients had (partial) diffuse subtypes of gastric adenocarcinoma with partial or complete signet cell morphology. All patients had metastatic disease and one patient had a microsatellite instability-high (MSI-H) tumor. In three patients, clinical signs of MAHA preceded the diagnosis of cancer, and in two patients, CR-MAHA indicated recurrent disease. All patients had severe hemolytic anemia and thrombocytopenia. Six patients experienced severe bone pain, and five patients had dyspnea. Systemic, 5-fluorouracil-based combination chemotherapy was initiated in six patients, which resulted in rapid initial response with significant improvement of clinical symptoms and blood values. Progression-free survival (PFS) of the whole cohort was 1.9 wk and median overall survival (OS) was 1.9 wk. For patients with chemotherapy, PFS was 9.0 wk and OS was 10.3 wk. The patient with the MSI-H tumor has been undergoing immunotherapy for more than 3 years.

#### CONCLUSION

The benefit of chemotherapy in CR-MAHA patients is limited. Immunotherapy for patients with MSI-H tumors may lead to long-term tumor control even in CR-MAHA patients.

**Key Words:** Microangiopathic hemolytic anemia; Gastric cancer; Chemotherapy; Second-line chemotherapy; Thrombocytopenia; Microsatellite instability-high tumor

©The Author(s) 2020. Published by Baishideng Publishing Group Inc. All rights reserved.

**Core Tip:** Microangiopathic hemolytic anemia (MAHA) with thrombopenia and organ failure caused by tumor-associated thrombotic microangiopathy is a rare and life-threatening oncological emergency. The only proven therapy is the treatment of the underlying malignancy. In our retrospective series, 6 of 8 cancer-related (CR)-MAHA patients with advanced gastric cancer received combination chemotherapy with an overall survival (OS) of 10.3 wk. For the whole cohort, OS was only 1.8 wk. Second-line treatment did not show any benefit. One patient with microsatellite instability-high tumor has been undergoing immunotherapy for more than 3 years, which to the best of our knowledge is the first reported case of long-term survival in a CR-MAHA patient with advanced disease.

**Citation:** Berger AK, Allgäuer M, Apostolidis L, Schulze-Schleithoff AE, Merle U, Jaeger D, Haag GM. Cancer-related microangiopathic hemolytic anemia in patients with advanced gastric cancer: A retrospective single-center analysis. *World J Gastrointest Oncol* 2020; 12(11): 1288-1295

**URL:** <https://www.wjgnet.com/1948-5204/full/v12/i11/1288.htm>

**DOI:** <https://dx.doi.org/10.4251/wjgo.v12.i11.1288>

#### INTRODUCTION

Tumor-associated thrombotic microangiopathy (TMA) caused by systemic microvascular metastases and bone marrow involvement is a life-threatening oncological emergency leading to microangiopathic hemolytic anemia (MAHA) with thrombocytopenia and organ failure of variable severity<sup>[1]</sup>. This alarming and often fatal clinical constellation is described as a rare event in several solid tumors entities and may sometimes reveal occult disseminated malignancy<sup>[2,3]</sup>. It has to be clearly distinguished from drug-induced TMA in cancer patients<sup>[4]</sup> and hereditary or acquired

Grade B (Very good): B  
 Grade C (Good): C, C  
 Grade D (Fair): 0  
 Grade E (Poor): 0

**Received:** July 7, 2020

**Peer-review started:** July 7, 2020

**First decision:** September 17, 2020

**Revised:** September 27, 2020

**Accepted:** October 19, 2020

**Article in press:** October 19, 2020

**Published online:** November 15, 2020

**P-Reviewer:** Chen L, Nishida T, Paydas S

**S-Editor:** Gao CC

**L-Editor:** Filipodia

**P-Editor:** Li JH



primary TMA syndromes such as ADAMTS13 deficiency or Shiga toxin-mediated TMA<sup>[5]</sup>. Those forms are also clinically characterized by MAHA, thrombocytopenia and organ injury, but based on diverging underlying pathomechanisms, immediate specific therapeutic measures like plasma exchange treatment or application of eculizumab<sup>[6,7]</sup> can be crucial for forms of primary TMA. For cancer patients with drug-induced TMA, removal of the causative drug is often sufficient<sup>[1]</sup>. In contrast, for patients with cancer-related (CR)-MAHA, the only beneficial therapy is the treatment of the underlying malignancy, highlighting the need for rapid diagnosis to avoid ineffective therapeutic interventions such as plasmapheresis. Still, the prognosis of this subgroup of cancer patients is very poor<sup>[8]</sup>.

To date, the most comprehensive clinical data for CR-MAHA patients come from two heterogeneous thrombotic thrombocytopenic purpura (TTP)-registry series that included 10 and 20 patients with different tumor types<sup>[2,9]</sup>. Gastric cancer was identified in 13.3% (4/30) of those patients. A large retrospective literature review covering a time period of 33 years reported on 168 CR-MAHA patients and identified another 40 patients with gastric cancer, reported mainly as single case reports<sup>[8]</sup>. Here, we add our experience with 8 patients presenting with CR-MAHA and gastric cancer treated at our university hospital center between 2012 and 2019. We present the patients' clinical and laboratory findings and outcomes, and report our experience with oncological treatment for this rare condition. To the best of our knowledge, this is the largest cohort of gastric cancer patients with CR-MAHA reported to date.

## MATERIALS AND METHODS

### Patients

We identified patients who were diagnosed with CR-MAHA and gastric adenocarcinoma at our center between January 2012 and January 2020. Patients who had CR-MAHA but other cancer types or cancer of unknown primary were excluded from this analysis. The data were obtained from an institutional prospectively maintained database. The basic requirements for inclusion were histologically proven diagnosis of gastric adenocarcinoma; and clinical diagnosis of hemolytic anemia with schistocytes with or without thrombocytopenia. The observation period for each patient started with the first day of documented symptoms. The follow-up period for this analysis ended on February 1, 2020.

### Assessment

If systemic treatment was initiated, the choice of treatment was up to the attending oncologist considering the individual patient's condition. When antitumor treatment was withheld, this was a shared decision considering the patient's choice, his condition, and the physician's advice. Clinical data were routinely collected and documented by the attending oncologists and medical staff *via* an electronic medical record. Information included: Time of first CR-MAHA-associated symptoms, time of diagnosis of MAHA from or to diagnosis of gastric cancer (prior, concurrent, after), site and histologic subtype of carcinoma, laboratory features, clinical signs of organ failure, histologic analysis of the bone marrow, start and stop date of antitumor treatment, response to therapy, and date of progression and date of death.

Overall survival (OS) was defined as the time from documented CR-MAHA diagnosis to death. Progression-free survival (PFS) was defined as the time from CR-MAHA diagnosis to documented tumor progression or death, whichever occurred first. Residual survival (RS) among patients with salvage therapy was defined as the time from start of second-line therapy to death. Diagnosis of CR-MAHA was defined as the timepoint when the term was documented the first time. Onset of CR-MAHA symptoms was defined as the first documented medical contact (as inpatient or outpatient) the patient had for associated symptoms (*e.g.*, dyspnea, pain, bleeding) or laboratory findings (anemia, thrombocytopenia, coagulopathy).

### Ethics approval

The study was approved by the local Ethics Committee University of Heidelberg, No. S-335/2014.

## RESULTS

### *Patients demographics*

We identified 8 patients meeting the inclusion criteria. An overview of the patients' characteristics is given in [Table 1](#). The median age was 50 years (range 28-76) for diagnosis of gastric cancer and 54 years (range 28-76) for diagnosis of CR-MAHA. Four patients were female. The gastric carcinoma was located in the stomach in 7 patients (87.5%), and at the gastroesophageal junction in 1 patient (12.5%). Histologically, 4 patients (50%) had adenocarcinomas of the diffuse subtype, and 4 patients (50%) showed mixed intestinal/diffuse differentiation. In all cases, the tumor was of partial or complete signet ring cell morphology. Five patients (62.5%) were human epidermal growth factor receptor 2 (HER2)-negative, and HER2 status was unknown in 3 patients (37.5%). One patient (12.5%) had microsatellite instability-high (MSI-H) tumor, and MSI status is unknown in all other patients. All patients had metastatic disease. Five patients (62.5%) had synchronous metastases, and 3 patients (37.5%) had secondary metastatic disease after definitive surgery that occurred 0.5, 2, and 10 years, respectively, after first treatment. For all patients, survival data were available. At time of database lock, 7 patients (87.5%) had died of their disease.

### *CR-MAHA*

In 3 patients (37.5%), clinical signs of MAHA preceded the diagnosis of cancer. Before admission to our hospital, these patients were inpatients or outpatients of external medical facilities. One patient was admitted to our hospital with severe backpain, anemia and thrombocytopenia, suspected to have "acute leukemia" only days after the patient sought medical attention for the first time. The second patient was transferred after 5 days with "unclear coagulopathy." The third patient had been under diagnostic evaluations for backpain and progressing anemia and thrombocytopenia for 3 wk. In 2 patients (25%), CR-MAHA indicated recurrent disease after 0.5 and 10 years, respectively. The patient with recurrent metastatic disease after 10 years was treated at an external hospital for severe backpain and thrombocytopenia for 6 d, and the patient with secondary metastases after 0.5 years presented in our emergency department with new back pain, fever and dyspnea. In 2 patients (25%), onset of CR-MAHA was concurrent with first cancer diagnosis, and 1 patient (12.5%) was under palliative chemotherapy (paclitaxel-ramucirumab) when CR-MAHA occurred.

In all patients, laboratory analysis revealed hemolytic anemia with a median hemoglobin concentration of 7.7 g/dL (range 5.4-8.4 g/dL, reference 12-16 g/dL), median schistocytes of 33% (range 15-97%, reference < 5%) and decreased haptoglobin (< 0.1 g/L, reference 0.3-2.0 g/L). The median platelet count was 40/nL (range 8-168/nL, reference 150-440/nL). Median lactate dehydrogenase level was 853 U/L (range 415-4765 U/L, reference < 249 U/L). At time of CR-MAHA, 1 patient (12.5%) had intermittent neurological symptoms (aphasia), 6 (75%) suffered from dyspnea and 5 (62.5%) complained about severe backpain, requiring analgesia with opioids. In 5 of 8 patients (62.5%), bone marrow biopsy was performed, of which 3 showed infiltration by adenocarcinoma ([Figure 1](#)). In 1 patient there were no signs of infiltration and 1 patient had a dry tap.

### *Antitumor treatment*

After diagnosis of CR-MAHA, systemic chemotherapy was administered in 6 patients (75%). Median time between CR-MAHA diagnosis at our center and start of chemotherapy was 1 d (range 0-2). Median time between first symptoms and start of chemotherapy was 5 d (range 0-22). All patients received 5-fluorouracil (5-FU)-based combinations. Three (37.5%) patients were treated with a triple combination according to the FLOT regimen<sup>[10]</sup>, 3 patients (37.5%) received doublet combinations (5-FU plus oxaliplatin in 2 cases, 5-FU plus irinotecan and ramucirumab in 1 case). Four patients (66.7% of patients starting treatment) showed rapid initial response to chemotherapy with significant improvement of clinical symptoms and blood values already before the second cycle at day 14 ([Table 2](#)). Two patients (25%) deteriorated rapidly despite chemotherapy and died only 1 and 5 d afterwards. Three patients (37.5%) received second-line chemotherapies (FOLFIRI, FOLFIRI-ramucirumab and paclitaxel, respectively). In one patient (patient 4), further analysis revealed a MSI-H tumor. Thus, after showing disease progression during treatment with FOLFIRI/ramucirumab, a checkpoint inhibitor therapy was initiated. A detailed summary of patients and treatment responses is given in [Table 2](#).

**Table 1 Patient characteristics**

Patient	Sex	Age <sup>1</sup>	Site of tumor	CR-MAHA <sup>2</sup>	Metastases	Initial symptoms	Onset symptoms to diagnosis in d	Chemotherapy for CR- MAHA
1	F	47	Stomach	Prior	OSS, LN, OVA	BP	1	Yes
2	M	68	Stomach	After	LR, PUL	DYS, BP	4	No
3	M	53	Stomach	Prior	OSS, LN	DYS, BP	22	Yes
4	F	36	GE-junction	After	OSS, HEP	DYS, BP	0	Yes
5	F	61	Stomach	Concurrent	OSS, PC, PUL, LN	DYS	0	Yes
6	M	54	Stomach	After	OSS, PUL	DYS, BP	6	Yes
7	F	28	Stomach	Concurrent	HEP	DYS, APH	10	Yes
8	M	76	Stomach	Prior	OSS, PUL	No	5	No

<sup>1</sup>age at microangiopathic hemolytic anemia diagnosis.

<sup>2</sup>time of diagnosis of microangiopathic hemolytic anemia from or to diagnosis of gastric cancer. APH: Aphasia; BP: Back pain; CR-MAHA: Cancer-related microangiopathic hemolytic anemia; DYS: Dyspnea; F: Female; GE: Gastroesophageal; HEP: Hepatic (liver); LN: Lymph node; LR: Local recurrence; M: Male; OSS: Osseous (bone); OVA: Ovary; PUL: Pulmonary; PC: Peritoneal carcinosis.

**Table 2 Treatment and response**

Patient number	1 <sup>st</sup> chemo therapy	2 <sup>nd</sup> chemo therapy	MAHA baseline			MAHA day 14			PFS in wk	RS in wk	OS in wk
			Pts	Hb	Sch	Plt	Hb	Sch			
1	FLO	FOLFIRI	8	5.9	31	84	9.6	12	9	1.1	10.3
2	No	NA	32	7.7	40	NA	NA	NA	0.1	NA	0.1
3	FLO	Paclitaxel	34	8.0	15	65	10.7	-	25.7	0.1	27.1
4	FOLFIRI-Ram <sup>1</sup>	NA	168	5.4	40	204	11.6	-	32.1	NA	NA
5	FLOT	No	130	7.8	35	NA	NA	NA	1.0	NA	1.0
6	FLOT	FOLFIRI-Ram	44	8.4	25	208	8.8	25	25.4	2.3	28.0
7	FLOT	No	46	6.9	97	NA	NA	NA	0.3	NA	0.3
8	No	NA	36	8.2	17	NA	NA	NA	1.86	NA	1.86

<sup>1</sup>Diagnosis of microsatellite instability-high tumor. FLO: 5-Fluorouracil (5-FU), leucovorin, oxaliplatin; FLOT: 5-FU, leucovorin, oxaliplatin, docetaxel; FOLFIRI: 5-FU, leucovorin, irinotecan; Hb: Hemoglobin (gram per deciliter); NA: Not applicable; OS: Overall survival; PFS: Progression-free survival; Plt: Platelet count (per nanoliter); RAM: Ramucirumab; RS: Residual survival; Sch: Schistocytes (per milliliter).

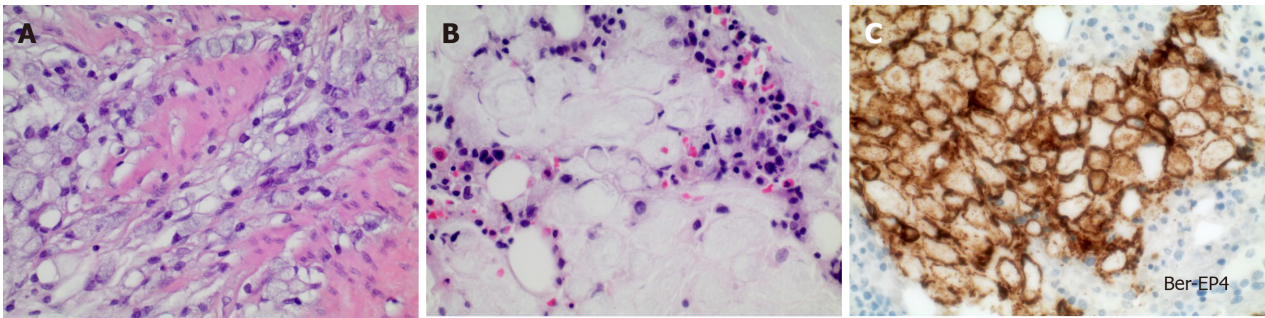
### Progression and survival

At time of analysis, 7 patients had died of their disease. The median PFS of the whole cohort was 1.9 wk (95% confidence interval [CI]: 0.0-12.9), median OS was 1.9 wk (95% CI: 0.0-14.7). For the 6 patients starting chemotherapy, PFS was 9.0 wk (95% CI: 0.0-38.3) and OS was 10.3 wk (95% CI: 0.0-41.7). For patients who received second-line chemotherapy after progression, median RS was 1.1 wk (95% CI: 0.0-3.2). The patient with the MSI-H tumor has been undergoing immunotherapy for more than 3 years.

## DISCUSSION

CR-MAHA was first described in 1970 by Brain *et al*<sup>[11]</sup> in 12 patients with metastatic mucin-secreting adenocarcinomas of which 6 were of gastric origin. Less than 50 patients with gastric cancer and CR-MAHA have been described, mainly as single case reports<sup>[11]</sup>. The pathogenesis of CR-MAHA is not completely understood. Microvascular obstruction with tumor emboli causing red cell fragmentation and





**Figure 1 Histopathology of diffuse type gastric adenocarcinoma, patient 2.** A: Discohesive tumor cells with a prominent intracytoplasmic mucin vacuole and peripherally displaced and compressed nucleus (signet ring cell morphology) diffusely infiltrate muscular layers of the gastric wall; B and C: Bone marrow core needle biopsy from the right iliac crest with residual hematopoietic elements and diffuse carcinomatous infiltrates composed of pale signet ring cells. Immunohistochemical staining for epithelial cell adhesion molecule is positive confirming the epithelial nature of cell infiltrates. A-C: Original magnification, 400 ×. A and B, hematoxylin and eosin staining.

platelet consumption especially in the bone marrow and the lung are supposed to be the underlying pathological mechanism<sup>[1,8]</sup>, which is in part supported by available autopsy data<sup>[12]</sup>. Of note, all of our patients showed, at least partial, signet ring cell morphology of their tumors. Brain *et al*<sup>[11]</sup> presumed that mucin-forming tumor cells may especially promote CR-MAHA. The incidence of CR-MAHA is estimated to be 0.25-0.45 persons per million per year<sup>[8]</sup> but data on CR-MAHA in overall cancer cases or for different cancer entities are lacking. At our center, between 2012 and 2020, approximately 4% of patients newly diagnosed with metastatic gastric cancer receiving palliative treatment developed CR-MAHA. This rather high rate might be explained by the fact that the awareness of our specialized oncologic center for CR-MAHA is high and that predominantly patients with high tumor burden and/or critical clinical symptoms are sent to our center.

Clinically, a rapid and precise distinction between CR-MAHA and other MAHA forms is crucial, since misdiagnosis, *e.g.*, as a primary TMA syndrome will result in inadequate and resource-consuming treatments, including therapeutic plasma exchange<sup>[13]</sup>. Given the observed often dramatic clinical deterioration of patients within days and the dismal survival times of 3 d reported by others<sup>[2]</sup>, it is evident that a prolonged diagnostic process can close the narrow time-window for application of systemic antitumor treatment. We had the experience that cross-specialty awareness for CR-MAHA leads to marked improvements in timely diagnosis of this condition. Helpful distinguishing clinical features of patients with CR-MAHA were published by Morton *et al*<sup>[1]</sup>. In line with these, dyspnea as well as the occurrence of severe back or bone pain, exceeding the extent of radiologically apparent metastatic disease, were recurrent clinical findings in our cohort. One of our patients developed CR-MAHA while under palliative chemotherapy with paclitaxel and ramucirumab. Drug-induced MAHA was considered unlikely using the Morton criteria, and a later bone marrow biopsy revealed metastatic infiltration by signet ring- cells. Distinguishing CR-MAHA from CR-disseminated intravascular coagulation (DIC) can be challenging. However, the vast majority (87.5%) of our patients had no signs of consumption coagulopathy or fibrinolysis when MAHA was diagnosed. In patients with a prolonged clinical history of MAHA-suspect symptoms, coagulation parameters might be altered since CR-MAHA itself can cause a secondary DIC due to organ damage. In addition, more severe microangiopathic changes on the blood smear can be observed in patients with CR-MAHA in comparison to DIC patients. In our patient with slight laboratory signs of coagulopathy, prolonged CR-MAHA was considered as the more appropriate clinical diagnosis in line with his significantly increased schistocytes and the severely decreased hemoglobin levels.

Our data show, that with prompt application of systemic chemotherapy a subset of patients can achieve tumor control and a relieve of symptoms for a limited time period (mostly few months). The small patient number does not allow for comparison of different chemotherapeutic regimen in this setting. Whether primary immunotherapy in MSI-H CR-MAHA patients would be more beneficial remains unclear, but the required prompt clinical response rather demands for combined chemotherapy to rapidly reduce tumor burden. However, the OS of CR-MAHA patients is clearly reduced compared to unaffected patients with metastatic gastric carcinoma where the median survival is currently in the range of 10-12 mo<sup>[14]</sup>. Of interest, among all of our patients undergoing second-line therapy, disease progression during first-line

treatment manifested with recurrent onset of bone pain and deterioration of blood test results. Thus, laboratory analysis should be performed diligently and could probably be used for early identification of insufficient tumor control. However, the RS after start of second-line treatment was dismal with only a few days. Therefore, the use of chemotherapy beyond the first-line situation seems questionable and should be discussed individually with the patient on a case-by-case basis.

To the best of our knowledge, this is the first report of a patient with CR-MAHA and a MSI-H tumor. Of note, this patient achieved long-term tumor control with the best long-term survival of all CR-MAHA patients reported to date. Thus, in patients with CR-MAHA and successful initial disease stabilization, further testing for MSI seems reasonable and may offer the chance for long-term survival.

## CONCLUSION

CR-MAHA is a rare event in patients with gastric cancer that can occur at every time point during the course of disease. Rapid diagnosis of CR-MAHA may allow for application of systemic chemotherapy, which is the only causative treatment. Chemotherapy can lead to a disease stabilization and relief of symptoms for a limited time period. The results of second-line approaches are disappointing. CR-MAHA patients with MSI-H tumors may benefit enormously from checkpoint inhibition including long-time tumor control. Thus, MSI testing is strongly recommended.

## ARTICLE HIGHLIGHTS

### **Research background**

Cancer-related microangiopathic hemolytic anemia (CR-MAHA) is an infrequent but alarming oncological emergency in patients with solid tumors. Advanced gastric cancer seems among the tumor types with the highest association with CR-MAHA. Data on appropriate treatment and patients' outcome are scarce.

### **Research motivation**

To obtain knowledge about CR-MAHA and the course of disease to help guide treatment decisions in future patients with CR-MAHA and gastric cancer.

### **Research objectives**

Frequency, patient and tumor characteristics, symptom load, treatment efficacy and patient outcomes.

### **Research methods**

We analyzed a prospectively maintained database for patients with CR-MAHA and gastric cancer at our high-volume university cancer center between 2012 and 2019.

### **Research results**

We identified 8 patients of whom 6 started polychemotherapy. Four of six showed initial response to treatment, but the survival was poor. Patients under chemotherapy had an overall survival (OS) of 10.3 wk. For the whole cohort, OS was 1.9 wk. One patient with microsatellite instability-high (MSI-H) tumor responded extremely well to immunotherapy with long-time survival exceeding 3 years.

### **Research conclusions**

CR-MAHA in gastric cancer patients is a condition with an overall limited prognosis. Some patients respond to first-line treatment for several months. Second-line treatment does not seem beneficial. Testing for MSI status is recommended.

### **Research perspectives**

First-line chemotherapy should be discussed with patients with CR-MAHA and gastric cancer, but the limited prognosis should be addressed by the attending oncologists. We do not encourage for second-line approaches. MSI-H tumors seem to act differently, even in fatal conditions such as CR-MAHA. It remains unclear, if combined chemo-immunotherapy in those patients would be beneficial.

## REFERENCES

- 1 **Morton JM**, George JN. Microangiopathic Hemolytic Anemia and Thrombocytopenia in Patients With Cancer. *J Oncol Pract* 2016; **12**: 523-530 [PMID: [27288467](#) DOI: [10.1200/JOP.2016.012096](#)]
- 2 **Francis KK**, Kalyanam N, Terrell DR, Vesely SK, George JN. Disseminated malignancy misdiagnosed as thrombotic thrombocytopenic purpura: A report of 10 patients and a systematic review of published cases. *Oncologist* 2007; **12**: 11-19 [PMID: [17227897](#) DOI: [10.1634/theoncologist.12-1-11](#)]
- 3 **Lin YC**, Chang HK, Sun CF, Shih LY. Microangiopathic hemolytic anemia as an initial presentation of metastatic cancer of unknown primary origin. *South Med J* 1995; **88**: 683-687 [PMID: [7777893](#) DOI: [10.1097/00007611-199506000-00021](#)]
- 4 **Hausberg M**, Felten H, Pfeffer S. Treatment of Chemotherapy-Induced Thrombotic Microangiopathy with Eculizumab in a Patient with Metastatic Breast Cancer. *Case Rep Oncol* 2019; **12**: 1-6 [PMID: [30792638](#) DOI: [10.1159/000495031](#)]
- 5 **George JN**, Nester CM. Syndromes of thrombotic microangiopathy. *N Engl J Med* 2014; **371**: 654-666 [PMID: [25119611](#) DOI: [10.1056/NEJMra1312353](#)]
- 6 **Bendapudi PK**, Hurwitz S, Fry A, Marques MB, Waldo SW, Li A, Sun L, Upadhyay V, Hamdan A, Brunner AM, Gansner JM, Viswanathan S, Kaufman RM, Uhl L, Stowell CP, Dzik WH, Makar RS. Derivation and external validation of the PLASMIC score for rapid assessment of adults with thrombotic microangiopathies: a cohort study. *Lancet Haematol* 2017; **4**: e157-e164 [PMID: [28259520](#) DOI: [10.1016/S2352-3026\(17\)30026-1](#)]
- 7 **Legendre CM**, Licht C, Muus P, Greenbaum LA, Babu S, Bedrosian C, Bingham C, Cohen DJ, Delmas Y, Douglas K, Eitner F, Feldkamp T, Fouque D, Furman RR, Gaber O, Herthelius M, Hourmant M, Karpman D, Lebranchu Y, Mariat C, Menne J, Moulin B, Nürnberger J, Ogawa M, Remuzzi G, Richard T, Sberro-Soussan R, Severino B, Sheerin NS, Trivelli A, Zimmerhackl LB, Goodship T, Loirat C. Terminal complement inhibitor eculizumab in atypical hemolytic-uremic syndrome. *N Engl J Med* 2013; **368**: 2169-2181 [PMID: [23738544](#) DOI: [10.1056/NEJMoa1208981](#)]
- 8 **Lechner K**, Obermeier HL. Cancer-related microangiopathic hemolytic anemia: clinical and laboratory features in 168 reported cases. *Medicine (Baltimore)* 2012; **91**: 195-205 [PMID: [22732949](#) DOI: [10.1097/MD.0b013e3182603598](#)]
- 9 **Oberic L**, Buffet M, Schwarzing M, Veyradier A, Clabault K, Malot S, Schleinitz N, Valla D, Galicier L, Bengrine-Lefèvre L, Gorin NC, Coppo P; Reference Center for the Management of Thrombotic Microangiopathies. Cancer awareness in atypical thrombotic microangiopathies. *Oncologist* 2009; **14**: 769-779 [PMID: [19684072](#) DOI: [10.1634/theoncologist.2009-0067](#)]
- 10 **Al-Batran SE**, Hartmann JT, Hofheinz R, Homann N, Rethwisch V, Probst S, Stoeckelmacher J, Clemens MR, Mahlberg R, Fritz M, Seipelt G, Sievert M, Pauligk C, Atmaca A, Jäger E. Biweekly fluorouracil, leucovorin, oxaliplatin, and docetaxel (FLOT) for patients with metastatic adenocarcinoma of the stomach or esophagogastric junction: a phase II trial of the Arbeitsgemeinschaft Internistische Onkologie. *Ann Oncol* 2008; **19**: 1882-1887 [PMID: [18669868](#) DOI: [10.1093/annonc/mdn403](#)]
- 11 **Brain MC**, Azzopardi JG, Baker LR, Pineo GF, Roberts PD, Dacie JV. Microangiopathic haemolytic anaemia and mucin-forming adenocarcinoma. *Br J Haematol* 1970; **18**: 183-193 [PMID: [5439525](#) DOI: [10.1111/j.1365-2141.1970.tb01433.x](#)]
- 12 **Francis KK**, Kojouri K and George JN. Occult systemic carcinoma masquerading as thrombotic thrombocytopenic purpura-hemolytic uremic syndrome. *Commun Oncol* 2005; **2**: 339-343 [DOI: [10.1016/S1548-5315\(11\)70904-4](#)]
- 13 **Choy B**, Alvarez Argote J, Treml A. Cancer-related microangiopathic hemolytic anemia. *Transfusion* 2016; **56**: 1937 [PMID: [27500918](#) DOI: [10.1111/trf.13634](#)]
- 14 **Wagner AD**, Syn NL, Moehler M, Grothe W, Yong WP, Tai BC, Ho J, Unverzagt S. Chemotherapy for advanced gastric cancer. *Cochrane Database Syst Rev* 2017; **8**: CD004064 [PMID: [28850174](#) DOI: [10.1002/14651858.CD004064.pub4](#)]



Retrospective Cohort Study

# Influence of primary tumor location and resection on survival in metastatic colorectal cancer

Zoé Tharin, Julie Blanc, Ikram Charifi Alaoui, Aurélie Bertaut, François Ghiringhelli

**ORCID number:** Zoé Tharin 0000-0002-3304-4822; Julie Blanc 0000-0003-4058-0794; Ikram Charifi Alaoui 0000-0002-5371-7086; Aurélie Bertaut 0000-0002-7934-9509; François Ghiringhelli 0000-0002-5465-8305.

**Author contributions:** All authors have contributed to the paper concept and design and agreed on the final content of the manuscript; Tharin Z and Charifi Alaoui I acquired the data; Blanc J and Bertaut A performed the statistical analysis; Tharin Z drafted the manuscript under the supervision of senior author Ghiringhelli F; all authors critically revised the manuscript and approved the final version of the manuscript.

**Institutional review board**

**statement:** I declare that, the database was registered and declared to the Clinical Trial database (NCT04031625). The study was conducted in accordance with standard procedures in France with approval from relevant institutional review boards called (CNIL).

**Informed consent statement:** I declare that all patients gave their informed consent before participating to this retrospective study.

**Zoé Tharin, François Ghiringhelli,** Department of Medical Oncology, Centre Georges-François Leclerc, Dijon 21000, France

**Julie Blanc, Ikram Charifi Alaoui, Aurélie Bertaut,** Department of Biostatistics, Centre Georges-François Leclerc, Dijon 21000, France

**Corresponding author:** Zoé Tharin, MD, Doctor, Department of Medical Oncology, Centre Georges-François Leclerc, 1 rue du Professeur Marion, Dijon 21000, France. [ztharin@cgfl.fr](mailto:ztharin@cgfl.fr)

## Abstract

### BACKGROUND

Patients with right sided colorectal cancer are known to have a poorer prognosis than patients with left sided colorectal cancer, whatever the cancer stage. To this day, primary tumor resection (PTR) is still controversial in a metastatic, non resectable setting.

### AIM

To explore the survival impact of PTR in patients with metastatic colorectal cancer (mCRC) depending on PTL.

### METHODS

We retrospectively collected data from all consecutive patients treated for mCRC at the Centre Georges François Leclerc Hospital. Univariate and multivariate Cox proportional hazard regression models were used to assess the influence of PTR on survival. We then evaluated the association between PTL and overall survival among patients who previously underwent or did not undergo PTR. A propensity score was performed to match cohorts.

### RESULTS

Four hundred and sixty-six patients were included. A total of 153 (32.8%) patients had unresected synchronous mCRC and 313 (67.2%) patients had resected synchronous mCRC. The number of patients with right colic cancer, left colic cancer and rectal cancer was respectively 174 (37.3%), 203 (43.6%) and 89 (19.1%). In the multivariate analysis only PTL, PTR, resection of hepatic and or pulmonary metastases and the use of oxaliplatin, EGFR inhibitors or bevacizumab throughout treatment were associated to higher overall survival rates. Survival evaluation depending on PTR and PTL found that PTR improved the prognosis of both left and right sided mCRC. Results were confirmed by using a weighted



**Conflict-of-interest statement:** All authors declare no conflict-of-interest related to this article.

**Data sharing statement:** No additional data are available.

**STROBE statement:** The authors have read the STROBE statement and the manuscript was prepared and revised according to the STROBE statement.

**Open-Access:** This article is an open-access article that was selected by an in-house editor and fully peer-reviewed by external reviewers. It is distributed in accordance with the Creative Commons Attribution NonCommercial (CC BY-NC 4.0) license, which permits others to distribute, remix, adapt, build upon this work non-commercially, and license their derivative works on different terms, provided the original work is properly cited and the use is non-commercial. See: <http://creativecommons.org/licenses/by-nc/4.0/>

**Manuscript source:** Unsolicited manuscript

**Specialty type:** Oncology

**Country/Territory of origin:** France

**Peer-review report's scientific quality classification**

Grade A (Excellent): 0  
Grade B (Very good): B  
Grade C (Good): C, C, C  
Grade D (Fair): D  
Grade E (Poor): 0

**Received:** June 8, 2020

**Peer-review started:** June 8, 2020

**First decision:** September 11, 2020

**Revised:** September 25, 2020

**Accepted:** October 28, 2020

**Article in press:** October 28, 2020

**Published online:** November 15, 2020

**P-Reviewer:** Aoki T, Boteon YL, Huang LY, MD JS, Yong T

**S-Editor:** Zhang L

**L-Editor:** A

**P-Editor:** Li JH

propensity score.

## CONCLUSION

In mCRC, PTR seems to confer a higher survival rate to patients whatever the PTL.

**Key Words:** Colorectal cancer; Metastatic; Primary tumor resection; Chemotherapy; Primary tumor location; Synchronous

©The Author(s) 2020. Published by Baishideng Publishing Group Inc. All rights reserved.

**Core Tip:** This article presents a large, real life, cohort of patients treated for a metastatic colorectal cancer. Primary tumor resection in this setting is not a validated systematic treatment. However, in our hospital, primary tumor resection is performed widely. In our study, primary tumor resection was associated to higher overall survival rates even in patients with a poor prognosis. We also looked at the impact of primary tumor resection depending on primary tumor location. Primary tumor location had no impact on the benefit provided by primary tumor resection.

**Citation:** Tharin Z, Blanc J, Charifi Alaoui I, Bertaut A, Ghiringhelli F. Influence of primary tumor location and resection on survival in metastatic colorectal cancer. *World J Gastrointest Oncol* 2020; 12(11): 1296-1310

**URL:** <https://www.wjgnet.com/1948-5204/full/v12/i11/1296.htm>

**DOI:** <https://dx.doi.org/10.4251/wjgo.v12.i11.1296>

## INTRODUCTION

Colorectal cancer (CRC) is a major public health issue and stands as the third most frequent cancer throughout the world with 1.8 million new cases diagnosed every year. It is the second cause of cancer related death with, according to GLOBOCAN estimates, 880000 deaths per year<sup>[1]</sup>. Between 20% and 30% of patients have metastases at the time of diagnosis<sup>[2,3]</sup> which classifies them as stage IV CRC. It has been established that primary tumor resection (PTR) and surgery of the metastases is a necessity for patients presenting resectable metastases as it allows to cure 20% to 25% of patients<sup>[4]</sup>. All resectable metastatic patients will undergo chemotherapy, in most cases they will receive peri-operative chemotherapy relying on the association of 5 fluorouracil (5 FU) and oxaliplatin<sup>[5,6]</sup>.

For 75% to 90% of patients, the cancer is unresectable, and they will receive palliative chemotherapy<sup>[7]</sup>. Recent data underlines that primary tumor location (PTL) is one of the most important prognostic factors in our study population. Indeed, the CALGB/SWOG 80405 found that survival was doubled for patients with left-sided primary tumors *vs* those with right-sided primary tumors<sup>[8,9]</sup>. This data was corroborated by a meta-analysis that pooled all clinical trials, available up to October 2016, which assessed the impact of PTL in metastatic CRC (mCRC)<sup>[10]</sup>.

For patients with unresectable metastases, PTR has not been validated as a systematic treatment in randomized clinical trials. At present, whether the patient will undergo PTR or not is decided in multidisciplinary reunions. This decision is based on quality of life improvement and prevention of complications related to the primary tumor for patients with unresectable metastases. In a recent analysis of the ARCAD patient data base, patients with synchronous metastases and no PTR had a significantly worse median overall survival (OS) (16.4 m) than patients with synchronous metastases who underwent PTR [22.2 m; hazard ratio (HR): 1.60, 95% carcinoembryonic antigen (CI): 1.43-1.78]<sup>[11]</sup>. Moreover, a meta-analysis of 21 studies, including 44226 patients, found that patients who had PTR had a better OS than the patients who received chemotherapy alone<sup>[12]</sup>.

However, to our knowledge, the outcome of PTR in terms of OS depending on PTL has never been evaluated.

The aim of this retrospective study, carried out at the Centre George François Leclerc Hospital in Dijon, was to evaluate if PTR allowed to improve the prognosis of





either left or right mCRC.

## MATERIALS AND METHODS

### Study population

Data was collected retrospectively from all consecutive patients treated at the Centre George François Leclerc Hospital for synchronous mCRC between January 31st, 2000 and the December 20th, 2018. Patients were included regardless of their tumor burden, of their resectability, of the treatments they had received (chemotherapy, molecular targeted agents, PTR, lung and/or liver metastases resection, hyperthermic chemotherapy). Patients were excluded if the PTL wasn't specified in the medical file, if the CRC wasn't the first or the only malignancy diagnosed or if it was appendiceal cancer.

### Data collection

The following parameters were retrospectively collected in the patients' medical file: Gender, age, performance status (PS), liver surgery or liver radiofrequency, lung surgery or lung radiofrequency, PTR, PTL: Right colon/Left colon/rectum (right colon cancers included right sided and transverse colon cancers; Left colon cancers included left sided and sigmoid cancers), number of metastatic sites, *KRAS* and *BRAF* mutations, type of medical treatment, levels of lactate dehydrogenase (LDH), carcinoembryonic antigen, leucocytes and alkaline phosphatase (ALP).

### Statistical analyses

The primary endpoint was to evaluate whether the use of PTR allowed to improve the prognosis of patients and if the benefit was correlated to PTL. All patients were followed until either their death or the date of last follow-up prior to the March 31st, 2020. The primary end point was OS, which was defined as the interval between the time of diagnosis of metastatic disease and the date of death as reported on medical record. Survivors were censored at last follow-up.

The characteristics of the whole population are presented according to whether PTR was performed and in function of PTL. Continuous variables were compared using ANOVA or Kruskal-Wallis tests depending on the distribution of the data. Qualitative variables were compared using either the  $\chi^2$  test or the Fisher exact test.

The median follow-up was estimated using the reverse Kaplan Meier method. OS was estimated using the Kaplan-Meier method, described using medians with its 95% confidence interval (95%CI), and compared using a log-rank test. Univariate Cox regressions were performed to estimate HR with its 95%CI. The multivariate Cox regression model was generated with all the variables with a  $P < 0.20$  and with less than 20% of missing data. The risks proportionality and log-linearity were verified for each variable. Correlations between all variables were tested and, in case of correlated variables, only one variable was included in the multivariate model. The interaction between PTL and PTR was tested.

A propensity score was generated using a multivariate logistic regression and stood as the likelihood of undergoing PTR. The inverse probability treatment weight was used to balance clinical variables associated with PTR and to eliminate potential selection biases. The weight allocated to patients who had undergone PTR was  $1/PS$  while the patients without PTR received a weight of  $1/(1-PS)$ . Then a weighted Cox regression model was built using the same variables introduced in the raw Cox model. Statistical analyses were performed using SAS® software version 9.4.

## RESULTS

### Characteristics of the patients

The data from 466 patients with synchronous mCRC was collected from the Centre Georges François Leclerc Hospital database between January 31st 2000 and December 20th 2018.

The male gender was slightly predominant (54.7%) but not statistically significant. The mean age was 64 years. PS was good for most patients with 83.6% of patients with a 0 or 1 PS. The number of patients with right colic cancer, left colic cancer and rectal cancer was respectively 174 (37.3%), 203 (43.6%) and 89 (19.1%). Three hundred and thirteen (67.2%) patients had undergone PTR, 153 (32.8%) patients had not been

operated on. One hundred and thirty seven (29.6%) patients were treated for their metastatic disease with curative intent with either liver and/or pulmonary surgery or radiofrequency. RAS status was available for 356 patients (76.4%), 154 patients had a RAS mutation. BRAF status was available for 294 patients (63.1%), 29 patients had a BRAF mutation.

Patients' characteristics according to PTR status are summarized in [Table 1](#). Age, PTL, PS, lung metastases, ACE, LDH, leucocyte and ALP and surgery or radiofrequency of lung and/or liver metastases were the significantly different variables between the groups.

Patients' characteristics depending on PTL are summarized in the supplementary data ([Supplementary Table 1](#)). PS, number of metastatic sites, lung and peritoneum metastases, *KRAS* and *BRAF* mutations, PTR, ALP levels, the use of EGFR inhibitors, chemotherapy regimen and surgery or radiofrequency of lung and/or liver metastases were the significantly different variables between the groups.

### Association between PTR, PTL and survival

Median follow up was 8 years. As expected, we found that left sided colon cancers were associated to a better OS than right sided colon cancers. Results shown in [Figure 1](#). As Kaplan Meier curves and Log Rank tests show that left colon cancers and rectal cancers share similar prognosis, we decided to pool them for further analyses. We found that patients who underwent PTR had higher OS rates than patients who didn't. Results shown in [Figure 2A](#). The benefit of PTR in terms of OS was observed regardless of PTR taking place before, primary PTR, or after the initiation of chemotherapy, secondary PTR. Results shown in [Figure 2B](#). As Kaplan Meier curves and Log Rank tests show that synchronous patients with primary PTR and synchronous patients with secondary PTR share similar prognosis, we decided to pool them for further analyses.

Using a univariate Cox model, we tested the impact of each clinical variable on OS. We found that left sided mCRC, a unique metastatic site, low levels of ACE, LDH, leucocytes and ALP, PTR, resection of hepatic and/or pulmonary metastases in curative intent, the use of intensive first line chemotherapy and the use of oxaliplatin, EGFR inhibitors or bevacizumab throughout treatment were associated to a better OS ([Table 2](#)).

Using a multivariate COX model which only included variables with  $P < 0.2$  on univariate analysis and with less than 20% of missing data, we observed that only left sided tumors, PTR, the use of oxaliplatin, EGFR inhibitors or bevacizumab throughout treatment and resection of hepatic and/or pulmonary metastases in curative intent were associated to higher OS rates. Harrell's C statistic of the multivariate model is 0.75 which indicates a good discrimination quality of the model. To allow for potential biases between patients who do and do not undergo PTR, we performed a weighted propensity score to match both cohorts: 304 patients were retained. The weighted multivariate COX model obtained similar results to the raw multivariate COX model. Results shown in Forrest Plot shown in [Figure 3A](#) and [B](#).

The interaction test carried out between PTR and PTL was not statistically significant ( $P = 0.2426$ ), thus suggesting that the positive effect of PTR is independent of PTL. The improvement of the HR of OS when PTR was performed was observed regardless of PTL. In the raw cohort, the one year survival rate for right sided tumors went from 40.32% (28.15-52.17) without PTR to 80.93% (72.26-87.13) with PTR; for the left sided tumors, it went from 73.26% (62.80-81.21) without PTR to 91.54% (86.75-94.66) with PTR. Similar results were observed in the weighted cohorts. Results shown in [Figure 4A](#) and [B](#).

## DISCUSSION

This retrospective study is in line with previous studies and supports the idea that PTR improves OS in patients with mCRC and suggests that PTR could be important in disease control of both left and right sided mCRC.

Many articles on PTR in mCRC have been published in the last 20 years. In the early 2000's, Cook *et al*<sup>[7]</sup> published the first article based on data extracted from a national prospective database in the United States, The Surveillance, Epidemiology and End Results where 26754 patients were included. Patients who underwent PTR had an improved survival<sup>[7]</sup>. In 2014, Ahmed *et al*<sup>[13]</sup> Published the first prospective observational study, designed to compare OS depending on PTR in patients with mCRC. All the results are in favor of PTR regardless of other important prognostic

**Table 1 Patients' characteristics according to primary tumor resection status**

	Total	PTR	No PTR	P value
Age				0.0065
<i>n</i>	466	313	153	
Mean (std)	64.0 (11.6)	63.0 (11.1)	66.1 (12.4)	
Median [min-max]	65.0 (24.0-92.0)	63.0 (29.0-90.0)	67.0 (24.0-92.0)	
Gender				0.9563
Male	255 (54.7%)	171 (54.6%)	84 (54.9%)	
Female	211 (45.3%)	142 (45.4%)	69 (45.1%)	
Primary tumor location				0.0010
Left colon + sigmoid	203 (43.6%)	153 (48.9%)	50 (32.7%)	
Right colon + transverse colon	174 (37.3%)	112 (35.8%)	62 (40.5%)	
Rectum	89 (19.1%)	48 (15.3%)	41 (26.8%)	
PS				0.0296
0-1	300 (83.6%)	202 (86.7%)	98 (77.8%)	
2-4	59 (16.4%)	31 (13.3%)	28 (22.2%)	
Missing values	107	80	27	
Number of metastatic sites				0.1080
1	283 (60.7%)	200 (63.9%)	83 (54.2%)	
2	133 (28.5%)	84 (26.8%)	49 (32.0%)	
> 2	50 (10.7%)	29 (9.3%)	21 (13.7%)	
Metastatic sites				
Liver				0.9689
No	89 (19.2%)	60 (19.2%)	29 (19.1%)	
Yes	375 (80.8%)	252 (80.8%)	123 (80.9%)	
Missing values	2	1	1	
Lung				0.0206
No	342 (73.9%)	240 (77.2%)	102 (67.1%)	
Yes	121 (26.1%)	71 (22.8%)	50 (32.9%)	
Missing values	3	2	1	
Peritoneum				0.8377
No	356 (76.9%)	240 (77.2%)	116 (76.3%)	
Yes	107 (23.1%)	71 (22.8%)	36 (23.7%)	
Missing values	3	2	1	
Other				0.2531
No	361 (78.1%)	247 (79.7%)	114 (75.0%)	
Yes	101 (21.9%)	63 (20.3%)	38 (25.0%)	
Missing values	4	3	1	
KRAS mutation				0.5956
No	202 (56.7%)	143 (57.7%)	59 (54.6%)	
Yes	154 (43.3%)	105 (42.3%)	49 (45.4%)	
Missing values	110	65	45	
BRAF mutation				0.3218

No	265 (90.1%)	188 (91.3%)	77 (87.5%)	
Yes	29 (9.9%)	18 (8.7%)	11 (12.5%)	
Missing values	172	107	65	
CEA				0.0002
≤ 200	251 (68.6%)	177 (75.3%)	74 (56.5%)	
> 200	115 (31.4%)	58 (24.7%)	57 (43.5%)	
Missing values	100	78	22	
LDH				< 0.0001
≤ 254	175 (53.2%)	130 (62.2%)	45 (37.5%)	
> 254	154 (46.8%)	79 (37.8%)	75 (62.5%)	
Missing values	137	104	33	
Leukocytes > 10000				0.0014
No	256 (70.9%)	175 (76.8%)	81 (60.9%)	
Yes	105 (29.1%)	53 (23.2%)	52 (39.1%)	
Missing values	105	85	20	
Alkaline phosphatase > 300				0.0008
No	261 (77.9%)	179 (83.6%)	82 (67.8%)	
Yes	74 (22.1%)	35 (16.4%)	39 (32.2%)	
Missing values	131	99	32	
Oxaliplatin				0.3478
No	35 (7.5%)	21 (6.7%)	14 (9.2%)	
Yes	431 (92.5%)	292 (93.3%)	139 (90.8%)	
5 FU or capecitabine				1.0000
No	3 (0.6%)	2 (0.6%)	1 (0.7%)	
Yes	463 (99.4%)	311 (99.4%)	152 (99.3%)	
Irinotecan				0.1278
No	105 (22.6%)	64 (20.5%)	41 (26.8%)	
Yes	360 (77.4%)	248 (79.5%)	112 (73.2%)	
Missing values	1	1	0	
Bevacizumab				0.1978
No	150 (32.4%)	95 (30.4%)	55 (36.4%)	
Yes	313 (67.6%)	217 (69.6%)	96 (63.6%)	
Missing values	3	1	2	
EGFR inhibitors				0.2681
No	267 (57.5%)	174 (55.8%)	93 (61.2%)	
Yes	197 (42.5%)	138 (44.2%)	59 (38.8%)	
Missing values	2	1	1	
1st line chemotherapy regimen				0.7568
Mono-chemotherapy	48 (10.4%)	32 (10.3%)	16 (10.5%)	
Bi-chemotherapy	326 (70.6%)	216 (69.7%)	110 (72.4%)	
Tri- chemotherapy	88 (19.0%)	62 (20.0%)	26 (17.1%)	
Missing values	4	3	1	
Lung or Liver surgery or radio-frequency				
				< 0.0001

No	326 (70.4%)	178 (57.4%)	148 (96.7%)
Yes	137 (29.6%)	132 (42.6%)	5 (3.3%)
Missing values	3	3	0

PTR: Primary tumor resection; PS: Performance status; CEA: Carcinoembryonic antigen; LDH: Lactate dehydrogenase; EGDR: Epidermal growth factor.

factors such as: Age, PS, comorbid illness and chemotherapy. However, many confounding factors could have influenced and biased these results.

More recently, using an Instrumental Variable analysis based on the annual hospital-levels of PTR rates, Alawadi *et al*<sup>[14]</sup> underlined in a large united states cohort that survival benefit linked to PTR is mainly related to inclusion biases and therefore do not recommend it in a non-resectable metastatic setting. A Japanese group reported, at the ASCO GI this year, the first clinical trial designed to evaluate the impact of primary PTR, in patients with unresectable mCRC. The study cohort only included 160 patients out of the 758 patients initially planned: 78 patients were assigned to the PTR + chemotherapy group, 83 were assigned to the chemotherapy alone group. They found that PTR followed by chemotherapy had no survival benefit over chemotherapy alone with respectively a 25.9 mo and 26.7 mo OS [hazard ratio: 1.10 (0.76-1.59), one-sided  $P = 0.69$ ]<sup>[15]</sup>.

In contrast, in our study, the multivariate Cox proportional analysis and weighted Cox proportional analyses were operated on the known bad prognostic risk factors in order to evaluate, independently, the association between survival and PTR. In these models, we continued to observe a strong association between PTR and prognosis.

Nevertheless, PTR in patients with unresectable mCRC cancer stays controversial. Indeed, the results of the studies encouraging PTR are thought to be biased by confounding factors such as age, PS, metastases resectability. One of the main arguments against PTR is the risk of post-operative complications and therefore delayed chemotherapy<sup>[16]</sup>. However, in our study, regardless of its limitations, PTR is associated to an increased OS independently of the known bad prognostic risk factors and chemotherapy treatment. Our study also shows that PTR is associated to better outcomes in both left and right sided mCRC.

The limits to our study are of course its retrospective design and the mono centric recruitment. However, we studied a large cohort of unselected patients and our results in terms of outcome and population are very similar to the results observed in clinical trials testing new strategies in mCRC<sup>[6,17]</sup> or in studies evaluating survival in mCRC<sup>[18]</sup>. Other limitations to our study are that it compares a heterogeneous population of patients in terms of tumor burden and that there is a statically significant difference when it comes to PTR between our groups. However, the aim of the propensity score was to balance the disparities observed within our population. The last limitation to our study is that the reason behind the decision of PTR was not recorded and we therefore cannot exclude a confounding factor.

## CONCLUSION

Our results support that PTR could be associated to OS improvement in patients with mCRC regardless of PTL. Our findings indicate a possible argument to promote surgical treatment for this category of patients. Such data needs to be validated in prospective clinical trials.



Table 2 Univariate Cox model

		HR	95%CI	P value
Age	<i>n</i> = 466			0.0714
> 65 yr <i>vs</i> ≤ 65 yr		1.209	[0.984-1.485]	
Gender	<i>n</i> = 466			0.3701
Female <i>vs</i> male		1.099	[0.894-1.350]	
Tumor location	<i>n</i> = 466			0.0022
Rectum <i>vs</i> left colon + sigmoid		1.019	[0.767-1.355]	
Right colon + transverse colon <i>vs</i> Left colon + sigmoid		1.464	[1.16-1.841]	
Number of metastatic sites	<i>n</i> = 466			0.0035
2 <i>vs</i> 1		1.219	[0.965-1.539]	
> 2 <i>vs</i> 1		1.749	[1.245-2.455]	
Number of metastatic sites	<i>n</i> = 466			0.0084
≥ 2 <i>vs</i> 1		1.328	[1.076-1.641]	
Liver metastases	<i>n</i> = 464			0.8836
Yes <i>vs</i> No		1.020	[0.782-1.330]	
Lung metastases	<i>n</i> = 463			0.6435
Yes <i>vs</i> No		1.057	[0.835-1.338]	
Peritoneum metastases	<i>n</i> = 463			0.0619
Yes <i>vs</i> No		1.260	[0.989-1.606]	
Other metastases	<i>n</i> = 462			0.0114
Yes <i>vs</i> No		1.377	[1.075-1.765]	
KRAS mutation	<i>n</i> = 356			0.0696
Yes <i>vs</i> No		1.256	[0.982-1.606]	
BRAF mutation	<i>n</i> = 294			< 0.0001
Yes <i>vs</i> No		2.276	[1.511-3.429]	
CEA	<i>n</i> = 366			< 0.0001
> 200 <i>vs</i> ≤ 200		1.654	[1.290-2.120]	
LDH	<i>n</i> = 329			< 0.0001
> 254 <i>vs</i> ≤ 254		2.022	[1.574-2.596]	
Leukocytes > 10000	<i>n</i> = 361			0.0016
Yes <i>vs</i> No		1.506	[1.168-1.941]	
Alkaline phosphatase > 300	<i>n</i> = 335			< 0.0001
Yes <i>vs</i> No		2.272	[1.713-3.014]	
PTR	<i>n</i> = 466			< 0.0001
Yes <i>vs</i> No		0.313	[0.250-0.392]	
Oxaliplatin	<i>n</i> = 466			< 0.0001
Yes <i>vs</i> No		0.361	[0.248-0.524]	
Irinotecan	<i>n</i> = 465			0.112
Yes <i>vs</i> No		0.807	[0.619-1.051]	
5 FU or Capecitabine	<i>n</i> = 466			0.2869
Yes <i>vs</i> No		0.539	[0.173-1.682]	
Bevacizumab	<i>n</i> = 463			0.0117

Yes vs No		0.750	[0.599-0.938]	
EGFR inhibitors	<i>n</i> = 464			0.0129
Yes vs No		0.769	[0.625-0.946]	
1st line chemotherapy regimen	<i>n</i> = 462			0.0080
Bi-chemotherapy vs Mono-chemotherapy		0.682	[0.496-0.937]	
Tri-chemotherapy vs Mono-chemotherapy		0.543	[0.368-0.799]	
Lung or liver surgery or radio-frequency	<i>n</i> = 463			< 0.0001
Yes vs No		0.302	[0.235-0.388]	

HR: Hazard ratio; CI: Carcinoembryonic antigen; CEA: Carcinoembryonic antigen; LDH: Lactate dehydrogenase; PTR: Primary tumor resection; 5 FU: 5 fluorouracil; EGFR: Epidermal growth factor.

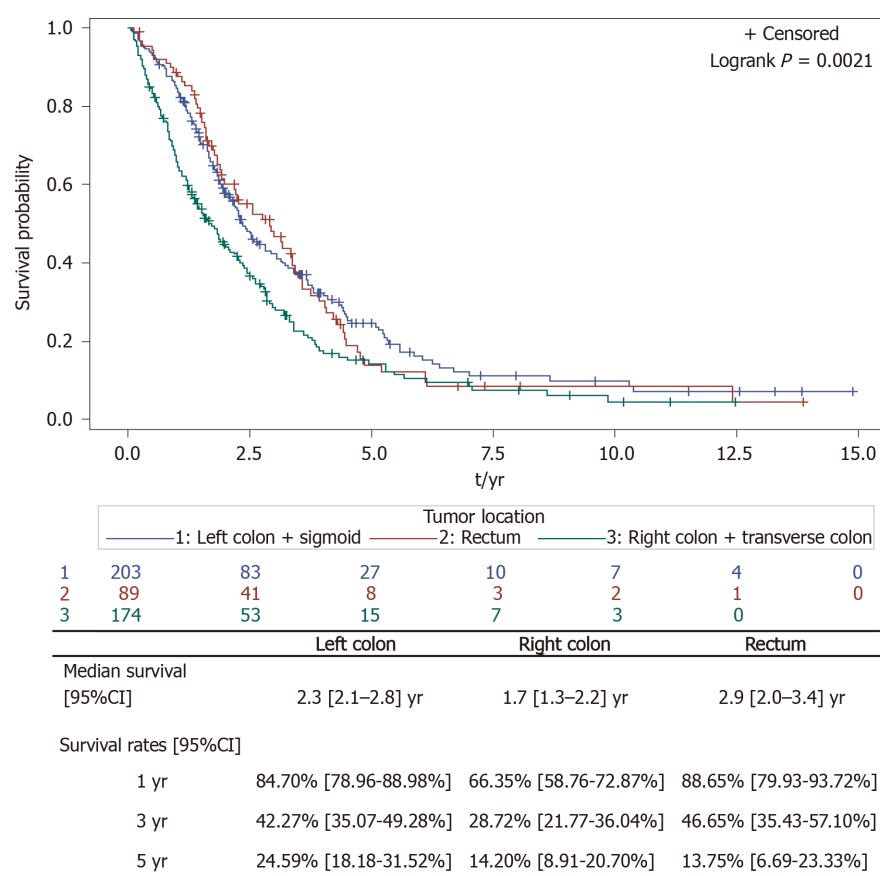
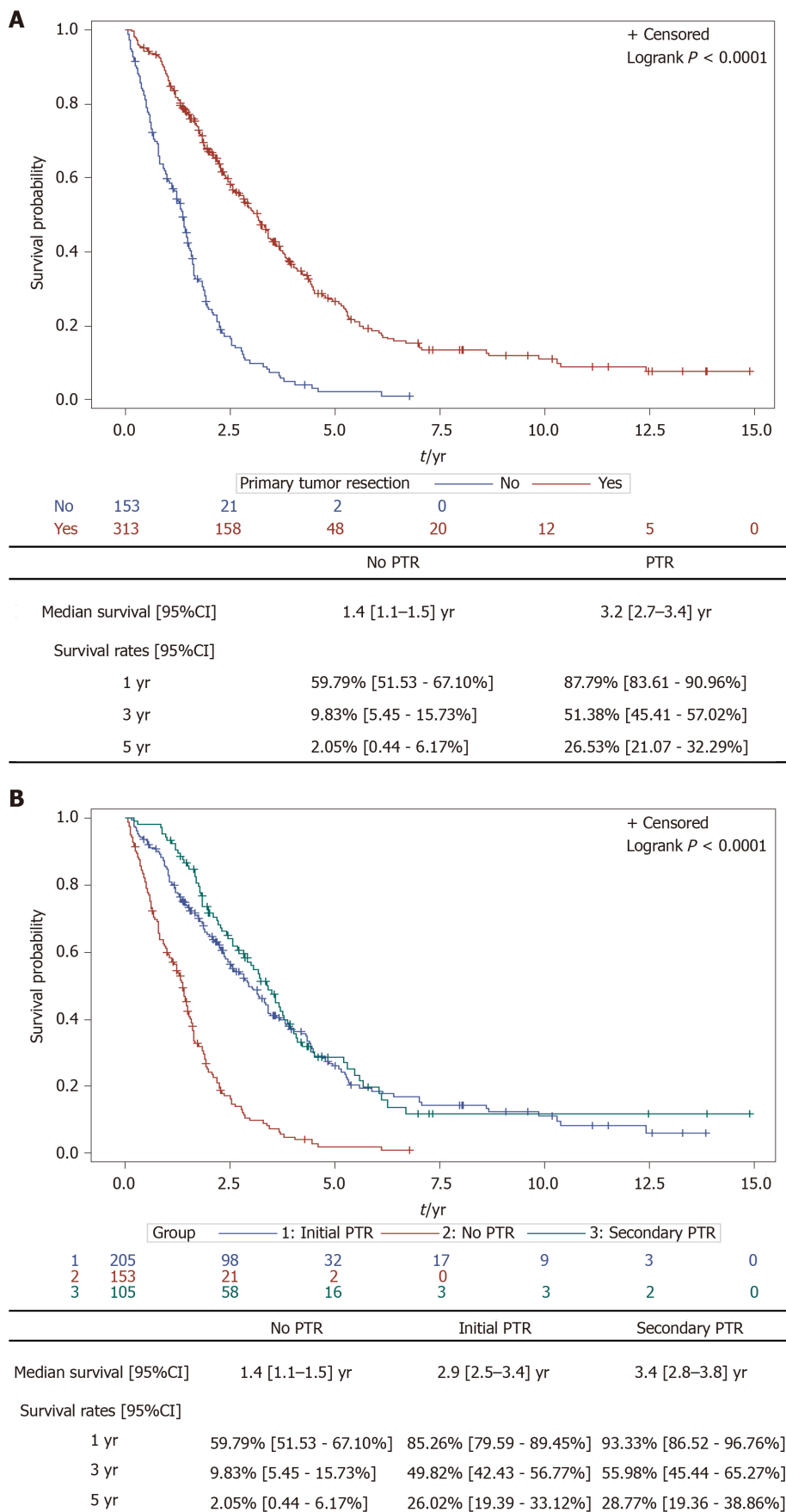
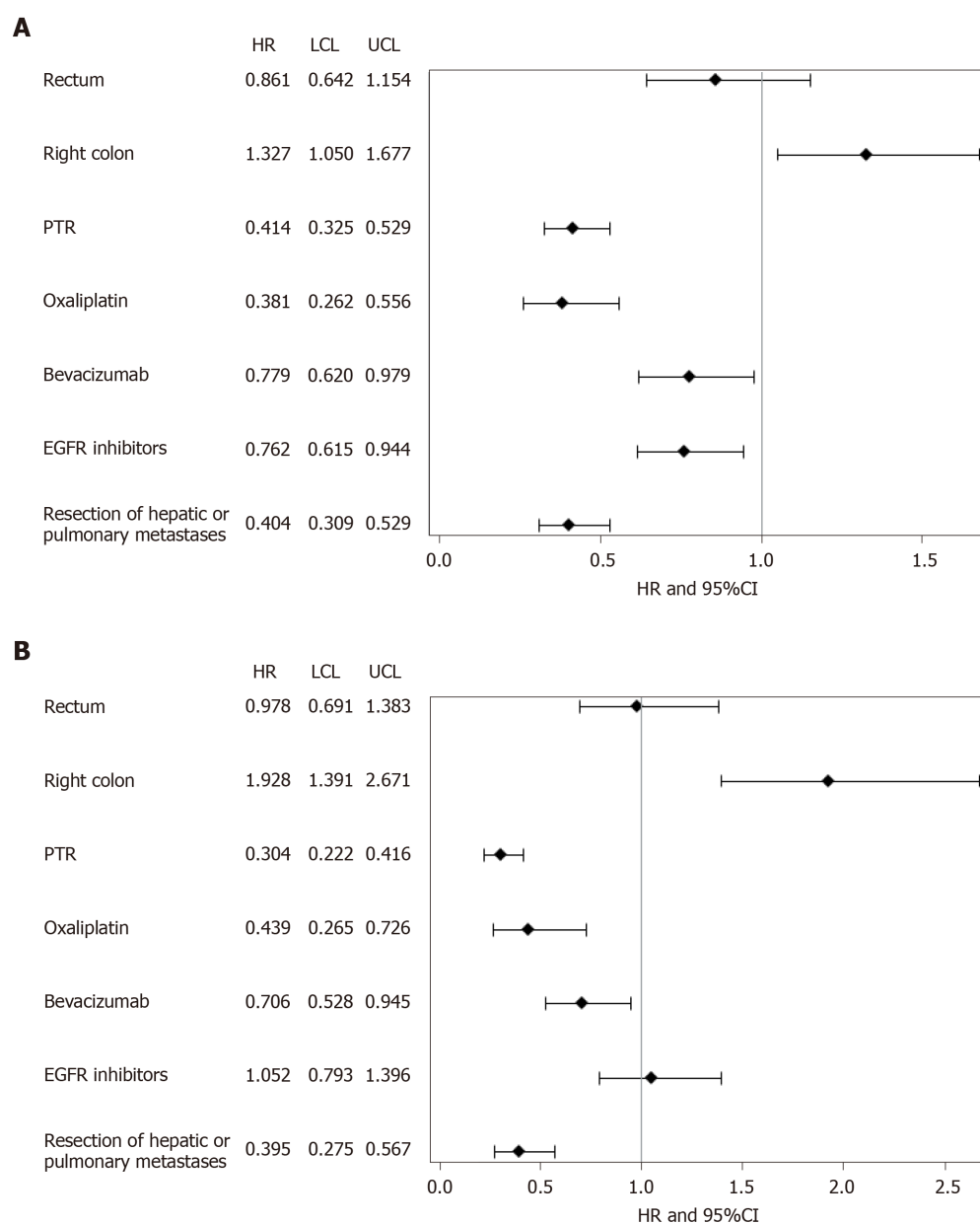


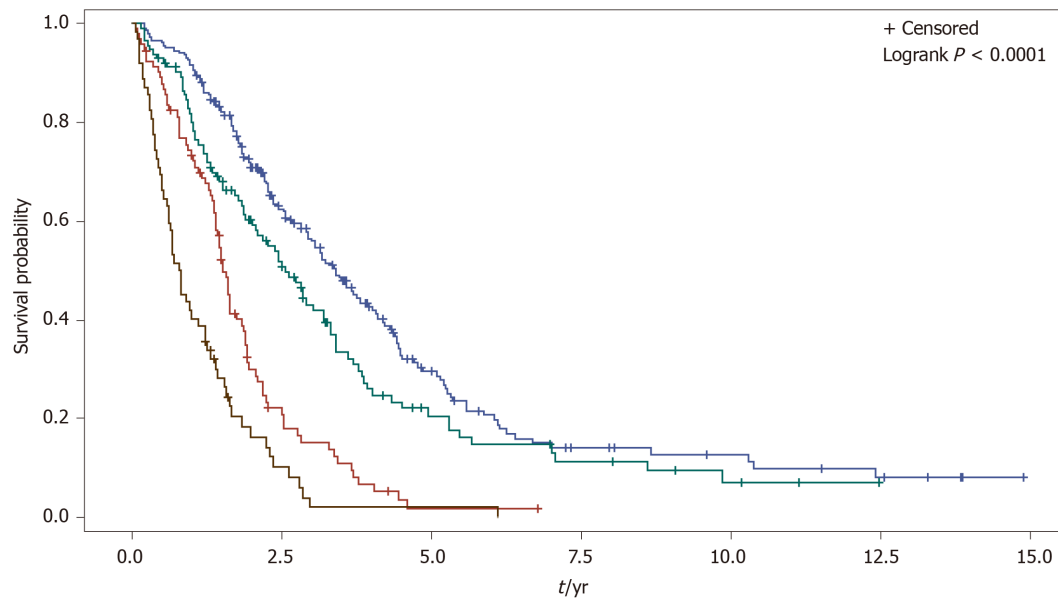
Figure 1 Survival depending on primary tumor location.



**Figure 2 Survival and primary tumor resection.** A: Survival depending on primary tumor resection; and B: Survival according to timing of primary tumor resection.



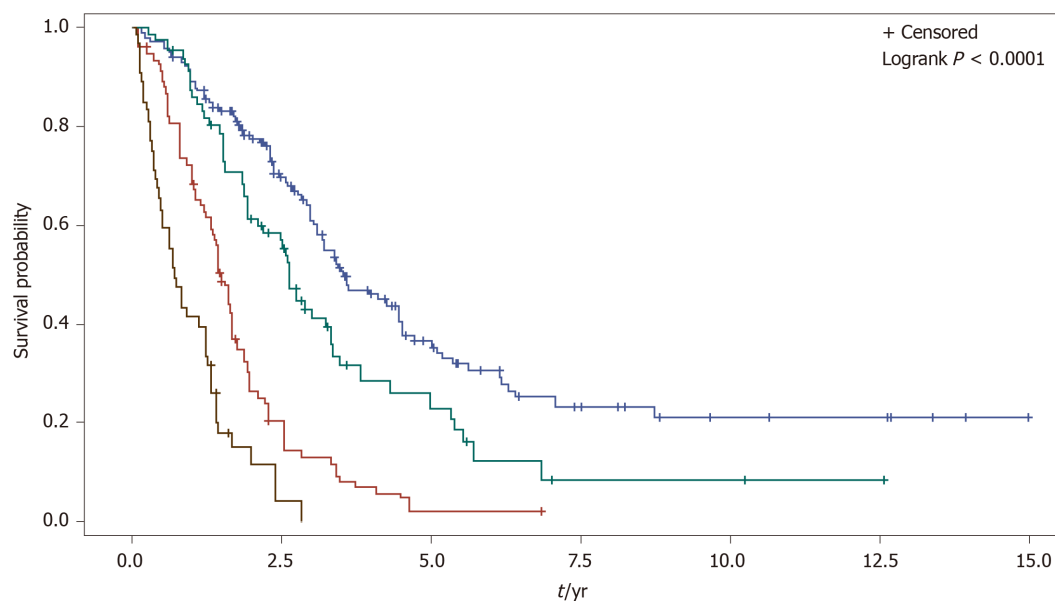
**Figure 3 Forrest plot raw and weighted Cox model.** A: Forrest plot raw multivariate Cox model; and B: Forrest plot weighted multivariate Cox model.

**A**

1	201	108	34	13	9	5	0
2	91	16	1	0			
3	112	48	14	7	3	0	
4	62	5	1	0			

	Right colon with no PTR	Right colon with PTR	Left colon and rectum with no PTR	Left colon and rectum with PTR
Median survival [95%CI]	0.8 [0.6–1.2] yr	2.6 [2.0–3.2] yr	1.5 [1.4–1.8] yr	3.4 [2.9–3.9] yr
Survival rates [95%CI]				
1 yr	40.32% [28.15 - 52.17%]	80.93% [72.26 - 87.13%]	73.26% [62.80 - 81.21%]	91.54% [86.75 - 94.66%]
3 yr	2.04% [0.17 - 9.34%]	43.08% [33.24 - 52.53%]	15.22% [8.30 - 24.09%]	55.90% [48.41 - 62.74%]
5 yr	2.04% [0.17 - 9.34%]	20.66% [12.81 - 29.82%]	1.85% [0.17 - 8.15%]	29.58% [22.50 - 36.98%]



**B**

1	102	19	5	0
2	107	2	0	
3	49	7	2	0
4	46	0		

	Right colon with no PTR	Right colon with PTR	Left colon and rectum with no PTR	Left colon and rectum with PTR
Median survival [95%CI]	0.7 [0.4–1.3] yr	2.6 [1.9–3.3] yr	1.5 [1.1–1.7] yr	3.5 [3.1–4.4] yr
Survival rates [95%CI]				
1 yr	41.54% [24.69 - 57.59%]	85.87% [73.32 - 92.79%]	68.44% [53.80 - 79.30%]	89.21% [82.38 - 93.50%]
3 yr		41.25% [27.52 - 54.45%]	13.06% [5.20 - 24.61%]	60.28% [50.58 - 68.67%]
5 yr		22.80% [11.51 - 36.37%]	2.02% [0.13 - 10.18%]	35.40% [26.09 - 44.82%]

**Figure 4 Survival depending on primary tumor resection and primary tumor location.** A: Survival depending on primary tumor resection and primary tumor location, raw cohort; and B: Survival depending on primary tumor resection and primary tumor location, weighted cohort.

## ARTICLE HIGHLIGHTS

### Research background

Patients with right sided colorectal cancer (CRC) are known to have a poorer prognosis than patients with left sided tumors and primary tumor resection (PTR) is controversial whatever the primary tumor location (PTL).

### Research motivation

Results concerning PTR in unresectable metastatic colorectal cancer (mCRC) are non-consensual and PTR is not a standard practice. To our knowledge, the outcome of PTR in terms of overall survival (OS) depending on tumor sidedness has never been evaluated.

### Research objectives

This study aimed to explore the survival impact of PTR in patients with mCRC

depending on PTL.

### Research methods

We retrospectively collected data from all consecutive patients treated for mCRC at the Centre Georges Francois Leclerc Hospital. Univariate and multivariate Cox proportional hazard regression models were used to assess the influence of PTR on survival. We then evaluated associations between PTL and OS among patients who previously underwent or did not undergo PTR. A propensity score was performed to match cohorts.

### Research results

Four hundred and sixty-six patients were included. A total of 153 (32.8%) patients had unresected synchronous mCRC and 313 (67.2%) patients had resected synchronous mCRC. The number of patients with right colic cancer, left colic cancer and rectal cancer was respectively 174 (37.3%), 203 (43.6%) and 89 (19.1%). In the multivariate analysis only PTL, PTR, resection of hepatic and or pulmonary metastases and the use of oxaliplatin, EGFR inhibitors or bevacizumab throughout treatment were associated to higher OS rates. Survival evaluation depending on PTR and PTL found that PTR improved the prognosis of both left and right sided unresectable mCRC. Results were confirmed by using a weighted propensity score.

### Research conclusions

In mCRC, PTR seems to confer higher survival rates whatever the PTL.

### Research perspectives

These results are in favor of PTR for patients treated for a mCRC but would need to be supported by a large scale, prospective trial.

## REFERENCES

- 1 **Bray F**, Ferlay J, Soerjomataram I, Siegel RL, Torre LA, Jemal A. Global cancer statistics 2018: GLOBOCAN estimates of incidence and mortality worldwide for 36 cancers in 185 countries. *CA Cancer J Clin* 2018; **68**: 394-424 [PMID: 30207593 DOI: 10.3322/caac.21492]
- 2 **Siegel RL**, Miller KD, Fedewa SA, Ahnen DJ, Meester RGS, Barzi A, Jemal A. Colorectal cancer statistics, 2017. *CA Cancer J Clin* 2017; **67**: 177-193 [PMID: 28248415 DOI: 10.3322/caac.21395]
- 3 **Leufkens AM**, van den Bosch MA, van Leeuwen MS, Siersema PD. Diagnostic accuracy of computed tomography for colon cancer staging: a systematic review. *Scand J Gastroenterol* 2011; **46**: 887-894 [PMID: 21504379 DOI: 10.3109/00365521.2011.574732]
- 4 **Brown RE**, Bower MR, Martin RC. Hepatic resection for colorectal liver metastases. *Surg Clin North Am* 2010; **90**: 839-852 [PMID: 20637951 DOI: 10.1016/j.suc.2010.04.012]
- 5 **Nordlinger B**, Sorbye H, Glimelius B, Poston GJ, Schlag PM, Rougier P, Bechstein WO, Primrose JN, Walpole ET, Finch-Jones M, Jaeck D, Mirza D, Parks RW, Collette L, Praet M, Bethe U, Van Cutsem E, Scheithauer W, Gruenberger T; EORTC Gastro-Intestinal Tract Cancer Group; Cancer Research UK; Arbeitsgruppe Lebermetastasen und-tumoren in der Chirurgischen Arbeitsgemeinschaft Onkologie (ALM-CAO); Australasian Gastro-Intestinal Trials Group (AGITG); Fédération Francophone de Cancérologie Digestive (FFCD). Perioperative chemotherapy with FOLFOX4 and surgery vs surgery alone for resectable liver metastases from colorectal cancer (EORTC Intergroup trial 40983): a randomised controlled trial. *Lancet* 2008; **371**: 1007-1016 [PMID: 18358928 DOI: 10.1016/S0140-6736(08)60455-9]
- 6 **Nordlinger B**, Sorbye H, Glimelius B, Poston GJ, Schlag PM, Rougier P, Bechstein WO, Primrose JN, Walpole ET, Finch-Jones M, Jaeck D, Mirza D, Parks RW, Mauer M, Tanis E, Van Cutsem E, Scheithauer W, Gruenberger T; EORTC Gastro-Intestinal Tract Cancer Group; Cancer Research UK; Arbeitsgruppe Lebermetastasen und-tumoren in der Chirurgischen Arbeitsgemeinschaft Onkologie (ALM-CAO); Australasian Gastro-Intestinal Trials Group (AGITG); Fédération Francophone de Cancérologie Digestive (FFCD). Perioperative FOLFOX4 chemotherapy and surgery vs surgery alone for resectable liver metastases from colorectal cancer (EORTC 40983): long-term results of a randomised, controlled, phase 3 trial. *Lancet Oncol* 2013; **14**: 1208-1215 [PMID: 24120480 DOI: 10.1016/S1470-2045(13)70447-9]
- 7 **Cook AD**, Single R, McCahill LE. Surgical resection of primary tumors in patients who present with stage IV colorectal cancer: an analysis of surveillance, epidemiology, and end results data, 1988 to 2000. *Ann Surg Oncol* 2005; **12**: 637-645 [PMID: 15965730 DOI: 10.1245/ASO.2005.06.012]
- 8 **Venook AP**. Right-sided vs left-sided colorectal cancer. *Clin Adv Hematol Oncol* 2017; **15**: 22-24 [PMID: 28212365]
- 9 **Venook AP**, Niedzwiecki D, Lenz HJ, Innocenti F, Fruth B, Meyerhardt JA, Schrag D, Greene C, O'Neil BH, Atkins JN, Berry S, Polite BN, O'Reilly EM, Goldberg RM, Hochster HS, Schilsky RL, Bertagnolli MM, El-Khoueiry AB, Watson P, Benson AB 3rd, Mulkerin DL, Mayer RJ, Blanke C. Effect of First-Line Chemotherapy Combined With Cetuximab or Bevacizumab on Overall Survival in Patients With KRAS Wild-Type Advanced or Metastatic Colorectal Cancer: A Randomized Clinical Trial. *JAMA* 2017; **317**: 2392-2401 [PMID: 28632865 DOI: 10.1001/jama.2017.7105]

- 10 **Holch JW**, Ricard I, Stintzing S, Modest DP, Heinemann V. The relevance of primary tumour location in patients with metastatic colorectal cancer: A meta-analysis of first-line clinical trials. *Eur J Cancer* 2017; **70**: 87-98 [PMID: [27907852](#) DOI: [10.1016/j.ejca.2016.10.007](#)]
- 11 **van Rooijen KL**, Shi Q, Goey KKH, Meyers J, Heinemann V, Diaz-Rubio E, Aranda E, Falcone A, Green E, de Gramont A, Sargent DJ, Punt CJA, Koopman M. Prognostic value of primary tumour resection in synchronous metastatic colorectal cancer: Individual patient data analysis of first-line randomised trials from the ARCAD database. *Eur J Cancer* 2018; **91**: 99-106 [PMID: [29353165](#) DOI: [10.1016/j.ejca.2017.12.014](#)]
- 12 **Clancy C**, Burke JP, Barry M, Kalady MF, Calvin Coffey J. A meta-analysis to determine the effect of primary tumor resection for stage IV colorectal cancer with unresectable metastases on patient survival. *Ann Surg Oncol* 2014; **21**: 3900-3908 [PMID: [24849523](#) DOI: [10.1245/s10434-014-3805-4](#)]
- 13 **Ahmed S**, Fields A, Pahwa P, Chandra-Kanthan S, Zaidi A, Le D, Haider K, Reeder B, Leis A. Surgical Resection of Primary Tumor in Asymptomatic or Minimally Symptomatic Patients With Stage IV Colorectal Cancer: A Canadian Province Experience. *Clin Colorectal Cancer* 2015; **14**: e41-e47 [PMID: [26140732](#) DOI: [10.1016/j.clcc.2015.05.008](#)]
- 14 **Alawadi Z**, Phatak UR, Hu CY, Bailey CE, You YN, Kao LS, Massarweh NN, Feig BW, Rodriguez-Bigas MA, Skibber JM, Chang GJ. Comparative effectiveness of primary tumor resection in patients with stage IV colon cancer. *Cancer* 2017; **123**: 1124-1133 [PMID: [27479827](#) DOI: [10.1002/ncr.30230](#)]
- 15 **Moritani K**, Kanemitsu Y, Shida D, Shitara K, Mizusawa J, Katayama H, Hamaguchi T, Shimada Y; Colorectal Cancer Study Group (CCSG) of Japan Clinical Oncology Group (JCOG). A randomized controlled trial comparing primary tumour resection plus chemotherapy with chemotherapy alone in incurable stage IV colorectal cancer: JCOG1007 (iPACS study). *Jpn J Clin Oncol* 2020; **50**: 89-93 [PMID: [31829404](#) DOI: [10.1093/jjco/hyz173](#)]
- 16 **Damjanov N**, Weiss J, Haller DG. Resection of the primary colorectal cancer is not necessary in nonobstructed patients with metastatic disease. *Oncologist* 2009; **14**: 963-969 [PMID: [19819916](#) DOI: [10.1634/theoncologist.2009-0022](#)]
- 17 **Loupakis F**, Cremolini C, Masi G, Lonardi S, Zagonel V, Salvatore L, Cortesi E, Tomasello G, Ronzoni M, Spadi R, Zaniboni A, Tonini G, Buonadonna A, Amoroso D, Chiara S, Carlomagno C, Boni C, Allegrini G, Boni L, Falcone A. Initial therapy with FOLFOXIRI and bevacizumab for metastatic colorectal cancer. *N Engl J Med* 2014; **371**: 1609-1618 [PMID: [25337750](#) DOI: [10.1056/NEJMoa1403108](#)]
- 18 **Kopetz S**, Chang GJ, Overman MJ, Eng C, Sargent DJ, Larson DW, Grothey A, Vauthey JN, Nagorney DM, McWilliams RR. Improved survival in metastatic colorectal cancer is associated with adoption of hepatic resection and improved chemotherapy. *J Clin Oncol* 2009; **27**: 3677-3683 [PMID: [19470929](#) DOI: [10.1200/JCO.2008.20.5278](#)]



Retrospective Study

## Highly accurate colorectal cancer prediction model based on Raman spectroscopy using patient serum

Hiroaki Ito, Naoyuki Uragami, Tomokazu Miyazaki, William Yang, Kenji Issha, Kai Matsuo, Satoshi Kimura, Yuji Arai, Hiromasa Tokunaga, Saiko Okada, Machiko Kawamura, Noboru Yokoyama, Miki Kushima, Haruhiro Inoue, Takashi Fukagai, Yumi Kamijo

**ORCID number:** Hiroaki Ito 0000-0002-0761-0632; Naoyuki Uragami 0000-0003-2974-8250; Tomokazu Miyazaki 0000-0002-6108-8945; William Yang 0000-0002-8476-3026; Kenji Issha 0000-0002-0782-6871; Kai Matsuo 0000-0001-7951-2444; Satoshi Kimura 0000-0002-6843-8127; Yuji Arai 0000-0002-7776-715X; Hiromasa Tokunaga 0000-0002-5842-9630; Saiko Okada 0000-0003-1814-6449; Machiko Kawamura 0000-0002-6138-1690; Noboru Yokoyama 0000-0003-1882-0018; Miki Kushima 0000-0002-1642-0478; Haruhiro Inoue 0000-0002-0551-7274; Takashi Fukagai 0000-0003-0261-6303; Yumi Kamijo 0000-0002-4562-6926.

**Author contributions:** Ito H conceived the study; Ito H, Miyazaki T, Kimura S, Kawamura M, Inoue H, Fukagai T, and Kamijo Y contributed to the study design; Ito H, Uragami N, Matsuo K, Arai Y, Tokunaga H, and Okada S collected the blood samples; Arai Y, Tokunaga H, and Okada S centrifuged the blood to prepare the serum samples; Ito H, Uragami N, Matsuo K, and Yokoyama N performed the experiments and delivered patients' clinical data; Miyazaki T, Yang W and Issha K participated in the measurements; Ito H, Uragami N, Matsuo K,

**Hiroaki Ito, Naoyuki Uragami, Kai Matsuo, Noboru Yokoyama, Haruhiro Inoue,** Digestive Disease Center, Showa University Koto Toyosu Hospital, Tokyo 135-8577, Japan

**Tomokazu Miyazaki,** Research Division, JSR Corporation, Tokyo 105-0021, Japan

**William Yang,** BaySpec Inc., San Jose, CA 95131, United States

**Kenji Issha,** Fuji Technical Research Inc., Yokohama 220-6215, Japan

**Satoshi Kimura,** Department of Laboratory Medicine and Central Clinical Laboratory, Showa University Northern Yokohama Hospital, Yokohama 224-8503, Japan

**Yuji Arai, Saiko Okada,** Department of Clinical Laboratory, Showa University Koto Toyosu Hospital, Tokyo 135-8577, Japan

**Hiromasa Tokunaga,** Department of Clinical Laboratory, Showa University Hospital, Tokyo 142-8555, Japan, BML Inc., Tokyo 151-0051, Japan

**Machiko Kawamura,** Department of Hematology, Saitama Cancer Center, Inamachi, Saitama 362-0806, Japan

**Miki Kushima,** Department of Pathology, Showa University Koto Toyosu Hospital, Tokyo 135-8577, Japan

**Takashi Fukagai,** Department of Urology, Showa University Koto Toyosu Hospital, Tokyo 135-8577, Japan

**Yumi Kamijo,** Showa University Koto Toyosu Hospital, Tokyo 135-8577, Japan

**Corresponding author:** Hiroaki Ito, MD, PhD, Associate Professor, Department of Surgery, Digestive Disease Center, Showa University Koto Toyosu Hospital, 5-1-38 Toyosu, Koto-ku, Tokyo 135-8577, Japan. [h.ito@med.showa-u.ac.jp](mailto:h.ito@med.showa-u.ac.jp)

### Abstract

#### BACKGROUND

Colorectal cancer (CRC) is an important disease worldwide, accounting for the second highest number of cancer-related deaths and the third highest number of

Miyazaki T, Kimura S, and Kawamura M contributed to the data interpretation; Ito H and Miyazaki T performed the statistical analysis; Inoue H, Fukagai T, and Kamijo Y contributed to developing an environment for promoting research; Yang W created the customized Raman spectrometer and measurement software used in this study; Issha K coordinated Raman spectroscopy and software production, and transported and maintained the completed Raman spectroscopy and software; Kushima M performed the histopathological diagnoses of the participants; All authors contributed to manuscript writing, revision, and final approval.

**Supported by** the Japanese Society for the Promotion of Science (JSPS), based on the JSPS KAKENHI Grants-in-Aid for Scientific Research (C), No. JP17K09022.

#### Institutional review board

**statement:** The study protocol was reviewed and approved (No. 18T5005) by the Institutional Review Board of Showa University Koto Toyosu Hospital.

**Informed consent statement:** All participants provided written consent for their participation in this study.

**Conflict-of-interest statement:** The authors declare no conflicts of interest.

**Data sharing statement:** The original dataset analyzed in this study was uploaded to "figshare" (<https://figshare.com/s/538980237eea527631a3>). All other data in this study are available upon reasonable request to the corresponding author.

**Open-Access:** This article is an open-access article that was selected by an in-house editor and fully peer-reviewed by external reviewers. It is distributed in accordance with the Creative Commons Attribution NonCommercial (CC BY-NC 4.0) license, which permits others to

new cancer cases. The blood test is a simple and minimally invasive diagnostic test. However, there is currently no blood test that can accurately diagnose CRC.

#### AIM

To develop a comprehensive, spontaneous, minimally invasive, label-free, blood-based CRC screening technique based on Raman spectroscopy.

#### METHODS

We used Raman spectra recorded using 184 serum samples obtained from patients undergoing colonoscopies. Patients with malignant tumor histories as well as those with cancers in organs other than the large intestine were excluded. Consequently, the specific diseases of 184 patients were CRC (12), rectal neuroendocrine tumor (2), colorectal adenoma (68), colorectal hyperplastic polyp (18), and others (84). We used the 1064-nm wavelength laser for excitation. The power of the laser was set to 200 mW.

#### RESULTS

Use of the recorded Raman spectra as training data allowed the construction of a boosted tree CRC prediction model based on machine learning. Therefore, the generalized  $R^2$  values for CRC, adenomas, hyperplastic polyps, and neuroendocrine tumors were 0.9982, 0.9630, 0.9962, and 0.9986, respectively.

#### CONCLUSION

For machine learning using Raman spectral data, a highly accurate CRC prediction model with a high  $R^2$  value was constructed. We are currently planning studies to demonstrate the accuracy of this model with a large amount of additional data.

**Key Words:** Colorectal cancer; Raman spectroscopy; Machine learning; Blood; Serum; Diagnosis

©The Author(s) 2020. Published by Baishideng Publishing Group Inc. All rights reserved.

**Core Tip:** We developed a comprehensive, spontaneous, minimally invasive, label-free, blood-based colorectal cancer (CRC) screening technique based on Raman spectroscopy. We used Raman spectra recorded using 184 serum samples obtained from patients undergoing colonoscopies. Use of the recorded Raman spectra as training data allowed the construction of a boosted tree CRC prediction model based on machine learning. The generalized  $R^2$  values for CRC was 0.9982. For machine learning using Raman spectral data, we are currently working on the construction of a more accurate CRC prediction model with a large amount of additional data.

**Citation:** Ito H, Uragami N, Miyazaki T, Yang W, Issha K, Matsuo K, Kimura S, Arai Y, Tokunaga H, Okada S, Kawamura M, Yokoyama N, Kushima M, Inoue H, Fukagai T, Kamijo Y. Highly accurate colorectal cancer prediction model based on Raman spectroscopy using patient serum. *World J Gastrointest Oncol* 2020; 12(11): 1311-1324

**URL:** <https://www.wjgnet.com/1948-5204/full/v12/i11/1311.htm>

**DOI:** <https://dx.doi.org/10.4251/wjgo.v12.i11.1311>

## INTRODUCTION

Colorectal cancer (CRC) is an important disease worldwide. According to Globocan 2018 (<http://gco.iarc.fr/today/data/factsheets/cancers/39-All-cancers-fact-sheet.pdf>), among all cancers, CRC accounted for the second highest number of deaths and the third highest number of new cases<sup>[1]</sup>. The blood test is a simple minimally invasive diagnostic test. However, presently, no blood test method can accurately diagnose CRC. Tumor marker tests such as those for carcinoembryonic antigen<sup>[2]</sup>, carbohydrate antigen 19-9 (CA 19-9)<sup>[3]</sup>, CA72-4<sup>[4]</sup>, and CA125<sup>[5]</sup> are minimally invasive tests for CRC patients and can be performed in many medical institutions. However, these



distribute, remix, adapt, build upon this work non-commercially, and license their derivative works on different terms, provided the original work is properly cited and the use is non-commercial. See: <http://creativecommons.org/licenses/by-nc/4.0/>

**Manuscript source:** Invited manuscript

**Specialty type:** Oncology

**Country/Territory of origin:** Japan

**Peer-review report's scientific quality classification**

Grade A (Excellent): 0  
Grade B (Very good): 0  
Grade C (Good): C, C  
Grade D (Fair): 0  
Grade E (Poor): 0

**Received:** July 31, 2020

**Peer-review started:** July 31, 2020

**First decision:** September 17, 2020

**Revised:** September 28, 2020

**Accepted:** October 19, 2020

**Article in press:** October 19, 2020

**Published online:** November 15, 2020

**P-Reviewer:** Chong CS, Kuo SH

**S-Editor:** Chen XF

**L-Editor:** Filipodia

**P-Editor:** Li JH



conventional tumor markers have low-detection sensitivity for CRC<sup>[6]</sup>; they are mostly used for prognostic<sup>[7]</sup> and recurrence predictions<sup>[8]</sup> rather than early diagnosis. The presence of cell-free DNA<sup>[9]</sup> and microRNA (miRNA)<sup>[10]</sup> has been reported in the blood of CRC patients; however, these tests have not yet become common practice. Circulating cancer cells<sup>[11]</sup> can be detected in the blood of CRC patients, but it is unclear whether the detection of circulating cancer cells is useful for the early diagnosis of CRC<sup>[12]</sup>.

Raman spectroscopy is a non-destructive method<sup>[13]</sup> used to analyze the components contained in a sample. This technique can analyze samples in various states (gases, liquids, and solids) without labeling. Research has also been conducted using Raman spectroscopy to diagnose cancer using a blood sample. Raman spectroscopy is useful for the diagnosis of colorectal<sup>[14]</sup>, gastric<sup>[15]</sup>, esophageal<sup>[16]</sup>, pancreatic<sup>[17]</sup>, lung<sup>[18]</sup>, breast<sup>[19]</sup>, prostate<sup>[20,21]</sup>, and bladder<sup>[22]</sup> cancers. Lin *et al*<sup>[14]</sup> reported the results of analysis of serum obtained from 38 CRC patients and 45 volunteers by gold nanoparticle-based surface-enhanced Raman spectroscopy, which had diagnostic sensitivity and specificity of 97.4% and 100%, respectively. However, the effectiveness of Raman spectroscopy in cancer diagnosis has not yet been evaluated. We recorded the highly sensitive surface-enhanced Raman scattering spectra of human serum samples using a silver nanocomplex biochip<sup>[23,24]</sup>. There were significant differences in the scattered light intensities of Raman shifts, attributed to specific molecular bonds, between the serum samples of cancer patients with stomach or colon cancer and those with benign disease. However, the procedure was complicated, and the detection of substances was limited by the fact that specific silver nanoparticles should be used. Thus, we decided to develop another comprehensive, label-free Raman technique to detect known and unknown substances in the serum. The subsequent preliminary study showed that our Raman spectroscopy system could detect spontaneous Raman scattering spectra from untreated human serum samples within 1 min<sup>[25]</sup>. Hence, we considered that serum analysis based on Raman spectroscopy could provide a rapid cancer diagnosis.

In this study, we confirmed the correlation between the Raman scattering spectra of the serum samples collected before examination and the endoscopic diagnosis of patients who underwent colonoscopies. Additionally, we constructed a model that predicts cancer with increased accuracy based on machine learning.

## MATERIALS AND METHODS

### Patients

This study included patients who underwent colonoscopies at the Showa University Koto Toyosu Hospital (Tokyo, Japan) between September 2018 and September 2019. Patients were excluded if they were < 20-years-old, > 80-years-old, had a history of malignancy, or had malignant diseases in organs other than the colon. The protocol in this study complied with the Declaration of Helsinki and the Clinical Trial Act in Japan. The study protocol was reviewed and approved (No. 18T5005) by the Institutional Review Board of Showa University Koto Toyosu Hospital. All participants provided written consent for their participation in this study. The study protocol was registered in the University Hospital Medical Information Network clinical trial registry (UMIN-CTR, No. UMIN000034306).

Based on previous clinical research at the Showa University Koto Toyosu Hospital, at least 150 patients were required to capture > 3 CRC patients. Therefore, 184 patients were recruited for the study (110 men and 74 women, aged between 20 and 80 years). The median and average ages were 57 and 56.9 years, respectively (Table 1).

In addition to colonoscopy, gastroscopy, computed tomography, ultrasonography, and magnetic resonance imaging were performed in 100, 51, 5, and 5 cases, respectively.

The primary diagnoses of the 184 patients recruited in this study were: CRC in 12 cases (3, tumor-node-metastasis [TNM] stage 0; 1, TNM stage I; 2, TNM stage II; 5, TNM stage III; 1, TNM stage IV), rectal carcinoids in 2 cases, colorectal adenomas in 68 cases, colon hyperplastic polyps in 18 cases, other diseases in 54 cases (1, leiomyoma; 9, nonspecific colitis; 2, ulcerative colitis; 24, colon diverticulum; 3, nonspecific ileitis; and 15, internal hemorrhoid), and no specific finding in 30 cases (Table 2). One CRC patient was also diagnosed with colorectal adenoma and another with ulcerative colitis. Sixteen of sixty-eight patients with colorectal adenoma were also diagnosed with colorectal hyperplastic polyps. All cancers and adenomas were histopathologically diagnosed by at least two qualified clinical pathologists. Polyps

**Table 1 Patients and evaluations**

Parameters	<i>n</i> = 184
Sex	
Male	110
Female	74
Age in yr, mean (range)	56.9 (20-80)
Gastroscopy	100
Computed tomography	51
Ultrasonography	5
Magnetic resonance imaging	5

**Table 2 Main diagnosis**

Main diagnosis	<i>n</i> = 184
Cancer	12
Colon, TNM stage 0-II	5
Colon, TNM stage III or IV	3
Rectum, TNM stage III or IV	3
Colon and rectum, double, TNM stage IIA	1
Malignant potential tumor	2
Rectal neuroendocrine tumor	2
Adenoma	68
Hyperplastic polyp	18
Other diseases	54
Leiomyoma	1
Nonspecific colitis	9
Ulcerative colitis	2
Colon diverticulum	24
Nonspecific ileitis	3
Internal hemorrhoids	15
No specific findings	30

TNM: Tumor node metastasis.

were diagnosed endoscopically as hyperplastic polyps are not usually treated.

### Materials

Blood samples were collected prior to endoscopic examinations. Serum samples were obtained by centrifuging blood samples for 5 min (1500 × g). The extracted serum samples were dispensed into 2.0 mL hyperplastic polypropylene microtubes (Biosphere® plus; Sarstedt Ag & Co. Kg, Sarstedtstraße, Nümbrecht, Germany), which were free from DNA, DNase/RNase, polymerase chain reaction inhibitor, adenosine triphosphate, and pyrogens/endotoxins. The specimens were preserved at -80 °C in an ultralow temperature freezer (MDF-C8V1; Panasonic Corporation, Osaka, Japan).

### Raman spectrometer

A Nomadic Raman microscope with a computer-controlled electrical stage running Pathologic System Software Version 1.0.1.0 (BaySpec Inc., San Jose, CA, United States) was used for analysis. The details of the Raman microscope used in this study have

been described in a previous paper<sup>[25]</sup>, and the outline is given below. A wavelength of 1064 nm was selected as the excitation laser. The power of the laser was set to 200 mW. A 20 × magnifying objective lens with a correction collar with near-infrared microscopy (LCPLN20XIR; Olympus Corporation, Tokyo, Japan) and a 2048 × 64 pixel thermoelectric cooled indium gallium arsenide, charge-couple device (CCD) detector, with a spectral range of 100–3200 cm<sup>-1</sup> (grating 4 cm<sup>-1</sup>) were used to record the spectra. A CCD camera with 1392 × 1040 colors and a maximum acquisition rate of 30 frames per second (Lw135R; Lumenera Corporation, Capella Court, Ottawa, ON, Canada) was used for focusing before each Raman scattering spectral acquisition (Figure 1). The dark background noise of the CCD camera was acquired in the form of a spectrum in the absence of a sample and was subtracted from all spectra acquired in which the sample was present. Baseline correction was performed for each spectrum with the Pathologic System Software (BaySpec Inc.). Moreover, some figures in this paper were created using RaspWin Ver 8.0.1 (HT SoftLab) and Adobe Illustrator CS6 Version 16.2.0 (Adobe Systems Incorporated, San Jose, CA, United States).

### Measurements

An overview of the measurement and analysis processes is summarized in Online resource 10. The cryopreserved serum was thawed immediately before the measurement and was set at 25 °C. We manually placed a drop of the serum stock solution on the tip of a thin stainless-steel tube. The serum was irradiated with a 1064-nm wavelength laser three times for 15 s, and the average value was recorded as the Raman scattering spectra. A new droplet was then prepared, and the same measurement was repeated three times for each serum sample.

### Data analysis

The scattered light intensity (15 range, A1–A15) of the Raman shift related to nucleic acids<sup>[26–34]</sup>, proteins<sup>[28,30–32,34,35]</sup>, and lipids<sup>[27,28,30,32,34,36–41]</sup> in serum was extracted from the obtained Raman spectra (Figures 2 and 3, Table 3). The average values of the three extracted scattered light intensities from each spectrum were analyzed as training data by the boosted tree model<sup>[42]</sup> with the use of JMP® Pro 14.3.0 (SAS Institute Inc., Cary, NC, United States). The average values for the three extracted scattered light intensities among the patient groups were evaluated for normality using the Tukey test. Intergroup differences in non-normally distributed data were compared using the Steel-Dwass nonparametric test. All analyses were performed using JMP® Pro 14.3.0 (SAS Institute Inc.).

The relevant definitions were: Entropy  $R$ -squared =  $1 - \text{Loglike}(\text{model}) / \text{Loglike}(0)$ ; Generalized  $R$ -squared =  $\{1 - [L(0)/L(\text{model})]^{(2/n)}\} / [1 - L(0)^{(2/n)}]$ ; Mean Logp =  $\sum -\text{Log}[p(j)] / n$ ; Root-mean-square error =  $\sqrt{\sum [y(j) - \rho(j)]^2 / n}$ ; Mean absolute deviation =  $\sum |y(j) - \rho(j)| / n$ ; and Misclassification rate =  $\sum [\rho(j) \neq \rho_{\text{Max}}] / n$  (Supplementary Table 1). The detailed conditions for the analysis based on the boosted tree model were: Number of layers = 200 (maximum number of layers to include in the final tree is 200); Splits per tree = 3 (number of splits for each layer is 3); Learning rate = 0.1; Overfit penalty = 0.0001; Minimum size split = 5; Row sampling rate = 1; and Column sampling rate = 1 (Supplementary Table 2).

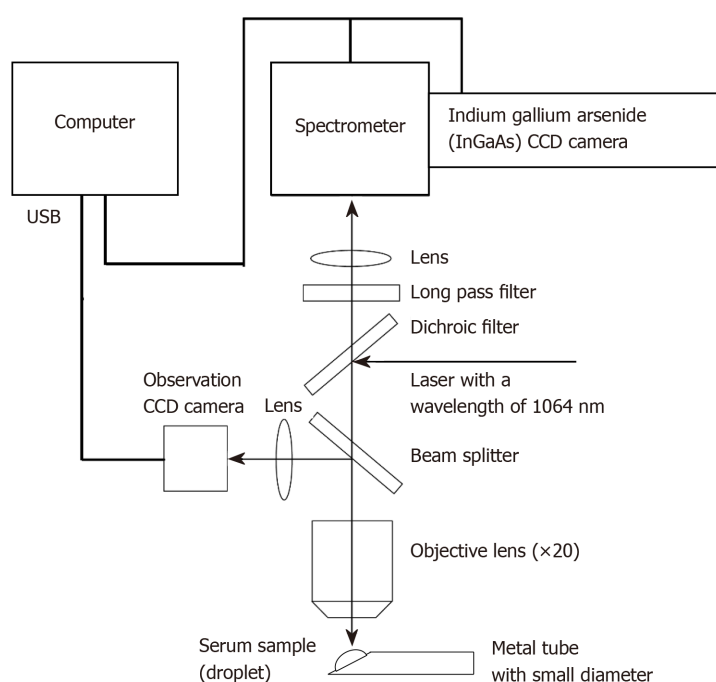
## RESULTS

### Boosted tree model using Raman spectra of patient serum as data

Raman spectra of all serum samples were recorded, and the highest values of the scattered light intensity, ranging from A1 to A15, were extracted (Figures 2 and 3). The boosted tree model was used to predict CRC, and a highly accurate model was constructed based on a generalized  $R^2$  value of 0.9977 and an entropy  $R^2$  value of 0.9982 (Supplementary Table 3). Similarly, the boosted tree model was used to predict colorectal adenomas and hyperplastic polyps, and a highly accurate adenoma prediction model was constructed based on a generalized  $R^2$  value of 0.9269, and an entropy  $R^2$  value of 0.9630 (Supplementary Table 4). Furthermore, a highly accurate hyperplastic polyp prediction model was constructed based on a generalized  $R^2$  value of 0.9947 and an entropy  $R^2$  value of 0.9962 (Supplementary Table 5). The boosted tree model was used to predict rectal neuroendocrine tumors based on data from two patients, and a highly accurate rectal neuroendocrine tumor prediction model was also constructed based on a generalized  $R^2$  value of 0.9985 and an entropy  $R^2$  value of 0.9986 (Supplementary Table 6).

**Table 3 Assignment of serum sample**

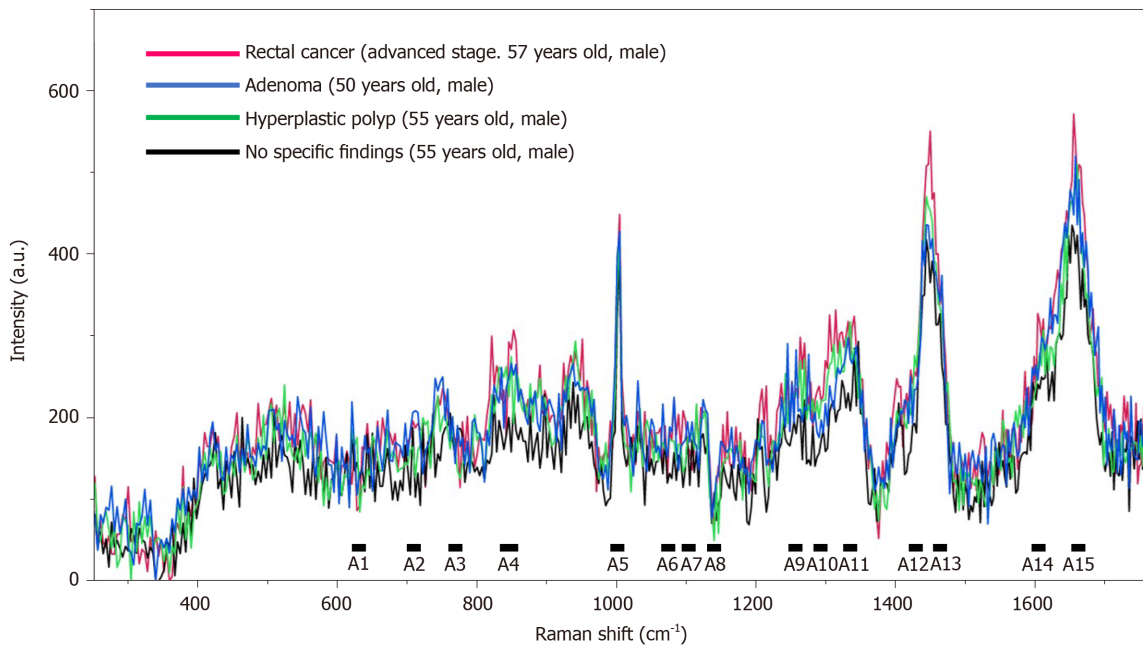
Raman shift, cm <sup>-1</sup>		Assignments		
		Nucleic acids	Proteins	Lipids
A1	611-631		Phenylalanine	
A2	700-720			Cholesterol, C-N-C
A3	751-771	DNA, pyrimidines	Tryptophan	
A4	830-859		Tyrosine, pro C-C	
A5	993-1013		Phenylalanine	
A6	1060-1080		Skeletal C-C, C-N	Skeletal C-C
A7	1091-1111	PO <sub>2</sub> stretching, DNA		Skeletal C-C
A8	1123-1143		Skeletal C-C, C-N	Skeletal C-C
A9	1244-1264	Adenine, thymine, cytosine	Amide III	=CH, CH <sub>2</sub>
A10	1275-1295		Amide III	
A11	1322-1343	Guanine, adenine	CH <sub>3</sub> CH <sub>2</sub>	CH
A12	1408-1428		COO <sup>-</sup>	
A13	1448-1468		CH <sub>2</sub>	CH <sub>2</sub>
A14	1596-1616	Cytosine	Phenylalanine, tyrosine	
A15	1647-1667	Thymine, guanine, cytosine	Amide I	C=C



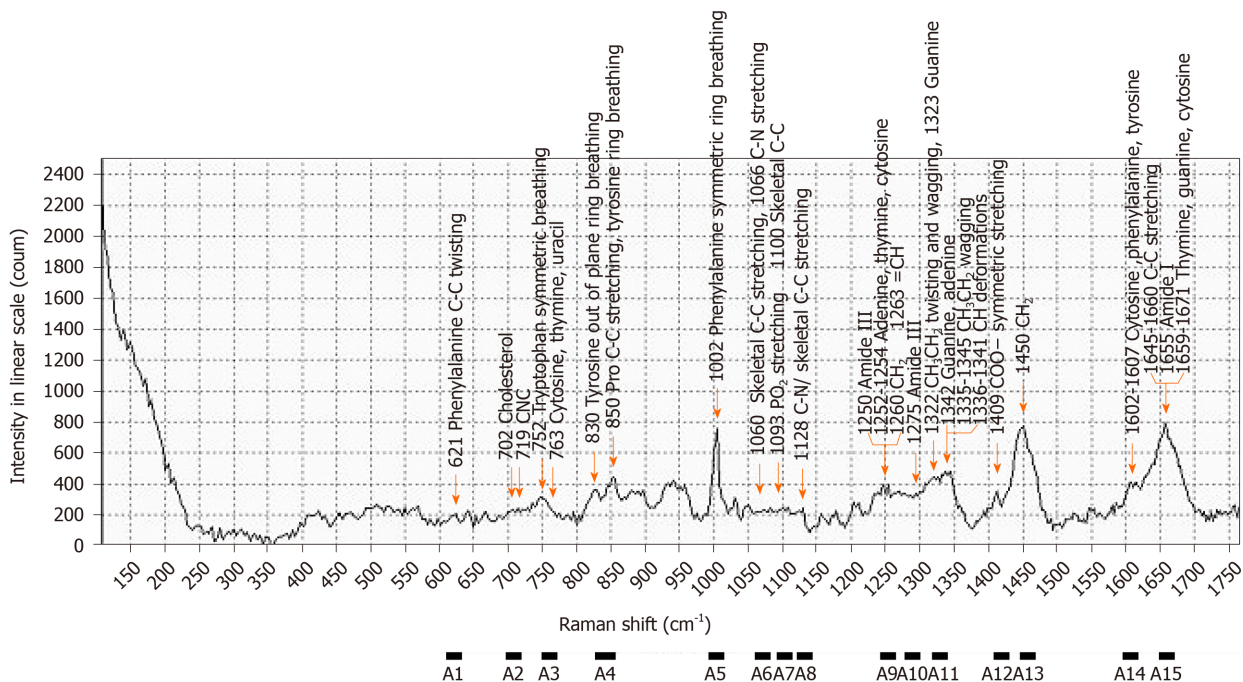
**Figure 1 Schematic of the confocal micro-Raman spectrometer used in this study.** A nomadic Raman microscope with an excitation laser at a wavelength of 1064 nm was used in this study. A 20 × magnifying objective lens with a correction collar with near-infrared microscopy (LCPLN20XIR; Olympus Corporation, Tokyo, Japan) and a 2048 × 64 pixel thermoelectric cooled indium gallium arsenide (InGaAs), charge-couple device (CCD) detector, with a spectral range of 100-3200 cm<sup>-1</sup> (grating 4 cm<sup>-1</sup>) were used to record the spectra.

### **Raman shifts contributed to the prediction of colorectal disease**

The major Raman shifts<sup>[17-19,21-37,43-45]</sup> that contributed to the prediction of the presence of CRC (effect > 0.1) were higher in the order of A10 (1275-1295 cm<sup>-1</sup>; amide III), A8 (1123-1143 cm<sup>-1</sup>; C-N and skeletal C-C), and A3 (751-771 cm<sup>-1</sup>; DNA, pyrimidines [cytosine, thymine, uracil], and tryptophan). The major Raman shifts that contributed to the



**Figure 2 Raman spectra of serum samples from patients.** The spectra of the serum samples from patients with rectal cancer, colon adenoma, and colon hyperplastic polyp, and the patient with no specific findings.



**Figure 3 Raman spectra of patient serum samples and assignments.** Raman spectra of serum sample from the patient with internal hemorrhoid (53-years-old, female), and selected range of Raman shift.

prediction of the presence of colorectal adenoma (effect > 0.1) were higher in the order of A4 (830-859  $\text{cm}^{-1}$ ; tyrosine and pro C-C), and A10 (1275-1295  $\text{cm}^{-1}$ ; amide III). The major Raman shifts that contributed to the prediction of colorectal polyps (effect > 0.1) were higher in the order of A7 (1091-1111  $\text{cm}^{-1}$ ;  $\text{PO}_2$  stretching and skeletal C-C), A1 (611-631  $\text{cm}^{-1}$ ; phenylalanine), and A4 (830-859  $\text{cm}^{-1}$ ; tyrosine and pro C-C). A10 (1275-1295  $\text{cm}^{-1}$ ; amide III) was the Raman shift that affected the prediction of the presence of cancer and adenomas. A4 (830-859  $\text{cm}^{-1}$ ; tyrosine and pro C-C) was the Raman shift that influenced the prediction of both adenomas and polyps. The only Raman shift that influenced the prediction of rectal neuroendocrine tumors was A11, which was different from those for the prediction of cancer, adenomas, and polyps (Table 4,



**Table 4 Boosted tree model for the prediction of colorectal disease**

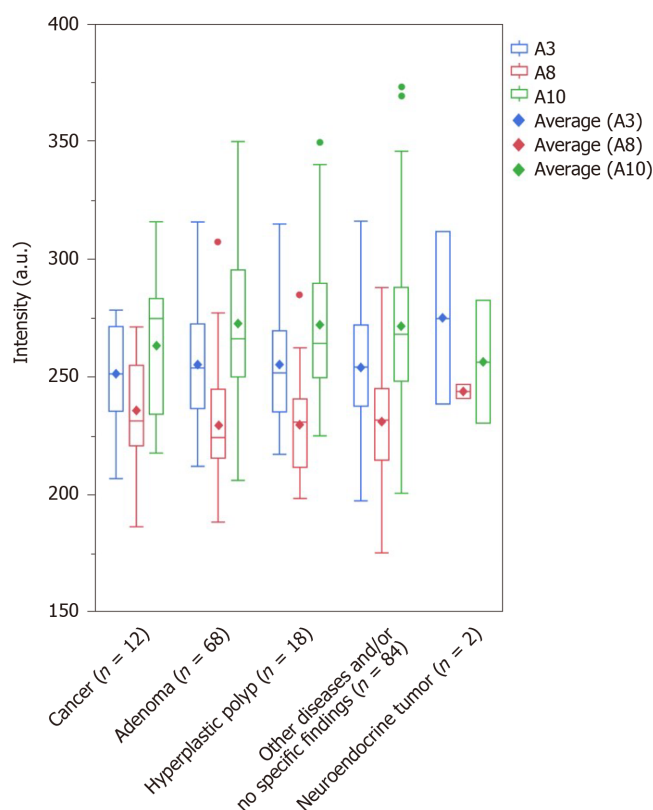
		Cancer	Adenoma	Hyperplastic polyp	NET
Measure		Training			
Entropy <i>R</i> -square		0.9977	0.9269	0.9947	0.9985
Generalized <i>R</i> -square		0.9982	0.9630	0.9962	0.9986
Raman shift, cm <sup>-1</sup>		Effect			
A1	611-631	0.0176	0.0285	0.2404	0.0148
A2	700-720	0.0191	0.0636	0.0476	0.0062
A3	751-771	0.1716	0.0479	0.0274	0.0182
A4	830-859	0.0580	0.2008	0.1936	0.0246
A5	993-1013	0.0084	0.0478	0.0054	0.0324
A6	1060-1080	0.0052	0.0555	0.0407	0.0000
A7	1091-1111	0.0686	0.0370	0.2886	0.0180
A8	1123-1143	0.1873	0.0722	0.0563	0.0412
A9	1244-1264	0.0481	0.0548	0.0129	0.0022
A10	1275-1295	0.2291	0.1146	0.0224	0.0000
A11	1322-1343	0.0505	0.0463	0.0149	0.7714
A12	1408-1428	0.0663	0.0551	0.0132	0.0662
A13	1448-1468	0.0089	0.0066	0.0041	0.0000
A14	1596-1616	0.0145	0.0758	0.0293	0.0049
A15	1647-1667	0.0470	0.0936	0.0033	0.0000

NET: Neuroendocrine tumor.

Supplementary Tables 3-6). We investigated the maximum scattered light intensities of the Raman shifts of A10, A8, and A3 that contributed to the prediction of the presence of CRC. Compared with the group with adenomas, hyperplastic polyps, and no specific findings and/or other diseases, the mean scattered light intensity of A8 tended to be higher, and the mean scattered light intensities of A3 and A10 tended to be lower in the cancer samples (Figure 4). However, there was no significant difference based on the Steel-Dwass test (Supplementary Table 7).

## DISCUSSION

Numerous studies have been performed to diagnose cancer using blood tests. However, tumor markers, free DNA<sup>[9]</sup>, miRNA<sup>[10]</sup>, and circulating cancer cells<sup>[11]</sup> have been the main targets of blood-based CRC diagnostic techniques. To date, high-precision technologies have not been developed. Additionally, standard blood-based procedures for cancer diagnosis have not yet been established. Raman spectroscopy is an analytical method that can quickly evaluate the components of unlabeled samples that have not been pre-treated<sup>[46]</sup>. However, the measurement of Raman spectra is strongly inhibited by autofluorescence<sup>[47]</sup>, and thus it is difficult to analyze a biological sample with high accuracy. Furthermore, given that the detection sensitivity of label-free, spontaneous Raman spectroscopy is lower than other labeling techniques, it is difficult to detect minute quantities of target substances. Correspondingly, it is necessary to enhance scattered light using various methods, including the use of surface-enhanced Raman spectroscopy. In fact, most Raman spectroscopic analyses of blood performed to date have utilized surface-enhanced Raman spectroscopy<sup>[19,20,48-50]</sup>. Some studies have used small sample sizes for blood-based diagnoses of CRC with Raman spectroscopy. Almost all of these studies have been based on the surface-enhanced Raman scattering technique<sup>[14,51-54]</sup>. Principal component analysis (PCA)<sup>[51]</sup>, partial least squares<sup>[52,53]</sup>, linear discriminant analysis (LDA)<sup>[52]</sup>, and PCA-LDA<sup>[14,54]</sup> were



**Figure 4 Comparison of intensity.** Outlier box plot depicting the intensity of the scattered light of the sera from the studied patients. The bottom and top parts of the box show the lower and upper quartiles, and the band across the box indicates the median. The lower and upper bars at the ends of the whiskers show the lowest data point within a range spanning 1.5 interquartile ranges of the lower quartile, and the highest data point within a range spanning 1.5 interquartile ranges of the upper quartile. The dots denote outliers that extend beyond the whiskers. The diagonal square indicates average values. However, with no significant difference, the mean scattered light intensity of A8 is higher in the cancer group (235.6) than in the adenoma (229.4), hyperplastic polyp (229.7), and other disease and/or no specific findings (231.0) groups. In addition, with no significant difference, the mean scattered light intensity of A10 is lower in the cancer group (263.4) than in the adenoma (272.4), hyperplastic polyp (272.1), and other disease and/or no specific findings (271.6) groups. With a slight difference, the mean scattered light intensity of A3 tended to be lower in the cancer group (251.3) than that in those with adenomas (255.2), hyperplastic polyps (254.9), and other disease and/or no specific findings (253.9).

used for evaluation, and respective diagnostic sensitivities and specificities of 86.4%-100% and 80%-100% were reported<sup>[14,51-54]</sup>. However, the surface-enhanced Raman scattering technique is highly sensitive. Furthermore, target substances are limited by the designed specifications of colloids based on precious metals, such as gold and silver. Therefore, important unknown substances that can be used for the detection of cancer may escape when surface-enhanced Raman scattering techniques are used. In fact, significant molecular bonds present in the serum and involved in cancer detection have varied<sup>[14,51-54]</sup>. Furthermore, the Raman scattered light enhancement technique does not have the advantages of Raman spectroscopy. For example, it is not label-free, more complex, and its response is slower. It would therefore be ideal if diagnosis could be established at high accuracy using ordinary, spontaneous Raman spectroscopy. Our label-free, spontaneous Raman spectroscopy system could detect known and unknown substances in a comprehensive manner. In this study, a highly accurate CRC prediction model with a generalized  $R^2$  value that exceeded 0.99 was constructed. We used a near-infrared laser as the excitation light source that was hardly affected by autofluorescence. Furthermore, a microtube was developed for serum measurements. Therefore, the Raman spectra of the serum could be obtained without a surface-enhanced Raman technique.

In this study, our system could accurately predict the presence of CRC, adenomas, and hyperplastic polyps. Even though our system could also predict the presence of rectal neuroendocrine tumors, the number of patients with rectal neuroendocrine tumors in this study was only two. Accordingly, findings should be confirmed with additional future studies. There is a possibility that our less invasive blood-based test could be used for screening CRC. In addition, this technique can comprehensively detect all known and unknown molecules contained in a sample. Therefore, by constructing an optimal algorithm based on the Raman spectrum, there is a possibility

that it can be applied to the diagnosis of various diseases, including congenital, genetic, and metabolic diseases.

The Raman shifts (effect > 0.1) in our CRC prediction model were in the ranges of 1275-1295  $\text{cm}^{-1}$  (amide III), 1123-1143  $\text{cm}^{-1}$  (C-N and skeletal C-C), and 751-771  $\text{cm}^{-1}$  [DNA, pyrimidines (cytosine, thymidine, uracil), and tryptophan] (Table 3). Additionally, the scattered light intensities of 1275-1295  $\text{cm}^{-1}$  (amide III), 1123-1143  $\text{cm}^{-1}$  (C-N and skeletal C-C), and 751-771  $\text{cm}^{-1}$  [DNA, pyrimidines (cytosine, thymidine, uracil), and tryptophan] of the sera obtained from CRC patients were respectively low, high, and low. Compared with the results of our study, Feng *et al.*<sup>[52]</sup> reported the exact opposite result with a surface-enhanced Raman scattering technique. Hong *et al.*<sup>[51]</sup> also reported that the scattered light of the serum from CRC patients was relatively high intensity at 1275-1295  $\text{cm}^{-1}$  (amide III). Other studies reported no difference regarding these Raman shifts<sup>[14,53,54]</sup>. These discrepancies may be attributed to differences between spontaneous Raman spectra and surface-enhanced Raman spectra or to the inaccuracies of the analyzed results owing to the small data sizes. In this study, only the disease was used as an index, and the effects of age, sex, presence or absence of co-morbidity, total protein concentration, albumin concentration, and other biological factors were not considered. We need to carefully analyze more samples after matching these factors to enhance our CRC prediction model.

The Raman shift that had a strong effect on the prediction of the presence of colorectal adenomas and hyperplastic polyps was partially consistent with the Raman shift used for the prediction of CRC. For the prediction of colorectal adenomas, effects larger than 0.01 were in the range of 830-859  $\text{cm}^{-1}$  (tyrosine and pro C-C) and 1275-1295  $\text{cm}^{-1}$  (amide III). Neither our or previous studies have shown a clear link between colorectal adenomas and serum tyrosine levels. The “adenoma-carcinoma sequence”<sup>[55]</sup> was estimated. Accordingly, it has been suggested that abnormalities in Wnt signaling in colorectal adenomas were associated with the development of CRC<sup>[56,57]</sup>. In this study, the amide III intensity level was a significant factor for CRC and adenomas. Furthermore, the amide III intensity level was low in cancer and high in adenomas. Thus, serum amide III levels may be used to assess the risk of CRC. For the prediction of hyperplastic colon polyps, effects were larger in the ranges of 1091-1111  $\text{cm}^{-1}$  ( $\text{PO}_2$  stretching and skeletal C-C), 611-631  $\text{cm}^{-1}$  (phenylalanine), and 830-859  $\text{cm}^{-1}$  (tyrosine and pro C-C). The Raman shift at 830-859  $\text{cm}^{-1}$  (tyrosine and pro C-C) was also the appropriate Raman shift for the prediction of colorectal adenomas. This overlap may be associated with the transition of hyperplastic colorectal polyps to colorectal adenomas and may be predictive for the development of colorectal adenomas<sup>[58]</sup>. In this study, all polyps were diagnosed endoscopically. Therefore, the possibility of adenomas cannot be ruled out.

The limitations of this study were as follows. First, the number of subjects was small; the total number of subjects was 184, of which only 12 were CRC patients. Additionally, since there were only two samples from patients with neuroendocrine tumors, we could not give definitive results for neuroendocrine tumors in this study. In the future, verification with more subjects must be performed. Second, this study did not consider the effects of biological factors other than diseases such as age, sex, presence or absence of co-morbidities, and total protein or albumin concentrations. We need to revalidate the technology in this study with prospective trials tailored to the subject's background. Third, the patients analyzed in this study received inconsistent clinical examinations that may have been associated with various degrees of accuracies regarding clinical diagnoses. They may have also had malignancies of organs other than the colon. Fourth, it was not clear whether our technology was able to detect high-risk states of carcinogenesis or the cancer cells themselves after the onset of carcinogenesis. If the moieties detected by our technology are derived from cancer cells, this technology can be used to determine the therapeutic effects of cancer.

In summary, we could present a model for diagnosing CRC with serum and machine learning in this study. However, the clinical usefulness of this model is still undecided. We plan to continue our research in the future to improve the accuracy of our results. First, we will include larger cohorts. Second, we will increase the number of target cancer types. Third, blood will be collected twice before and after the treatment, and the Raman spectra of the serum will be compared. From these results, we believe that the significance of our label-free, spontaneous Raman spectroscopy technology in cancer treatment will become clearer. Regarding the Raman spectral analysis, a comprehensive machine learning method capable of analyzing the entire spectrum will be designed and implemented.

## CONCLUSION

We studied a minimally invasive and accurate diagnostic method of CRC, which is the second most common cancer-related death worldwide. We evaluated that analysis of Raman spectrum of serum by machine learning could be an excellent diagnostic method for CRC. Since Raman spectroscopy is greatly affected by autofluorescence, it is technically difficult to analyze biological samples by Raman spectroscopy. We have succeeded in recording the Raman spectrum of untreated serum with high accuracy by using a near-infrared laser, which is less affected by autofluorescence, as the excitation light source. Then, using the recorded Raman spectra as data, we constructed a CRC prediction model by "Boosted Tree Model" which is a kind of machine learning. Although this model may predict CRC with high accuracy, we should analyze more clinical data to confirm the clinical usefulness of this model.

## ARTICLE HIGHLIGHTS

### **Research background**

Colorectal cancer (CRC) is an important disease worldwide. Among all cancers, CRC accounts for the second highest number of deaths and the third highest number of new cases. The blood test is a simple minimally invasive diagnostic test. However, presently, no blood test method can accurately diagnose cancer.

### **Research motivation**

We have tried to develop a comprehensive, spontaneous, minimally invasive, label-free, blood-based CRC screening technique based on Raman spectroscopy.

### **Research objectives**

We used Raman spectra recorded using 184 serum samples obtained from patients (CRC in 12 patients, rectal neuroendocrine tumor in 2 patients, colorectal adenoma in 68 patients, colorectal hyperplastic polyp in 18 patients, and others in 84 patients) undergoing colonoscopies.

### **Research methods**

We used Raman spectra recorded using 184 serum samples. We used 1064-nm wavelength laser for excitation.

### **Research results**

Use of the recorded Raman spectra as training data allowed the construction of a boosted tree CRC prediction model based on machine learning. Therefore, the generalized  $R^2$  values for CRC, adenomas, hyperplastic polyps, and neuroendocrine tumors were 0.9982, 0.9630, 0.9962, and 0.9986, respectively.

### **Research conclusions**

We could show a diagnostic model of machine learning using Raman spectral data, a highly accurate CRC prediction with a high  $R^2$  value.

### **Research perspectives**

We are currently planning studies to demonstrate the clinical usefulness of this model with a vast volume of additional data.

## ACKNOWLEDGEMENTS

We are grateful to the patients who donated blood. We are also grateful to the clinical staff at Showa University, Koto Toyosu Hospital. We would like to thank Ms. Iono A and Mr. Oi H (SAS Institute Inc.) for their dedicated support in machine learning.

## REFERENCES

- 1 Ciccolallo L, Capocaccia R, Coleman MP, Berrino F, Coebergh JW, Damhuis RA, Faivre J, Martinez-Garcia

- C, Møller H, Ponz de Leon M, Launoy G, Raverdy N, Williams EM, Gatta G. Survival differences between European and US patients with colorectal cancer: role of stage at diagnosis and surgery. *Gut* 2005; **54**: 268-273 [PMID: [15647193](#) DOI: [10.1136/gut.2004.044214](#)]
- 2 **Nicolini A**, Caciagli M, Zampieri F, Ciampalini G, Carpi A, Spisni R, Colizzi C. Usefulness of CEA, TPA, GICA, CA 72.4, and CA 195 in the Diagnosis of primary colorectal cancer and at its relapse. *Cancer Detect Prev* 1995; **19**: 183-195 [PMID: [7750106](#)]
- 3 **Morita S**, Nomura T, Fukushima Y, Morimoto T, Hiraoka N, Shibata N. Does serum CA19-9 play a practical role in the management of patients with colorectal cancer? *Dis Colon Rectum* 2004; **47**: 227-232 [PMID: [15043294](#) DOI: [10.1007/s10350-003-0041-6](#)]
- 4 **Filella X**, Molina R, Mengual PJ, Jo J, Ballesta AM. Significance of CA72.4 in patients with colorectal cancer. Comparison with CEA and CA19.9. *J Nucl Biol Med* 1991; **35**: 158-161 [PMID: [1816871](#)]
- 5 **Gao Y**, Wang J, Zhou Y, Sheng S, Qian SY, Huo X. Evaluation of Serum CEA, CA19-9, CA72-4, CA125 and Ferritin as Diagnostic Markers and Factors of Clinical Parameters for Colorectal Cancer. *Sci Rep* 2018; **8**: 2732 [PMID: [29426902](#) DOI: [10.1038/s41598-018-21048-y](#)]
- 6 **Shinkins B**, Nicholson BD, Primrose J, Perera R, James T, Pugh S, Mant D. The diagnostic accuracy of a single CEA blood test in detecting colorectal cancer recurrence: Results from the FACS trial. *PLoS One* 2017; **12**: e0171810 [PMID: [28282381](#) DOI: [10.1371/journal.pone.0171810](#)]
- 7 **Kanellos I**, Zacharakis E, Kanellos D, Pramateftakis MG, Betsis D. Prognostic significance of CEA levels and positive cytology in peritoneal washings in patients with colorectal cancer. *Colorectal Dis* 2006; **8**: 436-440 [PMID: [16684089](#) DOI: [10.1111/j.1463-1318.2006.00991.x](#)]
- 8 **Bhatti I**, Patel M, Dennison AR, Thomas MW, Garcea G. Utility of postoperative CEA for surveillance of recurrence after resection of primary colorectal cancer. *Int J Surg* 2015; **16**: 123-128 [PMID: [25771102](#) DOI: [10.1016/j.ijsu.2015.03.002](#)]
- 9 **Hamfjord J**, Guren TK, Dajani O, Johansen JS, Glimelius B, Sorbye H, Pfeiffer P, Lingjærde OC, Tveit KM, Kure EH, Pallisgaard N, Spindler KG. Total circulating cell-free DNA as a prognostic biomarker in metastatic colorectal cancer before first-line oxaliplatin-based chemotherapy. *Ann Oncol* 2019; **30**: 1088-1095 [PMID: [31046124](#) DOI: [10.1093/annonc/mdz139](#)]
- 10 **Desmond BJ**, Dennett ER, Danielson KM. Circulating Extracellular Vesicle MicroRNA as Diagnostic Biomarkers in Early Colorectal Cancer-A Review. *Cancers* **12**: 52 [PMID: [31878015](#) DOI: [10.3390/cancers12010052](#)]
- 11 **Yang C**, Zou K, Zheng L, Xiong B. Prognostic and clinicopathological significance of circulating tumor cells detected by RT-PCR in non-metastatic colorectal cancer: a meta-analysis and systematic review. *BMC Cancer* 2017; **17**: 725 [PMID: [29115932](#) DOI: [10.1186/s12885-017-3704-8](#)]
- 12 **Negin BP**, Cohen SJ. Circulating tumor cells in colorectal cancer: past, present, and future challenges. *Curr Treat Options Oncol* 2010; **11**: 1-13 [PMID: [20143276](#) DOI: [10.1007/s11864-010-0115-3](#)]
- 13 **Edwards HG**, Newton EM, Wynn-Williams DD, Lewis-Smith RL. Non-destructive analysis of pigments and other organic compounds in lichens using Fourier-transform Raman spectroscopy: a study of Antarctic epilithic lichens. *Spectrochim Acta A Mol Biomol Spectrosc* 2003; **59**: 2301-2309 [PMID: [12909143](#) DOI: [10.1016/s1386-1425\(03\)00073-8](#)]
- 14 **Lin D**, Feng S, Pan J, Chen Y, Lin J, Chen G, Xie S, Zeng H, Chen R. Colorectal cancer detection by gold nanoparticle based surface-enhanced Raman spectroscopy of blood serum and statistical analysis. *Opt Express* 2011; **19**: 13565-13577 [PMID: [21747512](#) DOI: [10.1364/OE.19.013565](#)]
- 15 **Chen Y**, Chen G, Zheng X, He C, Feng S, Chen Y, Lin X, Chen R, Zeng H. Discrimination of gastric cancer from normal by serum RNA based on surface-enhanced Raman spectroscopy (SERS) and multivariate analysis. *Med Phys* 2012; **39**: 5664-5668 [PMID: [22957632](#) DOI: [10.1118/1.4747269](#)]
- 16 **Li X**, Yang T, Li S, Wang D, Guan D. Detecting Esophageal Cancer Using Surface-Enhanced Raman Spectroscopy (SERS) of Serum Coupled with Hierarchical Cluster Analysis and Principal Component Analysis. *Appl Spectrosc* 2015; **69**: 1334-1341 [PMID: [26647057](#) DOI: [10.1366/14-07829](#)]
- 17 **Wang G**, Lipert RJ, Jain M, Kaur S, Chakraborty S, Torres MP, Batra SK, Brand RE, Porter MD. Detection of the potential pancreatic cancer marker MUC4 in serum using surface-enhanced Raman scattering. *Anal Chem* 2011; **83**: 2554-2561 [PMID: [21391573](#) DOI: [10.1021/ac102829b](#)]
- 18 **Zhang K**, Liu X, Man B, Yang C, Zhang C, Liu M, Zhang Y, Liu L, Chen C. Label-free and stable serum analysis based on Ag-NPs/PSi surface-enhanced Raman scattering for noninvasive lung cancer detection. *Biomed Opt Express* 2018; **9**: 4345-4358 [PMID: [30615731](#) DOI: [10.1364/BOE.9.004345](#)]
- 19 **Vargas-Obieta E**, Martínez-Espinosa JC, Martínez-Zerega BE, Jave-Suárez LF, Aguilar-Lemarroy A, González-Solís JL. Breast cancer detection based on serum sample surface enhanced Raman spectroscopy. *Lasers Med Sci* 2016; **31**: 1317-1324 [PMID: [27289243](#) DOI: [10.1007/s10103-016-1976-x](#)]
- 20 **Chen N**, Rong M, Shao X, Zhang H, Liu S, Dong B, Xue W, Wang T, Li T, Pan J. Surface-enhanced Raman spectroscopy of serum accurately detects prostate cancer in patients with prostate-specific antigen levels of 4-10 ng/mL. *Int J Nanomedicine* 2017; **12**: 5399-5407 [PMID: [28794631](#) DOI: [10.2147/IJN.S137756](#)]
- 21 **Shao X**, Pan J, Wang Y, Zhu Y, Xu F, Shanguan X, Dong B, Sha J, Chen N, Chen Z, Wang T, Liu S, Xue W. Evaluation of expressed prostatic secretion and serum using surface-enhanced Raman spectroscopy for the noninvasive detection of prostate cancer, a preliminary study. *Nanomedicine* 2017; **13**: 1051-1059 [PMID: [27979746](#) DOI: [10.1016/j.nano.2016.12.001](#)]
- 22 **Li S**, Li L, Zeng Q, Zhang Y, Guo Z, Liu Z, Jin M, Su C, Lin L, Xu J, Liu S. Characterization and noninvasive diagnosis of bladder cancer with serum surface enhanced Raman spectroscopy and genetic algorithms. *Sci Rep* 2015; **5**: 9582 [PMID: [25947114](#) DOI: [10.1038/srep09582](#)]
- 23 **Ito H**, Inoue H, Hasegawa K, Hasegawa Y, Shimizu T, Kimura S, Onimaru M, Ikeda H, Kudo SE. Use of surface-enhanced Raman scattering for detection of cancer-related serum-constituents in gastrointestinal cancer patients. *Nanomedicine* 2014; **10**: 599-608 [PMID: [24103303](#) DOI: [10.1016/j.nano.2013.09.006](#)]
- 24 **Ito H**, Hasegawa K, Hasegawa Y, Nishimaki T, Hosomichi K, Kimura S, Ohba M, Yao H, Onimaru M, Inoue I, Inoue H. Silver Nanoscale Hexagonal Column Chips for Detecting Cell-free DNA and Circulating Nucleosomes in Cancer Patients. *Sci Rep* 2015; **5**: 10455 [PMID: [25994878](#) DOI: [10.1038/srep10455](#)]



- 25 Ito H, Uragami N, Miyazaki T, Yokoyama N, Inoue H. Raman spectroscopic evaluation of human serum using metal plate and 785- and 1064-nm excitation lasers. *PLoS One* 2019; **14**: e0211986 [PMID: 30768643 DOI: 10.1371/journal.pone.0211986]
- 26 Sajjan D, Binoy J, Pradeep B, Venkata Krishna K, Kartha VB, Hubert Joe I, Jayakumar VS. NIR-FT Raman and infrared spectra and ab initio computations of glycinium oxalate. *Spectrochim Acta A Mol Biomol Spectrosc* 2004; **60**: 173-180 [PMID: 14670475 DOI: 10.1016/s1386-1425(03)00193-8]
- 27 Notingher I, Green C, Dyer C, Perkins E, Hopkins N, Lindsay C, Hench LL. Discrimination between ricin and sulphur mustard toxicity in vitro using Raman spectroscopy. *J R Soc Interface* 2004; **1**: 79-90 [PMID: 16849154 DOI: 10.1098/rsif.2004.0008]
- 28 Shetty G, Kendall C, Shepherd N, Stone N, Barr H. Raman spectroscopy: elucidation of biochemical changes in carcinogenesis of oesophagus. *Br J Cancer* 2006; **94**: 1460-1464 [PMID: 16622450 DOI: 10.1038/sj.bjc.6603102]
- 29 Farquharson S, Gift A, Shende C, Inscore F, Ordway B, Farquharson C, Murren J. Surface-enhanced Raman spectral measurements of 5-fluorouracil in saliva. *Molecules* 2008; **13**: 2608-2627 [PMID: 18946423 DOI: 10.3390/molecules13102608]
- 30 Chan JW, Taylor DS, Zwerdling T, Lane SM, Ihara K, Huser T. Micro-Raman spectroscopy detects individual neoplastic and normal hematopoietic cells. *Biophys J* 2006; **90**: 648-656 [PMID: 16239327 DOI: 10.1529/biophysj.105.066761]
- 31 Malini R, Venkatakrishna K, Kurien J, Pai KM, Rao L, Kartha VB, Krishna CM. Discrimination of normal, inflammatory, premalignant, and malignant oral tissue: a Raman spectroscopy study. *Biopolymers* 2006; **81**: 179-193 [PMID: 16231284 DOI: 10.1002/bip.20398]
- 32 Stone N, Kendall C, Smith J, Crow P, Barr H. Raman spectroscopy for identification of epithelial cancers. *Faraday Discuss* 2004; **126**: 141-157 [PMID: 14992404 DOI: 10.1039/b304992b]
- 33 Ruiz-Chica AJ, Medina MA, Sánchez-Jiménez F, Ramírez FJ. Characterization by Raman spectroscopy of conformational changes on guanine-cytosine and adenine-thymine oligonucleotides induced by aminoxy analogues of spermidine. *J Raman Spectrosc* 2004; **35**: 93-100 [DOI: 10.1002/jrs.1107]
- 34 De Gelder J, De Gussem K, Vandenabeele P, Moens L. Reference database of Raman spectra of biological molecules. *J Raman Spectrosc* 2007; **38**: 1133-1147 [DOI: 10.1002/jrs.1734]
- 35 Nijssen A, Bakker Schut TC, Heule F, Caspers PJ, Hayes DP, Neumann MH, Puppels GJ. Discriminating basal cell carcinoma from its surrounding tissue by Raman spectroscopy. *J Invest Dermatol* 2002; **119**: 64-69 [PMID: 12164926 DOI: 10.1046/j.1523-1747.2002.01807.x]
- 36 Cheng WT, Liu MT, Liu HN, Lin SY. Micro-Raman spectroscopy used to identify and grade human skin pilomatrixoma. *Microsc Res Tech* 2005; **68**: 75-79 [PMID: 16228983 DOI: 10.1002/jemt.20229]
- 37 Jyothi Lakshmi R, Kartha VB, Murali Krishna C, R Solomon JG, Ullas G, Uma Devi P. Tissue Raman spectroscopy for the study of radiation damage: brain irradiation of mice. *Radiat Res* 2002; **157**: 175-182 [PMID: 11835681 DOI: 10.1667/0033-7587(2002)157]
- 38 Huang Z, McWilliams A, Lui H, McLean DI, Lam S, Zeng H. Near-infrared Raman spectroscopy for optical diagnosis of lung cancer. *Int J Cancer* 2003; **107**: 1047-1052 [PMID: 14601068 DOI: 10.1002/ijc.11500]
- 39 Krafft C, Neudert L, Simat T, Salzer R. Near infrared Raman spectra of human brain lipids. *Spectrochim Acta A Mol Biomol Spectrosc* 2005; **61**: 1529-1535 [PMID: 15820887 DOI: 10.1016/j.saa.2004.11.017]
- 40 Koljenović S, Schut TB, Vincent A, Kros JM, Puppels GJ. Detection of meningioma in dura mater by Raman spectroscopy. *Anal Chem* 2005; **77**: 7958-7965 [PMID: 16351143 DOI: 10.1021/ac0512599]
- 41 Patil CA, Kalkman J, Faber DJ, Nyman JS, van Leeuwen TG, Mahadevan-Jansen A. Integrated system for combined Raman spectroscopy-spectral domain optical coherence tomography. *J Biomed Opt* 2011; **16**: 011007 [PMID: 21280894 DOI: 10.1117/1.3520132]
- 42 Hastie T, Tibshirani R, Friedman J. The elements of statistical learning: data mining, inference, and prediction. 2nd ed. Berlin: Springer Science+Business Media, 2009: 1-745
- 43 Ó Faoláin E, Hunter MB, Byrne JM, Kelehan P, McNamara M, Byrne HJ, Lyng FM. A study examining the effects of tissue processing on human tissue sections using vibrational spectroscopy. *Vib Spectrosc* 2005; **38**: 121-127 [DOI: 10.1016/j.vibspec.2005.02.013]
- 44 Short MA, Lui H, McLean D, Zeng H, Alajlan A, Chen XK. Changes in nuclei and peritumoral collagen within nodular basal cell carcinomas via confocal micro-Raman spectroscopy. *J Biomed Opt* 2006; **11**: 34004 [PMID: 16822054 DOI: 10.1117/1.2209549]
- 45 Lau DP, Huang Z, Lui H, Anderson DW, Berean K, Morrison MD, Shen L, Zeng H. Raman spectroscopy for optical diagnosis in the larynx: preliminary findings. *Lasers Surg Med* 2005; **37**: 192-200 [PMID: 16127671 DOI: 10.1002/Lsm.20226]
- 46 Gardiner DJ, Graves PR. Practical Raman spectroscopy. Berlin: Springer, 1989: 1-154
- 47 Huang Z, Lui H, McLean DI, Korbelik M, Zeng H. Raman spectroscopy in combination with background near-infrared autofluorescence enhances the in vivo assessment of malignant tissues. *Photochem Photobiol* 2005; **81**: 1219-1226 [PMID: 15869327 DOI: 10.1562/2005-02-24-RA-449]
- 48 Xue L, Yan B, Li Y, Tan Y, Luo X, Wang M. Surface-enhanced Raman spectroscopy of blood serum based on gold nanoparticles for tumor stages detection and histologic grades classification of oral squamous cell carcinoma. *Int J Nanomedicine* 2018; **13**: 4977-4986 [PMID: 30214201 DOI: 10.2147/IJN.S167996]
- 49 Tan Y, Yan B, Xue L, Li Y, Luo X, Ji P. Surface-enhanced Raman spectroscopy of blood serum based on gold nanoparticles for the diagnosis of the oral squamous cell carcinoma. *Lipids Health Dis* 2017; **16**: 73 [PMID: 28388900 DOI: 10.1186/s12944-017-0465-y]
- 50 Xiao R, Zhang X, Rong Z, Xiu B, Yang X, Wang C, Hao W, Zhang Q, Liu Z, Duan C, Zhao K, Guo X, Fan Y, Zhao Y, Johnson H, Huang Y, Feng X, Xu X, Zhang H, Wang S. Non-invasive detection of hepatocellular carcinoma serum metabolic profile through surface-enhanced Raman spectroscopy. *Nanomedicine* 2016; **12**: 2475-2484 [PMID: 27520725 DOI: 10.1016/j.nano.2016.07.014]
- 51 Hong Y, Li Y, Huang L, He W, Wang S, Wang C, Zhou G, Chen Y, Zhou X, Huang Y, Huang W, Gong T, Zhou Z. Label-free diagnosis for colorectal cancer through coffee ring-assisted surface-enhanced Raman spectroscopy on blood serum. *J Biophotonics* 2020; **13**: e201960176 [PMID: 31909563 DOI: 10.1002/jbph.202000176]

- 10.1002/jbio.201960176]
- 52 **Feng S**, Wang W, Tai IT, Chen G, Chen R, Zeng H. Label-free surface-enhanced Raman spectroscopy for detection of colorectal cancer and precursor lesions using blood plasma. *Biomed Opt Express* 2015; **6**: 3494-3502 [PMID: [26417518](#) DOI: [10.1364/BOE.6.003494](#)]
- 53 **Wang J**, Lin D, Lin J, Yu Y, Huang Z, Chen Y, Lin J, Feng S, Li B, Liu N, Chen R. Label-free detection of serum proteins using surface-enhanced Raman spectroscopy for colorectal cancer screening. *J Biomed Opt* 2014; **19**: 087003 [PMID: [25138208](#) DOI: [10.1117/1.JBO.19.8.087003](#)]
- 54 **Chen Y**, Chen G, Feng S, Pan J, Zheng X, Su Y, Chen Y, Huang Z, Lin X, Lan F, Chen R, Zeng H. Label-free serum ribonucleic acid analysis for colorectal cancer detection by surface-enhanced Raman spectroscopy and multivariate analysis. *J Biomed Opt* 2012; **17**: 067003 [PMID: [22734781](#) DOI: [10.1117/1.JBO.17.6.067003](#)]
- 55 **Hill MJ**, Morson BC, Bussey HJ. Aetiology of adenoma--carcinoma sequence in large bowel. *Lancet* 1978; **1**: 245-247 [PMID: [74668](#) DOI: [10.1016/s0140-6736\(78\)90487-7](#)]
- 56 **Prasetyanti PR**, Zimmerlin CD, Bots M, Vermeulen L, Melo Fde S, Medema JP. Regulation of stem cell self-renewal and differentiation by Wnt and Notch are conserved throughout the adenoma-carcinoma sequence in the colon. *Mol Cancer* 2013; **12**: 126 [PMID: [24144042](#) DOI: [10.1186/1476-4598-12-126](#)]
- 57 **Murakami T**, Mitomi H, Saito T, Takahashi M, Sakamoto N, Fukui N, Yao T, Watanabe S. Distinct WNT/ $\beta$ -catenin signaling activation in the serrated neoplasia pathway and the adenoma-carcinoma sequence of the colorectum. *Mod Pathol* 2015; **28**: 146-158 [PMID: [24925057](#) DOI: [10.1038/modpathol.2014.41](#)]
- 58 **Mohammadi M**, Kristensen MH, Nielsen HJ, Bonde JH, Holck S. Qualities of sessile serrated adenoma/polyp/lesion and its borderline variant in the context of synchronous colorectal carcinoma. *J Clin Pathol* 2012; **65**: 924-927 [PMID: [22782936](#) DOI: [10.1136/jclinpath-2012-200803](#)]

## Retrospective Study

# Subtotal gastrectomy combined with chemotherapy: An effective therapy for patients with circumscribed Borrmann type IV gastric cancer

Hai-Bo Huang, Zi-Ming Gao, An-Qi Sun, Wei-Tian Liang, Kai Li

**ORCID number:** Hai-Bo Huang 0000-0003-4268-8969; Zi-Ming Gao 0000-0002-8968-6015; An-Qi Sun 0000-0003-2756-8213; Wei-Tian Liang 0000-0002-5283-6411; Kai Li 0000-0002-1224-2088.

**Author contributions:** Huang HB and Li K designed the research; Gao ZM and Li K treated the patients and collected the material and clinical data from the patients; Huang HB and Sun AQ performed the assays; Liang WT and Huang HB analyzed the data; Huang HB wrote the paper.

**Institutional review board statement:** This study was reviewed and approved by the Ethics Committee of First Affiliated Hospital of China Medical University.

**Informed consent statement:** Written informed consent was obtained from each patient.

**Conflict-of-interest statement:** All authors declare no conflicts of interest.

**Data sharing statement:** No additional data are available.

**Open-Access:** This article is an open-access article that was

Hai-Bo Huang, Zi-Ming Gao, An-Qi Sun, Wei-Tian Liang, Kai Li, Department of Surgical Oncology and General Surgery, Key Laboratory of Precision Diagnosis and Treatment of Gastrointestinal Tumors, Ministry of Education, The First Affiliated Hospital of China Medical University, Shenyang 110001, Liaoning Province, China

**Corresponding author:** Kai Li, PhD, Professor, Department of Surgical Oncology and General Surgery, Key Laboratory of Precision Diagnosis and Treatment of Gastrointestinal Tumors, Ministry of Education, The First Affiliated Hospital of China Medical University, No. 155 Nanjing Street, Shenyang 110001, Liaoning Province, China. [cmu\\_likai@163.com](mailto:cmu_likai@163.com)

## Abstract

### BACKGROUND

Although Borrmann type IV (B-4) gastric cancer has a higher mortality rate and presents distant metastasis easily, especially peritoneal metastasis, when diagnosed, some B-4 patients were found to have no distant metastasis by preoperative detection and underwent curative surgery, which was defined as circumscribed B-4 in our study. In this study, we focused on the circumscribed B-4 patients without distant metastasis during surgery to identify factors related to prognosis and postoperative peritoneal cavity metastasis (PPCM), which is important for selecting an appropriate therapeutic strategy.

### AIM

To identify factors related to the prognosis and PPCM of B-4 patients.

### METHODS

A total of 117 B-4 patients who underwent gastrectomy between January 2005 and December 2012 were included in this study. Survival analysis was performed using Kaplan-Meier analysis and Cox multivariate models. Pearson correlation analyses were performed to identify the factors related to PPCM. All statistical analyses were performed using SPSS 20.0.

### RESULTS

Lymph node status, gastrectomy type, and postoperative chemotherapy were independent prognostic factors in 117 circumscribed B-4 patients. Subtotal gastrectomy combined with chemotherapy could significantly improve the long-term survival time. Six patients who were diagnosed with pN0 and received the

selected by an in-house editor and fully peer-reviewed by external reviewers. It is distributed in accordance with the Creative Commons Attribution NonCommercial (CC BY-NC 4.0) license, which permits others to distribute, remix, adapt, build upon this work non-commercially, and license their derivative works on different terms, provided the original work is properly cited and the use is non-commercial. See: <http://creativecommons.org/licenses/by-nc/4.0/>

**Manuscript source:** Unsolicited manuscript

**Specialty type:** Oncology

**Country/Territory of origin:** China

**Peer-review report's scientific quality classification**

Grade A (Excellent): 0  
Grade B (Very good): 0  
Grade C (Good): 0  
Grade D (Fair): 0  
Grade E (Poor): 0

**Received:** July 26, 2020

**Peer-review started:** July 26, 2020

**First decision:** August 9, 2020

**Revised:** August 20, 2020

**Accepted:** September 25, 2020

**Article in press:** September 25, 2020

**Published online:** November 15, 2020

**P-Reviewer:** Arigami T

**S-Editor:** Gao CC

**L-Editor:** Wang TQ

**P-Editor:** Li JH



combination therapy had a 3-year survival rate of 100% and a median survival of 77.7 mo. Even for patients with metastatic lymph nodes ( $n = 13$ ), the combination therapy also increased the 3-year overall survival rate to 57.1%. In addition, positive lymph node status was the only factor ( $P = 0.005$ ) correlated with PPCM in certain B-4 patients, and chemotherapy was useful for suppressing PPCM in patients with subtotal gastrectomy but not in those with total gastrectomy.

## CONCLUSION

Lymph node status is an independent prognostic factor for circumscribed B-4 patients. In addition, subtotal gastrectomy and postoperative chemotherapy could effectively improve prognosis and even suppress PPCM.

**Key Words:** Gastric cancer; Circumscribed; Borrmann type IV; Prognosis; Subtotal gastrectomy; Chemotherapy

©The Author(s) 2020. Published by Baishideng Publishing Group Inc. All rights reserved.

**Core Tip:** This is a retrospective study to evaluate the factors related to prognosis and prognostic postoperative peritoneal cavity metastasis for circumscribed Borrmann type IV (B-4) patients. We reported that lymph node metastatic status, gastrectomy type, and postoperative chemotherapy were the independent prognostic factors. Subtotal gastrectomy combined with chemotherapy could significantly improve the long-term survival time of circumscribed B-4 patients. And chemotherapy was also useful for suppressing postoperative peritoneal cavity metastasis in patients with subtotal gastrectomy. We believe that our study makes a significant contribution to the literature because it recommended reasonable treatment schedules for the B-4 patients, which can increase survival time to a certain extent.

**Citation:** Huang HB, Gao ZM, Sun AQ, Liang WT, Li K. Subtotal gastrectomy combined with chemotherapy: An effective therapy for patients with circumscribed Borrmann type IV gastric cancer. *World J Gastrointest Oncol* 2020; 12(11): 1325-1335

**URL:** <https://www.wjgnet.com/1948-5204/full/v12/i11/1325.htm>

**DOI:** <https://dx.doi.org/10.4251/wjgo.v12.i11.1325>

## INTRODUCTION

Gastric cancer (GC) is the fourth most common malignancy and the second most frequent cause of cancer-related death worldwide, with approximately 951600 new cases and 723100 deaths every year<sup>[1-3]</sup>. Borrmann type IV (B-4) GC, as an aggressive type of GC, accounts for approximately 10% of all GC cases in Asia<sup>[4,5]</sup>. B-4 lesions are characterized as lesions that diffusely infiltrate the gastric wall without ulceration or elevation. Compared with other types of GC, the occurrence rates of serosal invasion, positive lymph nodes, and distant metastasis in B-4 patients are higher.

Currently, surgery with chemotherapy is the major treatment method for advanced GC, which significantly improves the rate of long-term overall survival (OS). However, many B-4 patients are not suitable for surgical treatment at the time of diagnosis, and the 3-year OS rate of B-4 patients is only approximately 15%-20%<sup>[6-8]</sup>. Studies on the clinicopathology and prognosis of B-4 patients have had controversial findings<sup>[4,8-12]</sup>. Some B-4 patients were found to have no distant metastasis by preoperative detection and underwent curative surgery, which was defined as circumscribed B-4 in our study. Circumscribed B-4 accounts for relatively fewer cases of B-4 patients, and the clinicopathological characteristics and prognostic analysis of these patients would help us to understand the recurrence and metastasis of GC. There is no related research, especially for circumscribed B-4 patients.

In this study, we aimed to identify the factors related to prognosis and postoperative peritoneal cavity metastasis (PPCM) for circumscribed B-4 patients and to further explore the appropriate therapeutic strategies.

## MATERIALS AND METHODS

### **Patient selection**

A total of 1803 patients were diagnosed with GC and underwent gastrectomy at the First Affiliated Hospital of China Medical University from January 2005 to December 2012. Among them, 117 circumscribed B-4 patients were included in our analysis. The inclusion criteria for the patients were as follows: (1) B-4 gastric lesions and no distant metastasis were confirmed by preoperative detection and histopathology postoperatively; (2) Gastrectomy, including subtotal or total, was performed without neoadjuvant therapy; and (3) Detailed clinicopathological and follow-up data could be obtained for each patient. This study was approved by the Ethics Committee of China Medical University, and informed consent was obtained from the patients.

### **Data collection**

The following data were collected: Age, gender, tumor size, tumor location, radical degree (R0/R1), histological type (well/poor), tumor invasion depth (pT), lymph node status (pN), lymphatic vessel infiltration, subtotal/total gastrectomy, postoperative chemotherapy, PPCM, and overall survival time. Of these, highly or moderately differentiated adenocarcinoma was classified as the well differentiated histological type, while others were classified as the poorly differentiated histological type. Selection indication of chemotherapy for GC patients was based on the National Comprehensive Cancer Network (NCCN) Guidelines. The adjuvant chemotherapy regimen was FOLFOX6 in postoperative 6 mo, including 5-fluorouracil and platinum. Completion degree of chemotherapy was heterogeneous, with eight or less cycles. Follow-up was completed by December 2017, and stage was classified according to the 8<sup>th</sup> edition of the American Joint Committee on Cancer (AJCC) classification system.

### **Statistical analysis**

Continuous variables are expressed as the mean  $\pm$  standard deviation (SD), and categorical variables are expressed as frequencies. We performed multivariate analyses with the Cox proportional hazards model to identify independent prognostic factors. In addition, Kaplan-Meier analysis and the log-rank test were also used to evaluate the prognostic difference between groups. Pearson correlation analyses were performed for related factors of PPCM. The above statistical analyses were performed using SPSS 20.0, and  $P < 0.01$  was considered statistically significant.

## RESULTS

### **Baseline clinicopathological characteristics**

A total of 117 patients were diagnosed with circumscribed B-4 GC and finally included in our analyses. As shown in Table 1, the mean age of the patients was 57.55 years, and the mean diameter of tumors was 7.81 cm. According to TNM stage, there were 27 cases of stage II and 90 cases of stage III. Of these, 81 (69.2%) patients had stage pT4, and 65 (55.6%) had stage pN3. A total of 116 patients received D2 lymphadenectomy, and the other one underwent D2+ lymphadenectomy. None of the 117 patients had distant metastasis, and cytology result of peritoneal lavage fluid was negative in our study.

### **Results of univariate and multivariate prognostic analyses**

According to the Cox analysis, gastrectomy type ( $P = 0.003$ ), pN stage ( $P = 0.000$ ), and postoperative chemotherapy ( $P = 0.007$ ) were crucial for predicting the prognosis of these circumscribed B-4 patients (Table 2). As shown in Figure 1A, the prognosis of patients who underwent subtotal gastrectomy was better than that of patients who underwent total gastrectomy ( $P = 0.000$ ). After screening out patients with lower-middle lesions, the prognostic superiority of subtotal gastrectomy was consistent (Figure 1B). Notably, patients with a higher pN stage always had a worse prognosis (Figure 1C), but the prognostic value of pT stage was not significant (Figure 1D). In addition, as shown in Figure 1E, postoperative chemotherapy improved the long-term survival rate of circumscribed B-4 patients ( $P = 0.000$ ).

### **Role of postoperative chemotherapy in the circumscribed B-4 patient cohort**

The survival curves of chemotherapy for subtotal or total gastrectomy are shown in Figure 2A-B. We revealed that circumscribed B-4 patients who underwent subtotal



**Table 1** Main clinicopathological characteristics of patients with circumscribed Borrmann type IV gastric cancer

Variable	B-4 patients (n = 117)
Age (yr)	57.55 ± 10.69
Gender	
Male	75
Female	42
Diameter (cm)	7.81 ± 3.07
Tumor location	
Upper 1/3–1/2 (U or MU)	22
Lower 1/3–1/2 (M or L or ML)	59
Total (LAU or LMU)	36
Radical degree	
R0	45
R1+	72
Histological type	
Well	8
Poor	109
pT stage	
pT3	36
pT4	81
pN stage	
pN0	22
pN1	15
pN2	15
pN3	65
Venous/lymphatic infiltration	
Yes	74
No	43
Gastrectomy type	
Subtotal gastrectomy	26
Total gastrectomy	91
Adjuvant chemotherapy	
Yes	74
No	43

U: Upper; M: Middle; L: Lower; pT: Tumor invasion depth; pN: Lymph node status.

gastrectomy gained more benefit from postoperative chemotherapy ( $P = 0.003$ ) than those who underwent total gastrectomy ( $P = 0.04$ ). But therapeutic duration of chemotherapy was not the prognostic factor for circumscribed B-4. In addition, the efficacy of chemotherapy also seemed to be associated with patient age, and patients younger than 65 years had a better prognosis than the others (Figure 2C).

#### **Survival results of the 117 B-4 patients according to therapeutic strategy**

The prognostic results, including the median survival (MS) and 3-year OS rate, are shown in Figure 2. There was an obvious prognostic tendency of the different groups. For circumscribed B-4 patients with gastrectomy, postoperative chemotherapy could

**Table 2 Cox univariate and multivariate analyses of circumscribed Borrmann type IV patients**

Variable	Univariate analysis		Multivariate analysis	
	HR (95%CI)	P value	HR (95%CI)	P value
Age (yr)	1.012 (0.992-1.033)	0.226		
Gender	0.969 (0.638-1.470)	0.881		
Diameter (cm)	1.086 (1.013-1.164)	0.02		
Tumor location	1.206 (0.879-1.655)	0.246		
Radical degree	1.575 (0.687-3.612)	0.283		
Histological type	0.708 (0.310-1.620)	0.414		
pT stage	1.422 (1.021-1.982)	0.037		
pN stage	1.482 (1.224-1.794)	0.000	1.433 (1.179-1.742)	0.000
Venous/lymphatic infiltration	0.934 (0.615-1.418)	0.748		
Gastrectomy type	0.330 (0.182-0.595)	0.000	0.400 (0.219-0.728)	0.003
Postoperative chemotherapy	0.482 (0.320-0.727)	0.001	0.564 (0.373-0.853)	0.007

HR: Hazard ratio; CI: Confidence interval; pT: Tumor invasion depth; pN: Lymph node status.

significantly increase the MS time, regardless of lymph node metastasis. Notably, we revealed that circumscribed B-4 patients ( $n = 6$ ) who were diagnosed with pN0 and finally underwent subtotal gastrectomy and chemotherapy had a 3-year OS rate of 100% and a median survival of 77.7 mo. Even for patients with metastatic lymph nodes ( $n = 13$ ), combination therapy also increased the 3-year OS rate to 57.1% and the MS to 51.0 mo.

### **Analysis of circumscribed B-4 patients with PPCM**

Peritoneal metastasis is the most common type of GC metastasis. In our analysis, 79 (67.5%) patients were diagnosed with peritoneal cavity metastasis (PPCM) after gastrectomy, 11 (9.4%) had liver metastasis, and 5 (4.3%) had lung metastasis. We selected the other 22 patients without postoperative metastasis as a non-PPCM group. Positive pN stage was the only factor ( $P = 0.005$ ) correlated with PPCM in circumscribed B-4 patients by Pearson correlation analyses (Table 3). Notably, there was no difference in the PPCM rate between different pT stages (pT3 *vs* pT4). In addition, although chemotherapy did not seem to be associated with PPCM according to the results shown in Table 3, we further explored the association of chemotherapy and PPCM in different gastrectomy types. As shown in Table 4, postoperative chemotherapy was useful for suppressing PPCM in patients with subtotal gastrectomy ( $P = 0.018$ ) but not in those with total gastrectomy ( $P = 0.281$ ).

## **DISCUSSION**

In this study, we first defined B-4 patients without distant metastasis as circumscribed B-4 patients. By multivariate analysis, we revealed that subtotal/total gastrectomy, pN stage, and postoperative chemotherapy were independent prognostic factors for these patients. pN stage, but not pT stage, was crucial for predicting the prognosis of circumscribed B-4 patients. In a previous study, we suggested classifying B-4 patients into pT4b stage according to prognosis<sup>[4]</sup>. According to the statistical analysis, subtotal gastrectomy combined with chemotherapy can effectively improve the prognosis of circumscribed B-4. Even for the patients ( $n = 13$ ) with positive pN, the combination therapy also improved the 3-year OS rate to 57.1%.

Surgical resection remains the main therapeutic method for GC, but the role of curative resection in B-4 is controversial<sup>[10,13,14]</sup>. Luo *et al*<sup>[8]</sup> and Kim *et al*<sup>[10]</sup> reported that the 3- to 5-year OS of curative (R0) patients was higher than that of noncurative patients, but surgical curability was not an independent predictor of prognosis, particularly for B-4 patients. In addition, studies found that total gastrectomy had no advantages of long-term prognosis and led to nutritional deficiency and worse quality

**Table 3 Factors associated with postoperative peritoneal cavity metastasis in Borrmann type IV patients**

Variable	PPCM (79)	Non-PPCM (22)	Pearson <i>P</i> value
Tumor location			0.497
Upper 1/3–1/2 (U or MU)	13	4	
Lower 1/3–1/2 (M or L or ML)	41	13	
Total (LAU or LMU)	25	5	
Radical degree			0.107
R0	28	12	
R1+	51	10	
Gastrectomy type			0.112
Subtotal gastrectomy	13	7	
Total gastrectomy	66	15	
Venous/lymphatic infiltration			0.416
Yes	50	16	
No	29	6	
pT stage			0.559
pT3	23	5	
pT4	56	17	
pN stage			0.005 <sup>b</sup>
pN0	9	8	
pN1-3	70	14	
Chemotherapy			0.105
Yes	46	17	
No	33	5	

<sup>b</sup>*P* < 0.01. PPCM: Postoperative peritoneal cavity metastasis; U: Upper; M: Middle; L: Lower; pT: Tumor invasion depth; pN: Lymph node status.

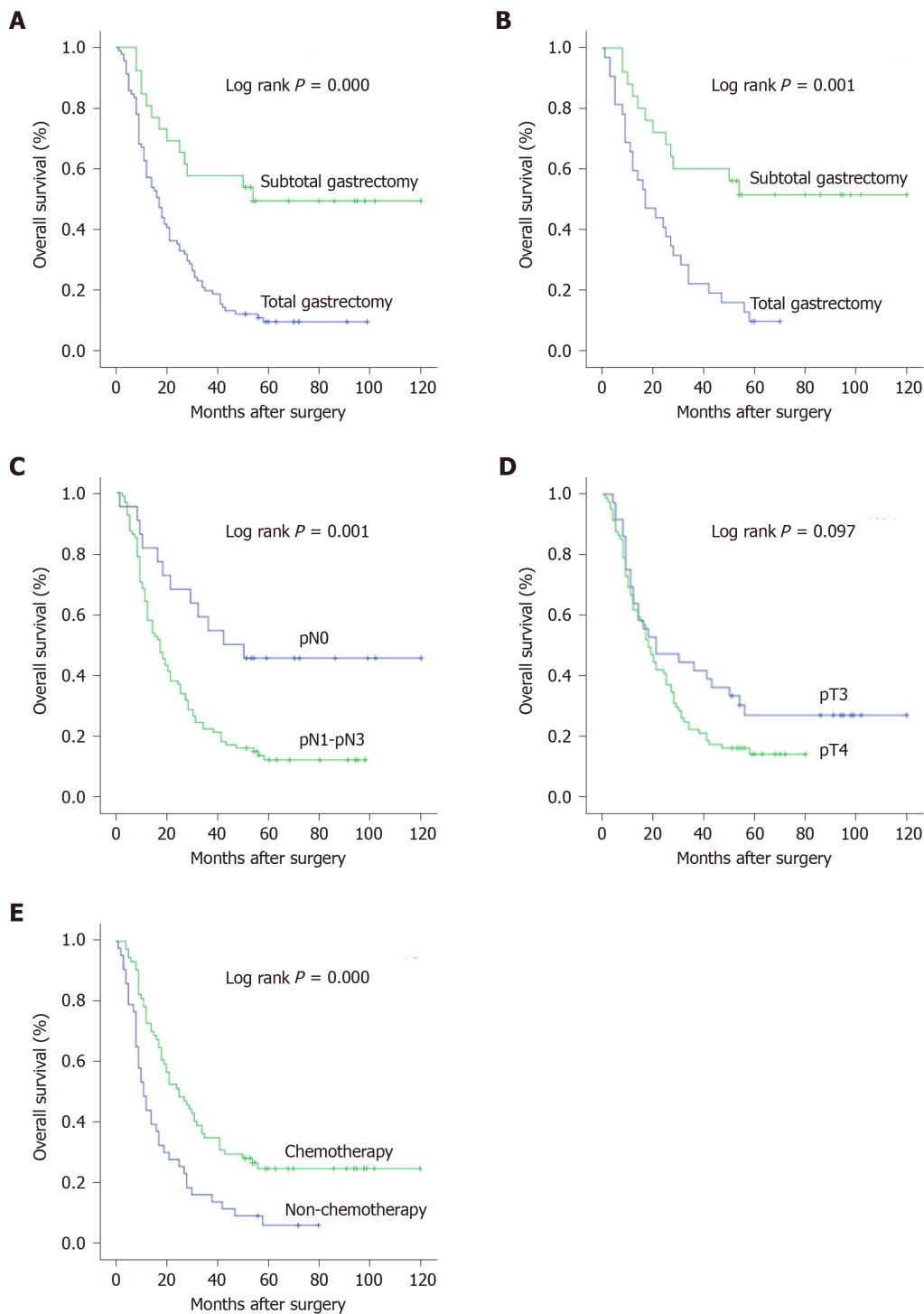
**Table 4 Role of chemotherapy in suppressing postoperative peritoneal cavity metastasis in patients who underwent different gastrectomy procedures**

Subtotal gastrectomy (20)			Total gastrectomy (81)		
	PPCM (13)	Non-PPCM (7)	PPCM (66)	Non-PPCM (15)	
Chemotherapy	4	6	45	8	0.018 <sup>a</sup>
Non-chemotherapy	9	1	21	7	0.281

<sup>a</sup>*P* < 0.05. PPCM: Postoperative peritoneal cavity metastasis.

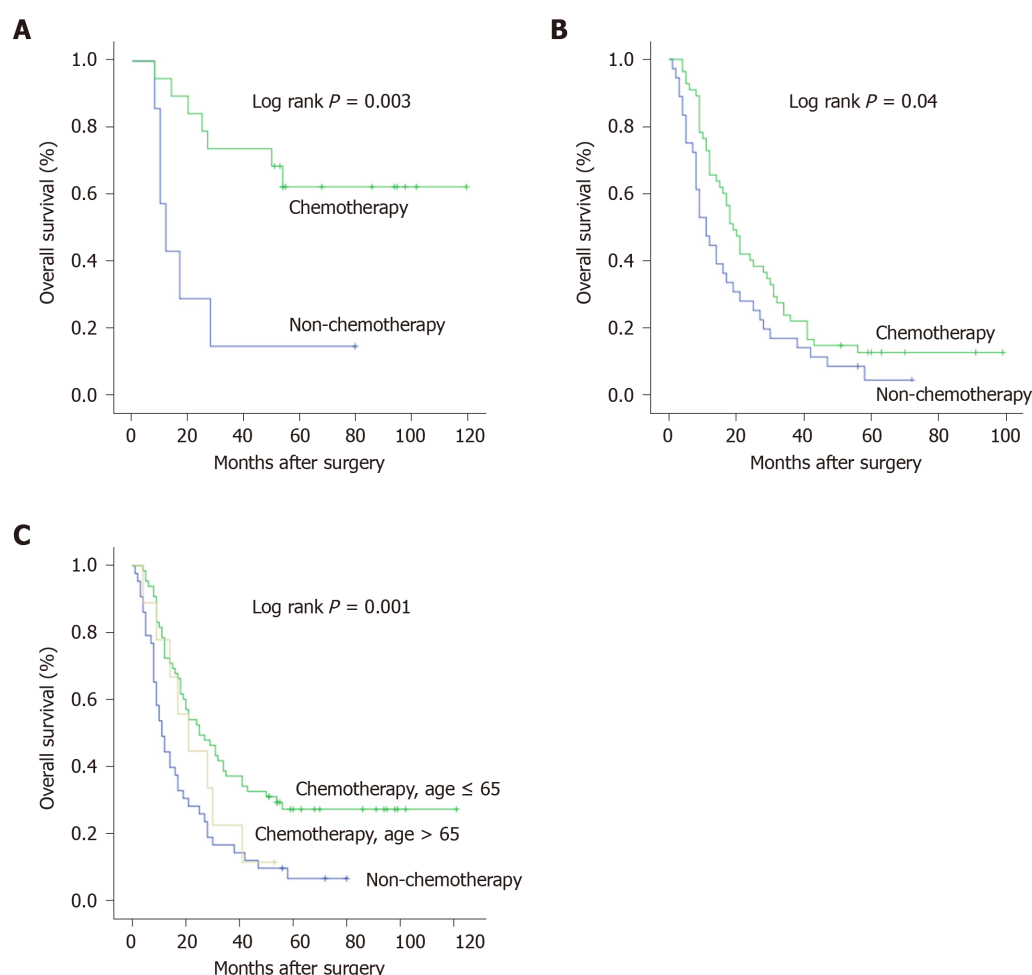
of life for advanced GC compared with subtotal gastrectomy<sup>[15-20]</sup>. In our analysis, we also found that no survival benefit existed in the R0 patients compared with the R1 patients, and subtotal gastrectomy could significantly improve the prognosis of circumscribed B-4 patients compared with total gastrectomy. The pathological features of B-4 GC suggested that the lesion invaded the whole layers of the gastric wall, and even if there was no venous or lymphatic infiltration, some micrometastases had occurred before macroscopic distant metastasis. Thus, it is difficult to restrict metastasis and improve survival by surgical resection. The results from circumscribed B-4 patients provided more evidence for this conclusion.

Considering the limited effect of surgery, adjuvant chemotherapy was also found to



**Figure 1** Survival curves of 117 patients according to the independent prognostic factors. A: Subtotal vs total gastrectomy; B: Subtotal vs total gastrectomy (lower-middle lesions); C: Lymph node status (pN stage); D: Tumor invasion depth (pT stage); E: Postoperative chemotherapy. pN: Lymph node status; pT: Tumor invasion depth.

be beneficial for survival in advanced GC. In a meta-analysis, 5-FU plus oxaliplatin (OXA) and 5-FU plus docetaxel (DOC) were recommended as postoperative chemotherapy regimens for advanced GC according to the efficacy<sup>[21]</sup>. In this study, chemotherapy, including 5-FU and platinum, significantly improved the prognosis of local B-4, serving as one of the independent factors, even for patients who were older than 65 years. Notably, as shown in [Supplementary Table 1](#), significant differences in age and pT stage existed between the chemotherapy and nonchemotherapy groups ( $P < 0.01$ ). Thus, we revealed that elderly patients with advanced GC stage seem to have a lower tendency to receive postoperative chemotherapy in the clinic, which should be rectified according to our conclusions. In addition, studies found that although S-1 or S-1/cisplatin might have positive effects against B-4, the prognostic role of



**Figure 2** Survival curves of chemotherapy for different Borrmann type IV patients. A: Patients with subtotal gastrectomy; B: Patients with total gastrectomy; C: Patients of different ages.

neoadjuvant chemotherapy did not reach the expected survival rate, with a median survival of only 17.3 mo and a 3-year OS rate of 24.5%<sup>[22-24]</sup>. Therefore, neoadjuvant chemotherapy was not included and analyzed in our study.

Above all, as shown in Figure 2, the survival time and OS rates of the two groups were significantly different, and there was an obvious tendency. Subtotal gastrectomy with chemotherapy improved the median survival of negative and positive pN patients to 77.7 mo and 51.0 mo, respectively. Thus, for advanced GC patients, after confirmation as circumscribed B-4, we recommend striving for subtotal gastrectomy and performing postoperative chemotherapy, especially for the lower 1/3-1/2 lesions, regardless of whether the patient has lymph node metastases.

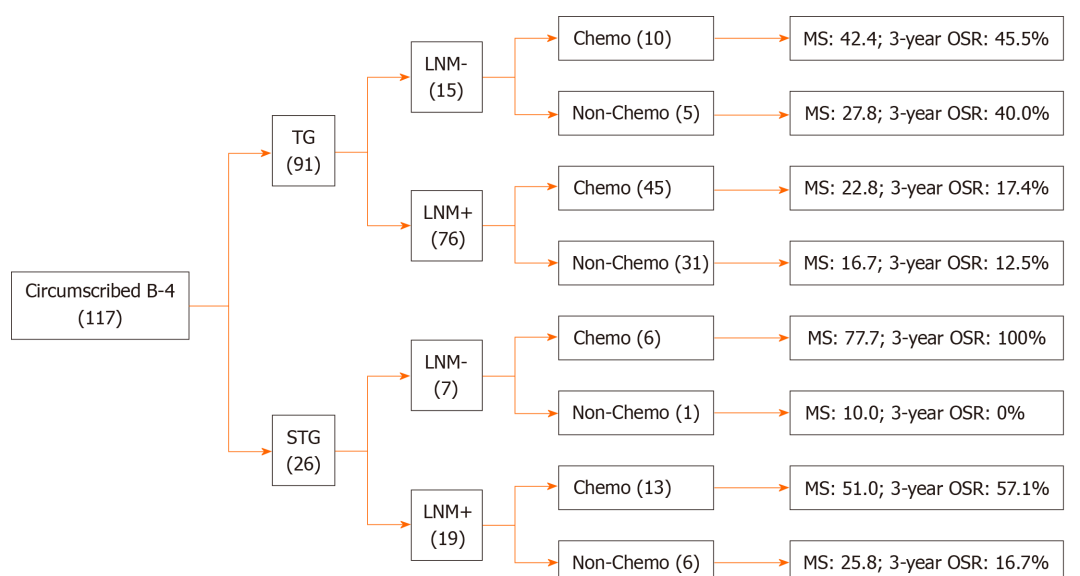
Additionally, our results showed that positive pN was correlated with the occurrence of PPCM in circumscribed B-4 patients, which indicated that lymph node metastasis was an important course for peritoneal metastasis. Some newly developed methods like endoscopic ultrasound guided fine needle aspiration may provide cytological confirmation for lymph node and other metastases<sup>[25-27]</sup>. Of course, serosal invasion and the shedding of cancer cells are also important routes for peritoneal metastasis.

There were also some limitations in our study. First, this is a retrospective, single-center and small-sample study, which reduced the significance of our study. For example, only one patient was divided in a group, as shown in Figure 3. Second, no data of neoadjuvant or targeted therapy were referred to in our study. Thus, a prospective study on a larger scale is necessary in the future.

## CONCLUSION

Lymph node metastasis is an independent risk factor for poor prognosis in





**Figure 3** Mean survival and 3-yr overall survival rates of different groups of 117 patients according to Cox multivariate analysis. TG: Total gastrectomy; STG: Subtotal gastrectomy; LNM: Lymph node metastasis; Chemo: Chemotherapy; MS: Median survival (mo); OSR: Overall survival rate.

circumscribed B-4 patients. Subtotal gastrectomy combined with postoperative chemotherapy could significantly improve the long-term OS rate and median survival time for circumscribed B-4 patients.

## ARTICLE HIGHLIGHTS

### Research background

Borrmann type IV (B-4) gastric cancer (GC) accounts for about 10% of all GC cases in Asia. Some B-4 patients were found to have no distant metastasis by preoperative detection and underwent curative surgery, which was defined as circumscribed B-4 in our study.

### Research motivation

Research of clinicopathological characteristics and prognosis in B-4 is rare, especially for the circumscribed B-4 patients.

### Research objectives

In this study, we aimed to identify the factors related to prognosis and postoperative peritoneal cavity metastasis (PPCM) for circumscribed B-4 patients and to further explore the appropriate therapeutic strategies.

### Research methods

A total of 117 circumscribed B-4 patients were included in this study. Survival analysis and Pearson correlation analyses were performed to identify the factors related to prognosis.

### Research results

Subtotal gastrectomy combined with chemotherapy could significantly improve the long-term survival time for circumscribed B-4. Positive lymph node status was the only factor correlated with PPCM, and chemotherapy was useful for suppressing PPCM in patients with subtotal gastrectomy but not in those with total gastrectomy.

### Research conclusions

Lymph node status is an independent prognostic factor for circumscribed B-4 patients. Subtotal gastrectomy and chemotherapy could effectively improve prognosis and suppress PPCM.

**Research perspectives**

This study recommended reasonable treatment schedules for circumscribed B-4 patients, but a multi-center study on a larger scale is necessary in the future.

**REFERENCES**

- 1 **Torre LA**, Bray F, Siegel RL, Ferlay J, Lortet-Tieulent J, Jemal A. Global cancer statistics, 2012. *CA Cancer J Clin* 2015; **65**: 87-108 [PMID: [25651787](#) DOI: [10.3322/caac.21262](#)]
- 2 **Ferro A**, Peleteiro B, Malvezzi M, Bosetti C, Bertuccio P, Levi F, Negri E, La Vecchia C, Lunet N. Worldwide trends in gastric cancer mortality (1980-2011), with predictions to 2015, and incidence by subtype. *Eur J Cancer* 2014; **50**: 1330-1344 [PMID: [24650579](#) DOI: [10.1016/j.ejca.2014.01.029](#)]
- 3 **Sak K**. A Hypothetical Approach on Gender Differences in Cancer Diagnosis. *J Transl Int Med* 2019; **7**: 90-92 [PMID: [31637178](#) DOI: [10.2478/jtim-2019-0020](#)]
- 4 **Huang JY**, Wang ZN, Lu CY, Miao ZF, Zhu Z, Song YX, Xu HM, Xu YY. Borrmann type IV gastric cancer should be classified as pT4b disease. *J Surg Res* 2016; **203**: 258-267 [PMID: [27363630](#) DOI: [10.1016/j.jss.2016.04.026](#)]
- 5 **An JY**, Kang TH, Choi MG, Noh JH, Sohn TS, Kim S. Borrmann type IV: an independent prognostic factor for survival in gastric cancer. *J Gastrointest Surg* 2008; **12**: 1364-1369 [PMID: [18516653](#) DOI: [10.1007/s11605-008-0516-9](#)]
- 6 **Dong RZ**, Guo JM, Zhang ZW, Zhou YM, Su Y. Prognostic impact and implications of extracapsular lymph node spread in Borrmann type IV gastric cancer. *Oncotarget* 2017; **8**: 97593-97601 [PMID: [29228635](#) DOI: [10.18632/oncotarget.18400](#)]
- 7 **Li C**, Oh SJ, Kim S, Hyung WJ, Yan M, Zhu ZG, Noh SH. Macroscopic Borrmann type as a simple prognostic indicator in patients with advanced gastric cancer. *Oncology* 2009; **77**: 197-204 [PMID: [19729977](#) DOI: [10.1159/000236018](#)]
- 8 **Luo Y**, Gao P, Song Y, Sun J, Huang X, Zhao J, Ma B, Li Y, Wang Z. Clinicopathologic characteristics and prognosis of Borrmann type IV gastric cancer: a meta-analysis. *World J Surg Oncol* 2016; **14**: 49 [PMID: [26912240](#) DOI: [10.1186/s12957-016-0805-9](#)]
- 9 **Zhu YL**, Yang L, Sui ZQ, Liu L, Du JF. Clinicopathological features and prognosis of Borrmann type IV gastric cancer. *J BUON* 2016; **21**: 1471-1475 [PMID: [28039710](#)]
- 10 **Kim EY**, Yoo HM, Song KY, Park CH. Limited significance of curative surgery in Borrmann type IV gastric cancer. *Med Oncol* 2016; **33**: 69 [PMID: [27251378](#) DOI: [10.1007/s12032-016-0783-3](#)]
- 11 **Yook JH**, Oh ST, Kim BS. Clinicopathological analysis of Borrmann type IV gastric cancer. *Cancer Res Treat* 2005; **37**: 87-91 [PMID: [19956485](#) DOI: [10.4143/crt.2005.37.2.87](#)]
- 12 **Kim DY**, Kim HR, Kim YJ, Kim S. Clinicopathological features of patients with Borrmann type IV gastric carcinoma. *ANZ J Surg* 2002; **72**: 739-742 [PMID: [12534387](#) DOI: [10.1046/j.1445-2197.2002.02523.x](#)]
- 13 **Yoshikawa T**, Tsuburaya A, Kobayashi O, Sairenji M, Motohashi H, Noguchi Y. Should scirrhus gastric carcinoma be treated surgically? *Hepatogastroenterology* 2001; **48**: 1509-1512 [PMID: [11677997](#)]
- 14 **Pedrazzani C**, Marrelli D, Pacelli F, Di Cosmo M, Mura G, Bettarini F, Rosa F, de Manzoni G, Roviello F. Gastric linitis plastica: which role for surgical resection? *Gastric Cancer* 2012; **15**: 56-60 [PMID: [21717092](#) DOI: [10.1007/s10120-011-0063-z](#)]
- 15 **Jang YJ**, Park MS, Kim JH, Park SS, Park SH, Kim SJ, Kim CS, Mok YJ. Advanced gastric cancer in the middle one-third of the stomach: Should surgeons perform total gastrectomy? *J Surg Oncol* 2010; **101**: 451-456 [PMID: [19924722](#) DOI: [10.1002/jso.21431](#)]
- 16 **Sugoor P**, Shah S, Dusane R, Desouza A, Goel M, Shrikhande SV. Proximal gastrectomy versus total gastrectomy for proximal third gastric cancer: total gastrectomy is not always necessary. *Langenbecks Arch Surg* 2016; **401**: 687-697 [PMID: [27143021](#) DOI: [10.1007/s00423-016-1422-3](#)]
- 17 **Bozzetti F**. Total versus subtotal gastrectomy in cancer of the distal stomach: facts and fantasy. *Eur J Surg Oncol* 1992; **18**: 572-579 [PMID: [1478289](#)]
- 18 **Liu Z**, Feng F, Guo M, Liu S, Zheng G, Xu G, Lian X, Fan D, Zhang H. Distal gastrectomy versus total gastrectomy for distal gastric cancer. *Medicine (Baltimore)* 2017; **96**: e6003 [PMID: [28151896](#) DOI: [10.1097/MD.0000000000006003](#)]
- 19 **Jentschura D**, Winkler M, Strohmeier N, Rumstadt B, Hagmüller E. Quality-of-life after curative surgery for gastric cancer: a comparison between total gastrectomy and subtotal gastric resection. *Hepatogastroenterology* 1997; **44**: 1137-1142 [PMID: [9261613](#)]
- 20 **Davies J**, Johnston D, Sue-Ling H, Young S, May J, Griffith J, Miller G, Martin I. Total or subtotal gastrectomy for gastric carcinoma? *World J Surg* 1998; **22**: 1048-1055 [PMID: [9747165](#) DOI: [10.1007/s002689900515](#)]
- 21 **Sun J**, Ren Z, Sun X, Hou H, Li K, Ge Q. Efficacy and safety comparison of chemotherapies for advanced gastric cancer: A network meta-analysis. *Oncotarget* 2017; **8**: 39673-39682 [PMID: [28562333](#) DOI: [10.18632/oncotarget.17784](#)]
- 22 **Kinoshita T**, Sasako M, Sano T, Katai H, Furukawa H, Tsuburaya A, Miyashiro I, Kaji M, Ninomiya M. Phase II trial of S-1 for neoadjuvant chemotherapy against scirrhus gastric cancer (JCOG 0002). *Gastric Cancer* 2009; **12**: 37-42 [PMID: [19390930](#) DOI: [10.1007/s10120-008-0496-1](#)]
- 23 **Iwasaki Y**, Sasako M, Yamamoto S, Nakamura K, Sano T, Katai H, Tsujinaka T, Nashimoto A, Fukushima N, Tsuburaya A; Gastric Cancer Surgical Study Group of Japan Clinical Oncology Group. Phase II study of preoperative chemotherapy with S-1 and cisplatin followed by gastrectomy for clinically resectable type 4 and large type 3 gastric cancers (JCOG0210). *J Surg Oncol* 2013; **107**: 741-745 [PMID: [23400787](#) DOI: [10.1002/jso.23301](#)]
- 24 **Mohri J**, Katada C, Ueda M, Sugawara M, Yamashita K, Moriya H, Komori S, Hayakawa K, Koizumi W, Atsuda K. Predisposing Factors for Chemotherapy-induced Nephrotoxicity in Patients with Advanced

- Esophageal Cancer Who Received Combination Chemotherapy with Docetaxel, Cisplatin, and 5-fluorouracil. *J Transl Int Med* 2018; **6**: 32-37 [PMID: [29607302](#) DOI: [10.2478/jtim-2018-0007](#)]
- 25 **Uberoi AS**, Bhutani MS. Has the role of EUS in rectal cancer staging changed in the last decade? *Endosc Ultrasound* 2018; **7**: 366-370 [PMID: [30531023](#) DOI: [10.4103/eus.eus\\_36\\_18](#)]
  - 26 **Mizuno S**, Nakai Y, Isayama H, Suzuki T, Saito K, Uchino R, Takahara N, Kogure H, Tada M, Koike K. EUS-FNA of gastric cancer metastatic to the head of pancreas using a forward oblique viewing echoendoscope in a case with Roux-en-Y anatomy. *Endosc Ultrasound* 2018; **7**: 420-421 [PMID: [29536952](#) DOI: [10.4103/eus.eus\\_107\\_17](#)]
  - 27 **Yang F**, Wang H, Liu X, Ge N, Guo J, Wang S, Song X, Cao L, Sun S. EUS-guided fine-needle technique-derived cancer organoids: A tailored "Shennong deity" for every patient with cancer. *Endosc Ultrasound* 2019; **8**: 73-75 [PMID: [31006704](#) DOI: [10.4103/eus.eus\\_13\\_19](#)]



Randomized Controlled Trial

## Diagnostic value of novel retroflexion colonoscopy in the right colon: A randomized controlled trial

Wen-Kun Li, Yun Wang, Ya-Dan Wang, Kui-Liang Liu, Chun-Mei Guo, Hui Su, Hong Liu, Jing Wu

**ORCID number:** Wen-Kun Li 0000-0001-7181-5184; Yun Wang 0000-0002-7563-0782; Ya-Dan Wang 0000-0002-7126-9360; Kui-Liang Liu 0000-0001-8163-0394; Chun-Mei Guo 0000-0002-6103-7849; Hui Su 0000-0002-0517-9981; Hong Liu 0000-0003-2443-7808; Jing Wu 0000-0002-2259-3926.

**Author contributions:** Wu J, Liu H, Liu KL, and Li WK completed the study concept and design; Li WK and Wang Y recruited the patients; Li WK and Wang Y acquired the data; Li WK performed statistical analysis and drafted the manuscript; Liu KL, Wang YD, Guo CM, and Su H performed colonoscopy; Wu J and Liu KL provided critical review of the manuscript; all authors read and approved the final manuscript.

**Supported by** Digestive Medical Coordinated Development Center of Beijing Hospitals Authority, No. XXZ015; Capital Citizens Health Cultivation Project of Beijing Municipal Science & Technology Commission, No. Z161100000116084; Medical and Health Public Foundation of Beijing, No. YWJKJHKYJJ-B17262-067; and Science and Technology Development Project of China State Railway Group, No. N2019Z004.

**Wen-Kun Li, Ya-Dan Wang, Kui-Liang Liu, Chun-Mei Guo, Hui Su, Hong Liu, Jing Wu,** Department of Gastroenterology, Beijing Shijitan Hospital, Capital Medical University, Beijing 100038, China

**Wen-Kun Li,** National Clinical Research Center for Digestive Diseases, Beijing 100050, China

**Yun Wang, Ya-Dan Wang, Kui-Liang Liu, Chun-Mei Guo, Hui Su, Hong Liu,** Department of Gastroenterology, Peking University Ninth School of Clinical Medicine, Beijing 100038, China

**Jing Wu,** Department of Gastroenterology, Beijing Friendship Hospital, Capital Medical University, National Clinical Research Center for Digestive Diseases, Beijing 100050, China

**Corresponding author:** Jing Wu, PhD, Director, Professor, Department of Gastroenterology, Beijing Friendship Hospital, Capital Medical University, National Clinical Research Center for Digestive Diseases, No. 95 Yong'an Road, Xicheng District, Beijing 100050, China. [bjsjtyywj@ccmu.edu.cn](mailto:bjsjtyywj@ccmu.edu.cn)

### Abstract

#### BACKGROUND

Colonoscopy is the accepted gold standard for the detection of colorectal cancer. However, colonoscopy is less effective in preventing colon cancer in the right side compared with the left side.

#### AIM

To investigate the feasibility of a novel type of retroflexion colonoscope, EC-3490Ti colonoscope, for detection of proximal colon lesions.

#### METHODS

In this prospective trial, we recruited patients who underwent colonoscopy for screening or surveillance. When the endoscopists could not grasp the whole observation of the right-side colon mucosa in the forward view (FV), insertion and withdrawal were repeatedly performed in the FV group with the EC38-i10F colonoscope while retroflexion was performed in the retroflexed view (RV) group with the EC-3490Ti colonoscope. Adenoma detection rate, the total number of adenomas per positive participant, the success rate of retroflexion, and endoscope withdrawal time were recorded and compared.

#### RESULTS

**Institutional review board**

**statement:** The study was reviewed and approved by the Institutional Review Board of Beijing Shijitan Hospital, Capital Medical University (Approval No. 2018-59).

**Clinical trial registration statement:**

This study is registered at <http://www.chictr.org.cn/>. The registration identification number is ChiCTR2000031186.

**Informed consent statement:**

All study participants provided informed written consent prior to study enrollment.

**Conflict-of-interest statement:**

The authors declare that there is no conflict of interests in this study.

**Data sharing statement:**

Dataset available from the corresponding author at [bjsjtyywj@ccmu.edu.cn](mailto:bjsjtyywj@ccmu.edu.cn).

**CONSORT 2010 statement:**

The authors have read the CONSORT 2010 Statement, and the manuscript was prepared and revised according to the CONSORT 2010 Statement.

**Open-Access:**

This article is an open-access article that was selected by an in-house editor and fully peer-reviewed by external reviewers. It is distributed in accordance with the Creative Commons Attribution NonCommercial (CC BY-NC 4.0) license, which permits others to distribute, remix, adapt, build upon this work non-commercially, and license their derivative works on different terms, provided the original work is properly cited and the use is non-commercial. See: <http://creativecommons.org/licenses/by-nc/4.0/>

**Manuscript source:** Unsolicited manuscript

**Specialty type:** Oncology

**Country/Territory of origin:** China

**Peer-review report's scientific quality classification**

Grade A (Excellent): 0

Grade B (Very good): B, B

The total adenoma detection rate (39.3% *vs* 37.7%,  $P = 0.646$ ) did not show any significant difference between the two groups. However, the polyp detection rate (59.6% *vs* 51.0%,  $P = 0.002$ ), adenoma detection rate in the right colon (21.6% *vs* 14.4%,  $P = 0.012$ ), and the total number of adenomas per positive participant (2.1 *vs* 1.7,  $P = 0.011$ ) reached statistical significance. Retroflexion was achieved in 91.7% of our cohort. Compared with the FV group, the withdrawal time was significantly prolonged in the RV group ( $586.1 \pm 124.4$  s *vs*  $508.8 \pm 129.6$  s,  $P < 0.001$ ). In contrast, the proportion of additional ancillary pressure decreased (27.4% *vs* 45.7%,  $P < 0.001$ ), and the visual analog scale pain scores did not increase ( $2.7 \pm 1.4$  *vs*  $2.8 \pm 1.4$ ,  $P = 0.377$ ).

**CONCLUSION**

Retroflexion in the proximal colon could be performed successfully and safely with the EC-3490Ti colonoscope. This maneuver could detect more adenomas effectively.

**Key Words:** Colorectal adenoma; Retroflexion; Right colon; Adenoma detection rate; Cancer

©The Author(s) 2020. Published by Baishideng Publishing Group Inc. All rights reserved.

**Core Tip:** The current prospective randomized trial assessed the feasibility and efficacy of retroflexion colonoscopy in the proximal colon. Unlike previous studies, retroflexion was performed when the mucosa could not be exposed completely in the forward view due to the folds and flexures, instead of second insertion and withdrawal. Retroflexion in the right colon could be performed successfully and safely with the EC-3490Ti colonoscope and detect more adenomas effectively.

**Citation:** Li WK, Wang Y, Wang YD, Liu KL, Guo CM, Su H, Liu H, Wu J. Diagnostic value of novel retroflexion colonoscopy in the right colon: A randomized controlled trial. *World J Gastrointest Oncol* 2020; 12(11): 1336-1345

**URL:** <https://www.wjgnet.com/1948-5204/full/v12/i11/1336.htm>

**DOI:** <https://dx.doi.org/10.4251/wjgo.v12.i11.1336>

**INTRODUCTION**

Colorectal cancer (CRC) is the third most commonly diagnosed malignancy and the second leading cause of cancer death worldwide<sup>[1]</sup>. According to the latest data of the Chinese National Cancer Center<sup>[2]</sup>, the incidence and mortality of CRC both ranked fifth in China. Pathological and genetic evidence<sup>[3,4]</sup> suggests that > 90% of CRCs gradually develop from adenomas, during a period of 7-12 years. Screening and endoscopic polypectomy can reduce the mortality rate of CRC remarkably. Therefore, colonoscopy is currently considered the gold standard for CRC screening. However, interval cancers (ICs) still occur in patients who have undergone colonoscopy screening, due to a low detection rate and high miss rate for adenoma<sup>[5,6]</sup>. Furthermore, colonoscopy has unsatisfactory protection for the right-side colon because of the anatomical and morphological characteristics of proximal colon neoplasms compared with those on the left side<sup>[7,8]</sup>. Corley *et al*<sup>[9]</sup> found that with every percent increase in adenoma detection rate (ADR), the morbidity of ICs decreased by 3% within 10 years.

Various potential methods have been applied to improve ADR, especially in the proximal colon. Proper colonic cleaning, a high rate of cecal intubation, sufficient withdrawal time, and specialized training to recognize subtle polyps are required. Moreover, various new instruments have been used by endoscopists, including image-enhanced endoscopy, full spectrum endoscopy (FUSE), extra-wide-angle-view colonoscopy (EWAVE), and third eye retroscopy (TER). However, the evidence supporting the efficacy of these measures is not sufficient<sup>[10]</sup>.

Retroflexion during withdrawal of a colonoscope refers to making a J-turn with the bending section of the colonoscope, primarily aiming to increase the diagnostic view



Grade C (Good): C  
 Grade D (Fair): 0  
 Grade E (Poor): 0

**Received:** July 13, 2020

**Peer-review started:** July 13, 2020

**First decision:** September 17, 2020

**Revised:** September 27, 2020

**Accepted:** October 15, 2020

**Article in press:** October 15, 2020

**Published online:** November 15, 2020

**P-Reviewer:** Dubois A, Sheu B, Vollmers H

**S-Editor:** Gao CC

**L-Editor:** Wang TQ

**P-Editor:** Li JH



in the rectum<sup>[11,12]</sup>. Retroflexion could improve the visualization of the back wall of the haustral folds and the inner curvatures of the colonic flexures, making it possible to detect more lesions in the right colon. Recently, PENTAX MEDICAL (Hoya, Tokyo, Japan) developed a novel type of retroflexion colonoscope, EC-3490Ti, with shorter bending section, wider retroflexion angle, and smaller retroflexion semidiameter (Figure 1), making retroflexion easier.

Therefore, we conducted a prospective randomized trial to assess the feasibility and efficiency of this new retroflexion colonoscope in the proximal colon.

## MATERIALS AND METHODS

### Study design

This was a single-center prospective randomized trial conducted in the Endoscopy Center of Beijing Shijitan Hospital, Capital Medical University (Beijing, China). The working protocol was approved by the ethics committee of Beijing Shijitan Hospital, Capital Medical University, and informed consent was obtained from each participant.

### Patients

We enrolled patients aged  $\geq 18$  years who underwent total colonoscopy for CRC screening or surveillance. The exclusion criteria included: (1) Familial adenomatous polyposis and hereditary non-polyposis colorectal cancer syndrome; (2) Inflammatory bowel disease; (3) Incomplete colonoscopy; (4) Inadequate bowel preparation [Boston bowel preparation scale (BBPS)  $< 6$ ]; (5) Advanced CRC; and (6) Receiving anticoagulant medication.

### Randomization

The enrolled patients were randomly assigned in a 1:1 ratio to the retroflexed view (RV) group or forward view (FV) group. Randomization was carried out using a computer-generated random sequence. The allocation was placed in a sealed envelope and kept by an independent nurse who was not involved in this study. The endoscopists were blinded to the result of randomization until the start of the colonoscopy.

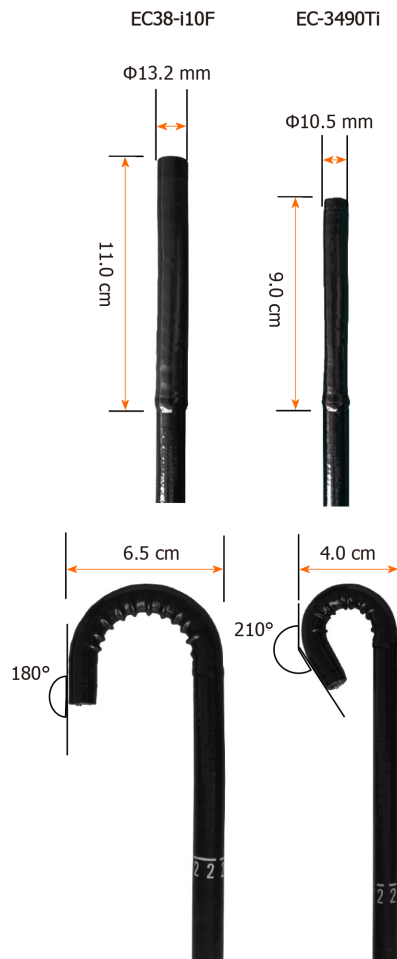
### Procedure

For bowel cleaning, all patients were advised to take a low-fiber diet for 3 d and were given 4 L of polyethylene glycol solution at split doses the day before colonoscopy. Endoscopists evaluated the quality of bowel preparation using the criteria of BBPS. Colonoscopy was performed without sedation. All procedures were performed by four experienced endoscopists, who had performed  $> 3000$  colonoscopies.

The right colon was defined as the colon from the cecum to the splenic flexure, including the cecum, ascending colon, hepatic flexure, and transverse colon. In each group, a colonoscope was intubated in the cecum routinely. Afterwards, the colonoscope was withdrawn to search for adenomas and other lesions. When the endoscopists could not grasp the whole observation of the right-side colon mucosa in the FV due to haustral folds and hepatic flexures in the proximal colon, insertion and withdrawal were repeatedly performed using the EC38-i10F colonoscope in the FV group while retroflexion was performed in the RV group with the EC-3490Ti colonoscope. Retroflexion was accomplished by using a maneuver similar to that used for rectal retroflexion. Successful retroflexion was defined as the insertion tube being visible to the endoscopist. After withdrawal to the splenic flexure, the rest of the colon was examined in a conventional FV in the two groups. The location and size, estimated by open biopsy forceps, were recorded for all detected polyps. The visualized lesions were removed by biopsy, endoscopic mucosal resection, or endoscopic submucosal dissection and sent for histopathological diagnoses by an experienced pathologist.

### Outcome measures

The primary outcome parameter of this study was ADR, which was the proportion of patients with at least one adenoma detected. The secondary outcome measures included ADR for the right colon (R-ADR), polyp detection rate (PDR), total number of adenomas per positive participant (APP), total number of adenomas per colonoscopy (APC), success rate of retroflexion, withdrawal duration, and degree of pain assessed with the visual analog scale (VAS).



**Figure 1** Compared with the EC38-i10F colonoscope, the EC-3490Ti colonoscope has shorter bending section, wider retroflexion angle, and smaller retroflexion semidiameter, making retroflexion easier.

### Sample size

According to the data of our center, the ADR of EC38-i10F endoscopy was 31.6% in 2018. Based on the results of previous studies, we hypothesized that ADR could be increased by 10% with retroflexion examination of the right colon, compared with forward withdrawal alone. Power analysis indicated that a minimum of 361 participants were required in each group, assuming a 0.05 significance level and 0.8 power using two-sided equivalence to test each hypothesis.

### Statistical analysis

IBM SPSS 23.0 (Armonk, NY, United States) was used for all statistical analyses. Continuous variables were compared using Student's *t* test if normally distributed and the Mann-Whitney test if not normally distributed. Pearson's  $\chi^2$  test or Fisher's exact test was used to analyze categorical data and compare proportions. Univariate analysis and logistic regression analysis were carried out to evaluate predictors associated with unsuccessful retroflexion in the proximal colon.  $P < 0.05$  was considered statistically significant. The statistical methods of this study were reviewed by Qing-Kun Song from Beijing Shijitan Hospital, Capital Medical University.

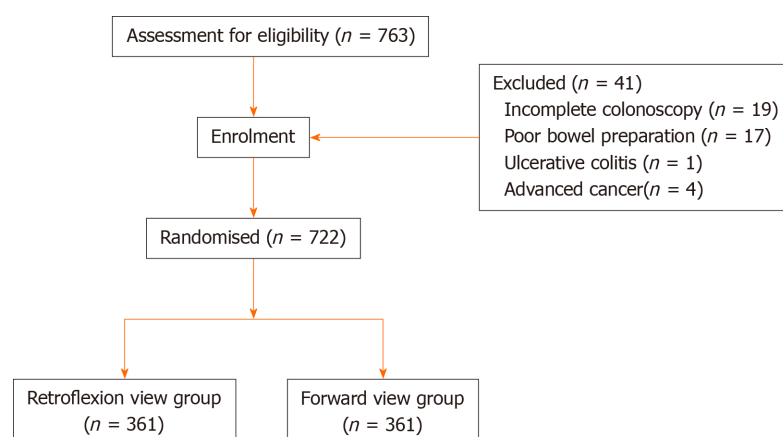
## RESULTS

During the 6-mo period, 763 patients consented to participate in the study. Forty-one participants were excluded as a consequence of incomplete colonoscopy ( $n = 19$ ), poor bowel preparation ( $n = 17$ ), ulcerative colitis ( $n = 1$ ), or advanced cancer ( $n = 4$ ). Finally, 361 patients were enrolled into each arm (Figure 2). Baseline demographic characteristics are listed in Table 1. The median age was 55 years in the RV group and FV group. There were no significant differences between the two groups with respect

**Table 1 Patients' baseline characteristics**

	RV ( <i>n</i> = 361)	FV ( <i>n</i> = 361)	<i>P</i> value
Age (yr)	55 (50-65)	55 (45-63)	0.052
Sex, <i>n</i> (%)			
Male	183 (50.7)	168 (46.5)	0.264
Female	178 (49.3)	193 (53.5)	
BMI (kg/m <sup>2</sup> )	24.38 (22.31-25.95)	24.22 (20.76-26.99)	0.055
Indication for colonoscopy, <i>n</i> (%)			
Screening (no history of colon polyps)	287 (79.5)	304 (84.2)	0.101
Surveillance (past history of colon polyps)	74 (20.5)	57 (15.8)	
Current smokers, <i>n</i> (%)	92 (25.5)	90 (25.5)	0.864
Family history of colorectal cancer, <i>n</i> (%)	111 (30.7)	104 (28.8)	0.569
BBPS	7 (7-8)	7 (7-8)	0.195

RV: Retroflexion view; FV: Forward view; BMI: Body mass index; BBPS: Boston bowel preparation scale.

**Figure 2 Flow diagram of participant enrollment and distribution into allocated groups.**

to age, sex, body mass index (BMI), indication for colonoscopy, smoking history, family history of CRC, and bowel preparation (Table 1). No immediate or delayed complications occurred.

The total number of polyps detected in the RV group was 497, including an additional 75 found by retroflexion. Histopathological analysis confirmed 297 adenomas, including 63 assigned to retroflexed vision. A total of 417 polyps and 235 adenomas were identified in the FV group. In the RV group, 142 (39.3%) patients had at least one lesion compared with 136 (37.7%) in the FV group. ADR, the primary outcome measure, showed no significant differences between the two groups ( $P = 0.646$ ). Among the secondary outcome parameters, there was also no significant difference in APC (0.8 *vs* 0.7,  $P = 0.280$ ) between the RV and FV groups. However, the PDR (59.6% *vs* 51.0%,  $P = 0.002$ ), R-ADR (21.6% *vs* 14.4%,  $P = 0.012$ ), and APP (2.1 *vs* 1.7,  $P = 0.011$ ) reached statistical significance between the two groups. Tables 2 and 3 show the details for the size and the location of lesions detected, respectively. Several pictures of detected lesions are shown in Figure 3.

To evaluate the applicability of the novel retroflexion colonoscopy, we calculated several related indicators. The colonoscope was inserted into the cecum in 351 (97.2%) of 361 cases. The scores of abdominal pain did not show a significant difference between the two groups during colonoscopy (RV  $2.7 \pm 1.4$  *vs* FV  $2.8 \pm 1.4$ ,  $P = 0.377$ ). The duration of withdrawal in the RV group was significantly longer than that of the FV group ( $586.1 \pm 124.4$  *vs*  $508.8 \pm 129.6$  s,  $P < 0.001$ ). Compared with conventional colonoscopy, the new approach required less ancillary pressure (27.4% *vs* 45.7%,  $P <$

**Table 2** Size of identified lesions

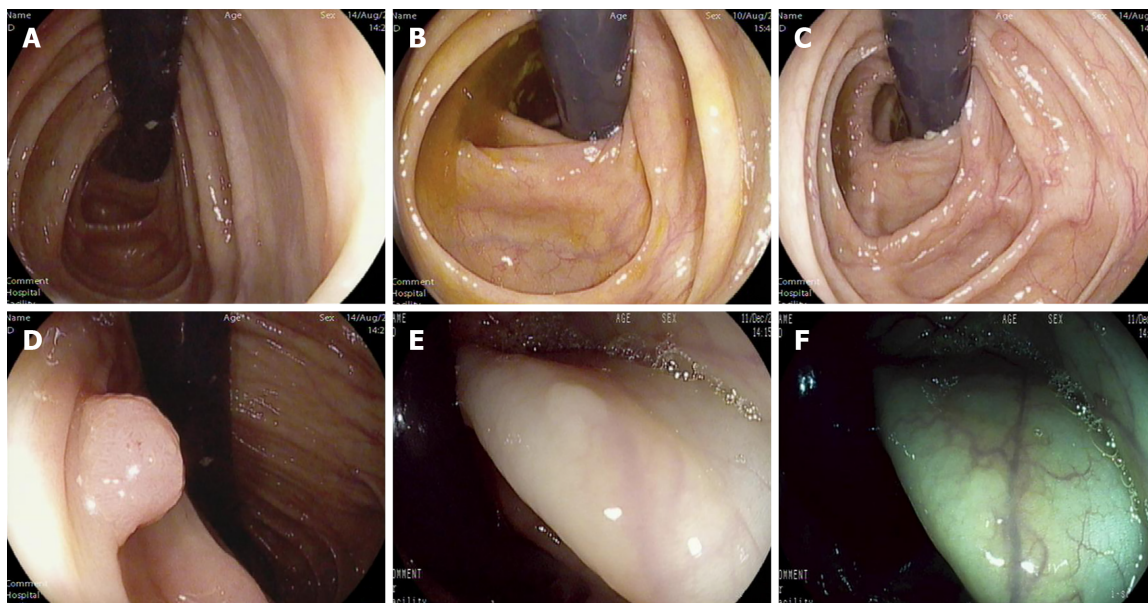
	Polyps		Adenomas	
	RV	FV	RV	FV
≤ 5 mm	295	314	126	133
6-10 mm	143	81	113	80
> 10 mm	59	22	58	22

RV: Retroflexion view; FV: Forward view.

**Table 3** Location of identified lesions

	Polyps		Adenomas	
	RV	FV	RV	FV
Right colon	244	141	145	90
Left colon	186	181	125	105
Rectum	67	95	27	40

RV: Retroflexion view; FV: Forward view.



**Figure 3** Detected lesions. A and B: The colonoscopy was successfully retroflexed in the ascending colon and the hepatic flexure, respectively; C and D: The same polyp hidden in the proximal side of the haustral folds in the distant view and the tight view, respectively; E and F: A flat lesion located on the haustral folds with white-light mode and i-SCAN mode, respectively.

0.001).

Retroflexion in the right-side colon was achieved in 331 (91.7%) of 361 patients. On univariate analysis, age, sex, abdominal surgery, and excessive looping were significantly associated with failure to retroflex. Body height, weight, BMI, bowel cleanliness, and smoking history were not related to the failure. Logistic regression analysis showed that age > 60 years, female sex, previous abdominal surgery, and instrumental looping were powerful predictors (Table 4).

**Table 4 Logistic regression analysis of predictors of failure to perform right-sided retroflexion**

	Odds ratio (95%CI)	P value
Age > 65 yr	5.26 (2.17-12.8)	< 0.001
Female sex	2.92 (1.17-7.31)	0.022
Previous abdominal surgery	5.83 (2.26-15.04)	< 0.001
Instrumental looping	3.49 (1.33-9.12)	0.011

CI: Confidence interval.

## DISCUSSION

Colorectal adenomas are considered to be a precancerous state of CRC. Benefiting from colonoscopy screening and polypectomy among adults aged  $\geq 50$  years, the morbidity of CRC declined by 2%-3% annually in Western developed countries<sup>[13]</sup>. However, about 20% of adenomas were missed during colonoscopy, which weakened the protective effect on CRC, especially in the proximal colon<sup>[6,14]</sup>.

Various colonoscopy techniques were attempted in several studies to improve adenoma detection. Compared with white-light imaging, narrow-band imaging could improve ADR and PDR significantly<sup>[15]</sup>. Nulsen *et al*<sup>[16]</sup> conducted a retrospective study, including 3998 participants, suggesting that overall ADR, ADR for the proximal colon, and ADR for advanced adenomas could be improved significantly after adopting FUSE. A multicenter randomized controlled trial conducted by Ikematsu *et al*<sup>[17]</sup> showed that blue-laser imaging significantly increased the mean number of adenomas per patient, rather than ADR.

Retroflexed inspection in the right-side colon has been proposed as a complementary maneuver following the routine forward withdrawal, which could potentially improve diagnostic visibility. However, the results of previous work have revealed controversial evidence for this maneuver. A prospective multicenter cohort study, conducted by Chandran *et al*<sup>[18]</sup> in 2014, showed that retroflexion following forward examination improved the ADR from 24.64% to 26.4%. There was no significant difference in ADR when the proximal colon was re-examined in the FV *vs* RV (46% *vs* 47%), as revealed in a high-quality randomized controlled trial<sup>[19]</sup>. A systematic review and meta-analysis<sup>[20]</sup>, including eight studies (with a total of 3660 cases), suggested that second examination of the proximal colon in retroflexion detected an additional 16.9% of right-sided adenomas that would have been missed by traditional colonoscopy. Recently, a multicenter randomized controlled trial suggested that a second examination of the right colon after standard withdrawal was associated with improvement of ADR, but by which method did not matter [RV (9%) or FV (12%)]<sup>[21]</sup>.

Our study aimed to evaluate the utility of the EC-3490Ti colonoscope in the retroflexion of the proximal colon. According to previous studies, compared with FV, retroflexion could not improve the ADR obviously in the second withdrawal, which is not feasible in clinical practice. Concerning this weakness, we did not perform a second withdrawal operation. Unlike previous studies, retroflexion was performed when the mucosa could not be exposed completely in the FV due to the folds and flexures of the colon, instead of the second insertion and withdrawal.

In the present study, the calculated ADR in the RV group was slightly higher than that in the control group (39.3% *vs* 37.3%,  $P = 0.646$ ). These results are in line with the previous study<sup>[19]</sup>. Proximal colon retroflexion failed to yield a higher ADR compared with that in the FV. We propose several explanations for this. First, visualization of the whole colon mucosa could not be achieved by retroflexion, as there were also some blind spots on the colon wall hidden by the insertion tube itself. During the examination, endoscopists attempted to compensate for this by rotating the insertion tube, but the results were still unsatisfactory. Second, adenomas located in the proximal colon were flatter or more depressed than those in the distal colon, which made it difficult to distinguish them from the normal mucosa. Third, it could be speculated that adenomas located in hidden positions on the proximal sides of folds and flexures of the colon were not the dominant mechanism resulting in unsuccessful detection during colonoscopy<sup>[22]</sup>. However, no other plausible mechanism has been put forward until now. Lastly, the ADR may not be comprehensive for the evaluation of colonoscopy detection, although it is targeted as one of the most critical indicators of



colonoscopy quality control<sup>[9]</sup>. In our study, additional 65 adenomas in 65/361 (18.0%) patients were identified. Still, the total ADR was only improved from 38.8% to 39.3% with additional retroflexion, excluding the cases with at least one adenoma detected on the initial forward withdrawal or detected in the distal colon. In this regard, the number of adenomas detected, as crucial as the ADR, should be used as an indicator to assess the endoscopic operation. Hence, we added other indicators to evaluate the detection efficiency of the novel endoscopy, such as APP, APC, R-ADR, and PDR. PDR, R-ADR, and APP were significantly increased with retroflexion during withdrawal in the proximal colon, compared with the FV. Based on these results, retroflexion in the right colon during withdrawal could facilitate detecting more adenomas and polyps.

In the present study, retroflexion in the right-side colon was successfully performed in approximately 92% of our cohort, which was identical to prior studies<sup>[18-20]</sup>. The significant predictors of failed retroflexion were advanced age, female sex, previous abdominal surgery, and instrumental looping. The observation time of RV was approximately 1 min longer than that of FV. We believe that this operation is new for our endoscopists, and retroflexion should be performed gently, which should take several seconds. Compared with conventional colonoscopy, the novel endoscopy requires less ancillary pressure during insertion, which may be associated with its flexible manipulation due to the shorter bending section and wider retroflexion angle. Besides, the new endoscopy did not increase the abdominal pain in patients, and the cecum arrival rate reached 95% as recommended in the guidelines. No major RV-related adverse event was noted in our study. Additionally, retroflexion could also provide valuable information to assess and remove lesions that are difficult to access in the prograde view<sup>[23,24]</sup>. The experience of our team suggests that retroflexion in the proximal colon is a safe and useful maneuver, as a complement to forward inspection. However, one serious adverse event of perforation was reported in the meta-analysis mentioned earlier<sup>[20]</sup>. We recommend that the procedure be stopped if any resistance is felt while turning the bending section.

There were several limitations in our study. First, the operators were experienced endoscopists, and the learning curve for the maneuver was unclear. Second, this trial did not adopt a double-blind design. Although the results could not reject bias altogether, we consider that there may have been some bias because it was impossible for our colleagues to overlook lesions in the FV group deliberately. Finally, this study was conducted in our center alone, thus large-scale multicenter trials are needed to explore the utility of retroflexion in the right-side colon.

## CONCLUSION

Retroflexion in the proximal colon can be performed successfully and safely with the EC-3490Ti colonoscope. This maneuver could increase the number of adenomas detected and improve ADR. As a result, we suggest that retroflexion should be adopted as a complementary maneuver during screening or surveillance colonoscopy in the right colon.

## ARTICLE HIGHLIGHTS

### Research background

Colonoscopy is the most effective method in the screening and prevention of colorectal cancer (CRC), and it could reduce the mortality from CRC. However, colonoscopy is less effective in preventing CRC in the right-side compared with the left-side colon.

### Research motivation

Failure to detect more preneoplastic lesions is regarded as one of the mechanisms in the development of interval CRC. Retroflexion in the proximal colon allows for better visualization of the folds and the hepatic flexure, which may increase adenoma detection rate (ADR).

### Research objectives

The current study aimed to investigate the effectiveness and safety of the EC-3490Ti colonoscope in detecting adenomas in the proximal colon.

### Research methods

We enrolled patients who underwent colonoscopy for screening or surveillance for CRC. When the endoscopists could not grasp the whole observation of the colon mucosa in the forward view, retroflexion was performed in the retroflexion view group with the EC-3490Ti colonoscope, while insertion and withdrawal were repeatedly conducted with the EC38-i10F colonoscope. ADR, total number of adenomas per positive participant (APP), success rate of retroflexion, and withdrawal time were compared.

### Research results

The success rate of proximal retroflexion was 91.7%. There were no complications with the maneuver. Polyp detection rate, ADR for the right colon, and APP were significantly increased with retroflexion during withdrawal in the proximal colon, compared with the forward view group.

### Research conclusions

Proximal retroflexion with the EC-3490Ti colonoscope in the right colon could be accomplished safely and effectively. Retroflexion in the proximal colon significantly increases the detection of adenomas compared with conventional colonoscopy.

### Research perspectives

Retroflexion should be adopted as a complementary procedure in the future for the improvement of CRC prevention.

## REFERENCES

- 1 **Bray F**, Ferlay J, Soerjomataram I, Siegel RL, Torre LA, Jemal A. Global cancer statistics 2018: GLOBOCAN estimates of incidence and mortality worldwide for 36 cancers in 185 countries. *CA Cancer J Clin* 2018; **68**: 394-424 [PMID: 30207593 DOI: 10.3322/caac.21492]
- 2 **Chen W**, Zheng R, Baade PD, Zhang S, Zeng H, Bray F, Jemal A, Yu XQ, He J. Cancer statistics in China, 2015. *CA Cancer J Clin* 2016; **66**: 115-132 [PMID: 26808342 DOI: 10.3322/caac.21338]
- 3 **Leslie A**, Carey FA, Pratt NR, Steele RJ. The colorectal adenoma-carcinoma sequence. *Br J Surg* 2002; **89**: 845-860 [PMID: 12081733 DOI: 10.1046/j.1365-2168.2002.02120.x]
- 4 **Wu Z**, Liu Z, Ge W, Shou J, You L, Pan H, Han W. Analysis of potential genes and pathways associated with the colorectal normal mucosa-adenoma-carcinoma sequence. *Cancer Med* 2018; **7**: 2555-2566 [PMID: 29659199 DOI: 10.1002/cam4.1484]
- 5 **Dawwas MF**. Adenoma detection rate and risk of colorectal cancer and death. *N Engl J Med* 2014; **370**: 2539-2540 [PMID: 24963578 DOI: 10.1056/NEJMc1405329]
- 6 **van Rijn JC**, Reitsma JB, Stoker J, Bossuyt PM, van Deventer SJ, Dekker E. Polyp miss rate determined by tandem colonoscopy: a systematic review. *Am J Gastroenterol* 2006; **101**: 343-350 [PMID: 16454841 DOI: 10.1111/j.1572-0241.2006.00390.x]
- 7 **Brenner H**, Chang-Claude J, Seiler CM, Rickert A, Hoffmeister M. Protection from colorectal cancer after colonoscopy: a population-based, case-control study. *Ann Intern Med* 2011; **154**: 22-30 [PMID: 21200035 DOI: 10.7326/0003-4819-154-1-201101040-00004]
- 8 **Rondagh EJ**, Bouwens MW, Riedl RG, Winkens B, de Ridder R, Kaltenbach T, Soetikno RM, Masclee AA, Sanduleanu S. Endoscopic appearance of proximal colorectal neoplasms and potential implications for colonoscopy in cancer prevention. *Gastrointest Endosc* 2012; **75**: 1218-1225 [PMID: 22482917 DOI: 10.1016/j.gie.2012.02.010]
- 9 **Corley DA**, Jensen CD, Marks AR, Zhao WK, Lee JK, Doubeni CA, Zauber AG, de Boer J, Fireman BH, Schottinger JE, Quinn VP, Ghai NR, Levin TR, Quesenberry CP. Adenoma detection rate and risk of colorectal cancer and death. *N Engl J Med* 2014; **370**: 1298-1306 [PMID: 24693890 DOI: 10.1056/NEJMoa1309086]
- 10 **ASGE Technology Committee**, Konda V, Chauhan SS, Abu Dayyeh BK, Hwang JH, Komanduri S, Manfredi MA, Maple JT, Murad FM, Siddiqui UD, Banerjee S. Endoscopes and devices to improve colon polyp detection. *Gastrointest Endosc* 2015; **81**: 1122-1129 [PMID: 25746978 DOI: 10.1016/j.gie.2014.10.006]
- 11 **Grobe JL**, Kozarek RA, Sanowski RA. Colonoscopic retroflexion in the evaluation of rectal disease. *Am J Gastroenterol* 1982; **77**: 856-858 [PMID: 7137139]
- 12 **Rex DK**, Vemulapalli KC. Retroflexion in colonoscopy: why? *Gastroenterology* 2013; **144**: 882-883 [PMID: 23499952 DOI: 10.1053/j.gastro.2013.01.077]
- 13 **Siegel RL**, Miller KD, Jemal A. Cancer statistics, 2018. *CA Cancer J Clin* 2018; **68**: 7-30 [PMID: 29313949 DOI: 10.3322/caac.21442]
- 14 **Baxter NN**, Warren JL, Barrett MJ, Stukel TA, Doria-Rose VP. Association between colonoscopy and colorectal cancer mortality in a US cohort according to site of cancer and colonoscopist specialty. *J Clin Oncol* 2012; **30**: 2664-2669 [PMID: 22689809 DOI: 10.1200/JCO.2011.40.4772]
- 15 **Vişovan II**, Tanţău M, Pascu O, Ciobanu L, Tanţău A. The role of narrow band imaging in colorectal polyp detection. *Bosn J Basic Med Sci* 2017; **17**: 152-158 [PMID: 28378694 DOI: 10.17305/bjbm.2017.1686]
- 16 **Nulsen B**, Ungaro RC, Davis N, Turvall E, Deutsch L, Lewis B. Changes in Adenoma Detection Rate With

- Implementation of Full-spectrum Endoscopy: A Report of 3998 Screening Colonoscopies. *J Clin Gastroenterol* 2018; **52**: 885-890 [PMID: 28787359 DOI: 10.1097/MCG.0000000000000874]
- 17 **Ikematsu H**, Sakamoto T, Togashi K, Yoshida N, Hisabe T, Kiriyaama S, Matsuda K, Hayashi Y, Matsuda T, Osera S, Kaneko K, Utano K, Naito Y, Ishihara H, Kato M, Yoshimura K, Ishikawa H, Yamamoto H, Saito Y. Detectability of colorectal neoplastic lesions using a novel endoscopic system with blue laser imaging: a multicenter randomized controlled trial. *Gastrointest Endosc* 2017; **86**: 386-394 [PMID: 28147226 DOI: 10.1016/j.gie.2017.01.017]
  - 18 **Chandran S**, Parker F, Vaughan R, Mitchell B, Fanning S, Brown G, Yu J, Efthymiou M. Right-sided adenoma detection with retroflexion versus forward-view colonoscopy. *Gastrointest Endosc* 2015; **81**: 608-613 [PMID: 25440687 DOI: 10.1016/j.gie.2014.08.039]
  - 19 **Kushnir VM**, Oh YS, Hollander T, Chen CH, Sayuk GS, Davidson N, Mullady D, Murad FM, Sharabash NM, Ruettgers E, Dassopoulos T, Easler JJ, Gyawali CP, Edmundowicz SA, Early DS. Impact of retroflexion vs. second forward view examination of the right colon on adenoma detection: a comparison study. *Am J Gastroenterol* 2015; **110**: 415-422 [PMID: 25732415 DOI: 10.1038/ajg.2015.21]
  - 20 **Cohen J**, Grunwald D, Grossberg LB, Sawhney MS. The Effect of Right Colon Retroflexion on Adenoma Detection: A Systematic Review and Meta-analysis. *J Clin Gastroenterol* 2017; **51**: 818-824 [PMID: 27683963 DOI: 10.1097/MCG.0000000000000695]
  - 21 **Núñez Rodríguez MH**, Díez Redondo P, Riu Pons F, Cimavilla M, Hernández L, Loza A, Pérez-Miranda M. Proximal retroflexion vs second forward view of the right colon during screening colonoscopy: A multicentre randomized controlled trial. *United European Gastroenterol J* 2020; **8**: 725-735 [PMID: 32379535 DOI: 10.1177/2050640620924210]
  - 22 **Harrison M**, Singh N, Rex DK. Impact of proximal colon retroflexion on adenoma miss rates. *Am J Gastroenterol* 2004; **99**: 519-522 [PMID: 15056095 DOI: 10.1111/j.1572-0241.2004.04070.x]
  - 23 **Pishvaian AC**, Al-Kawas FH. Retroflexion in the colon: a useful and safe technique in the evaluation and resection of sessile polyps during colonoscopy. *Am J Gastroenterol* 2006; **101**: 1479-1483 [PMID: 16863549 DOI: 10.1111/j.1572-0241.2006.00606.x]
  - 24 **Rex DK**, Khashab M. Colonoscopic polypectomy in retroflexion. *Gastrointest Endosc* 2006; **63**: 144-148 [PMID: 16377332 DOI: 10.1016/j.gie.2005.09.016]



## Efficacy and safety of anti-PD-1/anti-PD-L1 antibody therapy in treatment of advanced gastric cancer or gastroesophageal junction cancer: A meta-analysis

Li Yang, Xian-Zhe Dong, Xiao-Xuan Xing, Xiao-Hui Cui, Lin Li, Lan Zhang

**ORCID number:** Li Yang 0000-0001-8257-6094; Xian-Zhe Dong 0000-0002-5286-4623; Xiao-Xuan Xing 0000-0002-6792-4967; Xiao-Hui Cui 0000-0001-6905-8866; Lin Li 0000-0001-9218-1045; Lan Zhang 0000-0002-5220-3171.

**Author contributions:** Yang L and Dong XZ designed the study and wrote the manuscript; Yang L and Xing XX conducted the literature search; Yang L and Dong XZ collected and retrieved the data; Yang L and Cui XH analyzed the data; Dong XZ, Li L, and Zhang L critically reviewed and revised the manuscript; and all authors proofread the manuscript.

**Supported by** Beijing Hospitals Authority Ascent Plan, No. DFL20190803; Capital Science and Technology Leading Talent Training Project, No. Z191100006119017; National Nature and Science Foundation of China, No. 81773778; and China Postdoctoral Science Foundation, No. 2019M650775.

**Conflict-of-interest statement:** No conflict of interest.

**PRISMA 2009 Checklist statement:** The authors have read the PRISMA 2009 Checklist, and the manuscript was prepared and revised

**Li Yang, Xian-Zhe Dong, Xiao-Xuan Xing, Xiao-Hui Cui, Lin Li, Lan Zhang**, Department of Pharmacy, Xuanwu Hospital of Capital Medical University, National Clinical Research Center for Geriatric Diseases, Beijing Engineering Research Center for Nervous System Drugs, Beijing Institute for Brain Disorders, Key Laboratory for Neurodegenerative Diseases of Ministry of Education, Beijing 100053, China

**Li Yang**, College of Pharmacy, Zunyi Medical University, Zunyi 563000, Guizhou Province, China

**Corresponding author:** Lan Zhang, PhD, Professor, Department of Pharmacy, Xuanwu Hospital of Capital Medical University, National Clinical Research Center for Geriatric Diseases, Beijing Engineering Research Center for Nervous System Drugs, Beijing Institute for Brain Disorders, Key Laboratory for Neurodegenerative Diseases of Ministry of Education, No. 45 Changchun Street, Xicheng District, Beijing 100053, China. [lanizhg@126.com](mailto:lanizhg@126.com)

### Abstract

#### BACKGROUND

Faced with limited and inadequate treatment options for patients with advanced gastric cancer or gastroesophageal junction cancer (GC/GEJC), researchers have turned toward, with the support of promising clinical trials, anti-PD-1/anti-PD-L1 antibody therapy. But there are also different clinical trial results. To better assess its efficacy and safety, we integrated data from 13 eligible studies for a systematic review and meta-analysis.

#### AIM

To comprehensively evaluate the efficacy and safety of anti-PD-1/anti-PD-L1 antibody therapy in the treatment of advanced GC/GEJC patients.

#### METHODS

PubMed, Web of Science, Cochrane Library, and EMBASE databases were searched to identify eligible articles with outcomes including objective response rate (ORR), disease control rate (DCR), overall survival (OS), progression-free survival (PFS), and adverse events (AEs) of anti-PD-1/anti-PD-L1 antibody therapy.

#### RESULTS

Our study encompassed a total of 13 trials totaling 1618 patients. The outcomes

according to the PRISMA 2009 Checklist.

**Open-Access:** This article is an open-access article that was selected by an in-house editor and fully peer-reviewed by external reviewers. It is distributed in accordance with the Creative Commons Attribution NonCommercial (CC BY-NC 4.0) license, which permits others to distribute, remix, adapt, build upon this work non-commercially, and license their derivative works on different terms, provided the original work is properly cited and the use is non-commercial. See: <http://creativecommons.org/licenses/by-nc/4.0/>

**Manuscript source:** Unsolicited manuscript

**Specialty type:** Oncology

**Country/Territory of origin:** China

**Peer-review report's scientific quality classification**

Grade A (Excellent): 0  
Grade B (Very good): B  
Grade C (Good): 0  
Grade D (Fair): 0  
Grade E (Poor): 0

**Received:** June 9, 2020

**Peer-review started:** June 9, 2020

**First decision:** July 4, 2020

**Revised:** July 15, 2020

**Accepted:** September 18, 2020

**Article in press:** September 18, 2020

**Published online:** November 15, 2020

**P-Reviewer:** Byeon H

**S-Editor:** Huang P

**L-Editor:** Wang TQ

**P-Editor:** Wang LL



showed a pooled ORR and DCR of 15% (95% confidence interval [CI]: 14%-18%) and 40% (95% CI: 33%-46%), respectively. The pooled 6-mo OS and PFS were 54% (95% CI: 45%-64%) and 26% (95% CI: 20%-32%), respectively, and the 12-mo OS and PFS were 42% (95% CI: 21%-62%) and 11% (95% CI: 8%-13%), respectively. In addition, the incidence of any-grade AEs and grade  $\geq 3$  AEs was 64% (95% CI: 54%-73%) and 18% (95% CI: 16%-20%), respectively. Most importantly, PD-L1 positive patients exhibited a higher ORR rate than PD-L1 negative patients (odds ratio = 2.54, 95% CI: 1.56-4.15).

## CONCLUSION

Anti-PD-1/anti-PD-L1 antibody therapy has shown promising anti-tumor efficacy with manageable AEs in advanced GC/GEJC patients, with PD-L1 overexpressing patients exhibiting a higher ORR. What is more, the clinical efficacy of anti-PD-1/PD-L1 combined with traditional chemotherapy drugs is even better, although the occurrence of AEs still causes considerable concerns.

**Key Words:** Gastric cancer; Gastroesophageal junction cancer; Anti-PD-1/anti-PD-L1 antibody therapy; Meta-analysis; Systematic review

©The Author(s) 2020. Published by Baishideng Publishing Group Inc. All rights reserved.

**Core Tip:** Anti-PD-1/anti-PD-L1 antibody therapy, such as nivolumab and pembrolizumab, which has been approved by the FDA for marketing, enhances the body's cellular immune response to anti-tumor effects by regulating T cell function. At present, it has become the first-line treatment for extensive stage small cell lung cancer and other cancers. In recent years, some clinical trials have also shown that anti-PD-1/anti-PD-L1 antibody therapy has a reliable effect in advanced gastric cancer or gastroesophageal junction cancer (GC/GEJC) patients, but there is still controversy. The main purpose of this meta-analysis was to comprehensively evaluate the efficacy and safety of anti-PD-1/anti-PD-L1 antibody therapy in the treatment of advanced GC/GEJC patients.

**Citation:** Yang L, Dong XZ, Xing XX, Cui XH, Li L, Zhang L. Efficacy and safety of anti-PD-1/anti-PD-L1 antibody therapy in treatment of advanced gastric cancer or gastroesophageal junction cancer: A meta-analysis. *World J Gastrointest Oncol* 2020; 12(11): 1346-1363

**URL:** <https://www.wjgnet.com/1948-5204/full/v12/i11/1346.htm>

**DOI:** <https://dx.doi.org/10.4251/wjgo.v12.i11.1346>

## INTRODUCTION

Gastric cancer (GC) is the fifth most frequently diagnosed cancer and the third leading cause of cancer death worldwide<sup>[1]</sup>. Although GC incidence has been declining globally, there were still 1033701 new GC cases and 782685 death counts in 2018, with overall half occurring in East Asia, especially China<sup>[2]</sup>. Because GC patients often present nonspecific symptoms, diagnosis occurs predominantly at an advanced stage, where approximately 50% of patients have already developed locally advanced or metastatic tumor, bringing the 5-year survival rate from less than 30%<sup>[3,4]</sup> down to approximately 15%<sup>[5-7]</sup>.

Currently, the primary treatment option for GC patients is surgery and chemotherapy, with especially poor prognosis and overall survival (OS) rate for patients with advanced GC<sup>[8,9]</sup>. Current clinical guidelines recommend dual or triple platinum/fluorouracil combinations for human epidermal growth factor receptor 2 (HER-2) negative patients, and trastuzumab in combination with platinum and fluorouracil chemotherapy for HER-2 positive patients as the first-line treatment options, and taxanes, irinotecan, or ramucirumab for patients with performance status (PS) 0-1 as the second-line treatment options<sup>[10-12]</sup>. Nevertheless, despite these treatments, most patients with advanced gastric cancer or gastroesophageal junction cancer (GC/GEJC) continue to deteriorate after treatment<sup>[13,14]</sup>.

Immune checkpoint inhibitors, such as PD-1 and PD-L1 inhibitors, have become the



first-line treatment for multiple malignancies<sup>[15]</sup>. Inhibition of PD-1 and PD-L1 enhances the *in vitro* response of T cells as well as the antitumor activity in preclinical models<sup>[16,17]</sup>. The phase I studies with anti-PD-1 drugs, such as nivolumab and pembrolizumab, in non-small-cell lung cancer (NSCLC), advanced melanoma, renal cell carcinoma (RCC), and other solid tumor patients have demonstrated very promising response with controlled side effects. Inspired from this results, PD-1 blockers were studied for further trials and showed excellent response in phase III trial patients with advanced melanoma than in those with NSCLC and RCC<sup>[18]</sup>. Anti-PD-1/anti-PD-L1 antibody therapies exhibiting success in many clinical trials for various types of tumors regardless of pathologic grade with long-lasting responses and tolerable toxicity<sup>[18,19]</sup>. At present, the United States Food and Drug Administration (FDA) has approved PD-1 pathway inhibitors for cancer treatment including the monoclonal antibodies nivolumab (anti-PD-1; Bristol-Myers Squibb), pembrolizumab (anti-PD-1; Merck), atezolizumab (anti-PD-L1; Genentech/Roche), avelumab (anti-PD-L1; EMD Serono/Pfizer), and durvalumab (anti-PD-L1; AstraZeneca).

Several studies have shown the prevalent overexpression of PD-L1 in GC patients, and the expression of PD-L1 plays a key role in cancer immune escape and related tumor progression and poor prognosis<sup>[20,21]</sup>. Reducing the expression of PD-L1 in human gastric cancer cell line SGC-7901 can significantly inhibit cell proliferation and migration and tumor growth in subcutaneously transplanted mouse models<sup>[22]</sup>. In addition, many clinical studies have initially shown that PD-L1 blockers can significantly inhibit the tumor progression of many advanced cancers such as melanoma, GC, non-small cell lung cancer, ovarian cancer and so on<sup>[23,24]</sup>. Thus, anti-PD-1/anti-PD-L1 antibody therapy seemed promising as a potential approach for GC/GEJC.

In the meantime, several clinical trials have already evaluated the efficacy of anti-PD-1/anti-PD-L1 antibody therapy in advanced GC/GEJC patients, and the results show that this therapy has good anti-tumor activity and controllable adverse reactions for advanced GC/GEJC patients. However, one study suggested that not all tumors expressing PD-L1 respond to PD-1/PD-L1 inhibitors<sup>[16]</sup>. And the treatment regimen has not been included in the authoritative clinical practice guidelines, such as EMSO GC diagnosis and treatment guidelines, which means that there is yet no scholarly consensus on the efficacy and safety of PD-1/PD-L1 inhibitors in the treatment of advanced GC/GEJC. To address this need, we meta-analyzed all published clinical studies based on the Preferred Reporting Items for Systematic Reviews and Meta-analyses (PRISMA) statement<sup>[25]</sup>.

## MATERIALS AND METHODS

### Systematic literature search

PubMed, Web of Science, the Cochrane Library, and Embase were searched from inception up to March 5, 2020 using the following MeSHs headings (Gastric Cancer OR Stomach Cancer OR Stomach Neoplasm OR Gastric Neoplasm OR GC OR gastroesophageal OR Gastro Esophageal Junction Cancer OR GEJC) AND (Nivolumab OR MDX-1106 OR ONO-4538 OR BMS-936558 OR Opdivo OR Pembrolizumab OR lambrolizumab OR Keytruda OR MK-3475 OR SCH-900475 OR Atezolizumab OR anti-PDL1 OR MPDL3280A OR Tecentriq OR RG7446 OR Durvalumab OR MEDI4736 OR Imfinzi OR Avelumab OR Bavencio OR MSB0010682 OR MSB0010718C).

### Inclusion and exclusion criteria

The literature included in this study must meet all of the following criteria: (1) Prospective clinical trials in patients with advanced GC/GEJC; (2) Patients in the immunotherapy group were treated with anti-PD-1/PD-L1 drugs; and (3) The literature provides relevant anti-tumor activity and safety data [objective response rate (ORR), disease control rate (DCR), OS, progression-free survival (PFS), adverse events (AEs), or grade  $\geq 3$  AEs].

The exclusion criteria for this study were as follows: (1) Conference abstracts, case reports, comments, editorials, *etc.*; (2) For multiple publications that have been determined to be reported in the same clinical study, the publication with the most complete publication data is qualified; and (3) The literature information was insufficient to extract the required useful data.

### Selection of relevant studies

During the preliminary screening process, relevant studies were first independently selected by two authors (Yang L and Dong XZ) of this study. Any disagreements were then resolved through mutual discussion and consultation.

### Data extraction

Data were extracted independently by two researchers, including the name of the first author, year of publication, trial name, trial phase, number of participants, interventions, OS, PFS, ORR, DCR, AEs, tumor characteristics, and expression level of PD-L1 (positive expression as  $> 1\%$  and negative expression as  $\leq 1\%$ ). Any unavailable data were recorded as "NA".

### Quality assessment

Bias risk was assessed using the Cochrane Collaboration's tool<sup>[26]</sup> in the following domains: Random sequence generation, allocation concealment, blinding of outcome participants and personnel, blinding of outcome assessment, incomplete outcome data, selective reporting, and other biases. Each result was classified as low risk, high risk, or unclear risk. Quality assessment was done independently by two researchers with disagreements solved through discussion.

### Statistical analysis

To evaluate the efficacy of anti-PD-1/anti-PD-L1 antibody, the overall ORR and DCR as well as the combined OS and PFS rates (both 6 mo and 12 mo) were calculated. To assess its safety, the overall risk of AEs and grade  $\geq 3$  AEs were calculated. All statistical calculations were performed using Review Manager version 5.3 (Cochrane Collaboration's Information Management System) and STATA version 14.0 (STATA, College Station, TX, United States). Statistical heterogeneity across studies was assessed using the Cochran Q chi-square test and the  $I^2$  index. Whence significant heterogeneity was determined with either  $I^2 > 50\%$  or  $P$  value  $< 0.1$ , the random-effects model was applied<sup>[27]</sup>. Sensitivity analysis was performed by removing individual studies one by one to test the reliability of the results. Publication bias was determined using Begg's and Egger's methods.

## RESULTS

### Literature search

The whole process of study selection is shown in [Figure 1](#). Out of the 1220 initially retrieved records, 946 remained after the removal of duplicates. After the screening of titles and abstracts, 709 records were excluded and 237 were reviewed for full text. After further removal of conference reports, reviews, duplicates, and studies without clinical trials, 13 records were defined eligible<sup>[28-40]</sup>.

### Study characteristics

The detailed characteristics of the included studies are summarized in [Table 1](#). The 13 eligible studies include six single-arm trials<sup>[29,33-35,38,39]</sup>, five randomized controlled trials (RCTs)<sup>[28,30,31,37,40]</sup>, and two dose-escalation cohort expansion studies<sup>[32,36]</sup>. A total of 1618 GC/GEJC patients were included, of whom 787 received pembrolizumab, 429 received nivolumab, 375 received avelumab, and 27 received durvalumab. Pembrolizumab was intravenously administered at 200 mg in five trials<sup>[29,34,35,39,40]</sup> and 10 mg/kg in another<sup>[38]</sup>. Nivolumab was intravenously administered at 3 mg/kg in two studies<sup>[31,36]</sup>, and 360 mg in another<sup>[30]</sup>. Avelumab and durvalumab were administered at 10 mg/kg<sup>[28,32,33]</sup> and 20 mg/kg<sup>[37]</sup>, respectively.

### Quality assessment of included studies

The quality assessment was conducted using Review Manager 5.3. Details of risk of bias for each study are presented in [Figure 2](#). Due to the particularity of clinical trials in cancer treatment, the single-arm and dose-escalation trails are inherently considered high-risk in terms of bias. The 13 studies included in this meta-analysis were low-risk in terms of random sequence generation, allocation concealment, incomplete outcome data, and selective reporting. Blinding of outcome assessment and other biases might exist in two and four studies, respectively. Bias (blinding of outcome participants and personnel) was high risk. Generally speaking, the quality assessment of the included studies had a low risk of bias.

Table 1 Characteristics of included studies

Ref.	Trial	Clinical trials. gov. No.	Study design	Phase	Case, experimental vs control, (n)	Intervention methods	ORR (%)	DCR (%)	12- mo OS (%)	12- mo PFS (%)
Bang <i>et al</i> <sup>[28]</sup> 2018	JAVELIN Gastric 300	NCT02625623	RCT	III	371, 185 vs 186	Avelumab 10 mg/kg Q2 W vs paclitaxel 80 mg/m <sup>2</sup> or irinotecan 150 mg/m <sup>2</sup> 1, 8, 15 d of 4-wk cycles.	2.2	22.2	NA	NA
Bang <i>et al</i> <sup>[29]</sup> 2019	KEYNOTE-059 (cohorts 2 and 3)	NCT02335411	Single- arm	II	31	Pembrolizumab 200 mg on day 1 of 21-d cycles.	25.8	35.5	63.0	NA
Boku <i>et al</i> <sup>[30]</sup> 2019	ATTRACTION-4	NCT02746796	RCT	II	40, 21 vs 19	Nivolumab 360 mg Q3 W + SOX or Cape OX.	65.8	84.2	NA	NA
Chen <i>et al</i> <sup>[31]</sup> 2020	ATTRACTION-2	NCT02267343	RCT	III	493, 330 vs 163	Nivolumab 3 mg/kg Q2 W vs placebo 3 mg/kg Q2 W.	11.9	40.3	87.1	9.3
Chung <i>et al</i> <sup>[32]</sup> 2019	JAVELIN Solid Tumor	NCT01772004	Dose- escalation	I	150	Avelumab 10 mg/kg Q2 W.	6.7	45.3	38.0	12.6
Doi T <i>et al</i> <sup>[33]</sup> 2019	JAVELIN Solid Tumor JPN trial	NCT01943461	Single- arm	I	40	Avelumab 10 mg/kg Q2 W	10.0	52.5	31.0	NA
Fuchs <i>et al</i> <sup>[34]</sup> 2018	KEYNOTE-059 (cohorts 1)	NCT02335411	Single- arm	II	259	Pembrolizumab 200 mg Q3 W.	11.6	27.0	23.4	NA
Herbst <i>et al</i> <sup>[35]</sup> 2019	JVDF	NCT02443324	Single- arm	Ia/b	41	Pembrolizumab 200 mg on day 1 + ramucirumab 10 mg/kg days 1-8.	7.3	51.2	30.8	12.3
Janjigian <i>et al</i> <sup>[36]</sup> 2018	CheckMate-032	NCT01928394	Dose- escalation	I/II	59	Nivolumab 3 mg/kg Q2 W.	12.0	32.0	39.0	8.0
Kelly <i>et al</i> <sup>[37]</sup> 2020	NA	NCT02340975	RCT	Ib/II	27	Durvalumab 20 mg/kg + tremelimumab 1 mg/kg Q4W.	7.4	NA	37.0	NA
Muro <i>et al</i> <sup>[38]</sup> 2016	KEYNOTE-012	NCT01848834	Single- arm	Ib	39	Pembrolizumab 10 mg/ kg Q2 W.	22.0	33.0	42.0	NA
Shah <i>et al</i> <sup>[39]</sup> 2019	KEYNOTE-180	NCT02559687	Single- arm	II	121	Pembrolizumab 200 mg Q3 W.	9.9	30.6	28.0	NA
Shitara <i>et al</i> <sup>[40]</sup> 2018	KEYNOTE-061	NCT02370498	RCT	III	592, 296 vs 296	Pembrolizumab 200 mg Q3 W vs paclitaxel 80 mg/m <sup>2</sup> 1, 8, 15 d of 4-wk cycles	11.1	20.7	40.0	NA

ORR: Objective response rate; DCR: Disease control rate; OS: Overall survival; PFS: Progression-free survival; RCT: Randomized controlled trial; NA: Not available.

### ORR

ORR, which is the optimal number of partial responses (PR) or complete responses (CR) divided by the total number of patients receiving treatment, for all 1618 patients was recorded. Overall, the pooled ORR was 15% (95% confidence interval [CI]: 14%-18%,  $P < 0.001$ ), exhibiting significant heterogeneity ( $I^2 = 100\%$ ,  $P < 0.001$ ) (Figure 3). Within subgroup analysis, the pooled ORR for monotherapy was 12% (95%CI: 9%-15%,  $P < 0.001$ ) and 27% (95%CI: -6%-59%,  $P < 0.001$ ) for combined therapy.

### DCR

Only 12 trails including 1591 patients reported DCR, which is the sum of patients diagnosed with complete remission, partial remission, or stable disease. The pooled DCR was 40% (95%CI: 33%-46%,  $P < 0.001$ ), exhibiting high heterogeneity ( $I^2 = 100\%$ ,  $P < 0.001$ ) (Figure 4). Compared to patients in the monotherapy group, patients in the

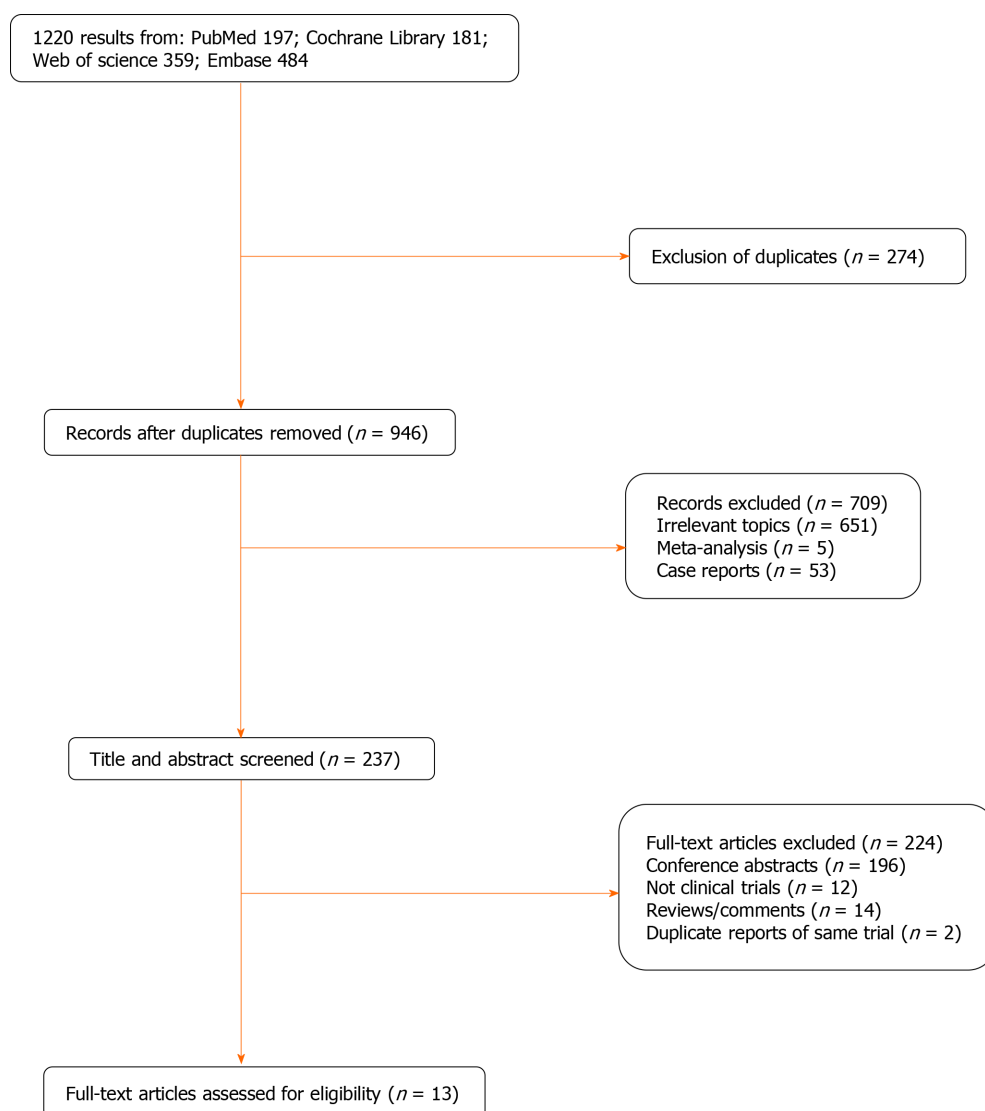


Figure 1 Record selection process.

combination group had a higher DCR (68%, 95%CI: 35%-100% *vs* 34%, 95%CI: 27%-41%).

### Survival benefits: OS and PFS

The 6-mo OS of 685 patients in six trials and 6-mo PFS of 708 patients in eight trials were reported. The pooled 6-mo OS and PFS were 54% (95%CI: 45%-64%,  $P < 0.001$ , Figure 5A) and 26% (95%CI: 20%-32%,  $P < 0.001$ , Figure 5B), respectively. Furthermore, the 6-mo OS and PFS of patients in the monotherapy group were 46% (95%CI: 45%-48%,  $P < 0.001$ ) and 21% (95%CI: 17%-26%,  $P < 0.001$ ), respectively, significantly lower than the corresponding OS of 72% (95%CI: 27%-116%,  $P < 0.001$ ) and PFS of 34% (95%CI: 3%-72%,  $P < 0.001$ ) of patients in the combination group.

The 12-mo OS and PFS were reported in 11 trials involving 1393 and 4 trials involving 580 patients. The pooled 12-mo OS and PFS were 42% (95%CI: 21%-62%,  $P < 0.001$ , Figure 5C) and 11% (95%CI: 8%-13%,  $P < 0.001$ ), respectively (Figure 5D). However, contrary to the 6-mo OS and PFS results in the subgroup analysis, the 12-mo OS of patients in the monotherapy group was 43% (95%CI: 21%-66%), significantly higher than that (34%; 95%CI: 28%-40%) of patients in the combination group, while the 12-mo PFS (12%, 95%CI: 11%-14%) of patients in the combination group was only slightly higher than that (10%, 95%CI: 7%-13%) of patients in the monotherapy group.

### PD-L1 expression and ORR

Of the 1191 patients in nine trials, the ORR was 15% (95%CI: 9%-21%,  $P < 0.001$ , Figure 6A) for patients with positive ( $> 1\%$ ) PD-L1 expression and 7% (95%CI: 3%-11%,  $P = 0.001$ , Figure 6B) for patients with negative ( $\leq 1\%$ ) PD-L1 expression. In

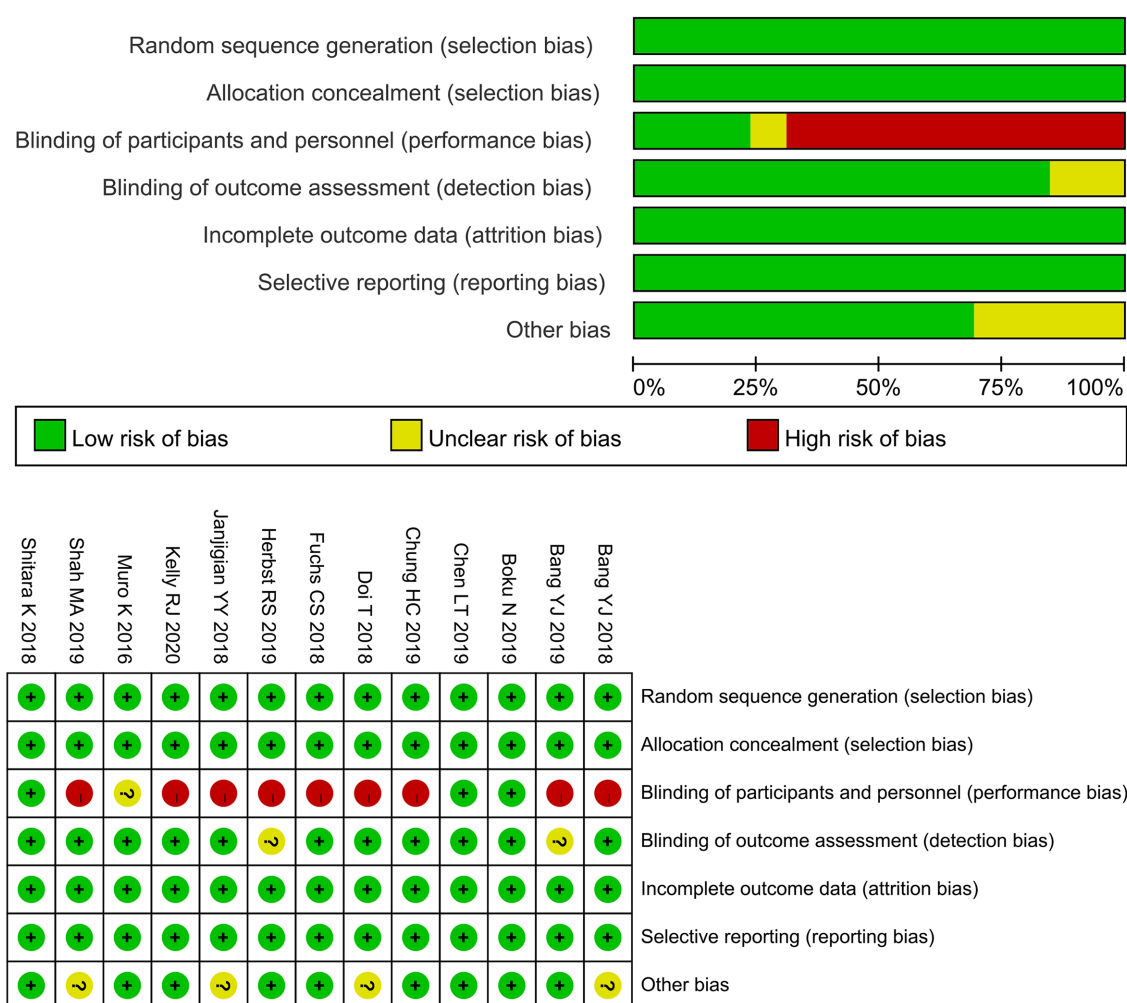


Figure 2 Risk of bias graph and summary.

addition, the pooled OR was 2.54 (95%CI: 1.56-4.15,  $P < 0.001$ ), indicating that the ORR of PD-L1 positive patients was significantly higher than that of negative patients (Figure 7).

### AEs related to treatment

Of the 1618 patients included in 13 trials reporting AEs, 869 (53.7%) experienced at least one AE and 237 (14.6%) experienced at least one grade  $\geq 3$  AE. The overall incidence of any-grade AEs was 64% (95%CI: 54%-73%,  $P < 0.001$ , Figure 8) with significantly more patients under the combination therapy than under monotherapy (84% *vs* 58%). The total incidence of grade  $\geq 3$  AEs was 18% (95%CI: 16%-20%,  $P < 0.001$ ). In the monotherapy group, the incidence of grade  $\geq 3$  AEs was 13% (95%CI: 11%-15%,  $P < 0.001$ ), which was 22% lower than that of the combination therapy group (Figure 9).

The most common any grade AEs was fatigue (15.8%; 95%CI: 11.1%-20.5%), followed by infusion reaction (13.8%; 95%CI: 1.3%-26.3%), pruritus (13.1%; 95%CI: 9.8%-16.4%), decreased appetite (9.6%), nausea (9.4%), abdominal pain (9.3%), diarrhea (8.3%) and pyrexia (8.0%). The most common grade  $\geq 3$  AEs was abdominal pain (2.8%, 95%CI: -3.4%-9.0%), and the incidence of other common grade  $\geq 3$  AEs was fairly low (Table 2).

### Publication bias and sensitivity analysis

Manual removal of any study for sensitivity analysis found no changes and reverse in the forest plot direction of all the results, indicating that the study results are both reliable and stable. Begg and Egger's tests on publication bias showed only presence of bias in 12-mo OS ( $P = 0.015 < 0.05$ ). No publication bias was found in other outcomes (Table 3).



**Table 2 Meta-analysis of common adverse events with anti-PD-1/PD-L1 antibody therapy**

Common AE	Any grade (%)	95%CI	Grade ≥ 3 (%)	95%CI
Fatigue	15.8	11.1-20.5	1.2	0.6-1.9
Infusion reaction	13.8	1.3-26.3	0.6	-0.2-1.4
Pruritus	13.1	9.8-16.4	NA	NA
Decreased appetite	9.6	5.7-13.5	0.9	0.2-1.6
Nausea	9.4	4.1-14.6	1.4	-2.5-5.4
Abdominal pain	9.3	-9.5-28.1	2.8	-3.4-9.0
Diarrhea	8.3	4.7-11.8	0.6	0.2-0.9
Pyrexia	8.0	1.3-14.6	NA	NA
Vomiting	7.8	0.1-15.4	NA	NA
Rash	7.3	5.2-9.4	0.9	-0.1-1.8
Arthralgia	6.2	3.4-9.0	NA	NA
Hypothyroidism	4.4	2.0-6.7	0.4	0-0.9
Elevated AST	4.1	2.1-6.2	1.5	-0.6-3.5
Asthenia	3.2	1.3-5.1	0.7	-0.2-1.6
Elevated ALT	2.7	1.2-4.1	0.9	-0.4-2.1
Pneumonitis	2.7	0-5.4	0.5	0-1.0
Elevated lipase	0.9	-0.4-2.2	0.7	-0.2-1.6
Colitis	0.8	0.2-1.4	0.4	0-0.8

AEs: Adverse events; CI: Confidence interval; ALT: Alanine aminotransferase; AST: Aspartate aminotransferase; NA: Not available.

**Table 3 P values of Begg and Egger's tests**

Test	ORR	DCR	6-mo OS	6-mo PFS	12-mo OS	12-mo PFS	AEs	Grade ≥ 3 AEs
Begg's <i>P</i> value	0.669	0.945	0.452	0.902	0.161	0.734	0.583	0.760
Egger's <i>P</i> value	0.973	0.890	0.810	0.448	0.015	0.821	0.924	0.992

ORR: Objective response rate; DCR: Disease control rate; OS: Overall survival; PFS: Progression-free survival; AEs: Adverse events.

## DISCUSSION

Immunoregulatory therapy has been shown to be effective in the control of advanced cancer. PD-1, a member of the CD28 family, is a receptor expressed on the surface of activated T cells that inhibits their activation and promotes apoptosis<sup>[41]</sup>. When bound to ligands, PD-1 can activate intracellular signaling pathways and inhibit the activation of immune cells, thereby reducing antibodies and cytokines secreted by immune cells and even depleting immune cells, thus maintaining the homeostasis of the immune system<sup>[42]</sup>. PD-L1 is the primary ligand of PD-1 and is expressed in certain tumor cells as well as activated B and T cells, dendritic cells, medullary cells, and endothelial cells. The molecule is also expressed in various tumor types and contributes to tumor immune escape<sup>[21,41]</sup>. The interaction between PD-1 and PD-L1 leads to down-regulation of T cells and their apoptosis and rejection by tumor microenvironment ultimately, which causes cancer cells to evade immune response<sup>[43]</sup>. Many studies have shown that blocking the interaction between PD-1 and PD-L1 can enhance T cell responses and mediate antitumor activity<sup>[44]</sup>.

Although numerous clinical trials have already confirmed the efficacy of manageable safety of anti-PD-1/PD-L1 therapy in patients with advanced GC/GEJC, so far the FDA has only approved pembrolizumab for advanced GC/GEJC patients<sup>[45]</sup>. This approval was merely based on KEYNOTE-059, a single-arm clinical

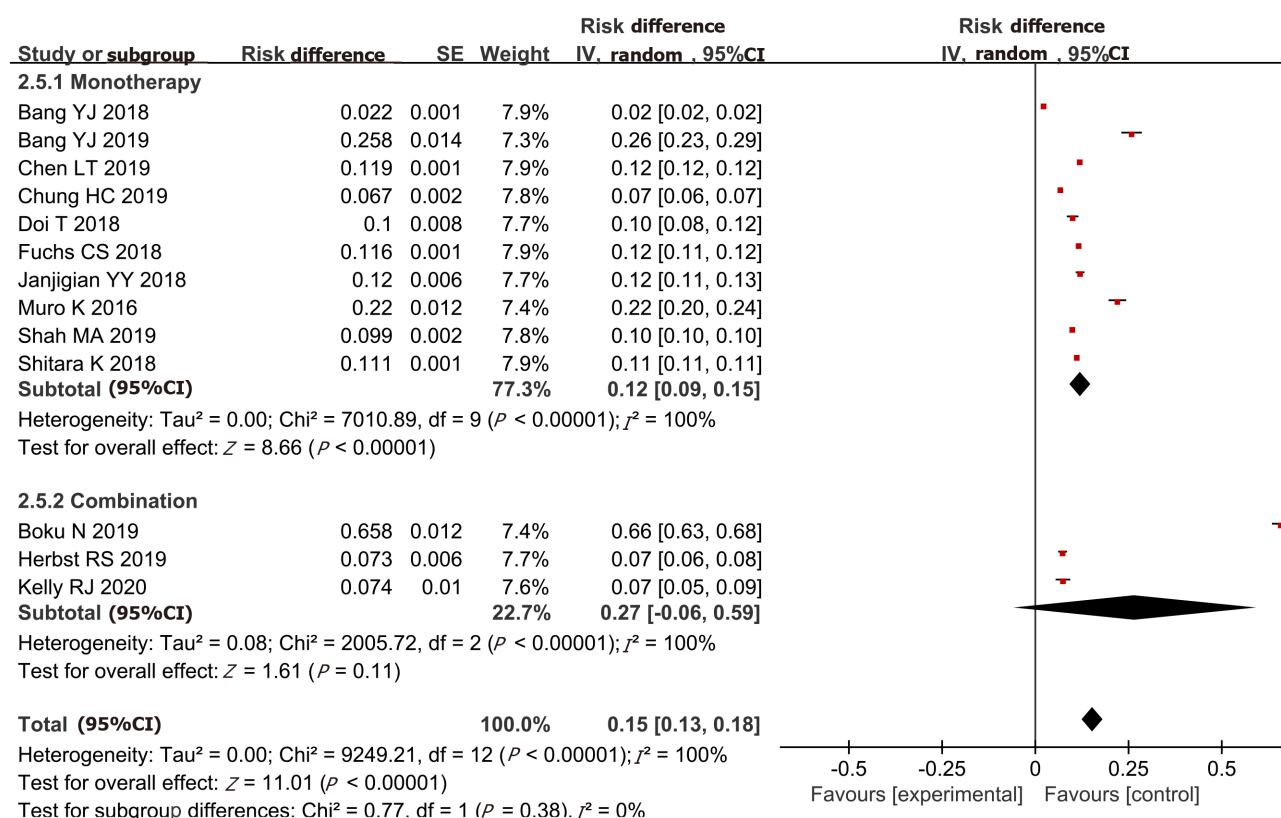


Figure 3 Pooled analysis of objective response rate.

trial, which showed an ORR of 11.6% (95%CI: 0.08-0.161) in Cohort 1, and 25.8% (95%CI: 0.119-0.46) in Cohorts 2 and 3 with a median OS of 20.7 mo (95%CI: 9.2-20.7)<sup>[29]</sup>, 15.5% (95%CI: 10.1%-22.4%) for PD-L1 positive patients and 6.4% (95%CI: 2.6%-12.8%) for PD-L1 negative patients<sup>[34]</sup>.

Contrary to the findings of KEYNOTE-059, KEYNOTE-061, which analyzed the different effects between pembrolizumab and paclitaxel in advanced GC/GEJC patients who had been previously treated<sup>[40]</sup>, and JAVELIN Gastric 300, which compared the efficacy and safety of avelumab and paclitaxel or irinotecan in GC/GEJC patients<sup>[28]</sup>, indicated that anti-PD-1/anti-PD-L1 antibody therapy is not significantly superior, in a significant way, to paclitaxel or irinotecan. ATTRACTION-2, the earliest randomized phase 3 study of an immune checkpoint inhibitor in advanced GC/GEJC patients, showed that nivolumab led to prolonged OS than placebo, and exhibited early and durable responses with a manageable safety profile<sup>[31,46]</sup>. Additionally, ATTRACTION-4, which studied the safety and efficacy of nivolumab in combination with S-1/capecitabine plus oxaliplatin in patients with previously untreated, unresectable, advanced or recurrent GC/GEJC, confirmed that nivolumab combined with chemotherapy led to manageable safety as well as clinically relevant antitumor activity with a reported ORR of 65.8%, DCR of 84.2%, and median OS over 13.9 mo.

Although the included clinical trials indicated different conclusions regarding the efficacy and safety of immune checkpoint inhibitors for advanced GC/GEJC patients, when combined, as shown in ORR, DCR, 6-mo OS, 6-mo PFS, 12-mo OS, and 12-mo PFS, it is both effective and manageably safe. A total of 15% of patients exhibited either a complete or a PR, and 40% showed progress in disease control. After treatment, 42% of patients survived for more than 1 year, with 26% exhibiting disease stability for 6 mo. Moreover, anti-PD-1/anti-PD-L1 antibody therapy also exhibited manageable safety and can, in fact, be tolerated by most patients. The total incidence of any grade AEs was 64%, with signs of fatigue (15.8%), infusion reaction (13.8%), and pruritus (13.1%), while that of grade  $\geq 3$  AEs was 18%, with signs of abdominal pain (2.8%), elevated AST (1.5%), and fatigue (1.2%). Although the immune-related AEs from anti-PD-1/anti-PD-L1 antibody occurred as a consequence of impaired self-tolerance from loss of T-cell inhibition<sup>[47]</sup>, these side effects were generally manageable but can be fatal in some cases. Therefore, doctors should pay close attention to the signs of AE during treatment and take appropriate counter measures. It should be noted that GC/GEJC patients with different PD-L1 levels reacted differently to the anti-PD-1/anti-PD-L1

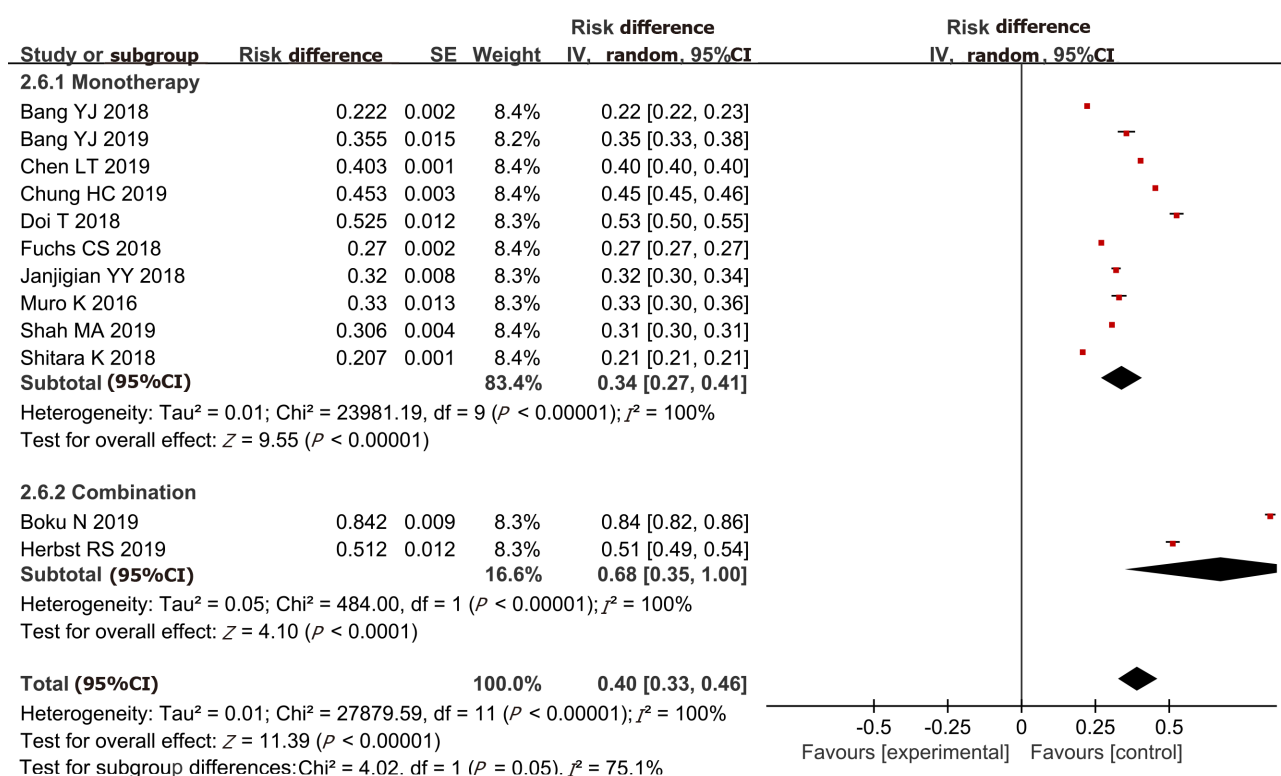


Figure 4 Pooled analysis of disease control rate.

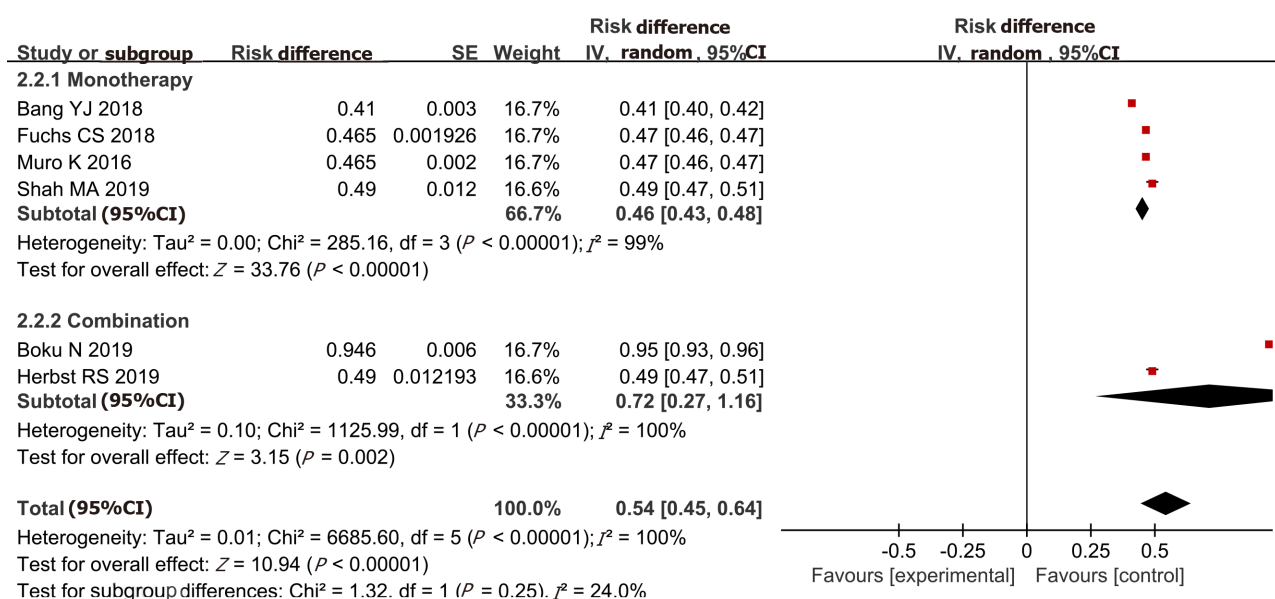
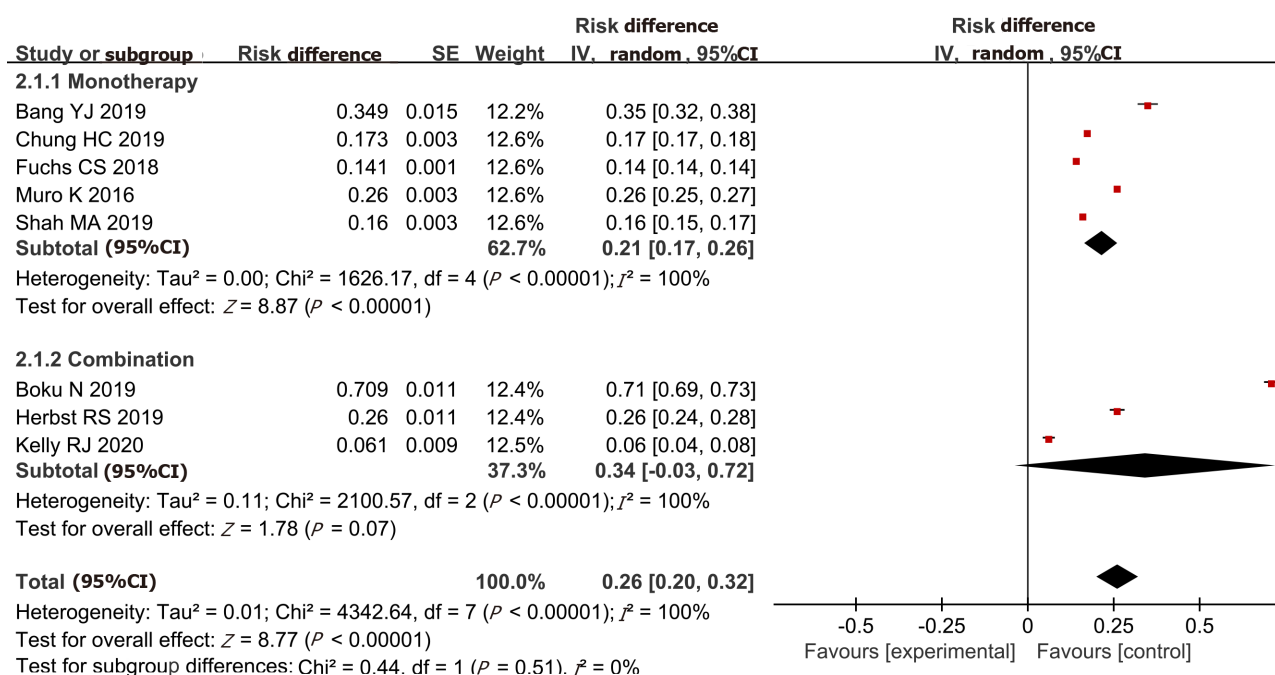
antibody therapy: Patients with PD-L1 overexpression achieved better clinical efficacy, as their ORR was 15% compared with only 7% for PD-L1 negative patients, consistent with a previous study<sup>[24]</sup>.

The Cancer Genome Atlas (TCGA) classifies gastric adenocarcinoma into four molecular subtypes: Epstein-Barr virus positive (EBV<sup>+</sup>), microsatellite instability-high (MSI-H), genomically stable, or chromosomal instability<sup>[23]</sup>. MSI-H is associated with high PD-L1 tumor expression, therefore making tumor more sensitive to immunotherapy<sup>[48,49]</sup>. Consistently, PD-L1 expression has been related to OS<sup>[50]</sup>. Additionally, a recent meta-analysis also indicated that EBV and MSI subtypes tended to express PD-L1, thus enabling PD-L1 to act as a potential screening predictor for screening for EBV and MSI subtype GC patients.

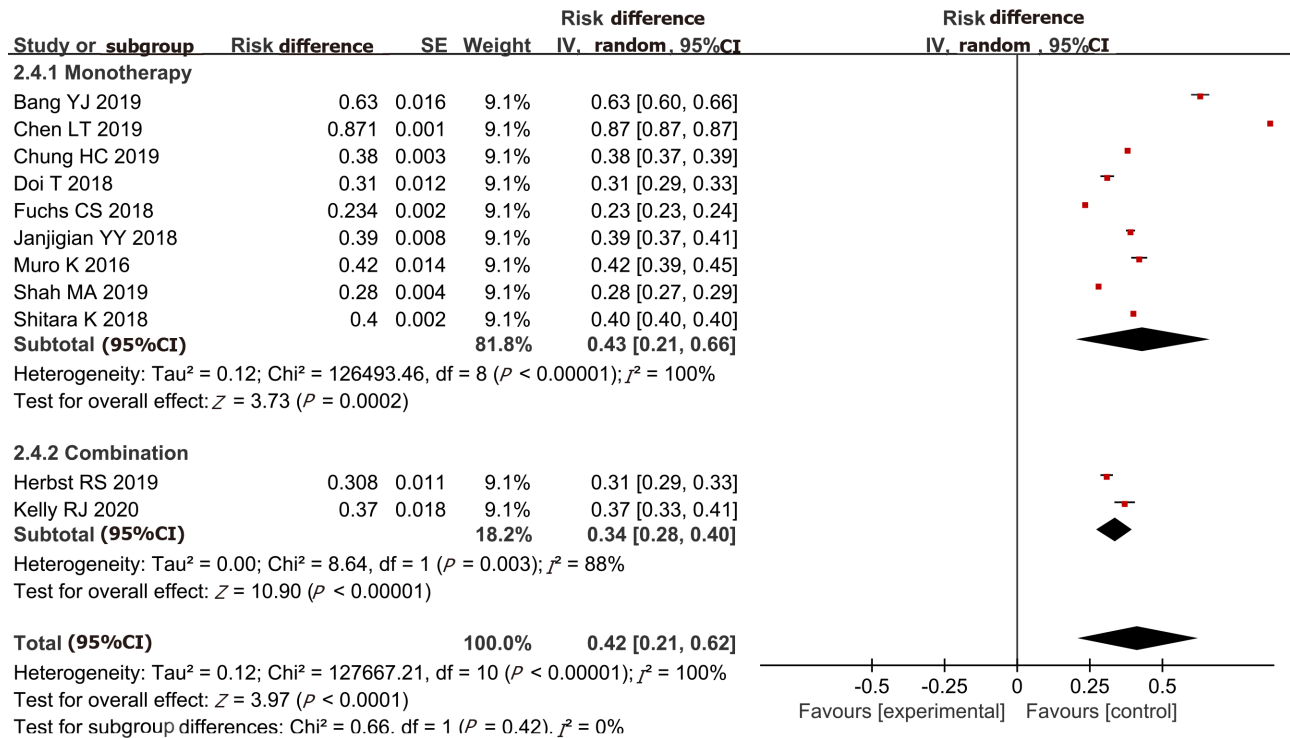
Monotherapy *vs* combination therapy analysis showed that while the ORR (27%), DCR (68%), 6-mo OS (72%), and 6-mo PFS (34%) of the combination therapy group were higher than those of the monotherapy group, the incidence rate of AEs was also higher, with 84% for any grade AEs and 35% for grade  $\geq 3$  AEs. A study in a melanoma mouse model also showed that the combined use of PD-1 inhibitors and TNF- $\alpha$  inhibitors has a better therapeutic effect than treatment with PD-1 inhibitors alone<sup>[51]</sup>. Thus, for patients who experienced reduced clinical efficacy, combination therapy may be a more potent option, although doctors should pay more attention to the potential development of AEs as well as the treatment progress of the pre-treated patients.

The efficacy and safety of combinational anti-PD-1/anti-PD-L1 antibody therapy still need to be explored. At present, only four trials were eligible to be included in this study, namely, KEYNOTE-590 (NCT03189719), CheckMate 649 (NCT02872116), KEYNOTE-062 (NCT02494583), and JAVELIN Gastric 100 (NCT02625610), which are all phase 3 clinical trials<sup>[30,35,37]</sup>. Notably, camrelizumab, a PD-1 inhibitor developed by Jiangsu Hengrui Medicine Co. Ltd., received approval in China in May 2019, although only conditionally for those who have already undergone at least two systemic chemotherapies for either relapsed or refractory classical Hodgkin lymphoma<sup>[52]</sup>. Additionally, two other phase 3 clinical trials on the efficacy and safety of camrelizumab combined with other chemotherapy drugs, NCT03691090 and NCT03813784, are under way.

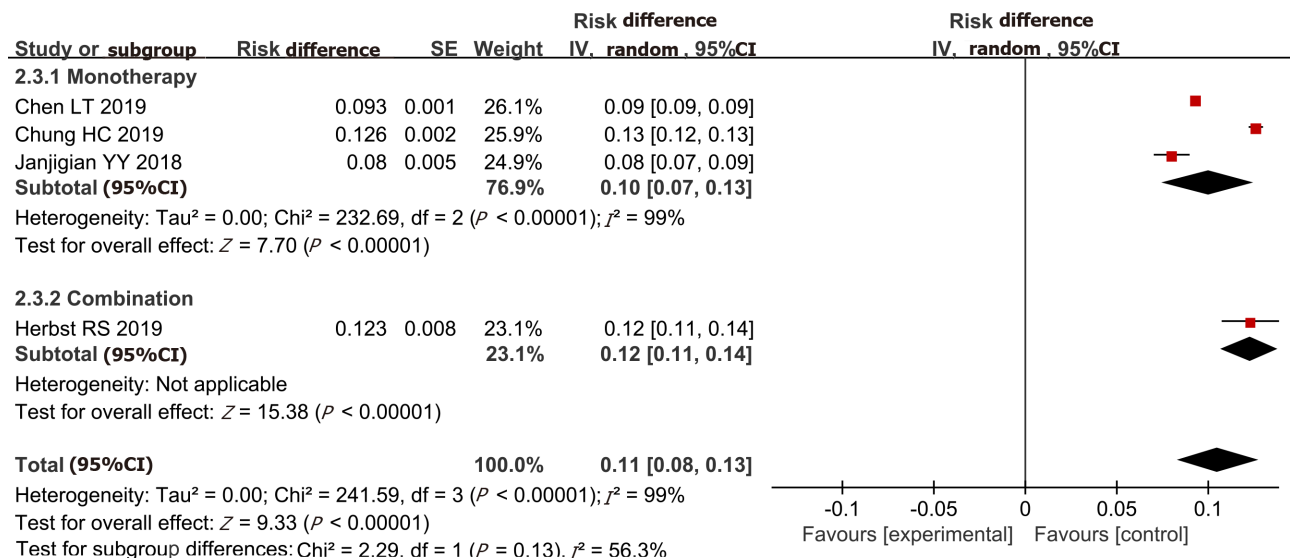
To be noted, despite the use of subgroup analysis and random effect model, our study is limited to the inherent heterogeneity of the included studies, in terms of both type and dosage of the drugs although publication bias was not found in most of the

**A****B**

C



D



**Figure 5 Overall survival and progression-free survival.** A: 6-mo overall survival (OS); B: 6-mo progression-free survival (PFS); C: 12-mo OS; D: 12-mo PFS.

studies. Out of the 13 trials, five were RCTs, while the rest were either single-arm trials or dose-escalation trials; this results in potential bias leading to the deviation of the final analysis results.

## CONCLUSION

Anti-PD-1/anti-PD-L1 antibody therapy is an effective treatment option with manageable AEs and high ORR for advanced GC/GEJC patients with overexpression



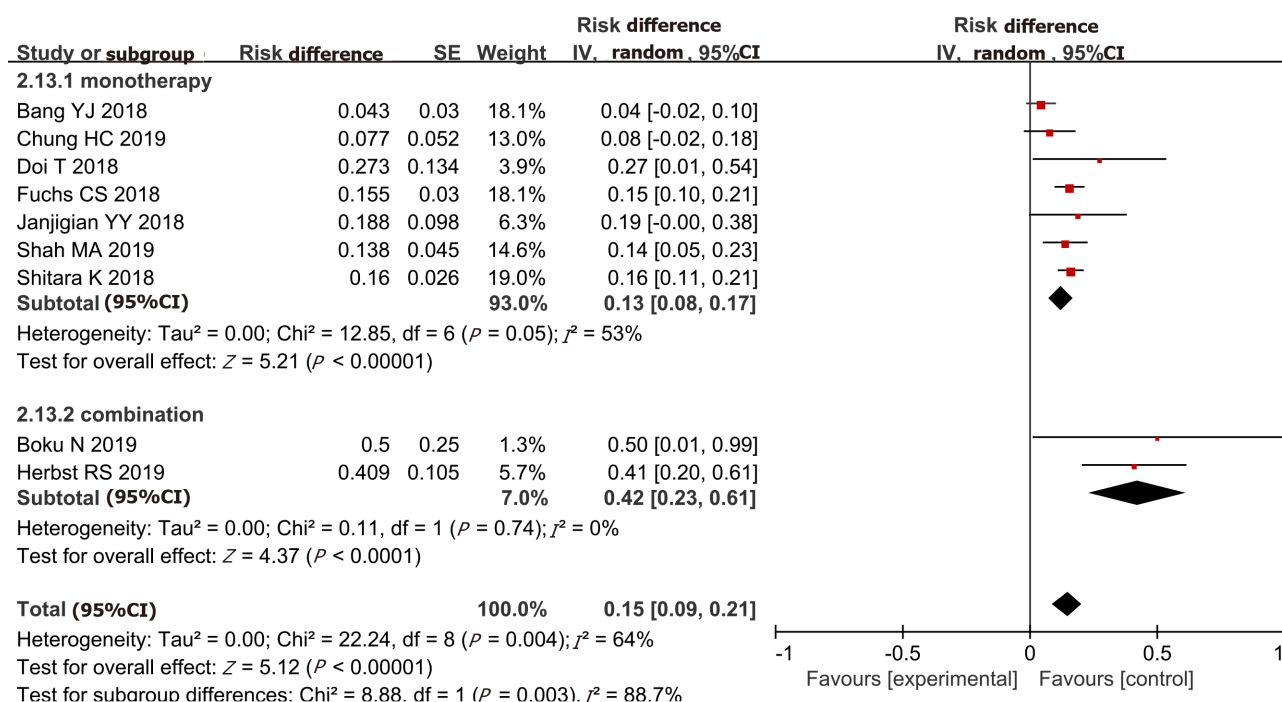
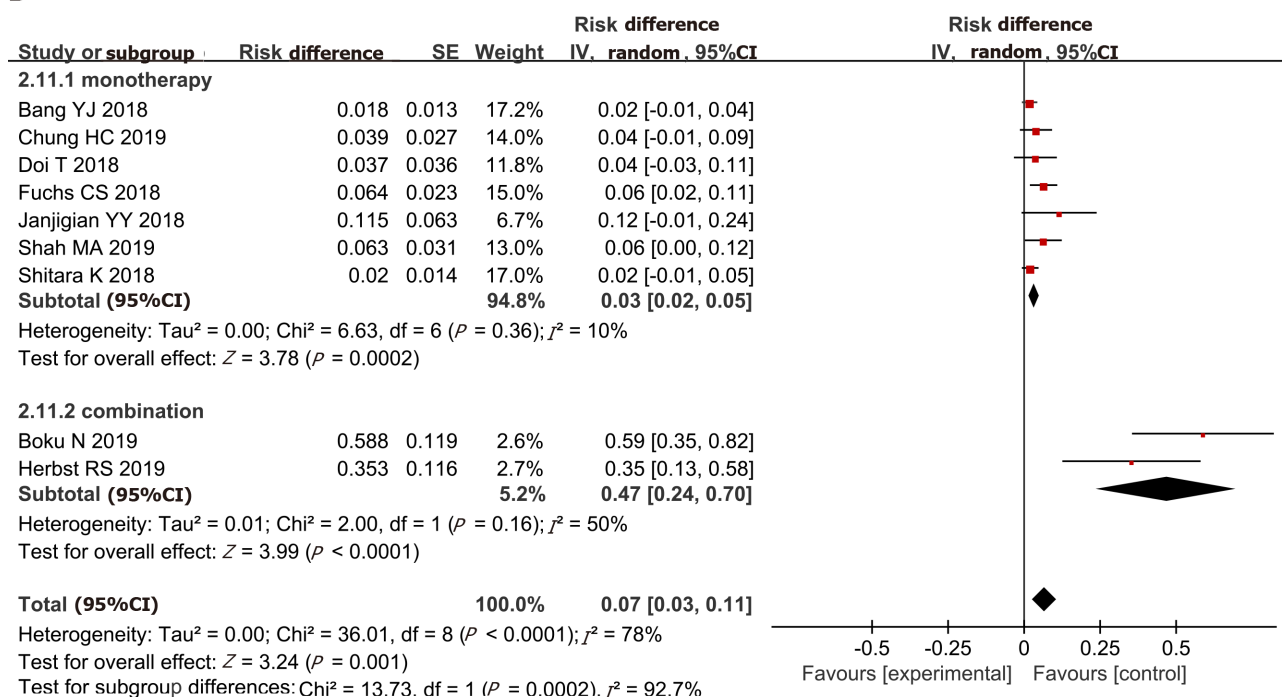
**A****B**

Figure 6 Objective response rate of PD-L1 positive (A) and negative patients (B).

of PD-L1. Furthermore, under the premise of paying close attention to safety of the treatment, it offers even better efficacy in combination with chemotherapy.

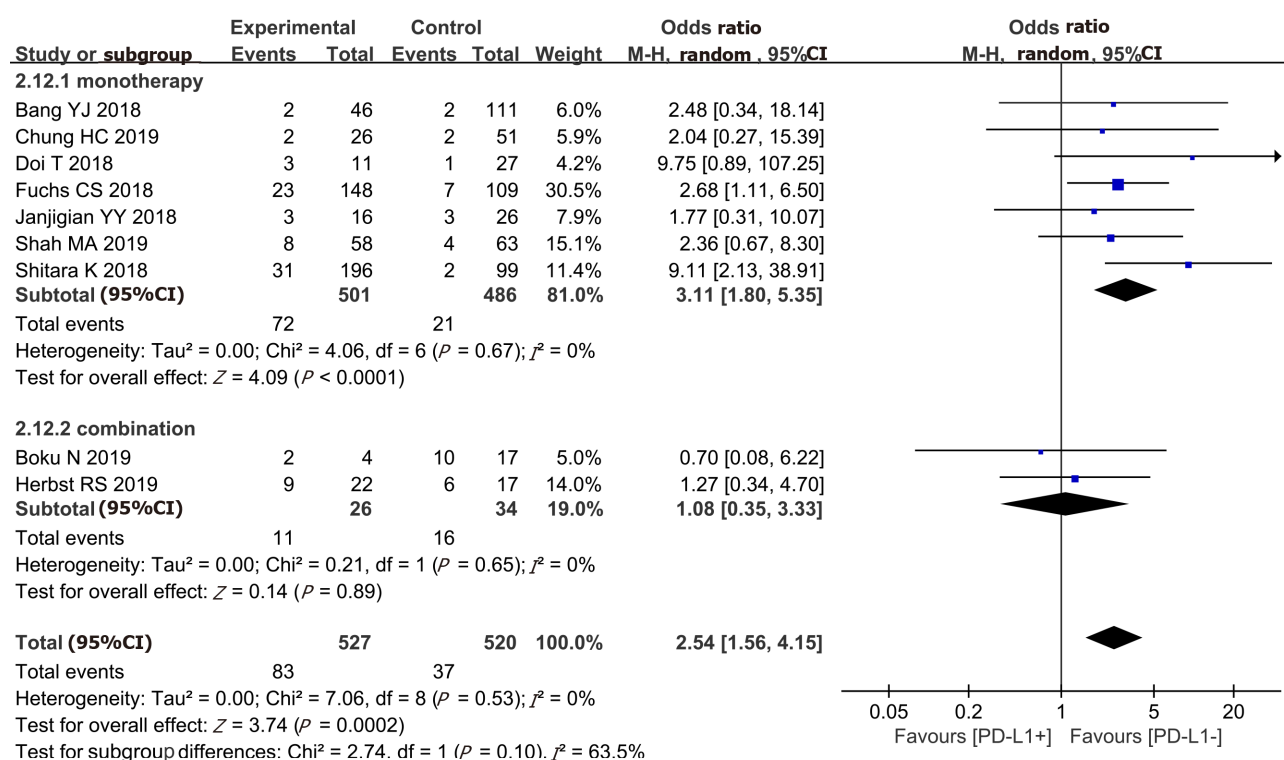


Figure 7 Comparison of objective response rate between PD-L1 positive and negative patients.

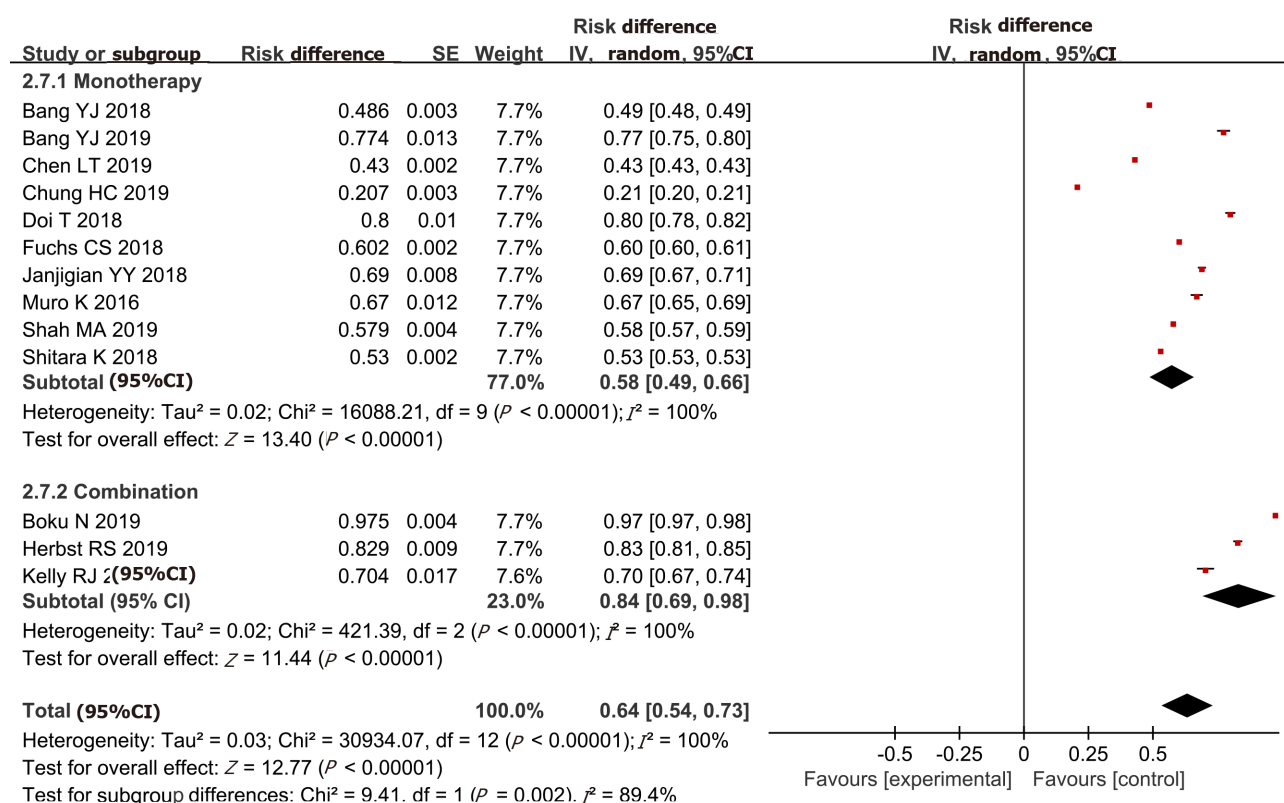
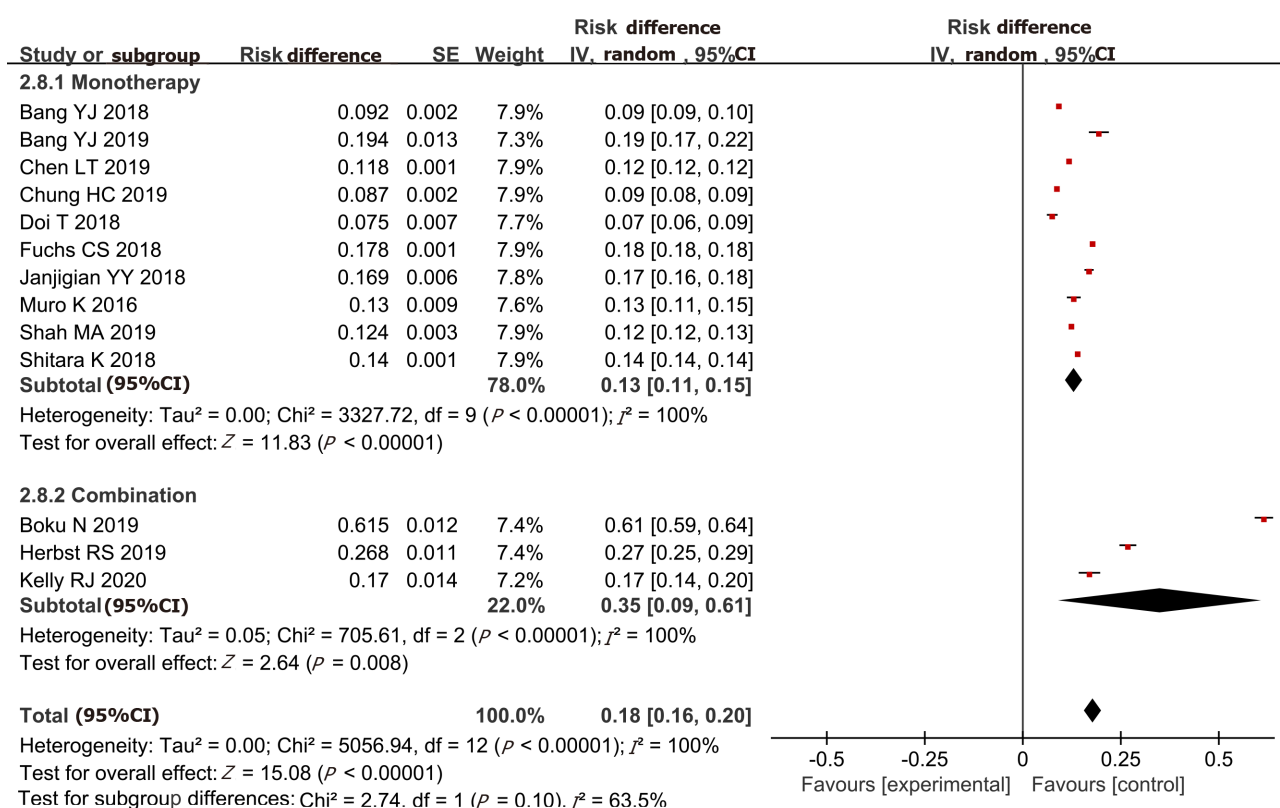


Figure 8 Pooled rate of any grade adverse events.

Figure 9 Pooled rate of grade  $\geq 3$  adverse events.

## ARTICLE HIGHLIGHTS

### Research background

Many clinical trials have confirmed that advanced gastric cancer or gastroesophageal junction cancer (GC/GEJC) patients can benefit from anti-PD-1/anti-PD-L1 antibody therapy. In addition, Epstein-Barr virus and microsatellite instability subtype gastric cancer patients tend to have high PD-L1 expression. Therefore, anti-PD-1/anti-PD-L1 antibody therapy may become a potential treatment for advanced GC/GEJC patients.

### Research motivation

To better assess the efficacy and safety of anti-PD-1/anti-PD-L1 antibody therapy, we integrated data from 13 eligible studies for a systematic review and meta-analysis.

### Research objectives

The purpose of this meta-analysis was to clarify the efficacy and safety of anti-PD-1/anti-PD-L1 antibody therapy in advanced GC/GEJC patients.

### Research methods

PubMed, Web of Science, Cochrane Library, and EMBASE databases were searched to extract relevant data according to the designed extraction scheme, and conduct statistical analysis using Review Manager 5.3 and STATA 14.0 software. The main outcomes of this study included the objective response rate (ORR), disease control rate (DCR), overall survival (OS), free survival (PFS), and adverse events (AEs).

### Research results

Our meta-analysis showed that the combined ORR and DCR were 15% (95%CI: 14%-18%) and 40% (95%CI: 33%-46%), respectively. The combined 6-mo OS and PFS were 54% (95%CI: 45%-64%) and 26% (95%CI: 20%-32%) respectively, and the 12-mo OS and PFS were 42% (95%CI: 21%-62%) and 11% (95%CI: 8%-13%). In addition, the incidence of any grade AEs and  $\geq 3$  grade AEs was 64% (95%CI: 54%-73%) and 18% (95%CI: 16%-20%), respectively.

## Research conclusions

Anti-PD-1/anti-PD-L1 antibody therapy has good anti-tumor efficacy with manageable AEs in advanced GC/GEJC patients. In addition, under the premise of paying close attention to safety of the treatment, it offers even better efficacy in combination with chemotherapy.

## Research perspectives

This meta-analysis demonstrated the efficacy and safety of anti-PD-1/anti-PD-L1 antibody therapy and high ORR for advanced GC/GEJC patients with overexpression of PD-L1. Furthermore, when paying close attention to the safety of treatment, it seems that combination with conventional chemotherapy treatment can achieve better clinical efficacy. This study has some limitations. The future research direction can be to verify the efficacy and safety of anti-PD-1/anti-PD-L1 antibody combined with chemotherapy in patients with advanced GC/GEJC.

## REFERENCES

- 1 **Bray F**, Ferlay J, Soerjomataram I, Siegel RL, Torre LA, Jemal A. Global cancer statistics 2018: GLOBOCAN estimates of incidence and mortality worldwide for 36 cancers in 185 countries. *CA Cancer J Clin* 2018; **68**: 394-424 [PMID: 30207593 DOI: 10.3322/caac.21492]
- 2 **Ang TL**, Fock KM. Clinical epidemiology of gastric cancer. *Singapore Med J* 2014; **55**: 621-628 [PMID: 25630323 DOI: 10.11622/smedj.2014174]
- 3 **den Hoed CM**, Kuipers EJ. Gastric Cancer: How Can We Reduce the Incidence of this Disease? *Curr Gastroenterol Rep* 2016; **18**: 34 [PMID: 27184043 DOI: 10.1007/s11894-016-0506-0]
- 4 **Luo G**, Zhang Y, Guo P, Wang L, Huang Y, Li K. Global patterns and trends in stomach cancer incidence: Age, period and birth cohort analysis. *Int J Cancer* 2017; **141**: 1333-1344 [PMID: 28614909 DOI: 10.1002/ijc.30835]
- 5 **Necula L**, Matei L, Dragu D, Neagu AI, Mambet C, Nedeianu S, Bleotu C, Diaconu CC, Chivu-Economescu M. Recent advances in gastric cancer early diagnosis. *World J Gastroenterol* 2019; **25**: 2029-2044 [PMID: 31114131 DOI: 10.3748/wjg.v25.i17.2029]
- 6 **Ajani JA**. Gastroesophageal cancers: progress and problems. *J Natl Compr Canc Netw* 2008; **6**: 813-814 [PMID: 18998257 DOI: 10.6004/jncn.2008.0061]
- 7 **Fontana E**, Smyth EC. Novel targets in the treatment of advanced gastric cancer: a perspective review. *Ther Adv Med Oncol* 2016; **8**: 113-125 [PMID: 26929787 DOI: 10.1177/1758834015616935]
- 8 **Venerito M**, Link A, Rokkas T, Malfertheiner P. Review: Gastric cancer-Clinical aspects. *Helicobacter* 2019; **24** Suppl 1: e12643 [PMID: 31486238 DOI: 10.1111/hel.12643]
- 9 **Dittmar Y**, Settmacher U. Individualized treatment of gastric cancer: Impact of molecular biology and pathohistological features. *World J Gastrointest Oncol* 2015; **7**: 292-302 [PMID: 26600929 DOI: 10.4251/wjgo.v7.i11.292]
- 10 **Smyth EC**, Verheij M, Allum W, Cunningham D, Cervantes A, Arnold D; ESMO Guidelines Committee. Gastric cancer: ESMO Clinical Practice Guidelines for diagnosis, treatment and follow-up. *Ann Oncol* 2016; **27**: v38-v49 [PMID: 27664260 DOI: 10.1093/annonc/mdw350]
- 11 **Goode EF**, Smyth EC. Immunotherapy for Gastroesophageal Cancer. *J Clin Med* 2016; **5** [PMID: 27669318 DOI: 10.3390/jcm5100084]
- 12 **Ajani JA**, D'Amico TA, Almhanna K, Bentrem DJ, Chao J, Das P, Denlinger CS, Fanta P, Farjah F, Fuchs CS, Gerdes H, Gibson M, Glasgow RE, Hayman JA, Hochwald S, Hofstetter WL, Ilson DH, Jaroszewski D, Johung KL, Keswani RN, Kleinberg LR, Korn WM, Leong S, Linn C, Lockhart AC, Ly QP, Mulcahy MF, Orringer MB, Perry KA, Poultsides GA, Scott WJ, Strong VE, Washington MK, Weksler B, Willett CG, Wright CD, Zelman D, McMillian N, Sundar H. Gastric Cancer, Version 3.2016, NCCN Clinical Practice Guidelines in Oncology. *J Natl Compr Canc Netw* 2016; **14**: 1286-1312 [PMID: 27697982 DOI: 10.6004/jncn.2016.0137]
- 13 **Ford HE**, Marshall A, Bridgewater JA, Janowitz T, Coxon FY, Wadsley J, Mansoor W, Fyfe D, Madhusudan S, Middleton GW, Swinson D, Falk S, Chau I, Cunningham D, Kareclas P, Cook N, Blazeby JM, Dunn JA; COUGAR-02 Investigators. Docetaxel versus active symptom control for refractory oesophagogastric adenocarcinoma (COUGAR-02): an open-label, phase 3 randomised controlled trial. *Lancet Oncol* 2014; **15**: 78-86 [PMID: 24332238 DOI: 10.1016/S1470-2045(13)70549-7]
- 14 **Smyth EC**, Moehler M. Late-line treatment in metastatic gastric cancer: today and tomorrow. *Ther Adv Med Oncol* 2019; **11**: 1758835919867522 [PMID: 31489035 DOI: 10.1177/1758835919867522]
- 15 **Sharma P**, Allison JP. The future of immune checkpoint therapy. *Science* 2015; **348**: 56-61 [PMID: 25838373 DOI: 10.1126/science.aaa8172]
- 16 **Hayashi H**, Nakagawa K. Combination therapy with PD-1 or PD-L1 inhibitors for cancer. *Int J Clin Oncol* 2020; **25**: 818-830 [PMID: 31549270 DOI: 10.1007/s10147-019-01548-1]
- 17 **Dong Y**, Sun Q, Zhang X. PD-1 and its ligands are important immune checkpoints in cancer. *Oncotarget* 2017; **8**: 2171-2186 [PMID: 27974689 DOI: 10.18632/oncotarget.13895]
- 18 **Alsaab HO**, Sau S, Alzhrani R, Tatiparti K, Bhise K, Kashaw SK, Iyer AK. PD-1 and PD-L1 Checkpoint Signaling Inhibition for Cancer Immunotherapy: Mechanism, Combinations, and Clinical Outcome. *Front Pharmacol* 2017; **8**: 561 [PMID: 28878676 DOI: 10.3389/fphar.2017.00561]
- 19 **Weber J**, Mandala M, Del Vecchio M, Gogas HJ, Arance AM, Cowey CL, Dalle S, Schenker M, Chiarion-Sileni V, Marquez-Rodas I, Grob JJ, Butler MO, Middleton MR, Maio M, Atkinson V, Queirolo P, Gonzalez

- R, Kudchadkar RR, Smylie M, Meyer N, Mortier L, Atkins MB, Long GV, Bhatia S, Lebbé C, Rutkowski P, Yokota K, Yamazaki N, Kim TM, de Pril V, Sabater J, Qureshi A, Larkin J, Ascierto PA; CheckMate 238 Collaborators. Adjuvant Nivolumab *versus* Ipilimumab in Resected Stage III or IV Melanoma. *N Engl J Med* 2017; **377**: 1824-1835 [PMID: [28891423](#) DOI: [10.1056/NEJMoa1709030](#)]
- 20 **Cancer Genome Atlas Research Network.** Comprehensive molecular characterization of gastric adenocarcinoma. *Nature* 2014; **513**: 202-209 [PMID: [25079317](#) DOI: [10.1038/nature13480](#)]
- 21 **Zhang M,** Dong Y, Liu H, Wang Y, Zhao S, Xuan Q, Wang Y, Zhang Q. The clinicopathological and prognostic significance of PD-L1 expression in gastric cancer: a meta-analysis of 10 studies with 1,901 patients. *Sci Rep* 2016; **6**: 37933 [PMID: [27892511](#) DOI: [10.1038/srep37933](#)]
- 22 **Li J,** Chen L, Xiong Y, Zheng X, Xie Q, Zhou Q, Shi L, Wu C, Jiang J, Wang H. Knockdown of PD-L1 in Human Gastric Cancer Cells Inhibits Tumor Progression and Improves the Cytotoxic Sensitivity to CIK Therapy. *Cell Physiol Biochem* 2017; **41**: 907-920 [PMID: [28222426](#) DOI: [10.1159/000460504](#)]
- 23 **Brahmer JR,** Tykodi SS, Chow LQ, Hwu WJ, Topalian SL, Hwu P, Drake CG, Camacho LH, Kauh J, Odunsi K, Pitot HC, Hamid O, Bhatia S, Martins R, Eaton K, Chen S, Salay TM, Alaparthi S, Grosso JF, Korman AJ, Parker SM, Agrawal S, Goldberg SM, Pardoll DM, Gupta A, Wigginton JM. Safety and activity of anti-PD-L1 antibody in patients with advanced cancer. *N Engl J Med* 2012; **366**: 2455-2465 [PMID: [22658128](#) DOI: [10.1056/NEJMoa1200694](#)]
- 24 **Bagley SJ,** Bauml JM, Langer CJ. PD-1/PD-L1 immune checkpoint blockade in non-small cell lung cancer. *Clin Adv Hematol Oncol* 2015; **13**: 676-683 [PMID: [27058572](#)]
- 25 **Moher D,** Liberati A, Tetzlaff J, Altman DG; PRISMA Group. Preferred reporting items for systematic reviews and meta-analyses: the PRISMA statement. *Int J Surg* 2010; **8**: 336-341 [PMID: [20171303](#) DOI: [10.1016/j.ijsu.2010.02.007](#)]
- 26 **Higgins JP,** Altman DG, Gøtzsche PC, Jüni P, Moher D, Oxman AD, Savovic J, Schulz KF, Weeks L, Sterne JA; Cochrane Bias Methods Group; Cochrane Statistical Methods Group. The Cochrane Collaboration's tool for assessing risk of bias in randomised trials. *BMJ* 2011; **343**: d5928 [PMID: [22008217](#) DOI: [10.1136/bmj.d5928](#)]
- 27 **Cumpston M,** Li T, Page MJ, Chandler J, Welch VA, Higgins JP, Thomas J. Updated guidance for trusted systematic reviews: a new edition of the Cochrane Handbook for Systematic Reviews of Interventions. *Cochrane Database Syst Rev* 2019; **10**: ED000142 [PMID: [31643080](#) DOI: [10.1002/14651858.ED000142](#)]
- 28 **Bang YJ,** Ruiz EY, Van Cutsem E, Lee KW, Wyrwicz L, Schenker M, Alsina M, Ryu MH, Chung HC, Evesque L, Al-Batran SE, Park SH, Lichinitser M, Boku N, Moehler MH, Hong J, Xiong H, Hallwachs R, Conti I, Taieb J. Phase III, randomised trial of avelumab *versus* physician's choice of chemotherapy as third-line treatment of patients with advanced gastric or gastro-oesophageal junction cancer: primary analysis of JAVELIN Gastric 300. *Ann Oncol* 2018; **29**: 2052-2060 [PMID: [30052729](#) DOI: [10.1093/annonc/mdy264](#)]
- 29 **Bang YJ,** Kang YK, Catenacci DV, Muro K, Fuchs CS, Geva R, Hara H, Golan T, Garrido M, Jalal SI, Borg C, Doi T, Yoon HH, Savage MJ, Wang J, Dalal RP, Shah S, Wainberg ZA, Chung HC. Pembrolizumab alone or in combination with chemotherapy as first-line therapy for patients with advanced gastric or gastroesophageal junction adenocarcinoma: results from the phase II nonrandomized KEYNOTE-059 study. *Gastric Cancer* 2019; **22**: 828-837 [PMID: [30911859](#) DOI: [10.1007/s10120-018-00909-5](#)]
- 30 **Boku N,** Ryu MH, Kato K, Chung HC, Minashi K, Lee KW, Cho H, Kang WK, Komatsu Y, Tsuda M, Yamaguchi K, Hara H, Fumita S, Azuma M, Chen LT, Kang YK. Safety and efficacy of nivolumab in combination with S-1/capecitabine plus oxaliplatin in patients with previously untreated, unresectable, advanced, or recurrent gastric/gastroesophageal junction cancer: interim results of a randomized, phase II trial (ATTRACTION-4). *Ann Oncol* 2019; **30**: 250-258 [PMID: [30566590](#) DOI: [10.1093/annonc/mdy540](#)]
- 31 **Chen LT,** Satoh T, Ryu MH, Chao Y, Kato K, Chung HC, Chen JS, Muro K, Kang WK, Yeh KH, Yoshikawa T, Oh SC, Bai LY, Tamura T, Lee KW, Hamamoto Y, Kim JG, Chin K, Oh DY, Minashi K, Cho JY, Tsuda M, Sameshima H, Kang YK, Boku N. A phase 3 study of nivolumab in previously treated advanced gastric or gastroesophageal junction cancer (ATTRACTION-2): 2-year update data. *Gastric Cancer* 2020; **23**: 510-519 [PMID: [31863227](#) DOI: [10.1007/s10120-019-01034-7](#)]
- 32 **Chung HC,** Arkenau HT, Lee J, Rha SY, Oh DY, Wyrwicz L, Kang YK, Lee KW, Infante JR, Lee SS, Kemeny M, Keilholz U, Melichar B, Mita A, Plummer R, Smith D, Gelb AB, Xiong H, Hong J, Chand V, Safran H. Avelumab (anti-PD-L1) as first-line switch-maintenance or second-line therapy in patients with advanced gastric or gastroesophageal junction cancer: phase 1b results from the JAVELIN Solid Tumor trial. *J Immunother Cancer* 2019; **7**: 30 [PMID: [30717797](#) DOI: [10.1186/s40425-019-0508-1](#)]
- 33 **Doi T,** Iwasa S, Muro K, Satoh T, Hironaka S, Esaki T, Nishina T, Hara H, Machida N, Komatsu Y, Shimada Y, Otsu S, Shimizu S, Watanabe M. Phase 1 trial of avelumab (anti-PD-L1) in Japanese patients with advanced solid tumors, including dose expansion in patients with gastric or gastroesophageal junction cancer: the JAVELIN Solid Tumor JPN trial. *Gastric Cancer* 2019; **22**: 817-827 [PMID: [30515672](#) DOI: [10.1007/s10120-018-0903-1](#)]
- 34 **Fuchs CS,** Doi T, Jang RW, Muro K, Satoh T, Machado M, Sun W, Jalal SI, Shah MA, Metges JP, Garrido M, Golan T, Mandala M, Wainberg ZA, Catenacci DV, Ohtsu A, Shitara K, Geva R, Bleeker J, Ko AH, Ku G, Philip P, Enzinger PC, Bang YJ, Levitan D, Wang J, Rosales M, Dalal RP, Yoon HH. Safety and Efficacy of Pembrolizumab Monotherapy in Patients With Previously Treated Advanced Gastric and Gastroesophageal Junction Cancer: Phase 2 Clinical KEYNOTE-059 Trial. *JAMA Oncol* 2018; **4**: e180013 [PMID: [29543932](#) DOI: [10.1001/jamaoncol.2018.0013](#)]
- 35 **Herbst RS,** Arkenau HT, Santana-Davila R, Calvo E, Paz-Ares L, Cassier PA, Bendell J, Penel N, Krebs MG, Martin-Liberal J, Isambert N, Soriano A, Wermke M, Cultrera J, Gao L, Widau RC, Mi G, Jin J, Ferry D, Fuchs CS, Petrylak DP, Chau I. Ramucicromab plus pembrolizumab in patients with previously treated advanced non-small-cell lung cancer, gastro-oesophageal cancer, or urothelial carcinomas (JVDF): a multicohort, non-randomised, open-label, phase 1a/b trial. *Lancet Oncol* 2019; **20**: 1109-1123 [PMID: [31301962](#) DOI: [10.1016/S1470-2045\(19\)30458-9](#)]
- 36 **Janjigian YY,** Bendell J, Calvo E, Kim JW, Ascierto PA, Sharma P, Ott PA, Peltola K, Jaeger D, Evans J, de Braud F, Chau I, Harbison CT, Dorange C, Tschaike M, Le DT. CheckMate-032 Study: Efficacy and



- Safety of Nivolumab and Nivolumab Plus Ipilimumab in Patients With Metastatic Esophagogastric Cancer. *J Clin Oncol* 2018; **36**: 2836-2844 [PMID: [30110194](#) DOI: [10.1200/JCO.2017.76.6212](#)]
- 37 **Kelly RJ**, Lee J, Bang YJ, Almanna K, Blum-Murphy M, Catenacci DVT, Chung HC, Wainberg ZA, Gibson MK, Lee KW, Bendell JC, Denlinger CS, Chee CE, Omori T, Leidner R, Lenz HJ, Chao Y, Reblatto MC, Brohawn PZ, He P, McDevitt J, Sheth S, Englert JM, Ku GY. Safety and Efficacy of Durvalumab and Tremelimumab Alone or in Combination in Patients with Advanced Gastric and Gastroesophageal Junction Adenocarcinoma. *Clin Cancer Res* 2020; **26**: 846-854 [PMID: [31676670](#) DOI: [10.1158/1078-0432.CCR-19-2443](#)]
  - 38 **Muro K**, Chung HC, Shankaran V, Geva R, Catenacci D, Gupta S, Eder JP, Golan T, Le DT, Burtness B, McRee AJ, Lin CC, Pathiraja K, Lunceford J, Emancipator K, Juco J, Koshiji M, Bang YJ. Pembrolizumab for patients with PD-L1-positive advanced gastric cancer (KEYNOTE-012): a multicentre, open-label, phase 1b trial. *Lancet Oncol* 2016; **17**: 717-726 [PMID: [27157491](#) DOI: [10.1016/S1470-2045\(16\)00175-3](#)]
  - 39 **Shah MA**, Kojima T, Hochhauser D, Enzinger P, Raimbourg J, Hollebecque A, Lordick F, Kim SB, Tajika M, Kim HT, Lockhart AC, Arkenau HT, El-Hajbi F, Gupta M, Pfeiffer P, Liu Q, Lunceford J, Kang SP, Bhagia P, Kato K. Efficacy and Safety of Pembrolizumab for Heavily Pretreated Patients With Advanced, Metastatic Adenocarcinoma or Squamous Cell Carcinoma of the Esophagus: The Phase 2 KEYNOTE-180 Study. *JAMA Oncol* 2019; **5**: 546-550 [PMID: [30570649](#) DOI: [10.1001/jamaoncol.2018.5441](#)]
  - 40 **Shitara K**, Özgüroğlu M, Bang YJ, Di Bartolomeo M, Mandalà M, Ryu MH, Fornaro L, Olesiński T, Caglevic C, Chung HC, Muro K, Goekkurt E, Mansoor W, McDermott RS, Shacham-Shmueli E, Chen X, Mayo C, Kang SP, Ohtsu A, Fuchs CS; KEYNOTE-061 investigators. Pembrolizumab versus paclitaxel for previously treated, advanced gastric or gastro-oesophageal junction cancer (KEYNOTE-061): a randomised, open-label, controlled, phase 3 trial. *Lancet* 2018; **392**: 123-133 [PMID: [29880231](#) DOI: [10.1016/S0140-6736\(18\)31257-1](#)]
  - 41 **Zou W**, Wolchok JD, Chen L. PD-L1 (B7-H1) and PD-1 pathway blockade for cancer therapy: Mechanisms, response biomarkers, and combinations. *Sci Transl Med* 2016; **8**: 328rv4 [PMID: [26936508](#) DOI: [10.1126/scitranslmed.aad7118](#)]
  - 42 **Jiang X**, Wang J, Deng X, Xiong F, Ge J, Xiang B, Wu X, Ma J, Zhou M, Li X, Li Y, Li G, Xiong W, Guo C, Zeng Z. Role of the tumor microenvironment in PD-L1/PD-1-mediated tumor immune escape. *Mol Cancer* 2019; **18**: 10 [PMID: [30646912](#) DOI: [10.1186/s12943-018-0928-4](#)]
  - 43 **Iwai Y**, Hamanishi J, Chamoto K, Honjo T. Cancer immunotherapies targeting the PD-1 signaling pathway. *J Biomed Sci* 2017; **24**: 26 [PMID: [28376884](#) DOI: [10.1186/s12929-017-0329-9](#)]
  - 44 **Dermani FK**, Samadi P, Rahmani G, Kohlan AK, Najafi R. PD-1/PD-L1 immune checkpoint: Potential target for cancer therapy. *J Cell Physiol* 2019; **234**: 1313-1325 [PMID: [30191996](#) DOI: [10.1002/jcp.27172](#)]
  - 45 **Fashoyin-Aje L**, Donoghue M, Chen H, He K, Veeraraghavan J, Goldberg KB, Keegan P, McKee AE, Pazdur R. FDA Approval Summary: Pembrolizumab for Recurrent Locally Advanced or Metastatic Gastric or Gastroesophageal Junction Adenocarcinoma Expressing PD-L1. *Oncologist* 2019; **24**: 103-109 [PMID: [30120163](#) DOI: [10.1634/theoncologist.2018-0221](#)]
  - 46 **Kang YK**, Boku N, Satoh T, Ryu MH, Chao Y, Kato K, Chung HC, Chen JS, Muro K, Kang WK, Yeh KH, Yoshikawa T, Oh SC, Bai LY, Tamura T, Lee KW, Hamamoto Y, Kim JG, Chin K, Oh DY, Minashi K, Cho JY, Tsuda M, Chen LT. Nivolumab in patients with advanced gastric or gastro-oesophageal junction cancer refractory to, or intolerant of, at least two previous chemotherapy regimens (ONO-4538-12, ATTRACTION-2): a randomised, double-blind, placebo-controlled, phase 3 trial. *Lancet* 2017; **390**: 2461-2471 [PMID: [28993052](#) DOI: [10.1016/S0140-6736\(17\)31827-5](#)]
  - 47 **Spain L**, Diem S, Larkin J. Management of toxicities of immune checkpoint inhibitors. *Cancer Treat Rev* 2016; **44**: 51-60 [PMID: [26874776](#) DOI: [10.1016/j.ctrv.2016.02.001](#)]
  - 48 **Dudley JC**, Lin MT, Le DT, Eshleman JR. Microsatellite Instability as a Biomarker for PD-1 Blockade. *Clin Cancer Res* 2016; **22**: 813-820 [PMID: [26880610](#) DOI: [10.1158/1078-0432.CCR-15-1678](#)]
  - 49 **Ma C**, Patel K, Singhi AD, Ren B, Zhu B, Shaikh F, Sun W. Programmed Death-Ligand 1 Expression Is Common in Gastric Cancer Associated With Epstein-Barr Virus or Microsatellite Instability. *Am J Surg Pathol* 2016; **40**: 1496-1506 [PMID: [27465786](#) DOI: [10.1097/PAS.0000000000000698](#)]
  - 50 **Gu L**, Chen M, Guo D, Zhu H, Zhang W, Pan J, Zhong X, Li X, Qian H, Wang X. PD-L1 and gastric cancer prognosis: A systematic review and meta-analysis. *PLoS One* 2017; **12**: e0182692 [PMID: [28796808](#) DOI: [10.1371/journal.pone.0182692](#)]
  - 51 **Bertrand F**, Montfort A, Marcheteau E, Imbert C, Gilhodes J, Filleron T, Rochemaux P, Andrieu-Abadie N, Levade T, Meyer N, Colacios C, Séguin B. TNF $\alpha$  blockade overcomes resistance to anti-PD-1 in experimental melanoma. *Nat Commun* 2017; **8**: 2256 [PMID: [29273790](#) DOI: [10.1038/s41467-017-02358-7](#)]
  - 52 **Markham A**, Keam SJ. Camrelizumab: First Global Approval. *Drugs* 2019; **79**: 1355-1361 [PMID: [31313098](#) DOI: [10.1007/s40265-019-01167-0](#)]



## Inferior mesenteric arteriovenous fistula during treatment with bevacizumab in colorectal cancer patient: A case report

Ayako Doi, Hiroyuki Takeda, Kumiko Umemoto, Ryosuke Oumi, Shinji Wada, Shingo Hamaguchi, Hidefumi Mimura, Hiroyuki Arai, Yoshiki Horie, Takuro Mizukami, Naoki Izawa, Takashi Ogura, Takako Eguchi Nakajima, Yu Sunakawa

**ORCID number:** Ayako Doi 0000-0003-3140-2654; Hiroyuki Takeda 0000-0002-2847-7105; Kumiko Umemoto 0000-0001-8698-3893; Ryosuke Oumi 0000-0001-8071-828X; Shinji Wada 0000-0001-7172-1508; Shingo Hamaguchi 0000-0003-0354-417X; Hidefumi Mimura 0000-0002-5205-6394; Hiroyuki Arai 0000-0001-5447-4197; Yoshiki Horie 0000-0001-5568-6562; Takuro Mizukami 0000-0002-9960-5629; Naoki Izawa 0000-0003-3653-5325; Takashi Ogura 0000-0002-6326-9993; Takako Eguchi Nakajima 0000-0002-4589-2335; Yu Sunakawa 0000-0002-0163-7543.

**Author contributions:** Doi A was the patient's medical oncologist, reviewed the literature, and contributed to manuscript drafting; Takeda H, Umemoto K, Arai H, Horie Y, Mizukami T, Izawa N, Ogura T, Nakajima TE, and Sunakawa Y reviewed the literature and contributed to manuscript drafting; Oumi R was the gastroenterology disease consultation, reviewed the literature, and drafted the manuscript; Wada S, Hamaguchi S, and Mimura H interpreted the imaging findings and contributed to manuscript drafting; All authors issued final approval for the version to be submitted.

**Informed consent statement:**

Ayako Doi, Hiroyuki Takeda, Kumiko Umemoto, Hiroyuki Arai, Yoshiki Horie, Takuro Mizukami, Naoki Izawa, Takashi Ogura, Yu Sunakawa, Department of Clinical Oncology, St. Marianna University School of Medicine, Kanagawa 216-8511, Japan

Ryosuke Oumi, Department of Gastroenterology, St. Marianna University School of Medicine, Kanagawa 216-8511, Japan

Shinji Wada, Shingo Hamaguchi, Hidefumi Mimura, Department of Radiology, St. Marianna University School of Medicine, Kanagawa 216-8511, Japan

Takako Eguchi Nakajima, Innovation Center for Next Generation Clinical Trials and iPS Cell Therapy, Kyoto University Hospital, Kyoto 606-8507, Japan

**Corresponding author:** Yu Sunakawa, PhD, Associate Professor, Department of Clinical Oncology, St. Marianna University School of Medicine, 2-16-1, Sugao, Miyamae-ku, Kawasaki, Kanagawa 216-8511, Japan. [y.sunakawa@marianna-u.ac.jp](mailto:y.sunakawa@marianna-u.ac.jp)

### Abstract

#### BACKGROUND

Fistula formation is a severe adverse event related to antiangiogenic agents such as bevacizumab and inferior mesenteric arteriovenous fistula (IMAVF) is a result of acquired factor, especially colon surgery. However, IMAVF occurs very rarely and there are few reports in patients during chemotherapy. We report a case of a patient who developed IMAVF during treatment with bevacizumab in metastatic colorectal cancer (mCRC) after colon surgery.

#### CASE SUMMARY

An 81-year-old man was diagnosed with descending colon cancer and underwent left hemicolectomy without any complications. He was definitely diagnosed with high-risk stage 2 and received tegafur-uracil plus leucovorin as adjuvant chemotherapy. Three years and 6 mo after the operation, the cancer relapsed with peritoneal dissemination. The patient underwent CyberKnife radiosurgery targeting the recurrent tumor and received chemotherapy with S-1 plus bevacizumab. At 1 year after chemotherapy, he complained of severe diarrhea, which is suspected drug-induced colitis. As diarrhea worsened despite the termination of treatment, he underwent colonoscopy and computed tomography

Informed written consent was obtained from the patient for publication of this report and any accompanying images.

**Conflict-of-interest statement:** All authors have declared no conflicts of interest.

**CARE Checklist (2016) statement:** The authors have read the CARE Checklist (2016), and the manuscript was prepared and revised according to the CARE Checklist (2016).

**Open-Access:** This article is an open-access article that was selected by an in-house editor and fully peer-reviewed by external reviewers. It is distributed in accordance with the Creative Commons Attribution NonCommercial (CC BY-NC 4.0) license, which permits others to distribute, remix, adapt, build upon this work non-commercially, and license their derivative works on different terms, provided the original work is properly cited and the use is non-commercial. See: <http://creativecommons.org/licenses/by-nc/4.0/>

**Manuscript source:** Unsolicited manuscript

**Specialty type:** Oncology

**Country/Territory of origin:** Japan

**Peer-review report's scientific quality classification**

Grade A (Excellent): 0  
Grade B (Very good): 0  
Grade C (Good): C  
Grade D (Fair): 0  
Grade E (Poor): 0

**Received:** June 24, 2020

**Peer-review started:** June 24, 2020

**First decision:** August 9, 2020

**Revised:** August 20, 2020

**Accepted:** September 22, 2020

**Article in press:** September 22, 2020

**Published online:** November 15, 2020

**P-Reviewer:** Jesus-Silva SG

**S-Editor:** Ma YJ

**L-Editor:** Filipodia

**P-Editor:** Li JH

(CT) scans that revealed edematous change from sigmoid to rectosigmoid colon. CT scans also revealed an aneurysm adjacent to the inferior mesenteric vein and multidetector CT angiography showed the IMAVF. Elective angiography confirmed the diagnosis of an IMAVF and it was successfully treated by arterial embolization. The patient resumed chemotherapy with only S-1 6 mo after embolization.

## CONCLUSION

Clinicians should keep in mind the probability of severe diarrhea arose from IMAVF in mCRC patients treated with bevacizumab.

**Key Words:** Metastatic cancer; Colon surgery; Chemotherapy; Fistula formation; Inferior mesenteric artery; Interventional radiology; Case report

©The Author(s) 2020. Published by Baishideng Publishing Group Inc. All rights reserved.

**Core Tip:** Gastrointestinal perforation and fistula formation are s bevacizumab-induced serious adverse events (SAEs). Arteriovenous fistula may occur during bevacizumab treatment *via* the action of antiangiogenetic agent. Inferior mesenteric arteriovenous fistula (IMAVF) arises from acquired factors especially colon surgery, although there has been no report related to chemotherapy including bevacizumab. We report a case of IMAVF in metastatic colorectal cancer (mCRC) during bevacizumab treatment. This patient complained of severe diarrhea caused by ischemic colitis due to IMAVF. As fistula may be lethal complications, clinicians should pay attention to SAEs including IMAVF for mCRC patients during bevacizumab treatment.

**Citation:** Doi A, Takeda H, Umemoto K, Oumi R, Wada S, Hamaguchi S, Mimura H, Arai H, Horie Y, Mizukami T, Izawa N, Ogura T, Nakajima TE, Sunakawa Y. Inferior mesenteric arteriovenous fistula during treatment with bevacizumab in colorectal cancer patient: A case report. *World J Gastrointest Oncol* 2020; 12(11): 1364-1371

**URL:** <https://www.wjgnet.com/1948-5204/full/v12/i11/1364.htm>

**DOI:** <https://dx.doi.org/10.4251/wjgo.v12.i11.1364>

## INTRODUCTION

Angiogenesis is important for cancer proliferation and promotion since blood vessels in tumors supply oxygen and nutrients, which support cancer growth. Vascular endothelial growth factor (VEGF) is a key factor for angiogenesis, promoting new blood vessel formation<sup>[1-3]</sup>. Bevacizumab is a recombinant humanized monoclonal IgG1 antibody that acts as an antiangiogenic drug targeting VEGF-A related to angiogenesis and inhibits the growth of tumor vessels as well as tumor proliferation. Hence, it has survival benefits for patients with metastatic colorectal cancer (mCRC) and is a useful standard therapy not only in the first-line but also for second-line treatment of mCRC<sup>[4-6]</sup>.

Major adverse events (AEs) of bevacizumab include secondary hypertension, wound healing complications, and proteinuria. Practitioners should also be aware of certain rare but fatal bevacizumab-induced AEs such as hemorrhage, thrombosis, gastrointestinal (GI), non-GI perforation, and fistula formation. Although perforation and fistula formation have been reported in various cancers, they have been predominantly observed in GI sites and very rarely in non-GI sites. Non-GI fistula formation has been reported at tracheoesophageal, bronchopleural, biliary, vaginal, renal, and bladder sites in patients treated with bevacizumab; however, few have been observed in patients with mCRC. Alternative drugs for mCRC targeting angiogenesis include aflibercept, ramucirumab, and regorafenib. The incidence of fistula formation during treatment with antiangiogenetic agents ranged from less than 1% to 1.5% across previous phase III clinical trials of mCRC, specifically 0.9% (6/694) during bevacizumab treatment<sup>[6]</sup>, 1.5% (9/611) during aflibercept treatment<sup>[7]</sup>, 0.8% (4/529) during ramucirumab treatment<sup>[8]</sup>, and 0.4% (2/500) during regorafenib treatment<sup>[9]</sup>.

To inform clinicians of the possibility of this rare AE, we herein report a patient who



developed an inferior mesenteric arteriovenous fistula (IMAVF) during bevacizumab treatment.

## CASE PRESENTATION

### Chief complaints

An 81-year-old man complained of frequent diarrhea more than 10 times per day without bleeding and abdominal pain. The patient's symptom started 1 year after the start of palliative chemotherapy with S-1 plus bevacizumab. The diarrhea worsened progressively, and we suspected S-1-induced AE. However, despite the termination of treatment for 1 mo, severe diarrhea did not improve; therefore, a careful investigation was conducted into the cause of the serious adverse event (SAE).

### History of present illness

The patient was diagnosed with descending colon cancer and underwent laparoscopic left hemicolectomy without any complications at 5 years prior to this report. However, he was later pathologically diagnosed with high-risk stage 2 descending colon cancer with venous and lymph duct invasion for which he received tegafur-uracil plus leucovorin for 6 mo as an adjuvant chemotherapy. At 3 years and 6 mo after the operation, the cancer relapsed with peritoneal dissemination in front of the left kidney. Stereotactic CyberKnife radiosurgery targeting the limited margin of the recurrent tumor resulting in tumor shrinkage, and the patient went onto palliative chemotherapy with S-1 plus bevacizumab for the remaining tumors.

### History of past illness

He underwent surgery for appendicitis in his 20s and received *Helicobacter pylori* eradication therapy for gastric ulcer in his 80s.

### Physical examination

The patient's temperature was 36.5 °C, heart rate was 86 beats per min, respiratory rate was 18 breaths per min, blood pressure was 122/71 mmHg, and oxygen saturation in room air was 98%. In clinical abdominal examination, his abdomen was soft, flat with spontaneous pain and tenderness in the left lower quadrant.

### Laboratory examinations

Laboratory test results were almost normal. Blood analysis revealed that hemoglobin and hematocrit were slightly decreased at 12.2 g/dL and 37.0%, respectively, with normal leukocyte and platelet count. Prothrombin percentage activity was slightly decreased at 71% with normal activated partial thromboplastin time and d-dimers were slightly increased at 0.9 µg/mL. Serum C-reactive protein was slightly increased at 1.58 mg/dL (normal range < 0.3 mg/dL) and erythrocyte sedimentation rate at 21 mm/h. The blood biochemistries were almost normal. Urine analysis revealed mild proteinuria at 50 mg/dL. Chest X-ray was normal and electrocardiogram showed QT prolongation without clinical importance.

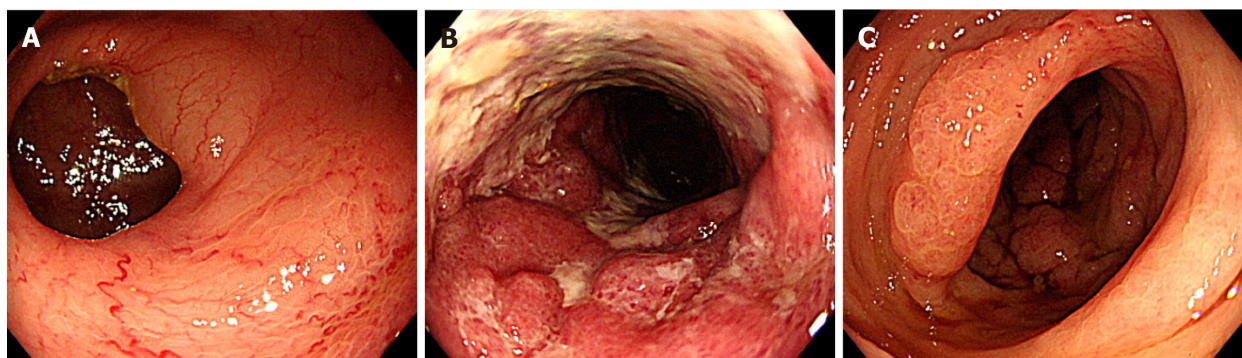
### Imaging examinations

Colonoscopy showed abnormal colonic edematous mucosa with multiple ulcers stretching from the sigmoid colon (distal to the anastomotic site) to the rectosigmoid colon (Figure 1). Abdominal contrast-enhanced computed tomography (CT) scans revealed edematous change from the sigmoid colon to the rectum and a 1.8 cm × 1.3 cm aneurysm adjacent to the inferior mesenteric vein (IMV) (Figure 2A and B). Multidetector CT (MDCT) angiography showed the arteriovenous fistula with nidus involving the branches of the inferior mesenteric artery (IMA) and IMV (Figure 2C). An elective angiography of the IMA confirmed the existence of an IMAVF and defined several shunting points of the fistula from the branch of the IMA (Figure 3A and B).

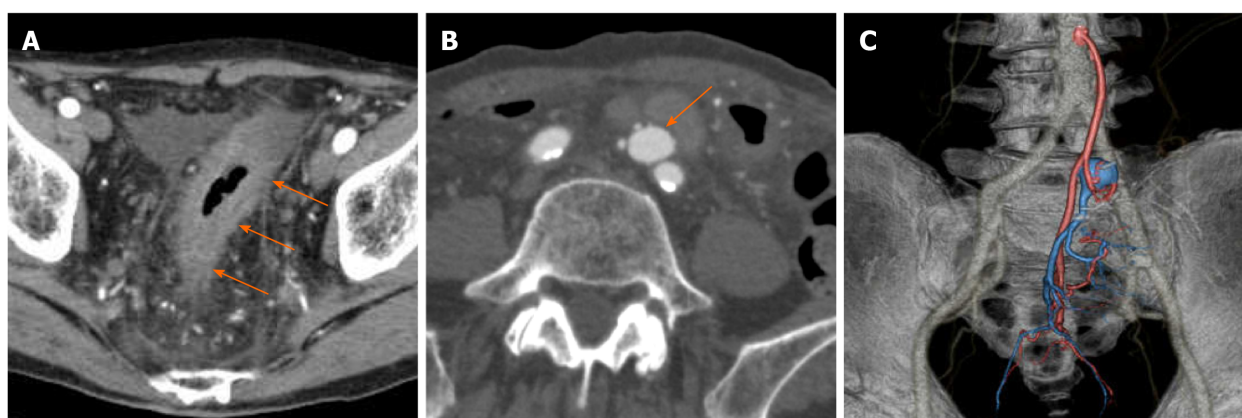
## FINAL DIAGNOSIS

The final diagnosis of the presented case was IMAVF with ischemic colitis.





**Figure 1** Colonoscopy showed abnormal colonic edematous mucosa with multiple ulcers from the sigmoid colon, distal to the anastomotic site, to the rectosigmoid colon and rectum below the peritoneal reflection. A: Mild inflammation in the anastomotic site; B: Severe inflammation with multiple ulcers and edematous mucosa in the sigmoid colon; C: Rectum below the peritoneal reflection with almost normal findings.



**Figure 2** Abdominal contrast-enhanced computed tomography at 5 year after left hemicolectomy and at 1 year after the start of palliative chemotherapy. A: Computed tomography (CT) showed edematous change from the sigmoid colon to the rectum (triple arrow); B: An aneurysm adjacent to the inferior mesenteric vein (IMV) (arrow); C: Multidetector CT angiography (three-dimensional volume-rendered image) showed the arteriovenous fistula with nidus involving the branches of the inferior mesenteric artery and IMV.

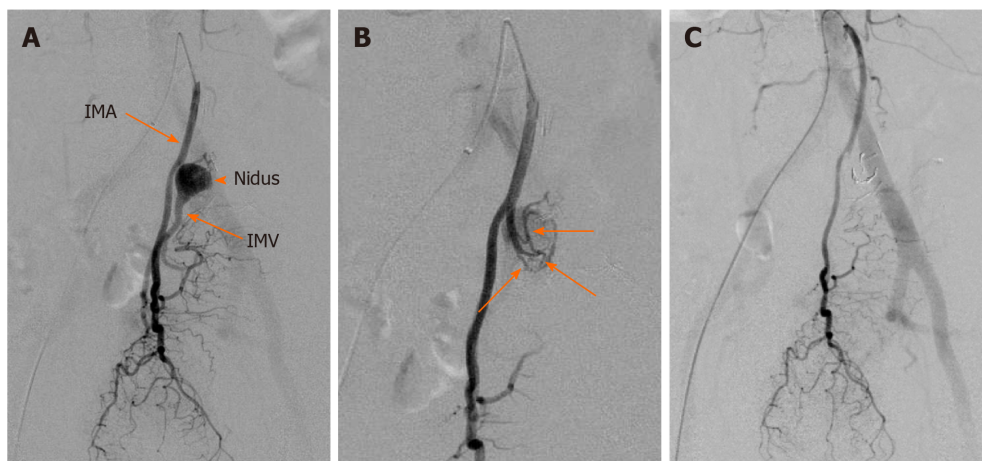
## TREATMENT

This diagnosis was followed by treatment with interventional radiology (IR) on the same day. Abdominal angiography revealed that four small feeding arteries from the branch of the IMA were involved in AVF. Interventional radiologists judged that this case was candidate for transcatheter arterial embolization (TAE). TAE was performed by using detachable micro coils with 2 mm in diameter through the microcatheter, which was utilized to access the AVF. We did not use a liquid agent because there was a risk of rectal ischemia by accidental embolization of the superior rectal artery distal to AVF. Treatment succeeded without any complications and the AVF completely disappeared (Figure 3C).

## OUTCOME AND FOLLOW-UP

Twelve days after fistula embolization, the patient's symptom improved, and CT findings indicated an improvement in the edematous change of the colon. Reattempt colonoscopy also showed improvement of the colonic edematous mucosa. At 6 mo after the procedure, the patient recovered and resumed palliative chemotherapy with only S-1. He has continued the same treatment without any complications as of June 2020.





**Figure 3 An elective angiography of the inferior mesenteric artery.** A: Angiography revealed the nidus of fistula supplied by the inferior mesenteric artery (IMA) (arrow head); B: Several shunting points of the fistula from the branch of the IMA (arrows), which confirmed the existence of an inferior mesenteric arteriovenous fistula (IMAVF); C: The IMAVF completely disappeared after arterial embolization. IMV: Inferior mesenteric vein.

## DISCUSSION

Previous studies<sup>[10,11]</sup> have reported the risk factors for GI perforation or fistula formation, which induce several types of cancer such as colorectal, ovarian, or renal cell cancer, as well as untreated primary tumor, colorectal surgery, abdominal irradiation, and chemotherapy-induced colitis. More than once surgery, irradiation, peritoneal dissemination, and cancer infiltration of the digestive tract were shown to be particularly high-risk factors<sup>[10,11]</sup>. The average period for the development of perforation or fistula formation after the start of treatment with bevacizumab was around 15 wk in several studies<sup>[11,12]</sup>. Most fistula formation occurs as a rectoperineal or colovesical fistulae in GI sites<sup>[12]</sup>, while an AVF in CRC is extremely rare.

We report a case in which a patient with CRC developed an IMAVF during cancer treatment with bevacizumab after colorectal surgery. AVF including the IMA has been reported in only 35 cases so far. Among them, only seven articles available in the English language reported IMAVF following colorectal surgery from the PubMed database. Four of these patients were males and three females, with a median age of 63 years (range, 59–81 years) (Table 1)<sup>[13–17]</sup>. Most cases received surgical resection of the left colon involving the IMA and IMV. The median interval to diagnosis after the surgery was 5 years, and common symptoms were abdominal pain and GI bleeding. Only three cases of IMAVF have been observed in patients with CRC<sup>[16–18]</sup>. However, there has been no reported case of IMAVF related to chemotherapy, such as treatment with bevacizumab or other antiangiogenic agents.

Angiography is useful for diagnosis of the IMAVF as it provides specific findings such as influent artery dilatation, abnormal blood vessel gathering, and early venous return. Recently, it has been shown that minimally invasive examinations including MR angiography and three- or four-dimensional CT angiography are also effective for diagnosis of IMAVF<sup>[18–20]</sup>. Treatment for the IMAVF includes surgery, IR, or both<sup>[13,14]</sup>. In the previous reported IMAVF cases, about half of the patients underwent surgical treatment or intra-arterial embolization, and only one patient underwent both treatments due to failure of the first embolization treatment<sup>[13–17]</sup>. Recently, IR has become the preferred method of treatment as it is easily repeatable and less invasive. It presents a good option in cases with identified fistula sites or when surgery is difficult due to complications. In the present case, the IMAVF was diagnosed by abdominal MDCT, and the diagnosis was confirmed by angiography. Since the location of the fistula and its feeding vessels were known, the IMAVF was treated by using arterial embolization. However, embolization may cause extensive arterial thrombosis followed by organ ischemia or recurrence in cases with more than one feeding vessel; therefore, it should not be performed in cases where the fistula has developed in a large vessel or has multiple feeding vessels<sup>[13,21]</sup>. In this case, an alternative possible treatment for ischemic colitis is resection of sigmoid colon and part of the rectum that are supplied by the IMA. Surgery may also be required in complications such as rebleeding, intestinal stenosis, or necrosis after IR.

To the best of our knowledge, the current case is the first report of an IMAVF in a patient with CRC who received palliative chemotherapy. The IMAVF occurred at 5

**Table 1 Cases of inferior mesenteric arteriovenous fistula after colorectal surgery**

Ref.	Sex	Age	Surgery	Interval to diagnosis	Symptoms	Treatment
Capron <i>et al</i> <sup>[14]</sup> , 1984	F	60	Colon resection	11 yr	Abdominal pain, Meteorism	Embolization
Peer <i>et al</i> <sup>[15]</sup> , 1989	M	63	Anterior resection of rectum	5 wk	Abdominal pain, Upper GI bleeding	Left colectomy
Pietri <i>et al</i> <sup>[13]</sup> , 1990	M	72	Left colectomy	Unknown	Abdominal mass	Left colectomy
	F	60	Left colectomy	Unknown	Lower GI bleeding	Embolization
Okada <i>et al</i> <sup>[16]</sup> , 2002	F	69	Sigmoidectomy	8 yr	Abdominal mass	Left colectomy
Gorospa <i>et al</i> <sup>[17]</sup> , 2012	M	59	Right hemicolectomy	5 yr	Abdominal pain, Lower GI bleeding, Diarrhea	Embolization, Total colectomy
Current case	M	81	Left hemicolectomy	5 yr	Diarrhea	Embolization

F: Female; GI: Gastrointestinal; M: Male.

years after surgery (similar to the previously reported median time post-surgery) and 1 year after the initiation of bevacizumab treatment, which was later the average period of perforation or fistula formation after bevacizumab treatment initiation<sup>[12-17]</sup>. Also, although irradiation is considered to be a risk factor for perforation or fistula formation, it is unlikely to be the cause of the fistula in this case, because the recurrent site treated with CyberKnife stereotactic radiosurgery was distant from the site of the IMAVF and irradiation was limited to the margin of the tumor.

An AVF could occur due to acquired factors such as the spontaneous rupture of an aneurysm, trauma, or surgery. These are responsible for fistula formation in approximately 60% of cases, whereas 25% of fistula are due to congenital factors such as arteriovenous malformation<sup>[13]</sup>. AVF most often develops in the celiac artery or one of its branches, especially the hepatic artery (45%), or the splenic artery (30%). An IMAVF may cause ischemic colitis by steal syndrome causing a reduction in blood flow supply to the bowel wall because arterial blood directly flows into venous blood<sup>[13,21]</sup>. Several reports have indicated the IMAVF formation after colectomy to hematoma or infection followed by necrosis of the vessel wall with pseudoaneurysm formation, such as vessel injury and ligation, during surgical procedures<sup>[22,23]</sup>. However, the mechanisms by which surgery or chemotherapy with antiangiogenic agent or both treatments cause IMAVF formation remain unclear. The risk of IMAVF formation during treatment with antiangiogenic agent in CRC patients after colorectal surgery has significant implications for clinicians. Most patients with IMAVF complained of symptoms such as abdominal pain and GI bleeding followed by diarrhea<sup>[13-17]</sup>, which overlapped in some cases. These symptoms are very common in mCRC patients due to cancer itself or other drug related adverse events and they are many mCRC patients during treatment with antiangiogenic agent, which is most bevacizumab, after colorectal surgery. Therefore, this is an extremely important case report that clinician need to know. In order to avoid SAEs like this case, we should pay attention to abdominal related symptoms, such as pain, bloody stool and diarrhea, then diagnose and treat a patient as rapidly as possible.

## CONCLUSION

We report on a case of IMAVF to have occurred during bevacizumab treatment in a patient with mCRC after colon surgery. There are many recurrent CRC patients after colon surgery and they routinely receive bevacizumab in clinical practice; however, as this case indicates, clinicians need to pay attention to SAEs related to bevacizumab. Formation of IMAVF and other fistula are potentially lethal complications causing massive bleeding and peritonitis. Accordingly, the clinician should keep in mind the probability of vascular-related AEs, including IMAVF, if patients complain of severe diarrhea during treatment with bevacizumab or other antiangiogenic agents.

## REFERENCES

- 1 **Dvorak HF.** Vascular permeability factor/vascular endothelial growth factor: a critical cytokine in tumor angiogenesis and a potential target for diagnosis and therapy. *J Clin Oncol* 2002; **20**: 4368-4380 [PMID: 12409337 DOI: 10.1200/JCO.2002.10.088]
- 2 **Hicklin DJ, Ellis LM.** Role of the vascular endothelial growth factor pathway in tumor growth and angiogenesis. *J Clin Oncol* 2005; **23**: 1011-1027 [PMID: 15585754 DOI: 10.1200/JCO.2005.06.081]
- 3 **Folkman J.** Tumor angiogenesis: therapeutic implications. *N Engl J Med* 1971; **285**: 1182-1186 [PMID: 4938153 DOI: 10.1056/NEJM197111182852108]
- 4 **Giantonio BJ, Catalano PJ, Meropol NJ, O'Dwyer PJ, Mitchell EP, Alberts SR, Schwartz MA, Benson AB 3rd, Eastern Cooperative Oncology Group Study E3200.** Bevacizumab in combination with oxaliplatin, fluorouracil, and leucovorin (FOLFOX4) for previously treated metastatic colorectal cancer: results from the Eastern Cooperative Oncology Group Study E3200. *J Clin Oncol* 2007; **25**: 1539-1544 [PMID: 17442997 DOI: 10.1200/JCO.2006.09.6305]
- 5 **Kozloff M, Yood MU, Berlin J, Flynn PJ, Kabbinnavar FF, Purdie DM, Ashby MA, Dong W, Sugrue MM, Grothey A; Investigators of the BRiTE study.** Clinical outcomes associated with bevacizumab-containing treatment of metastatic colorectal cancer: the BRiTE observational cohort study. *Oncologist* 2009; **14**: 862-870 [PMID: 19726453 DOI: 10.1634/theoncologist.2009-0071]
- 6 **Saltz LB, Clarke S, Diaz-Rubio E, Scheithauer W, Figer A, Wong R, Koski S, Lichinitser M, Yang TS, Rivera F, Couture F, Sirzén F, Cassidy J.** Bevacizumab in combination with oxaliplatin-based chemotherapy as first-line therapy in metastatic colorectal cancer: a randomized phase III study. *J Clin Oncol* 2008; **26**: 2013-2019 [PMID: 18421054 DOI: 10.1200/JCO.2007.14.9930]
- 7 **Van Cutsem E, Tabernero J, Lakomy R, Prenen H, Prausová J, Macarulla T, Ruff P, van Hazel GA, Moiseyenko V, Ferry D, McKendrick J, Polikoff J, Tellier A, Castan R, Allegra C.** Addition of aflibercept to fluorouracil, leucovorin, and irinotecan improves survival in a phase III randomized trial in patients with metastatic colorectal cancer previously treated with an oxaliplatin-based regimen. *J Clin Oncol* 2012; **30**: 3499-3506 [PMID: 22949147 DOI: 10.1200/JCO.2012.42.8201]
- 8 **Tabernero J, Yoshino T, Cohn AL, Obermannova R, Bodoky G, Garcia-Carbonero R, Ciuleanu TE, Portnoy DC, Van Cutsem E, Grothey A, Prausová J, Garcia-Alfonso P, Yamazaki K, Clingan PR, Lonardi S, Kim TW, Simms L, Chang SC, Nasroulah F; RAISE Study Investigators.** Ramucicromab vs placebo in combination with second-line FOLFIRI in patients with metastatic colorectal carcinoma that progressed during or after first-line therapy with bevacizumab, oxaliplatin, and a fluoropyrimidine (RAISE): a randomised, double-blind, multicentre, phase 3 study. *Lancet Oncol* 2015; **16**: 499-508 [PMID: 25877855 DOI: 10.1016/S1470-2045(15)70127-0]
- 9 **Grothey A, Van Cutsem E, Sobrero A, Siena S, Falcone A, Ychou M, Humblet Y, Bouché O, Mineur L, Barone C, Adenis A, Tabernero J, Yoshino T, Lenz HJ, Goldberg RM, Sargent DJ, Cihon F, Cupit L, Wagner A, Laurent D; CORRECT Study Group.** Regorafenib monotherapy for previously treated metastatic colorectal cancer (CORRECT): an international, multicentre, randomised, placebo-controlled, phase 3 trial. *Lancet* 2013; **381**: 303-312 [PMID: 23177514 DOI: 10.1016/S0140-6736(12)61900-X]
- 10 **Hapani S, Chu D, Wu S.** Risk of gastrointestinal perforation in patients with cancer treated with bevacizumab: a meta-analysis. *Lancet Oncol* 2009; **10**: 559-568 [PMID: 19482548 DOI: 10.1016/S1470-2045(09)70112-3]
- 11 **Sliesoraitis S, Tawfik B.** Bevacizumab-induced bowel perforation. *J Am Osteopath Assoc* 2011; **111**: 437-441 [PMID: 21803880]
- 12 **Ganapathi AM, Westmoreland T, Tyler D, Mantyh CR.** Bevacizumab-associated fistula formation in postoperative colorectal cancer patients. *J Am Coll Surg* 2012; **214**: 582-8; discussion 588-90 [PMID: 22321523 DOI: 10.1016/j.jamcollsurg.2011.12.030]
- 13 **Pietri J, Remond A, Reix T, Abet D, Sevestre H, Sevestre MA.** Arterioportal fistulas: twelve cases. *Ann Vasc Surg* 1990; **4**: 533-539 [PMID: 2261320 DOI: 10.1016/S0890-5096(06)60834-0]
- 14 **Capron JP, Gineston JL, Remond A, Lallement PY, Delamarre J, Revert R, Veyssier P.** Inferior mesenteric arteriovenous fistula associated with portal hypertension and acute ischemic colitis. Successful occlusion by intraarterial embolization with steel coils. *Gastroenterology* 1984; **86**: 351-355 [PMID: 6690362]
- 15 **Peer A, Slutski S, Witz E, Abrahmsohn R, Bogokowsky H, Leonov Y.** Transcatheter occlusion of inferior mesenteric arteriovenous fistula: a case report. *Cardiovasc Intervent Radiol* 1989; **12**: 35-37 [PMID: 2496926 DOI: 10.1007/BF02577124]
- 16 **Okada K, Furusyo N, Sawayama Y, Ishikawa N, Nabeshima S, Tsuchihashi T, Kashiwagi S, Hayashi J.** Inferior mesenteric arteriovenous fistula eight years after sigmoidectomy. *Intern Med* 2002; **41**: 543-548 [PMID: 12132522 DOI: 10.2169/internalmedicine.41.543]
- 17 **Gorospe EC, Leggett CL, Sun G.** Inferior mesenteric arteriovenous malformation: an unusual cause of ischemic colitis. *Ann Gastroenterol* 2012; **25**: 165 [PMID: 24714150]
- 18 **Kai K, Sano K, Higuchi K, Uchiyama S, Sueta H, Nanashima A.** A rare case of simultaneous rectal and gastric carcinomas accompanied with inferior mesenteric arterioportal fistula: case report. *Surg Case Rep* 2019; **5**: 82 [PMID: 31102060 DOI: 10.1186/s40792-019-0630-9]
- 19 **Lee S, Chung J, Ahn B, Lee S, Baek S.** Inferior mesenteric arteriovenous fistula. *Ann Surg Treat Res* 2017; **93**: 225-228 [PMID: 29094033 DOI: 10.4174/astr.2017.93.4.225]
- 20 **Cheng L, Zhao R, Guo D, Cai K, Zou K, Yang J, Zhu L.** Inferior mesenteric arteriovenous fistula with nonpulsatile abdominal mass: A case report and a mini-review. *Medicine (Baltimore)* 2017; **96**: e8717 [PMID: 29310345 DOI: 10.1097/MD.00000000000008717]
- 21 **Metcalf DR, Nivatvongs S, Andrews JC.** Ischemic colitis: an unusual case of inferior mesenteric arteriovenous fistula causing venous hypertension. Report of a case. *Dis Colon Rectum* 2008; **51**: 1422-1424 [PMID: 18521673 DOI: 10.1007/s10350-008-9377-2]
- 22 **Rossi P, Carillo FJ, Alfidi RJ, Ruzicka FF Jr.** Iatrogenic arteriovenous fistulas. *Radiology* 1974; **111**: 47-51 [PMID: 4856165 DOI: 10.1148/111.1.47]

- 23 **Athanasίου A**, Michalinos A, Alexandrou A, Georgopoulos S, Felekouras E. Inferior mesenteric arteriovenous fistula: case report and world-literature review. *World J Gastroenterol* 2014; **20**: 8298-8303 [PMID: 25009407 DOI: 10.3748/wjg.v20.i25.8298]



## Cutaneous metastases of pancreatic carcinoma to the labia majora: A case report and review of literature

Ying Shi, Shan-Shan Li, Dan-Yan Liu, Yan Yu

**ORCID number:** Ying Shi 0000-0002-3249-6632; Shan-Shan Li 0000-0001-5745-7835; Dan-Yan Liu 0000-0001-5631-6387; Yan Yu 0000-0003-1227-7448.

**Author contributions:** All authors contributed equally to this paper with the conception and design of the study, literature review and analysis, manuscript drafting, critical revision, and editing, and approval of the final version.

**Informed consent statement:**

Informed consent was obtained from the patient.

**Conflict-of-interest statement:** All the authors are aware of the content of the manuscript and have no conflict of interest to disclose.

**CARE Checklist (2016) statement:**

The authors have read the CARE Checklist (2016), and the manuscript was prepared and revised according to the CARE Checklist (2016).

**Open-Access:** This article is an open-access article that was selected by an in-house editor and fully peer-reviewed by external reviewers. It is distributed in accordance with the Creative Commons Attribution NonCommercial (CC BY-NC 4.0) license, which permits others to distribute, remix, adapt, build

**Ying Shi, Yan Yu,** Department of Dermatology, First Hospital of Jilin University, Changchun 130021, Jilin Province, China

**Shan-Shan Li,** Department of Dermatology and Venereology, First Hospital of Jilin University, Changchun 130021, Jilin Province, China

**Dan-Yan Liu,** Department of Radiology, First Hospital of Jilin University, Changchun 130021, Jilin Province, China

**Corresponding author:** Yan Yu, MD, Chief Doctor, Department of Dermatology, First Hospital of Jilin University, No. 71 Xinmin Street, Changchun 130021, Jilin Province, China. [yuyan741206@126.com](mailto:yuyan741206@126.com)

### Abstract

#### BACKGROUND

Cutaneous metastases originating from pancreatic cancer are relatively rare. The most common reported site of metastasis is the umbilicus, and this manifestation is known as the Sister Mary Joseph's nodule. Non-umbilical cutaneous metastases are far less common, with only a few cases reported in the literature. Our case is the first case report, to our knowledge, on metastasis involving the labia majora and flat papules.

#### CASE SUMMARY

A 49-year-old Chinese female patient presented with a number of red, swollen papules on the vulva for 2 mo. Histological examination of the labia majora lesion revealed metastatic adenocarcinoma. The serum levels of tumor biomarkers CA199, CA242, and CA125 were significantly elevated. B-mode ultrasound-guided needle biopsy of the pancreas demonstrated moderately and poorly differentiated adenocarcinoma. The patient finally declined treatment for financial reasons and died 3 mo later.

#### CONCLUSION

Metastatic cutaneous lesions could indicate pancreatic cancer. Serum levels of tumor biomarkers may aid in diagnosing metastatic pancreatic adenocarcinoma.

**Key Words:** Pancreatic cancer; Cutaneous; Metastasis; Non-umbilical; Biomarker; Case report



upon this work non-commercially, and license their derivative works on different terms, provided the original work is properly cited and the use is non-commercial. See: <http://creativecommons.org/licenses/by-nc/4.0/>

**Manuscript source:** Unsolicited manuscript

**Specialty type:** Oncology

**Country/Territory of origin:** China

**Peer-review report's scientific quality classification**

Grade A (Excellent): 0

Grade B (Very good): 0

Grade C (Good): 0

Grade D (Fair): 0

Grade E (Poor): 0

**Received:** August 12, 2020

**Peer-review started:** August 12, 2020

**First decision:** September 16, 2020

**Revised:** September 29, 2020

**Accepted:** October 19, 2020

**Article in press:** October 19, 2020

**Published online:** November 15, 2020

**P-Reviewer:** Buanes T

**S-Editor:** Gao CC

**L-Editor:** Wang TQ

**P-Editor:** Li JH



©The Author(s) 2020. Published by Baishideng Publishing Group Inc. All rights reserved.

**Core Tip:** Cutaneous metastasis from pancreatic cancer is uncommon. The most common site of the skin lesion is the umbilicus. The majority of skin lesions are singular, particularly in patients exhibiting the Sister Mary Joseph's nodule. We describe an unusual case of flat papules on the labia majora that metastasized from pancreatic cancer. The lesion was the first sign of metastatic disease, and serum levels of CA199, CA242, and CA125 were also elevated. We report this case to improve the understanding of cutaneous metastasis of pancreatic cancer and emphasize the importance of serum levels of CA199, CA242, and CA125 in diagnosing pancreatic cancer.

**Citation:** Shi Y, Li SS, Liu DY, Yu Y. Cutaneous metastases of pancreatic carcinoma to the labia majora: A case report and review of literature. *World J Gastrointest Oncol* 2020; 12(11): 1372-1380

**URL:** <https://www.wjgnet.com/1948-5204/full/v12/i11/1372.htm>

**DOI:** <https://dx.doi.org/10.4251/wjgo.v12.i11.1372>

## INTRODUCTION

Pancreatic cancer is one of the most lethal human malignancies and is often diagnosed late in the course of the disease. Cutaneous metastases originating from pancreatic cancer are relatively rare. The most common reported site of metastasis is the umbilicus, and this manifestation is known as the Sister Mary Joseph's nodule. Non-umbilical cutaneous metastases are far less common, with only a few cases reported in the literature. To our knowledge, there are no previous reports on metastasis involving the labia majora and flat papules. This report describes a case of cutaneous pancreatic metastases on the labia majora in a Chinese woman, and a review of previously reported non-umbilical cutaneous pancreatic carcinoma metastases (by conducting a detailed PubMed search). Furthermore, an analysis of 34 reported cases of non-umbilical cutaneous metastasis from pancreatic cancer was conducted with regard to the clinical characteristics.

## CASE PRESENTATION

### Chief complaints

A 49-year-old female patient with a number of red, swollen papules on the vulva for 2 mo was referred to our department.

### History of present illness

The patient had developed red, swollen papules on the vulva 3 mo previously. She attended a local hospital, where she was diagnosed with contact dermatitis and took regular anti-allergy treatment. There was no obvious improvement in her symptoms. Erythema gradually affected the abdomen and lower extremities. The patient had experienced intermittent shortness of breath and coughed up white sputum during this period.

### History of past illness

The patient had experienced hypertension for 2 years and had a history of sulfonamide allergy.

### Personal and family history

There was not a personal or family history of pancreatic cancer.

### Physical examination

Physical examination revealed diffuse erythema and swelling on the chest, abdomen, and vulva; right leg edema; and a number of flat skin-colored or gray papules on the

labia majora (Figure 1).

### Laboratory examinations

Routine laboratory testing revealed that the patient was human immunodeficiency virus (HIV) negative; the results of blood and urine tests and levels of renal and hepatic markers and antinuclear antibodies were within the normal ranges. There was a remarkable elevation in the serum concentrations of tumor markers, comprising cytokeratin 19 (8.98 g/L; normal: < 5 µg/L), CA242 (> 500 U/mL; normal: < 20 U/mL), CA125 (52.41 U/mL; normal: < 35 U/mL), and CA199 (726.54 U/mL; normal: < 37 U/mL).

### Imaging examinations

An ultrasound scan showed bilateral mammary gland hyperplasia, no other gynecological abnormalities, and right leg lymphedema. A chest computerized tomography (CT) scan revealed inflammation, with patterns of interstitial change scattered across both lungs and a little pleural effusion in the left lung. An abdominal CT scan demonstrated many enlarged lymph nodes, associated with the abdominal aorta, bilateral iliac artery, and bilateral inguinal region, as well as changes in the pancreatic and peripancreatic morphology. A positron emission tomography (PET)-CT scan showed increased metabolic activity in the tail of the pancreas and multiple enlarged lymph nodes throughout the body, as well as subcutaneous tissue edema (Figure 2).

### Further diagnostic work-up

A punch biopsy was performed on the abdomen and labia majora lesions. The abdominal epidermis was normal, and there were dilated small blood vessels and lymph vessels in the dermis, and small quantities of infiltrating lymphocytes. Histological examination of the labia majora papules showed nests of moderately differentiated atypical cells partly forming adenomatous structures in the collagen bundles of the dermis and lymphangiectasia (pathologic dilation of the lymph vessels) in the dermis (Figure 3). The immunohistochemical staining results (Figure 4) were as follows: CK7 (+), panCK (+), CK19 (+), CA19-9 (+), CDX-2 (+), CK20 (+), D2-40 (-), and P63 (-), which is consistent with a possible pancreatic source of the metastasis.

In addition, a large amount of milky fluid was drained from the skin biopsy sites. While the serum triglyceride level was normal, the level in the fluid was 1.55 mmol/L, indicating lymphocytosis. Neither bacteria (including *Mycobacterium tuberculosis*) nor fungi were found in the fluid. According to the laboratory and histopathologic findings, a diagnosis of chylous reflux fluid was made.

Thereafter, B-mode ultrasound-guided needle biopsy of the pancreas demonstrated moderately and poorly differentiated adenocarcinoma (Figure 5).

## FINAL DIAGNOSIS

According to the clinical manifestations and histopathologic findings, a diagnosis of metastatic pancreatic carcinoma was established.

## TREATMENT

The patient declined treatment for financial reasons.

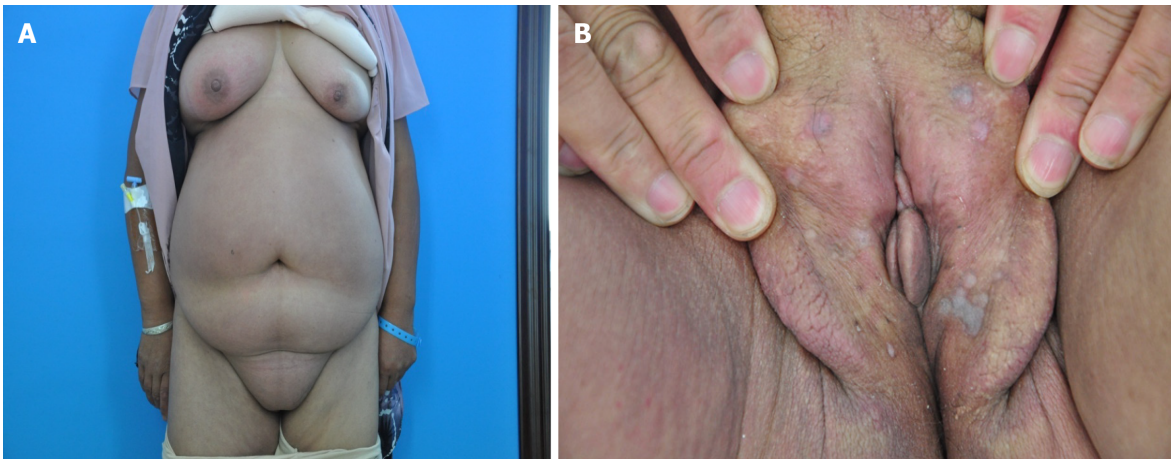
## OUTCOME AND FOLLOW-UP

The patient died 3 mo later.

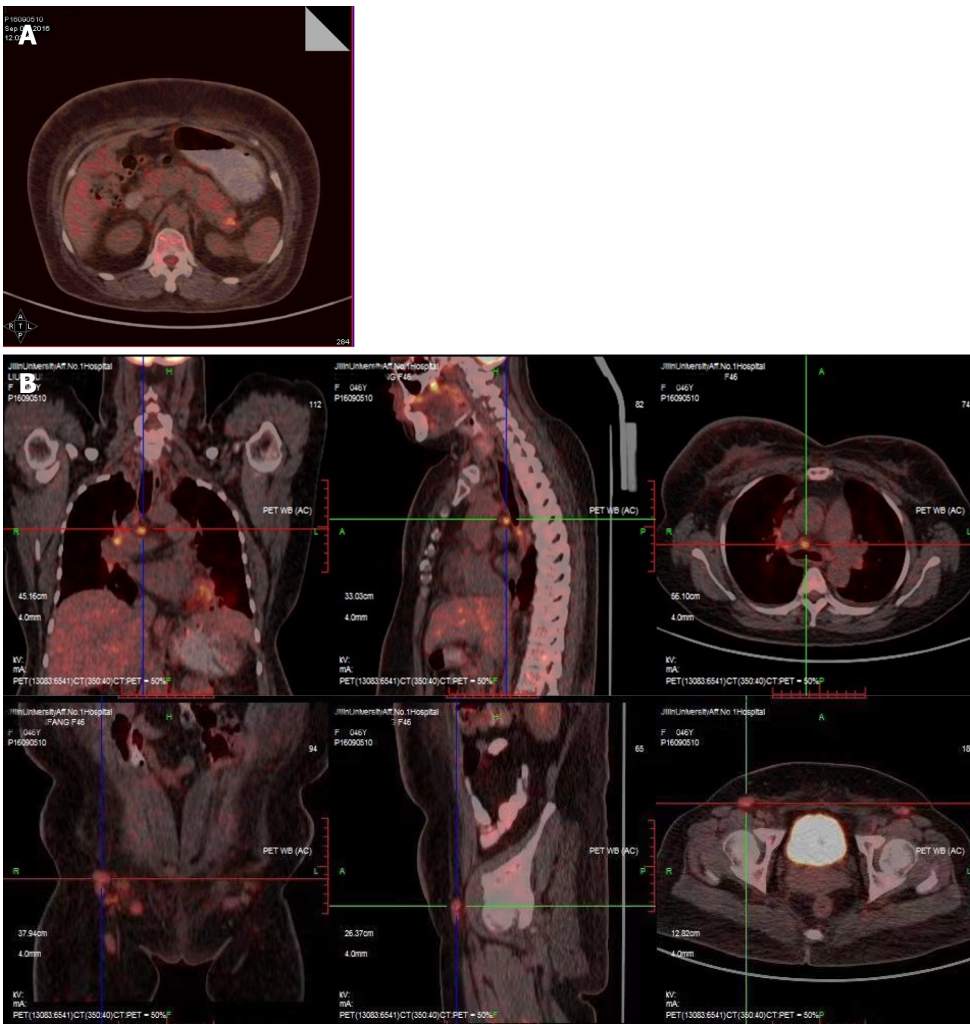
## DISCUSSION

Cutaneous metastases are rare, occurring in 0.7%-9.0% of all patients with cancer<sup>[1]</sup>. Breast, lung, and colon cancer are the most frequent origins of cutaneous metastases.

Pancreatic cancer is one of the most lethal cancers, with a 5 year survival rate of 5%.



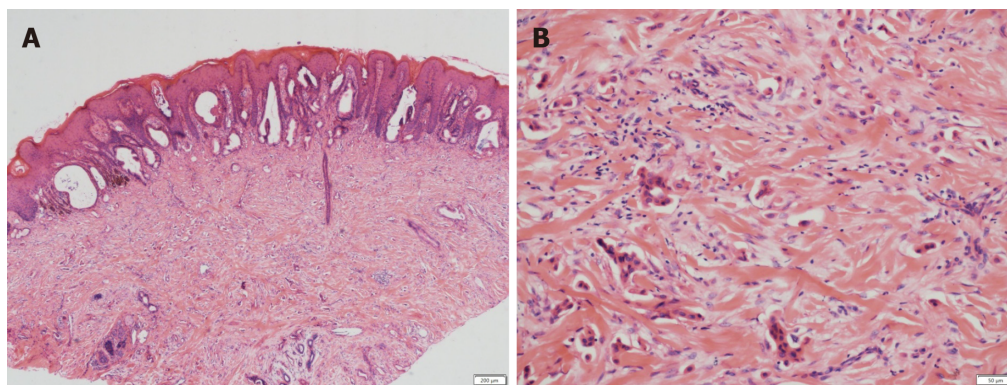
**Figure 1** Photographs of our patient. A: Diffuse erythema and swelling on the chest, abdomen, and right leg; B: Edema and a number of flat skin-colored or gray papules on the labia majora.



**Figure 2** Positron emission tomography-computed tomography scan showing increased metabolic activity. A: The tail of the pancreas; B: Mediastinum, hilus of the lung, and postperitoneal lymph nodes.

Owing to a lack of early clinical features and the fulminant disease course, early diagnosis is difficult and the metastasis rate is high, with a median overall survival of 5 mo<sup>[2]</sup>. Pancreatic cancer is often known to metastasize *via* the lymphatic system, with direct invasion at an early stage and hematogenous dissemination at a later stage. The incidence of cutaneous metastases is significantly more frequent for cancers of the





**Figure 3 Pathology of cutaneous metastasis.** A: Histological examination of the labia majora papule showing nests of moderately differentiated atypical cells partly forming adenomatous structures in the collagen bundle of the dermis and lymphangiectasis in the dermis [hematoxylin-eosin (HE) staining,  $\times 40$ ]; B: Dermis occupied by mass of numerous tumor cells (HE staining,  $\times 200$ ).

pancreatic body and tail than for pancreatic head cancer<sup>[3]</sup>.

The most frequent organs involved in the metastasis are the liver, peritoneum, lungs, bones, and brain<sup>[2]</sup>. Indeed, only 2% of the first metastases from pancreatic cancer are cutaneous metastases, making cutaneous metastases relatively rare<sup>[4]</sup>. The most common site of cutaneous metastasis from the pancreas is the umbilicus, and this manifestation is known as Sister Mary Joseph's nodule<sup>[5]</sup>. Horino *et al*<sup>[6]</sup> reviewed 42 reported cases of pancreatic metastasis from 1950 to 2011, and included only 14 cases of non-umbilical cutaneous metastasis, involving the head, neck, and truncal region. The patients with pancreatic metastasis had such symptoms as subcutaneous nodules (in 26 patients) and inflammatory erythema (in 3 patients).

We collected all case reports of non-umbilical metastatic skin cancer from 1950 to 2020 on the electronic PubMed database ([www.ncbi.nlm.nih.gov/pubmed](http://www.ncbi.nlm.nih.gov/pubmed); up to July 2020) by searching using Medical Subject Headings ([www.nlm.nih.gov/mesh](http://www.nlm.nih.gov/mesh)) and keywords, and by limiting the search to human studies (Table 1)<sup>[1-4,6-30]</sup>. The terms pancreatic cancer, pancreatic neoplasm, pancreatic carcinoma, cutaneous metastasis, and skin metastasis were used. The abstracts were reviewed, and articles that were associated with umbilical metastasis were excluded. Duplicate references as well as repeated publications were discarded. All of the studies that were considered to be eligible were retrieved and the final selection was based on the full article.

Our case is unique in that the cutaneous pancreatic cancer metastases were found on the labia majora. Our patient had papules on the labia majora, with diffuse swelling on the skin of the chest, abdomen, and vulva. In addition, there was oozing of chyle from the skin biopsy sites.

Chyle originates in the bowel lacteals (lymphatic capillaries that absorb dietary fats), is absorbed by the intestinal lymphatic vessels, passes through the collecting lymphatic vessels into the intestinal trunk (truncus intestinalis), and then passes through the cisterna chyli and thoracic duct to the bloodstream. If the reflux is obstructed, chylous reflux occurs; the chyle flows backward or leaks into the serosal cavity, external genitalia, lower limbs, *etc.* Chylous reflux is divided into primary and secondary types. Secondary chylous reflux is usually caused by neoplasia, trauma, inflammation, or surgery<sup>[7]</sup>. According to the PET-CT scan, the metastatic cancer cells may have traveled to the labia majora *via* the lymphatic pathways. The abnormal lymphatic system, caused by tumor metastasis, may have been the underlying cause for the backflow of chyle to the skin. The patient was advised to undergo lymphangiography to confirm this, but declined for financial reasons.

The serum levels of tumor biomarkers CA199, CA242, and CA125 were significantly elevated in our case. It has been shown that the sensitivity and specificity of CA199 for diagnosing pancreatic cancer are 77% and 88%, respectively. Ozkan *et al*<sup>[8]</sup> revealed that CA242 was significantly increased in 75% of pancreatic cancer patients. To sum up, Mao *et al*<sup>[9]</sup> suggested that assessment of the combination of CA199, CA242, CEA, and CA125 levels is a simple, noninvasive, and effective method for early diagnosis of pancreatic cancer.

We present a case of pancreatic adenocarcinoma metastasizing to the vulva, with a number of flat papules. This condition is extremely rare and easy to misdiagnose.

Table 1 Review of case reports of nonumbilical cutaneous metastasis from pancreatic cancer

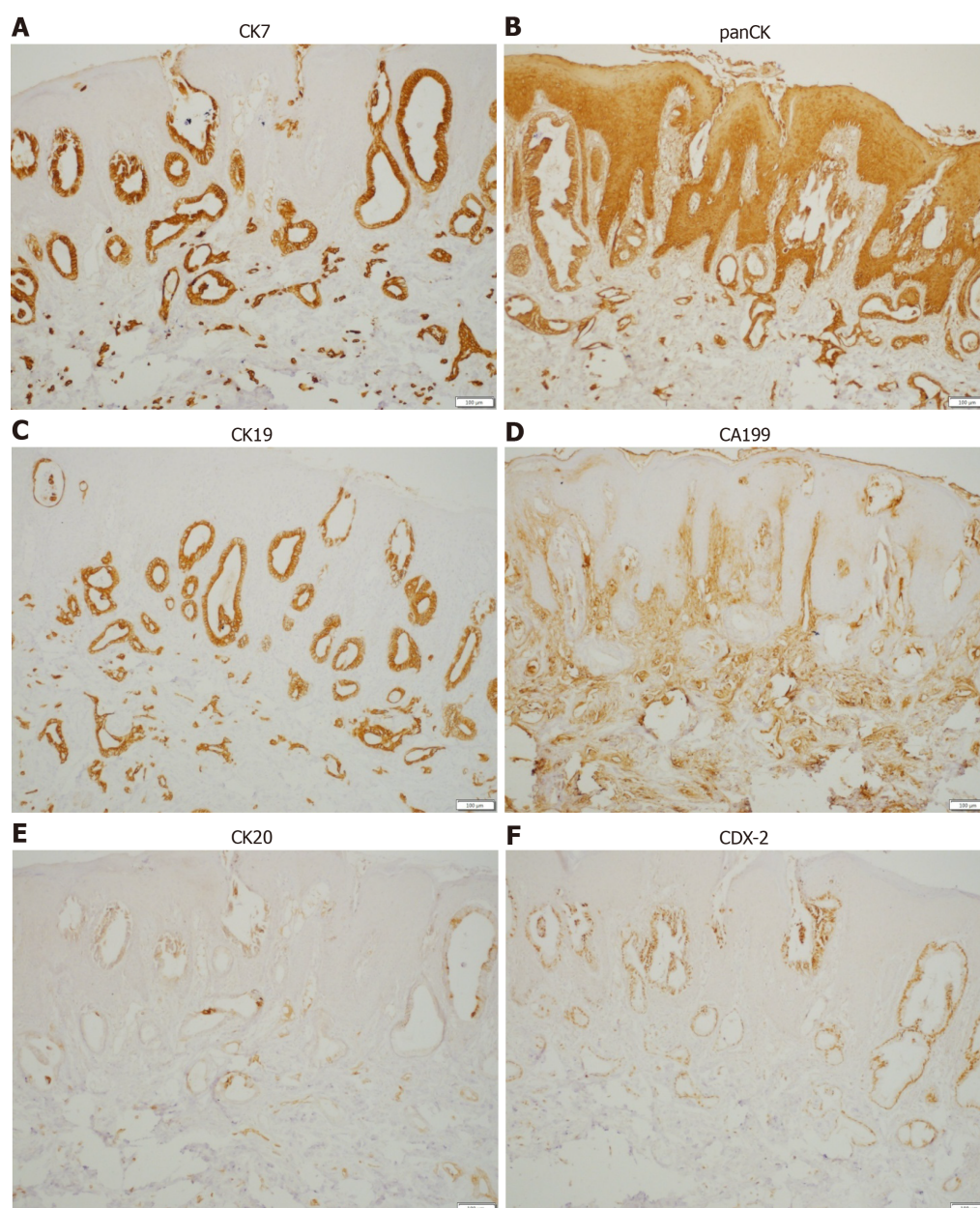
	Ref.	Age (yr)	Sex	Appearance	Metastatic site	Primary	Year
1	Edelstein <i>et al</i> <sup>[10]</sup>	60	M	Cellulitis	Face, neck	NA	1950
2	Sakai <i>et al</i>	47	M	Herpes zoster-like	No details	Head	1969
3	Sironi <i>et al</i> <sup>[12]</sup>	72	M	Nodule	Right thigh	Head	1991
4	Lookingbill <i>et al</i> <sup>[13]</sup>	No details	No details	Nodule	Abdomen	No details	1993
5	Taniguchi <i>et al</i> <sup>[4]</sup>	63	F	Erythematousplaques, nodule	Left axilla, chest	No details	1994
6	Ohashi <i>et al</i>	79	M	Nodule	Neck, chest, abdomen	No details	1995
7	Ohashi <i>et al</i>	65	M	Nodule	Back	No details	1995
8	Fukui <i>et al</i>	49	M	Nodule	Face, chest	No details	1995
9	Puri <i>et al</i> <sup>[14]</sup>	45	M	Nodule	Scalp, face, neck, back	No details	1995
10	Nakano <i>et al</i> <sup>[15]</sup>	80	M	Nodule	Occipital scalp	Tail	1996
11	Miyahara <i>et al</i> <sup>[16]</sup>	43	M	Nodule	Scalp	Uncus	1996
12	Miyahara <i>et al</i> <sup>[16]</sup>	65	M	Nodule	Mentum	Uncus	1996
13	Horino <i>et al</i> <sup>[17]</sup>	65	F	Nodule	Chest wall	Head	1999
14	Flórez <i>et al</i> <sup>[18]</sup>	48	M	Nodule	Buttock	Head	2000
15	Gawrieh <i>et al</i> <sup>[19]</sup>	45	F	Nodule	Temporal scalp	No details	2002
16	Takeuchi <i>et al</i> <sup>[3]</sup>	77	M	Nodule	Left axilla	Tail	2003
17	Otegbayo <i>et al</i> <sup>[20]</sup>	59	M	Nodule	Face, chest, abdomen, back	No details	2005
18	Jun <i>et al</i> <sup>[21]</sup>	68	M	Nodule	Right forearm, chest	Body, tail	2005
19	Ambro <i>et al</i> <sup>[22]</sup>	63	M	Nodule	Scalp	Ductal	2006
20	Takemura <i>et al</i> <sup>[23]</sup>	85	M	Nodule	Left temple	No details	2007
21	Hafez <i>et al</i> <sup>[24]</sup>	55	F	Nodule	Neck	Head	2008
22	Kimura <i>et al</i>	50	M	Nodule	Lateral abdomen	Body	2008
23	van Akkooi <i>et al</i> <sup>[25]</sup>	59	M	Nodule	Scalp	No details	2010
24	Bdeiri <i>et al</i> <sup>[1]</sup>	59	F	Nodule	Scalp	Tail	2010
25	Pontinen <i>et al</i> <sup>[26]</sup>	67	F	Nodule	Lower abdomen	Tail	2010
26	Saif <i>et al</i> <sup>[27]</sup>	46	F	Nodule	Chest, abdomen, right supraclavicular area	No details	2011
27	Horino <i>et al</i> <sup>[6]</sup>	58	F	Nodule	Lower abdomen	Body	2012
28	Horino <i>et al</i> <sup>[6]</sup>	65	F	Nodule	Lower abdomen	Tail	2012
29	Bdeiri <i>et al</i> <sup>[1]</sup>	70	F	Nodule	Scalp	Tail	2013
30	Kaoutzanis <i>et al</i> <sup>[28]</sup>	43	M	Nodule	Scalp	Head	2013
31	Zhou <i>et al</i> <sup>[2]</sup>	76	F	Nodule	Scalp, chest, abdomen	Tail	2014
32	Shin <i>et al</i> <sup>[29]</sup>	60	M	Mass	Left hip	Body	2015
33	Kotsantis <i>et al</i> <sup>[11]</sup>	62	M	Edema	Scrotum, trunk, chest wall	Head	2017
34	Ito <i>et al</i> <sup>[30]</sup>	71	F	Ulcer	Scalp	Tail	2020

NA: Not available; F: Female; M: Male.

## CONCLUSION

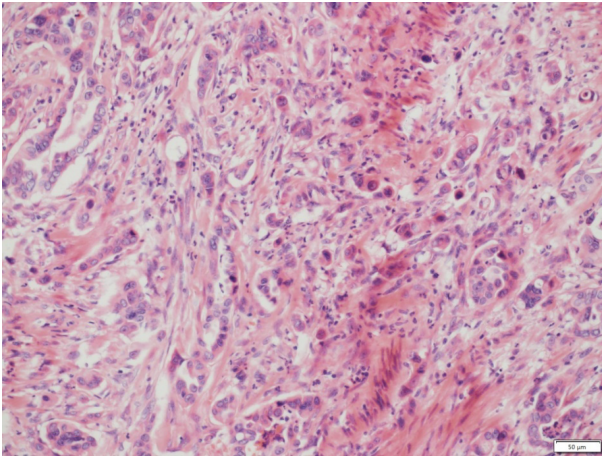
Cutaneous metastasis from pancreatic carcinoma is a rare finding and mostly occurs around the umbilicus. Subcutaneous nodules are the most common clinical manifestation. To our knowledge, we describe the first case of cutaneous pancreatic metastasis to the vulva, with a number of flat papules. Clinicians should be aware of the possibility of metastatic cutaneous lesions in pancreatic adenocarcinoma and





**Figure 4** Neoplastic glands showing a positive reaction to immunohistochemical staining (100  $\times$ ). A: CK7 (+); B: panCK (+); C: CK19 (+); D: CA199 (+); E: CK20 (+); F: CDX-2 (+).

screen for tumor markers as promptly as possible.



**Figure 5** B-mode ultrasound-guided needle biopsy of the pancreas showing the moderately and poorly differentiated adenocarcinoma (hematoxylin-eosin staining, × 200).

## REFERENCES

- 1 **Bdeiri K**, Kamar FG. Cutaneous metastasis of pancreatic adenocarcinoma as a first clinical manifestation: a case report and review of the literature. *Gastrointest Cancer Res* 2013; **6**: 61-63 [PMID: [23745161](#)]
- 2 **Zhou HY**, Wang XB, Gao F, Bu B, Zhang S, Wang Z. Cutaneous metastasis from pancreatic cancer: A case report and systematic review of the literature. *Oncol Lett* 2014; **8**: 2654-2660 [PMID: [25364444](#) DOI: [10.3892/ol.2014.2610](#)]
- 3 **Takeuchi H**, Kawano T, Toda T, Minamisono Y, Nagasaki S, Yao T, Sugimachi K. Cutaneous metastasis from pancreatic adenocarcinoma: a case report and a review of the literature. *Hepatogastroenterology* 2003; **50**: 275-277 [PMID: [12630040](#) DOI: [10.1016/j.fct.2008.12.023](#)]
- 4 **Taniguchi S**, Hisa T, Hamada T. Cutaneous metastases of pancreatic carcinoma with unusual clinical features. *J Am Acad Dermatol* 1994; **31**: 877-880 [PMID: [7525667](#) DOI: [10.1016/s0190-9622\(94\)70250-0](#)]
- 5 **Gabriele R**, Conte M, Egidi F, Borghese M. Umbilical metastases: current viewpoint. *World J Surg Oncol* 2005; **3**: 13 [PMID: [15723695](#) DOI: [10.1186/1477-7819-3-13](#)]
- 6 **Horino K**, Takamori H, Ikuta Y, Nakahara O, Chikamoto A, Ishiko T, Beppu T, Baba H. Cutaneous metastases secondary to pancreatic cancer. *World J Gastrointest Oncol* 2012; **4**: 176-180 [PMID: [22844548](#) DOI: [10.4251/wjgo.v4.i7.176](#)]
- 7 **Huang HY**, Chiu WT. Primary chylous reflux presenting with vulvar vesicles. *Arch Dermatol* 2010; **146**: 683-684 [PMID: [20566942](#) DOI: [10.1001/archdermatol.2010.122](#)]
- 8 **Ozkan H**, Kaya M, Cengiz A. Comparison of tumor marker CA 242 with CA 19-9 and carcinoembryonic antigen (CEA) in pancreatic cancer. *Hepatogastroenterology* 2003; **50**: 1669-1674 [PMID: [14571813](#) DOI: [10.1002/jcb.20532](#)]
- 9 **Mao QQ**, Yan WL, Sun X, Hu Y, Zhong L. The value of serum CA199, CA242 and CA125 in the diagnosis and prognosis of pancreatic cancer. *Biaoji Mianyi Fenxi Yu Linchunag Zazhi* 2009; **16**: 79-82 [DOI: [10.3969/j.issn.1006-1703.2009.02.006](#)]
- 10 **EDELSTEIN JM**. Pancreatic carcinoma with unusual metastasis to the skin and subcutaneous tissue simulating cellulitis. *N Engl J Med* 1950; **242**: 779-781 [PMID: [15416899](#) DOI: [10.1056/NEJM195005182422003](#)]
- 11 **Kotsantis I**, Economopoulou P, Dritsakos K, Oikonomopoulos N, Bakogeorgos M, Rapti C, Kentepozidis N. Extensive cutaneous metastases of pancreatic adenocarcinoma: a case report and review of the literature. *Clin Case Rep* 2017; **5**: 51-56 [PMID: [28096990](#) DOI: [10.1002/ccr.3.737](#)]
- 12 **Sironi M**, Radice F, Taccagni GL, Braga M, Zerbi M. Fine needle aspiration of a pancreatic oxyphilic carcinoma with pulmonary and subcutaneous metastases. *Cytopathology* 1991; **2**: 303-309 [PMID: [1724921](#) DOI: [10.1111/j.1365-2303.1991.tb00505.x](#)]
- 13 **Lookingbill DP**, Spangler N, Helm KF. Cutaneous metastases in patients with metastatic carcinoma: a retrospective study of 4020 patients. *J Am Acad Dermatol* 1993; **29**: 228-236 [PMID: [8335743](#) DOI: [10.1016/0190-9622\(93\)70173-q](#)]
- 14 **Puri AS**, Saraswat VA, Krishnani N, Salunke PN. Cutaneous metastases in pancreatic adenocarcinoma. *Indian J Pathol Microbiol* 1995; **38**: 99-101 [PMID: [8919476](#)]
- 15 **Nakano S**, Narita R, Yamamoto M, Ogami Y, Osuki M. Two cases of pancreatic cancer associated with skin metastases. *Am J Gastroenterol* 1996; **91**: 410-411 [PMID: [8607535](#) DOI: [10.2958/suizo.24.521](#)]
- 16 **Miyahara M**, Hamanaka Y, Kawabata A, Sato Y, Tanaka A, Yamamoto A, Ueno T, Nishihara K, Suzuki T. Cutaneous metastases from pancreatic cancer. *Int J Pancreatol* 1996; **20**: 127-130 [PMID: [8968868](#)]
- 17 **Horino K**, Hiraoka T, Kanemitsu K, Tsuji T, Inoue K, Tanabe D, Takamori H, Matsuoka M, Kitamura N. Subcutaneous metastases after curative resection for pancreatic carcinoma: a case report and review of the literature. *Pancreas* 1999; **19**: 406-408 [PMID: [10547202](#) DOI: [10.1097/00006676-199911000-00013](#)]
- 18 **Flórez A**, Rosón E, Sánchez-Aguilar D, Peteiro C, Toribio J. Solitary cutaneous metastasis on the buttock: a disclosing sign of pancreatic adenocarcinoma. *Clin Exp Dermatol* 2000; **25**: 201-203 [PMID: [10844494](#) DOI: [10.1046/j.1365-2230.2000.00614.x](#)]
- 19 **Gawrieh S**, Massey BT, Komorowski RA. Scalp metastases as the first manifestation of pancreatic cancer.

- Dig Dis Sci* 2002; **47**: 1469-1471 [PMID: [12141802](#) DOI: [10.1023/a:1015842413562](#)]
- 20 **Otegbayo JA**, Oluwasola OA, Akere A, Yakubu A, Daramola OO, Ogun GO. Pancreatic carcinoma presenting as cutaneous nodules in a diabetic Nigerian male. *West Afr J Med* 2005; **24**: 180 [PMID: [16092324](#)]
- 21 **Jun DW**, Lee OY, Park CK, Choi HS, Yoon BC, Lee MH, Lee DH. Cutaneous metastases of pancreatic carcinoma as a first clinical manifestation. *Korean J Intern Med* 2005; **20**: 260-263 [PMID: [16295788](#) DOI: [10.3904/kjim.2005.20.3.260](#)]
- 22 **Ambro CM**, Humphreys TR, Lee JB. Epidermotropically metastatic pancreatic adenocarcinoma. *Am J Dermatopathol* 2006; **28**: 60-62 [PMID: [16456328](#) DOI: [10.1097/01.dad.0000157460.72334.fa](#)]
- 23 **Takemura N**, Fujii N, Tanaka T. Cutaneous metastasis as the first clinical manifestation of pancreatic adenocarcinoma: a case treated with gemcitabine. *J Dermatol* 2007; **34**: 662-664 [PMID: [17727372](#) DOI: [10.1111/j.1346-8138.2007.00353.x](#)]
- 24 **Hafez HZ**. Cutaneous pancreatic metastasis: a case report and review of literature. *Indian J Dermatol* 2008; **53**: 206-209 [PMID: [19882039](#) DOI: [10.4103/0019-5154.44806](#)]
- 25 **van Akkooi AC**, Dokter J, Boxma H. Unusual first presentation of metastatic pancreatic cancer as skin metastases in a burn patient. *Burns* 2010; **36**: e111-e114 [PMID: [20392566](#) DOI: [10.1016/j.burns.2009.12.004](#)]
- 26 **Pontinen T**, Melin A, Varadi G, Khanmoradi K, Chewaproug D, Kung SC, Zaki R, Ortiz J. Cutaneous metastasis of pancreatic adenocarcinoma after kidney transplant: a case report and review of the literature. *Exp Clin Transplant* 2010; **8**: 273-276 [PMID: [21143091](#)]
- 27 **Saif MW**, Brennan M, Penney R, Hotchkiss S, Kaley K. Cutaneous metastasis in a patient with pancreatic cancer. *JOP* 2011; **12**: 306-308 [PMID: [21546714](#)]
- 28 **Kaoutzanis C**, Chang MC, Abdul Khalek FJ, Kreske E. Non-umbilical cutaneous metastasis of a pancreatic adenocarcinoma. *BMJ Case Rep* 2013; **2013** [PMID: [23307465](#) DOI: [10.1136/bcr-2012-007931](#)]
- 29 **Shin WY**, Lee KY, Ahn SI, Park SY, Park KM. Cutaneous metastasis as an initial presentation of a non-functioning pancreatic neuroendocrine tumor. *World J Gastroenterol* 2015; **21**: 9822-9826 [PMID: [26361431](#) DOI: [10.3748/wjg.v21.i33.9822](#)]
- 30 **Ito H**, Tajiri T, Hiraiwa SI, Sugiyama T, Ito A, Shinma Y, Kaneko M, Anzai K, Tsuda S, Ichikawa H, Nagata J, Kojima S, Watanabe N. A Case of Rare Cutaneous Metastasis from Advanced Pancreatic Cancer. *Case Rep Oncol* 2020; **13**: 49-54 [PMID: [32110219](#) DOI: [10.1159/000505322](#)]



Published by **Baishideng Publishing Group Inc**  
7041 Koll Center Parkway, Suite 160, Pleasanton, CA 94566, USA

**Telephone:** +1-925-3991568

**E-mail:** [bpgoffice@wjgnet.com](mailto:bpgoffice@wjgnet.com)

**Help Desk:** <https://www.f6publishing.com/helpdesk>

<https://www.wjgnet.com>

